MEASUREMENTS OF HEAT CAPACITY AND HEAT TRANSFER COEFFICIENT OF WATER-OXYGEN MIXTURES AT NEAR CRITICAL CONDITIONS

By

Sanja Boskovic

B.Sc. (Mechanical Eng.) University of Sarajevo, 1985

A THESIS SUBMITTED IN PARTIAL FULFILLMENT OF THE REQUIREMENTS

FOR THE DEGREE OF MASTER OF APPLIED SCIENCE

in

THE FACULTY OF GRADUATE STUDIES DEPARTMENT OF MECHANICAL ENGINEERING

We accept this thesis as conforming to the required standard

THE UNIVERSITY OF BRITISH COLUMBIA

November, 2001

ABSTRACT:

The constant-pressure heat capacity, C_p, and local forced convection heat transfer coefficient, h, for water-oxygen mixtures flowing inside horizontal smooth tubes were obtained experimentally. Data were obtained for pressures of 24 to 26 MPa; flow rates 0.636 to 1.27 l/min, average heat fluxes 34 to 160 kW/m^2, mass velocities 351 to 701 kg/m^{2}s and temperatures from 330 to 430 °C. Oxygen flow was 2 to 8 weight percentage of the total mixture flow. For a given flow and heat supplied to the mixture, C_p is determined from the bulk temperature in a heated tube. The heat transfer coefficient, h is determined from the difference in bulk and wall temperatures. The temperature at which the maximum heat capacity occurs (T_{pc}) is lower for water-oxygen mixtures than for pure water. Another effect of oxygen addition is a reduction in magnitude of the maximum C_p and h. The enhancement near the critical point appears to be less at high heat flux.

TABLE OF CONTENTS

LIST OF FIGURES

LIST OF TABLES

NOMENCLATURE

A – area, m^2

C_p – heat capacity, kJ/kgK

E – temperature ratio

Fc – coefficient, Eqs. (3a) and (3b)

h – heat transfer coefficient, W/m^2K

i – enthalpy, kJ/kg

k - thermal conductivity, W/mK

L – test section length, m

m – mass flow rate, kg/h

n_1 – coefficient, Eq. 3b.

n_2 – coefficient, Eq. 3b.

Nu – Nuselt number

P - pressure, MPa

Pr – Prandtl number

q - heat flux, kJ/ m^2

Q – heat power supplied to water-oxygen mixtures, kW

R - tube radius, m

Re – Reynolds number

T – temperature, °C

T_{out} – temperature, K

V - voltage reading, V

V_o – zero offset, V

w_{Cp} – error for heat capacity measutrement

w_m – error for oxygen mass flow rate measurement

w_T – error for temperature measurement

w_h – error for heat transfer coefficient measurement

Greek:

ρ – density, kg/m^3

Δx – axial distance between thermocouples, m

Subscript:

b – bulk

c - critical

f – fluid

i – inlet

o – outlet

r – reduced temperature

w – wall

m – pseudocritical condition

ACKNOWLEDGMENT

First and foremost I would like to thank Dr. Steven Rogak, my supervisor, whose insight and support was never ending. His support kept me motivated throughout the whole course of this study.

I wish to thank Dr. Richard Branion for his support, kindness, and time he spent to correct my mistakes. I also would like to thank Dr. Clive Brereton for serving in my examination board and for his invaluable comments.

I was lucky to meet and be with a number of wonderful fellow graduate students during my stay at UBC. I should thank Tazim Rehmat as well as Majid Bazargan, Mohamed Khan and Ivette Vera-Perez . My specially thanks go to Wang Shuo who was my office-mate as well as a very good friend.

My appreciate also goes to the technical support stuff in mechanical shop and electronic shop, secretaries in the department.

Loving gratitude is extended to my husband and son.

I thank my brother, his family, my relatives from Slovenia and friends, who kept me going and kept me smiling.

I thank my parents who taught me the most important lessons, showed me the path, and shaped my life.

Finally, the financial support provided by NSERC of Canada are gratefully acknowledged.

Dedicated to my husband and son and my very best friends Davor and Andrej.

Thank you.

1. INTRODUCTION

1.1 Supercritical Water Oxidation

Supercritical Water Oxidation (SCWO), sometimes referred to as Hydrothermal Oxidation (HTO), is a thermal process capable of destroying a wide variety of hazardous organic wastes. SCWO exploits the ability of supercritical water to dissolve both oxygen and nonpolar organic compounds thereby allowing wastewater containing organic wastes such as oils and sewage to be completely oxidized to carbon dioxide and water. In a typical SCWO waste treatment system (Fig. 1.1), dilute aqueous organic waste is combined with an oxidizer at elevated pressure and temperature (P> 22.1 MPa, T>550 °C) in a reactor for residence times on the order of 30 – 90 seconds depending on the reaction temperature. Since supercritical water is an excellent solvent as well as an ideal media for heat transfer, the reaction occurs quickly within the reactor. The products of the reaction are cooled and separated. This feature is very useful when treating highly toxic wastes. Research is ongoing to assist in developing the utilization of SCWO technology on an industrial scale.

The high temperature environment within SCWO reactors and processing systems can present significant reliability and performance problems. Unlike most organic materials, inorganic compounds tend to be highly soluble in liquid water at ambient conditions but have extremely low solubility under supercritical conditions. The resulting inorganic salts can precipitate causing sticky deposits on the reactor wall and can even plug the reactor tube through high local deposition rates. Even if plugging does

not occur, salt deposition significantly affects the pressure drop and flow characteristics as well as the heat transfer rate.

One very important aspect of the design of a SCWO facility is having knowledge of the heat transfer rates. Maximizing the heat transfer rate is a major task for the design process of any heat transfer equipment.

1.2 Heat transfer to supercritical fluids

There are no available data for heat transfer coefficients for water-oxygen mixtures and there are limited heat transfer data for supercritical water covering various ranges of geometry, pressure, mass flow and heat flux (Bazargan, 2001).

Such information might provide the necessary knowledge for the optimal design of a SCWO system. To accomplish this goal, the present study focuses on thermodynamic properties and heat transfer to supercritical water-oxygen mixtures flowing in a pipe.

Experimental results to date (Swenson *et al.*, 1965: Yamagata *et al.*, 1972: Kondratev, 1967) have shown different heat transfer behavior for supercritical fluids compared to that observed during single-phase forced convection under subcritical conditions including different features like enhanced and deteriorated heat transfer.

1.3 Enhanced heat transfer

Suppose the temperature of a fluid flowing in a heated tube at supercritical pressure was raised until the wall temperature was slightly above the "pseudocritical temperature". Sabaresky *et al.* (1967) describe the pseudocritical temperature as follows: "The temperature at which the thermodynamic and transport properties have their maximum rate of change with temperature at constant pressure. Its significance is that below the pseudocritical temperature, the fluid has liquid-like properties while above, it closely resembles a vapor". Under such conditions many investigators have reported a significant enhancement of the heat transfer rate at low heat fluxes. Swenson *et al.* (1965) demonstrated a correlation between the heat transfer enhancement and pressure for supercritical water flowing in a smooth, vertical tube. Pitla *et al.* (1998) in their review article pointed out that Shitsman (1963) and Krasnoshchekov *et al.* (1970) observed an improvement in heat transfer when the wall temperature was less than the critical temperature and the fluid bulk temperature was greater than the critical temperature. The improvement of heat transfer during cooling occurs because of the formation of a lower temperature, liquid like layer near the wall of the tube. This layer has higher thermal conductivity than the bulk fluid. Perhaps the most important factor affecting heat transfer is high heat capacity near the pseudocritical point.

1.4 Deteriorated heat transfer

Yamagata *et al.* (1972) and Kondratev (1967) studied the effect of heat flux on heat transfer to supercritical fluids. They showed that when the heat flux increased, the heat transfer coefficient decreased in the pseudocritical region. At very high heat fluxes, heat transfer deterioration is a very serious problem and can cause tube failure. Sabaresky and Hauptmann (1967) measured forced convective heat transfer from a flat plate to carbon dioxide near the critical point and showed that at larger heat-transfer rates, the heat transfer coefficient exhibited a sharp drop when the free stream (bulk) temperature slightly exceeded the pseudocritical temperature. Jackson and Hall (1979) derived an expression for the onset of impaired heat transfer at high heat flux during forced convection. They suggested that the validity of the expression needed to be investigated experimentally.

1.5 Thermodynamic and transport properties

A complete set of thermodynamic properties of supercritical water-oxygen mixture is not available in the literature. From data provided by Christoforakos and Franck (1986), phase equilibria were calculated and P-V-T-x relations for water-oxygen developed.

With this Equation of State (EOS) density and mixture heat capacity were calculated (Saur *et al.*, 1993). Viscosity and thermal conductivity were obtained as deviations from values for low density gases. Van der Waals "one fluid theory" was used

for mixture rules. Wang (2001) calculated the phase boundary, constant pressure heat capacity and density using the Hard Sphere equation of state and Redlich-Kwong-Soave equation of state. Oh *et al.* (1997) calculated thermodynamic and transport properties for SCWO fluids (water, ethanol, isopropyl alcohol, nitrogen, oxygen, and carbon dioxide) using the Redlich-Kwong-Soave cubic equation of state. Details are presented in Appendix B.

It is difficult to predict the phase equilibrium of two-component or multi-component systems because changes of the fractions of the each component in the liquid and vapor phases need to be considered. A T – x phase diagram for water-oxygen mixtures at pressure 25 MPa was obtained (Wang 2001) Figure 1.2. The phase curve (ABCDE) divided liquid, vapor and liquid-vapor regions from each other. Point C is the critical point. Curve AC represents the fraction in the vapor phase, and curve CE represents in the liquid phase. For example, at 580K (line B-D), the vapor is approximately 55% H_2O while the liquid is over 98% H_2O.

1.6 Nusselt number correlation

Non-dimensional relations are usually developed to make experimental results more general. Nusselt number correlations are used for forced convection heat transfer in pipe flows. They have the following form:

$$Nu = a\,\mathrm{Re}^{b}\,\mathrm{Pr}^{c} \qquad (1)$$

where a,b,c are constants to be determined from the experimental data. Near the critical region, the fluid properties are changing significantly with temperature. Because of that behaviour, the simple Nusselt number correlation, which assumes constant property values and fully developed flow, is not generally applicable for supercritical conditions. To account for the effect of property variations some correction factors have been introduced to the Nusselt number correlation. The ratio of the specific heat, density or viscosity at the wall and bulk temperature, or combinations of these are usually employed. The following are some examples of correlations presented in the literature.

Swenson *et al.* (1965) developed the following correlatio from their experiments with heated turbulent flow:

$$Nu_w = 0.00459(\mathrm{Re}_b)^{0.923}\left(\overline{Cp}\frac{\mu_w}{k_w}\right)^{0.612}\left(\frac{\rho_w}{\rho_b}\right)^{0.231} \qquad (2)$$

where the integrated heat capacity is given by

$$\overline{C_p} = \left(\frac{i_w - i_b}{T_w - T_b}\right)$$

The subscripts w and b refer to conditions at the wall and bulk respectively.

Yamagata *et al.* (1972) examined data from horizontal and vertical test sections to develop the following more complicated correlation:

$$Nu_b = 0.0135\left(\mathrm{Re}_b\right)^{0.85}\left(\mathrm{Pr}_b\right)^{0.8} F_c \qquad (3a)$$

where the correction factor F_c depends on the temperature

$$F_c = 1 \text{ for } E = \frac{T_m - T_b}{T_w - T_b} > 1$$

$$F_c = 0.67\left(\mathrm{Pr}_m\right)^{-0.05}\left(\frac{\overline{Cp}}{Cp_b}\right)^{n1} \quad \text{for} \quad 0 \le E \le 1 \tag{3b}$$

$$F_c = \left(\frac{\overline{Cp}}{Cp_b}\right)^{n2} \quad \text{for} \quad E < 0$$

the exponents n_1 and n_2 are

$$n1 = -0.77\left(1 + \frac{1}{\mathrm{Pr}_m}\right) + 1.49$$

$$n2 = 1.44\left(1 + \frac{1}{\mathrm{Pr}_m}\right) - 0.53$$

and Pr_m is the Prandtl number at the pseudocritcal point.

The subscript m refers to conditions at the pseudocritical temperature.

Shown in Figure 1.3 is a comparision of some available correlations with experimental data P=25.2 MPa, Q = 307 kW/m^2 and G = 965 kg/m^{2}s (Bazargan, 2001). The sources of disagreement between the results are due to: (a) differences in the test conditions, mainly in terms of the heat flux and buoyancy effects, which can not be fully reflected in a typical Nusselt number correlation and, (b) differences in values of the thermophysical properties used in various correlations either because of different sources of information or difficulty in applying the proper values (as a result of their large variation with small changes in pressure and temperature in the critical region).

To apply such Nusselt number correlations to supercritical water-oxygen mixtures, reliable thermodynamic properties in the supercritical region are needed.

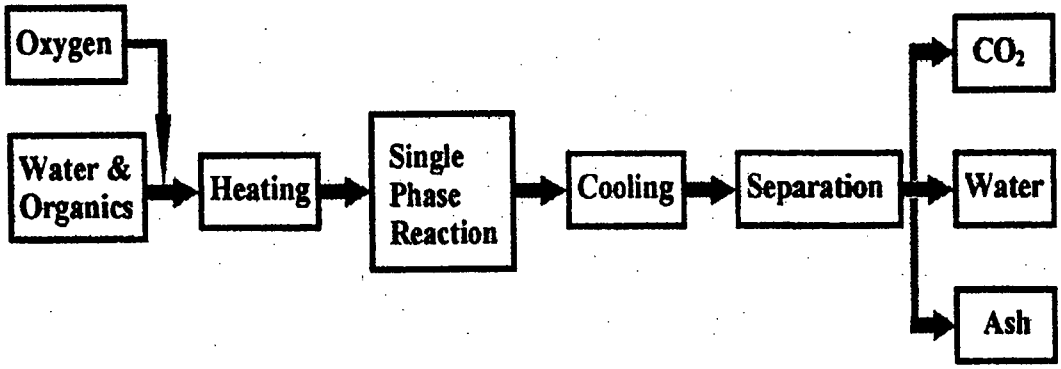

Figure 1.1 SCWO process flow diagram

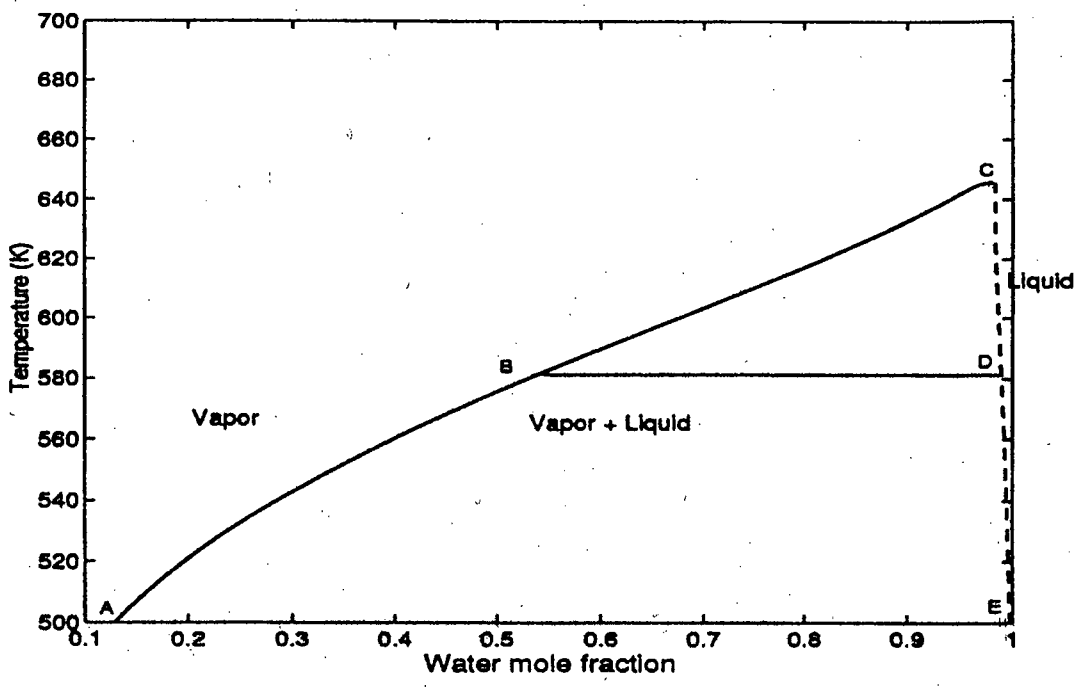

Figure 1.2 Phase equilibrium of binary mixtures for P= 25 MPa, calculated from RKS EOS, (Wang, 2001)

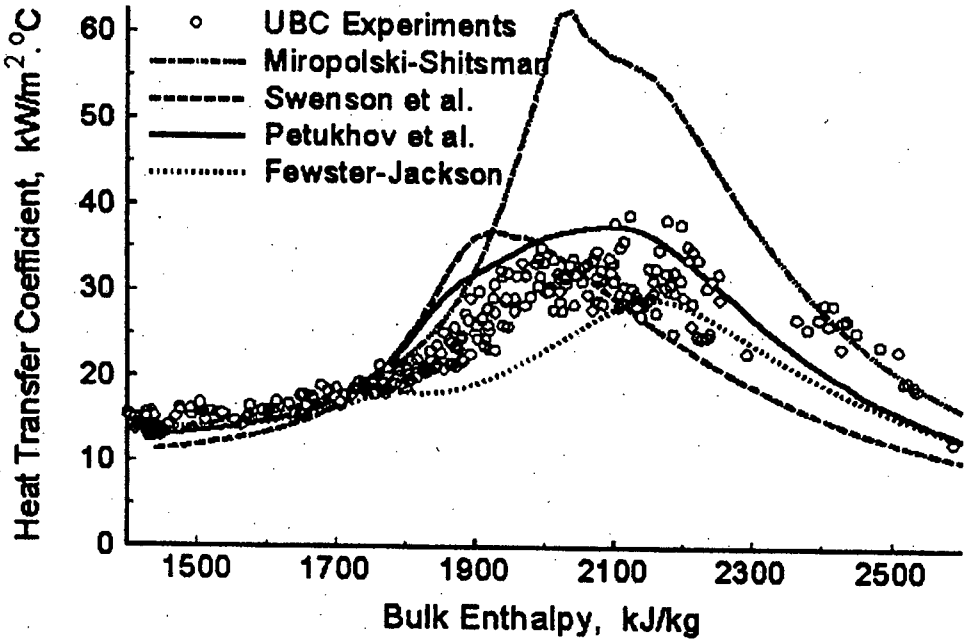

Figure 1.3 Variation of heat transfer coefficient with temperature for supercritical water, P = 25.2 MPa,Q = 307 kW/m^2 and G = 965 kg/m^{2}s (Bazargan, 2001)

2. EXPERIMENTAL SYSTEM

2.1 The UBC/NORAM pilot plant

The UBC/NORAM SCWO facility (Figure 2.1) was constructed for research and development of a tubular-type reactor, for the destruction of wet organic wastes. A range of pressures, heat fluxes temperatures and mass flows can be achieved. Two 550 L cylindrical storage tanks supply the system with water and waste. Water is pressurized with a triplex plunger pump while oxygen is pressurized using an air-operated booster. Water flow is measured with a graduated cylinder and stop watch, at the system outlet when it is cold (without oxygen). Oxygen flow is measured using a differential pressure transmitter installed across an orifice plate downstream of the booster. Details about transmitter calibration are given in Appendix C.

The main heat transfer elements of the SCWO system are the regenerative heat exchanger, two preheaters, the test section, the reactor, and the process cooler. The process cooler is 6.1 m of 9.5 mm stainless steel tube. All other tubing is made of Alloy 625 high pressure tubing (6.2 mm ID and 9.5 mm OD). An electrical current through the tube wall provides the heat supplied to the system (Fig. 2.2). The power is supplied from silicon controlled rectifiers (SCR). The power goes from the SCR panel through two step-down transformers to each preheater. The preheaters are controlled separately from the SCR panel. The power to Preheater 1 is adjusted manually on the SCR panel. The power to Preheater 2 can be adjusted with a feedback temperature controller. The heating for the test section is achieved in the same way as for the preheaters, but power control is always manual. The test section is made from four tube sections (Fig. 2.3). Two shorter

sections (0.3 m), placed at the inlet and the outlet of the test section are not heated. The other two (1.52 m each) are electrically heated. The regenerative heat exchanger is designed to recover approximately 30 kW of power from the test section outlet. The tubing is insulated in 15.25 cm x 15.25 cm boxes of ceramic board (Kaowool). There is one absolute pressure transducer located at the beginning of the test section and a differential pressure transducer which measures the pressure drop along the test section. The last one is also used for pressure drop measurement through the venturi, which is placed at the end of the test section. The venturi was used for preliminary density measurements as described in Wang (2001). The temperature measurements are made using 29 surface thermocouples (high temperature thermocouple wire with ceramic fiber insulation) and three bulk temperature thermocouples.

2.2 Temperature measurement

All thermocouples are K – type (Chromel Alumel) with twisted shielded extension wire.

Three thermocouples were placed in the test section (Fig. 2.4). Previously all of them were used for heat capacity and heat transfer measurements. Runs #28-35 had only two bulk thermocouples working in the test section (Fig.2.5).

The test section has 20 top surface thermocouples and 10 bottom ones. All of them were spot-welded. Thermocouple error is in range 2 – 3 °C, but it was possible to measure difference of less than 0.5 °C, by cross calibrating thermocouples against each other.

2.3 Pressure measurement

The absolute pressure transducer is used for the system pressure control. The pressure range of the transducer is 0 – 34.5 MPa and output signal is in range 0-10 volts. The calibration was done with a digital calibrator (0 – 51.7 MPa) with water as a working fluid. A correlation between the absolute pressure and the voltage was linear:

$$P = 6.8119V + 0.0444 \quad (4)$$

Where P is the system pressure (MPa), V is voltage reading (V). This relation gives an error of 0.04-0.1% (0.01 MPa – 0.028 MPa on interval of 21.9 MPa – 26.9 MPa).

2.4 Flow rate measurement

Water flow rate is measured by using a graduated cylinder and a stopwatch after the system is pressurized, and before oxygen is introduced and heat is supplied.

For Runs #1-22 and #36-38 oxygen flow rate was measured with Validyne variable reluctance pressure transducer – DP303. The differential pressure transducer cell was capable of detecting pressure differences up to 5.5 MPa. The calibration was performed by supplying nitrogen to the booster and measuring the low pressure outlet flow with a dry gas meter. The correlation between oxygen mass flow rate and voltage signal is as follows:

$$m = (V*\rho/44.4)^{1/2} \quad (5)$$

where:

m – mass flow rate, kg/h

V – voltage reading, V

ρ – oxygen density at 27.4 MPa

More details about calibration are available in Gairns and Rogak (1999).

Oxygen flow is measured with a transmitter (Foxboro E13DH_ISAM2) for Runs # 23-35. The diameter of the orifice is 0.86 mm. The pressure drop is measured by a transmitter. The output signal is in the range 4 – 20 mA. To provide an acceptable output signal for the data acquisition (0 – 10 V) a 500 Ohm resistor was connected in the line.

The orifice was calibrated using oxygen at the 27.2 MPa (Appendix C). The correlation between oxygen mass flow rate and voltage signal is as follows:

$$m = 4.16(V-V_o)^{1/2} \quad (6)$$

where:

m – mass flow rate, kg/h

V – voltage reading, V

V_o – zero offset, V

The error of measurement is around 16% considering calibration error and zero-offset drift (the major factor). The transmitter maximum flow rate measurement is 12 kg/h. Zero offset varies with the working pressure and it is depends on the possible overloading of the transmitter. A ball valve is used as a bypass to protect the transmitter.

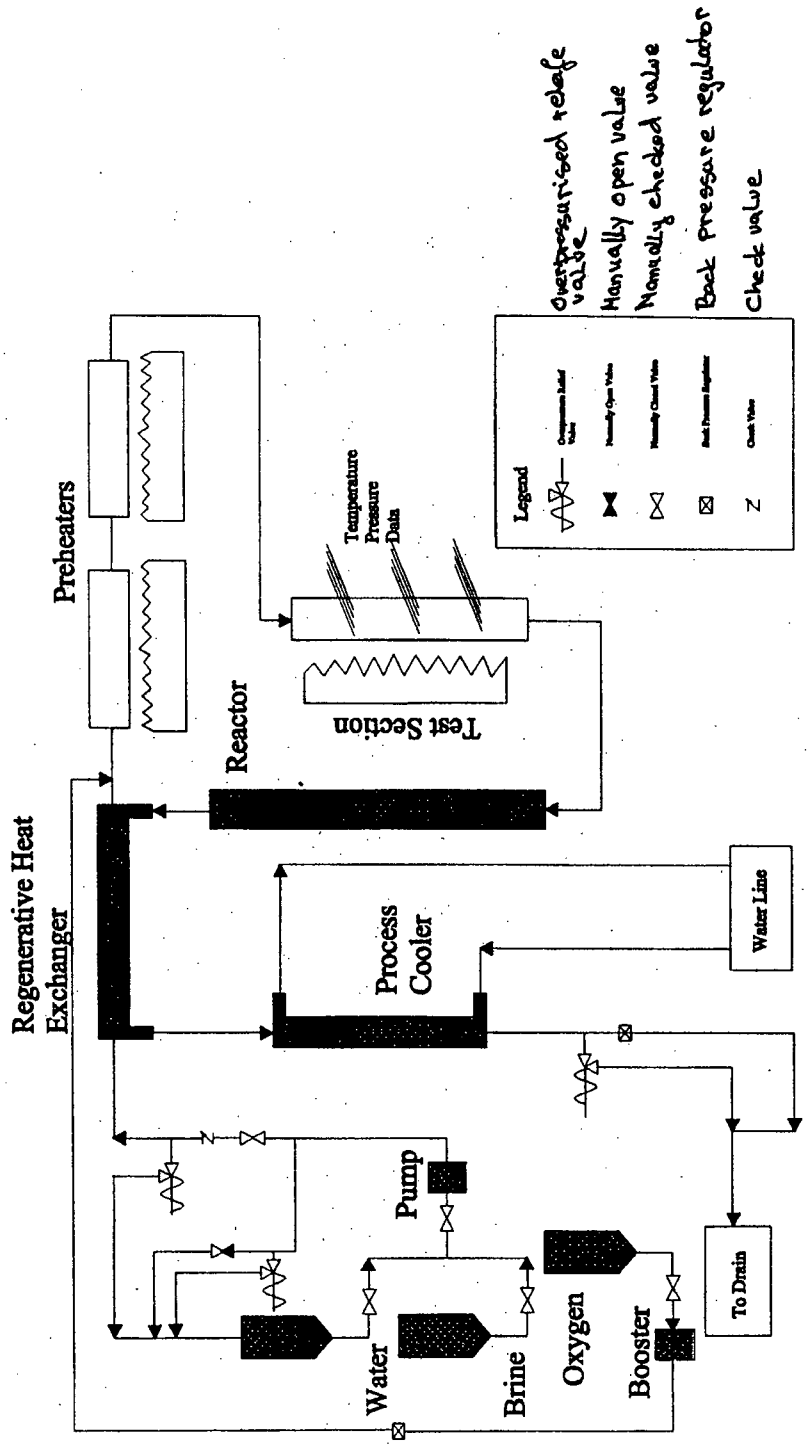

Figure 2.1 UBC/NORAM Pilot Plant
Note that all preheaters and test section are horizontal

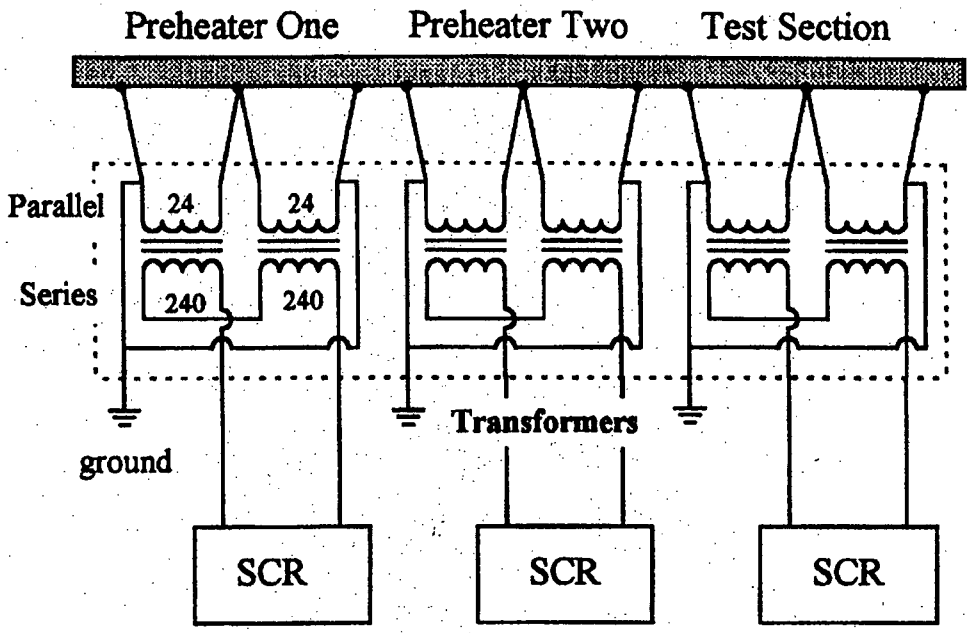

Figure 2.2 Electrical heating system (Teshima, 1997)

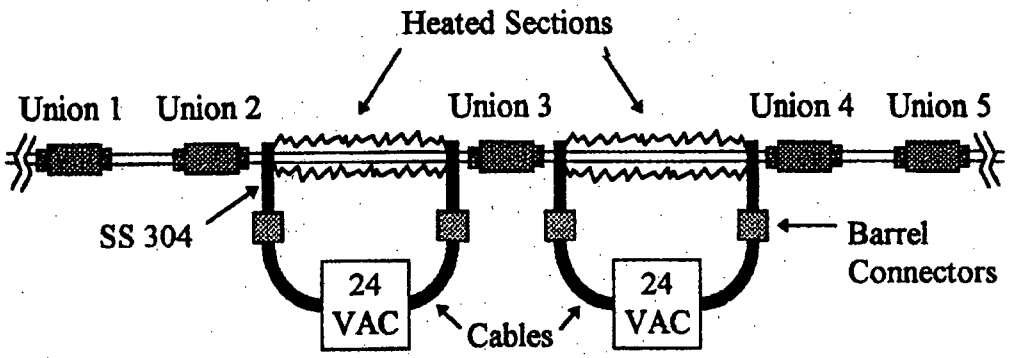

Figure 2.3 Test section (Teshima, 1997)

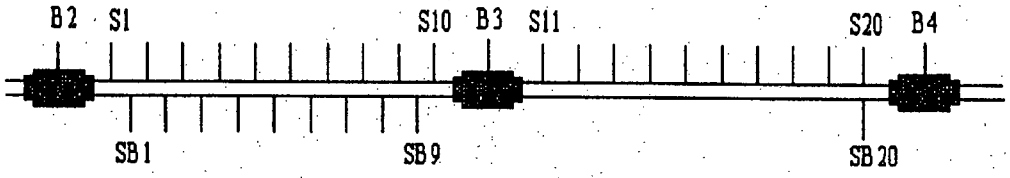

Figure 2.4 Thermocouple setting for the test section (before the venturi was installed)

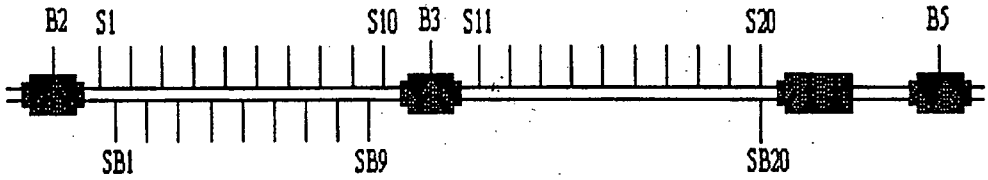

Figure 2.5 Thermocouple setting for the test section (after the venturi was installed)

3. MEASUREMENTS OF CONSTANT PRESSURE HEAT CAPACITY AND HEAT TRANSFER COEFFICIENT FOR WATER-OXYGEN MIXTURE:

3.1 Constant heat capacity measurement

For a given system pressure, measurements were done by slowly increasing the temperature of the system. The power supplied to the working fluid was calculated using a heat loss model (Appendix A). Power supplied to the fluid was calibrated in pure-water (known *Cp*) measurements at temperature far from T_c. In order to quantify the small transient thermal effect and non-constant heat losses, a 1-D transient thermal model was developed (Appendix A). This model was used to correct the supplied power for all experiments. The difference between the correct supplied power and the adiabatic case was 20%, which represents total heat loss. The transient effect is only 20% of the total heat loss. Heat capacity was calculated as:

$$Cp = Q_f / m(T_{bout} - T_{bin}) \tag{7}$$

where Q_f is the power supplied to the working fluid, T_{out} is the temperature at the test section outlet and T_{in} is the temperature at the test section inlet.

The mean value of inlet and outlet temperature was used as the nominal temperature for reporting *Cp* values.

Figure 3.1 gives the comparison between the measurements, exact values from IAPWS-95 (International Association of Properties of Water and Steam) and values from

IAPWS – 95 averaged over the ΔT of the test section for the actual experiments for pure water at 24.4 MPa. From the location of the peak in Cp, it appears that the measured temperature is 2 degrees too high. A discrepancy of 2°C appeared, which could be related to errors in the thermocouple readings (the thermocouples were not calibrated at high temperature and all other tests done on this facility gave a similar offset).

3.2 Heat transfer coefficient measurement

As written before, the thermocouples are welded to the outer surface of the tube. Technically it is very difficult to measure the inner wall temperature in a small bore tube without violating the flow pattern. Thus the inside wall temperature was calculated from measured outside temperatures. The differential equation for the temperature distribution is given by:

$$\frac{d}{dr}\left(rk\frac{dT}{dr}\right) = -\frac{2qR_i r}{\left(R_o^2 - R_i^2\right)} \tag{8}$$

where r is distance measured from the center of the tube, k is the thermal conductivity of the tube wall (Alloy 625) and assumed to be constant across the tube, R_i is the inside tube radius, R_o is the outside tube radius and q is heat flux. The boundary conditions at the outer tube surface ($r = R_o$) are:

$$T = T_o \tag{9}$$

$$dT/dr = -q_{loss}/k$$

The solution of the equation for the temperature distribution across the wall to get the inside wall temperature T_i, at $r = R_i$ is:

$$T_i = T_o + \frac{qA(R_o^2 - R_i^2)}{4k} + \frac{R_o}{k}\left(\frac{qR_oA}{2} - q_{loss}\right)\left(\ln R_i - \ln R_o\right) \qquad (10)$$

$$A = \frac{2R_i}{\left(R_o^2 - R_i^2\right)}$$

This correction results in heat transfer coefficients about 10% higher than those based on the raw outside temperature.

To calculate the local heat transfer coefficient, the local bulk temperature needs to be known. The bulk temperature of the fluid as a function of the axial position, x, can be estimated from an energy balance $Q = m\Delta i$, where $\Delta i = C_p(T_{b(j+1)} - T_{bj})$, C_p is heat capacity for water-oxygen mixtures and T_{bi} and $T_{b(i+1)}$ are bulk temperatures at axial position j and j+1 respectively, i is enthalpy. Those bulk temperatures are calculated as follows (assuming that the pressure drop along the test section is small and that the enthalpy of the fluid is only a function of the bulk temperature):

$$T_{b_{i+1}} = \frac{q_L \Delta x}{mC_p} + T_{b_i} \qquad (11)$$

where $q_L = Q_f/L$

Q_f – heat power supplied to water-oxygen mixtures, kW

L – test section length, m

m – flow rate, kg/s

C_p – heat capacity, kJ/kgK

Δx – axial distance between thermocouples, m

Knowing the inside wall and bulk temperatures, the local heat transfer coefficient can be obtained by:

$$h = \frac{q}{(T_w - T_b)} \tag{12}$$

where:

$q = Q_f/A$ and

Q_f – heat power supplied to water-oxygen mixture, kW

A – area, m^2

T_w – inlet wall temperature, K

T_b – bulk temperature, K

Heat loss model

The heat power supplied to the working fluid is primarily a function of applied voltage, but also depends on steady and transient heat losses to the tubing, fitting, insulation, and surroundings. Appendix A describes the methods used to determine these heat losses.

The first component of the thermal model is a one-dimensional transient heat loss model, which uses measured tube wall temperatures as a boundary condition. This model is shown to reproduce transient heat fluxes quite well.

The second component is a model to predict the electrical power dissipated in the tube and transferred to the flow and the losses mentioned above. Finally, a method for using these models in the heat capacity measurements is described.
Details of the model are given in Appendix A.

3.3 Data processing

A MatLab program (heatdata.m) was developed for the data processing. The outline of the program is given in Appendix F. Raw data are used as input in the program. The program consists of filtering data (running median calculation), heat loss, heat capacity, electrical power and heat transfer coefficient calculations. For all runs, the number of 5 seconds measurements averaged was nav = 20. Final results are heat capacity and heat transfer coefficient data, which can be, used for graphical presentation either using a MatLab program or any other program.

3.4 Evaluation of the error of the measurements

The major errors for the heat capacity and heat transfer coefficient measurements are the errors in the oxygen flow rate measurements and the temperature measurements. The estimated error for the transmitter is 16% and for thermocouple (ΔT) is 20%. The estimated error for heat flux is 4%. Since heat capacity is function of flow rate, heat flux and temperature, the total error of heat capacity measurements is obtained by differentially Eq. 7:

$$w_{C_p} = \left[\left(w_m \frac{\partial C_p}{\partial m} \right)^2 + \left(w_T \frac{\partial C_p}{\partial \Delta T} \right)^2 + \left(w_Q \frac{\partial C_p}{\partial Q} \right)^2 \right]^{\frac{1}{2}} \quad (13)$$

where:

w_{Cp} – error for heat capacity measutrement

w_m – error for oxygen mass flow rate measurement

w_T – error for temperature measurement

w_Q – error for heat flux measurement

The estimated error for heat capacity measurement is 26%. Heat capacity error for pure water far from the critical point is less than 4% (Figure 3.1).

The heat transfer coefficient measurement error is estimated using the same expression considering that the heat transfer coefficient is function of heat capacity, bulk temperature and oxygen flow rate.

$$w_h = \left[\left(w_m \frac{\partial h}{\partial m} \right)^2 + \left(w_T \frac{\partial h}{\partial T} \right)^2 + \left(w_{C_p} \frac{\partial h}{\partial C_p} \right)^2 \right]^{\frac{1}{2}} \quad (14)$$

The estimated error for the heat transfer coefficient is 36 %

Figure 3.1 Heat capacity for pure water,
Run #11 (P = 24.4 MPa, m = 1.01 l/min, Q = 93 kW/m^2)

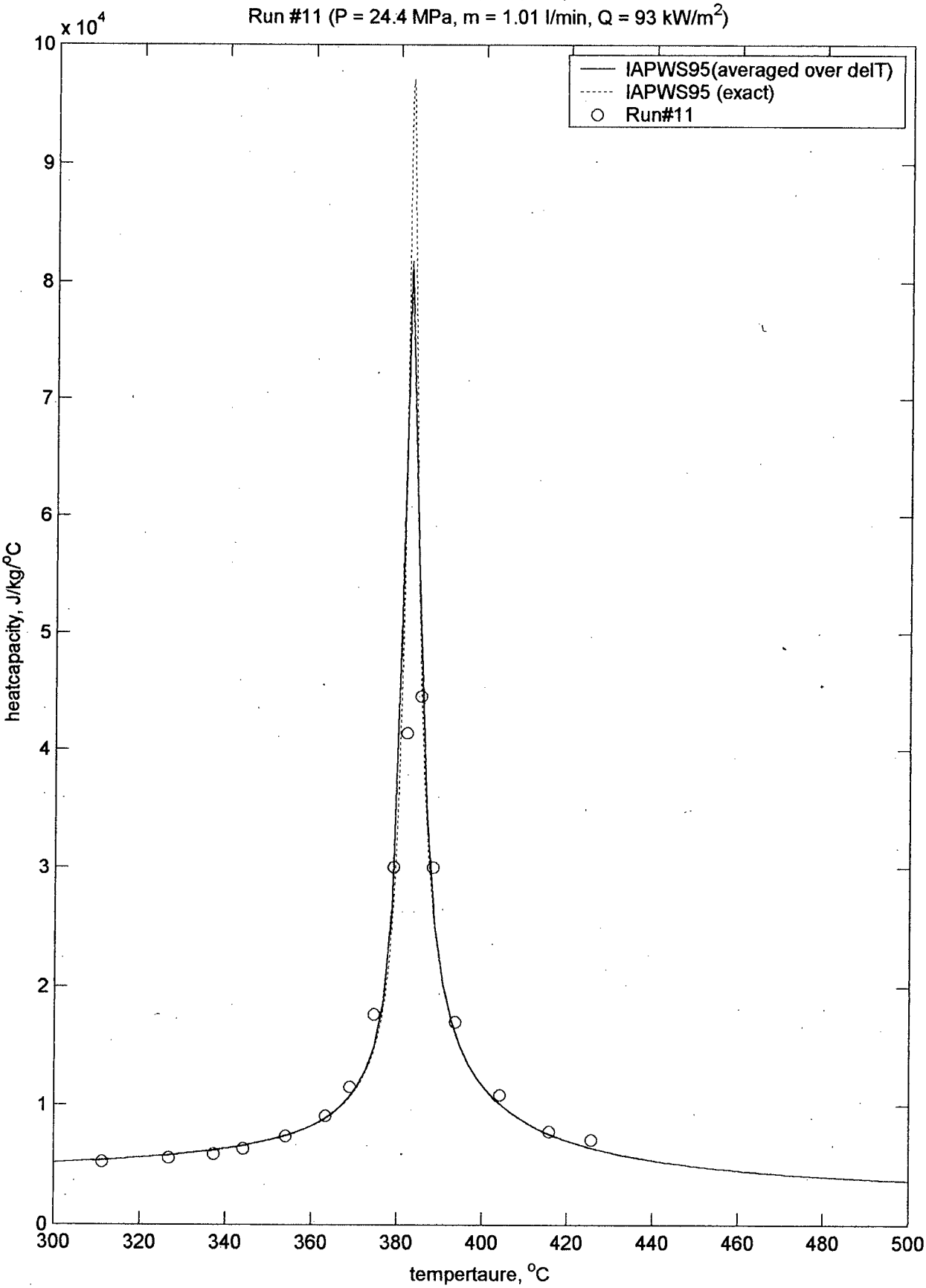

4. RESULTS

4.1 Constant pressure heat capacity for water-oxygen mixtures

Figure 4.1a shows measurements at system pressures of 24 MPa (Run#12) and 26MP (Run #15) with 2% oxygen by weight. The peaks are clearly smaller and appear at a lower temperature than for pure water (Run #11), but have the same trends as for pure water. Figure 4.2a gives the oxygen concentration effect on values and positions of the peaks of heat capacity. It is clear that with an increase of the oxygen concentration, the peak value of heat capacity is lower and the position of the peak occurs at a lower temperature. Complete results, which include 3% and 8% of oxygen concentrations, are presented in Appendix E1.

4.2 Heat transfer coefficient to supercritical water-oxygen mixtures

Figures 4.1b,c show measurements of the heat transfer coefficient at system pressures of 24 (Run #12) and 26 (Run #15) MPa with a 2% oxygen weight concentration. Figures 4.2b,c give the oxygen concentration effect on the values and positions of the peaks in the heat transfer coefficient. It is clear that with an increase in the oxygen concentration, the peak values of the heat transfer coefficient are lower and the positions of the peaks are occurring at lower temperatures. The effect of heat flux on heat transfer coefficient was also explored. With an increase of heat flux, the peak of heat transfer coefficient is lower, but it is not dramatically lower as it is for pure water

(Figs. 4.3a,b). Figures 4.4a,b show the flow rate effect on the heat transfer coefficient. With an increase in flow rate the heat transfer coefficient peak is higher.

For all cases heat transfer coefficient is higher for the top surfaces than for bottom surfaces (Figures 4.1b,c, 4.2b,c, 4.3a,b, 4.4a,b). These plots also include predictions of heat transfer coefficient for pure water. The heat transfer coefficient was calculated using Swenson et al. correlation (Eq. 2) for Nusselt number for supercritical water. In each case, the correlation was evaluated at the same values of the reported pressures, flows, and heat fluxes. The mass flow used in the correlation was the water flow without oxygen flow. It can be seen that in all cases Swenson correlation over predicts the heat transfer coefficient.

Figure 4.5 shows a difference between temperature at the peaks of heat capacity for water-oxygen mixtures and for pure water as a function of oxygen concentrations.

Figure 4.6 shows a ratio between heat capacity for water-oxygen mixtures and for pure water as a function of oxygen concentrations.

Table 4.1 summary results for the Run #11 to # 34. An average heat transfer coefficient was calculated based on a C_p weighted average +/- 15 °C of the temperature at C_p peak.

Table 4.1 Summary for Runs #11 - #34

Run #	Pressure MPa	Water flow l/min	Oxygen %	Average flux kW/m^2	Temperature at peak, °C water-IAPWS	Temperature at peak, °C	Heat capacity at peak, kJ/kg/K water-IAPWS	Heat capacity at peak, kJ/kg/K	Average heat transfer coefficient KW/m^2K
11	24.4	1.01	0	93	383	385	96	45	9.7
12	24.5	1.01	2.0	97	383	379	92	39	9.7
13	24.2	1.01	4.9	96	382	372	110	30	9.6
14	25.8	1.01	4.7	97	388	381	58	21	8.9
15	26.4	1.01	2.1	95	390	386	50	26	9
17	25.4	1.05	4	95	386	373	66	24	9.1
18	25.6	1.05	6.2	96	387	366	62	19	8.5
19	24.5	0.636	0	-15	383	heat loss test	92	-	-
20	24.9	0.636	0	-19	384	heat loss test	80	-	-
21	24.5	1.3	0	-12	383	heat loss test	92	-	-
27	25.2	1.03	5.8	95	386	373	70	16	8.7
28	25.2	1.27	0	83	386	392	70	40	8.1
29	25.1	1.27	3	96	385	383	72	28	9.4
30	25.2	1.01	3	95	386	382	70	34	10
31	25.3	1.01	7.9	98	386	373	68	27	8.2
32	25.2	1.01	8	160	386	374	70	21	6.1
33	25.3	1.01	7.6	37	386	372	68	27	5.9
34	24	1.01	7.8	34	381	370	121	29	8.2

Figure 4.1a Heat capacity for Run #11(P = 24.4 MPa, m = 1.01 l/min, Q = 93 kW/m^2),
Run #12 (P = 24.5 MPa, m = 1.01 l/min, Q = 97 kW/m^2, O2 = 2%),
Run #15 (P = 26.4 MPa, m = 1.01 l/min, Q = 95 kW/m^2, O2 = 2.1%)

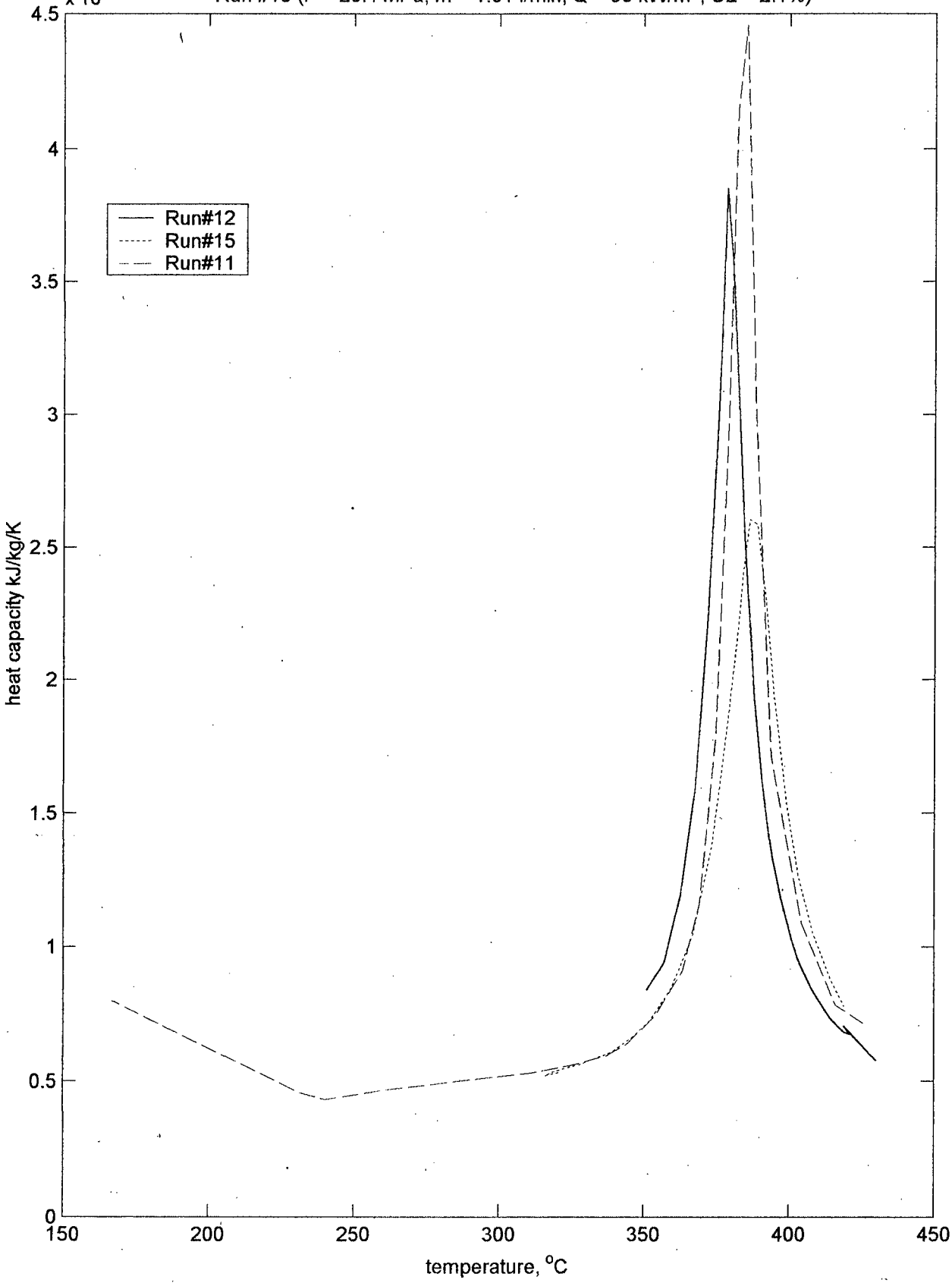

Figure 4.1b Heat transfer coefficient (bottom)
Run #12 (P=24.5 MPa, m=1.01 l/min, Q=97 kW/m^2, O2=2%),
Run #15 (P=26.4 MPa, m=1.01 l/min, Q=95 kW/m^2, O2=2.1%)

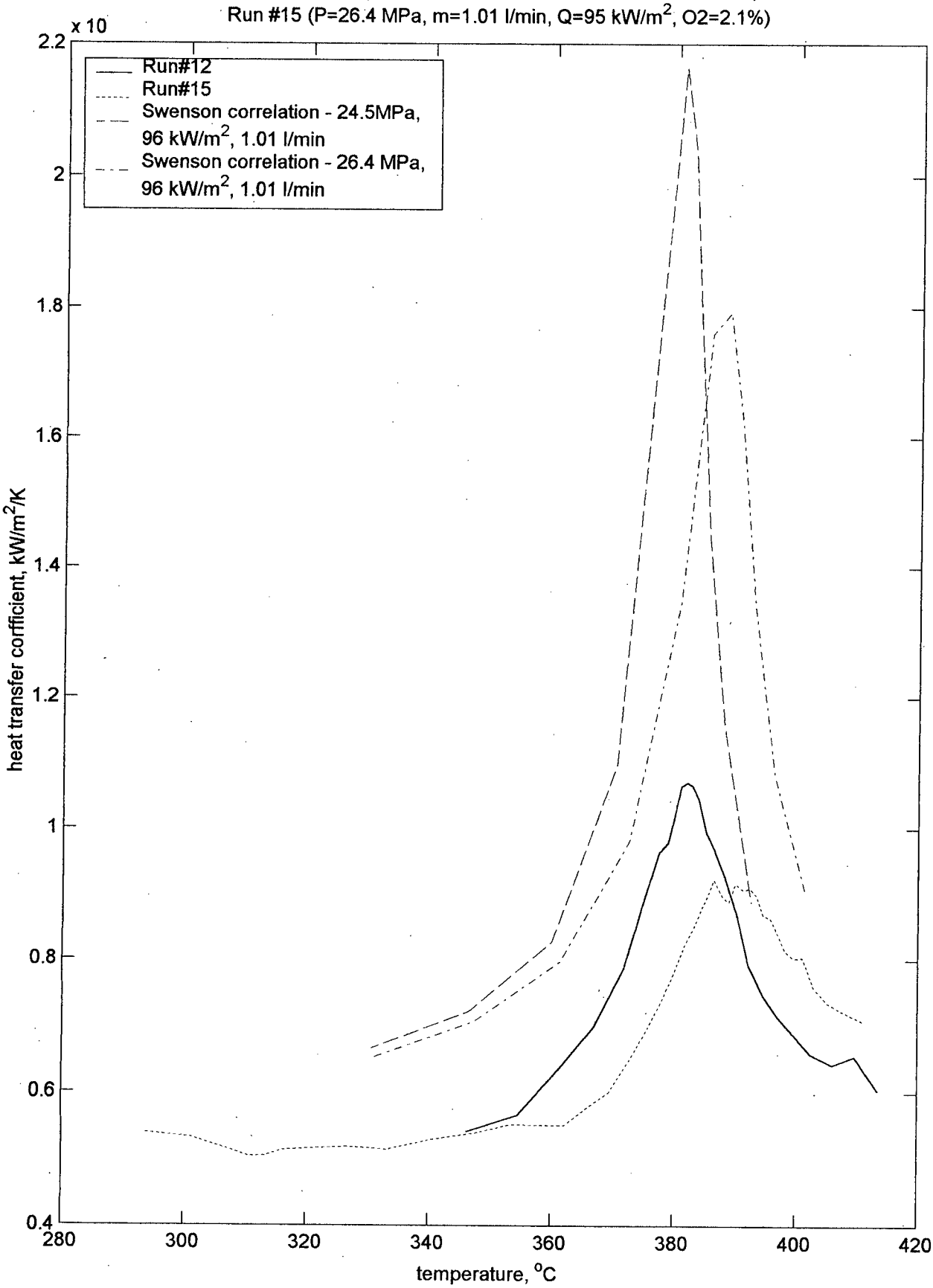

Figure 4.1c Heat transfer coefficient (top) for
Run #12 (P=24.5 MPa, m=1.01 l/min, Q=97 kW/m^2, O2=2%),
Run #15 (P=26.4 MPa, m=1.01 l/min, Q=95 kW/m^2, O2=2.1%)

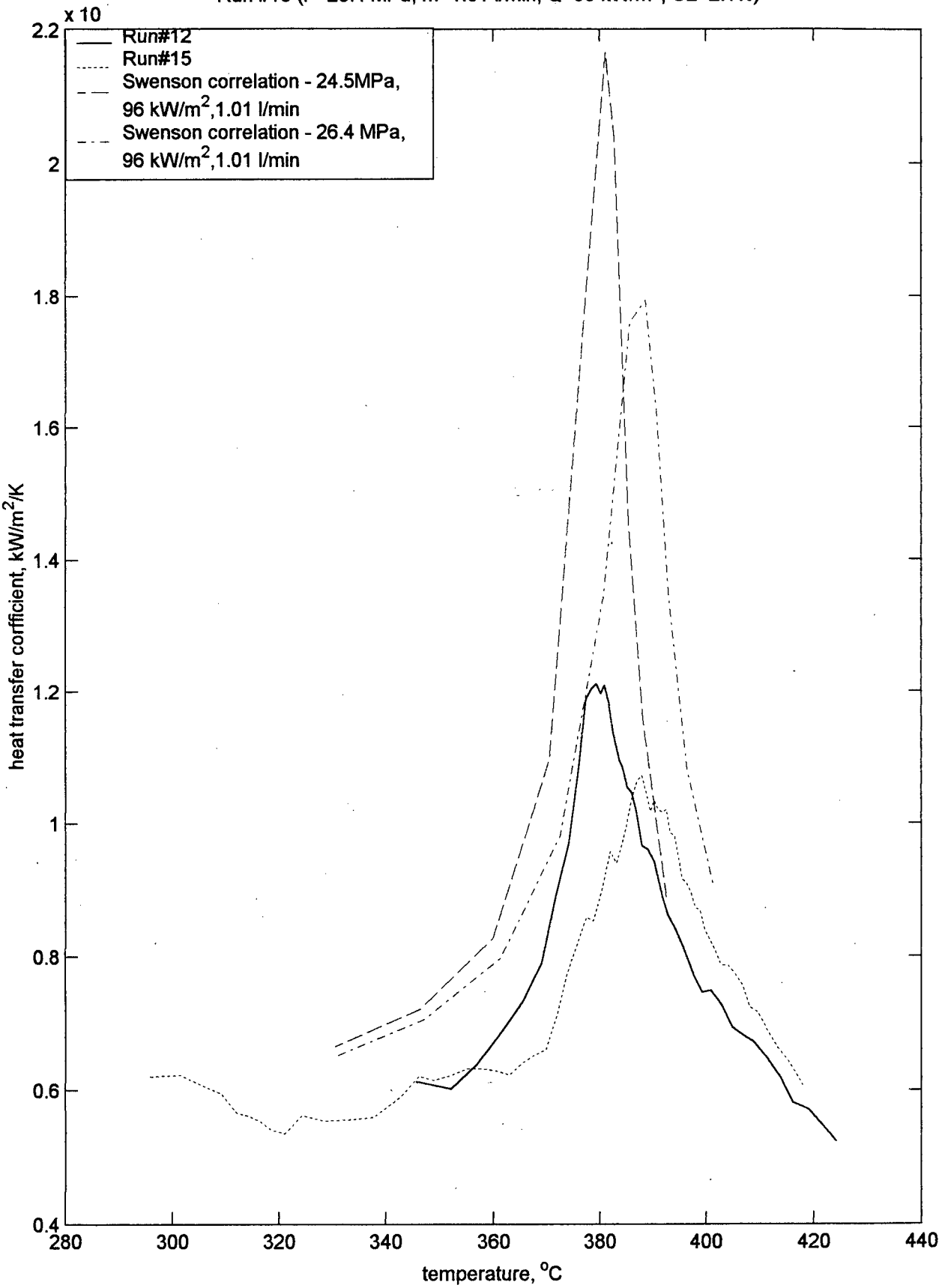

Figure 4.2a Heat capacity for Run #11(P=24.2MPa, m=1.01l/min, Q=93 kW/m^2, O2=0),
Run #12 (P=24.5 MPa, m=1.01 l/min, Q=97 kW/m^2, O2=2%),
Run #13 (P=24.2 MPa, m=1.01 l/min, Q=96 kW/m^2, O2=4.9%)

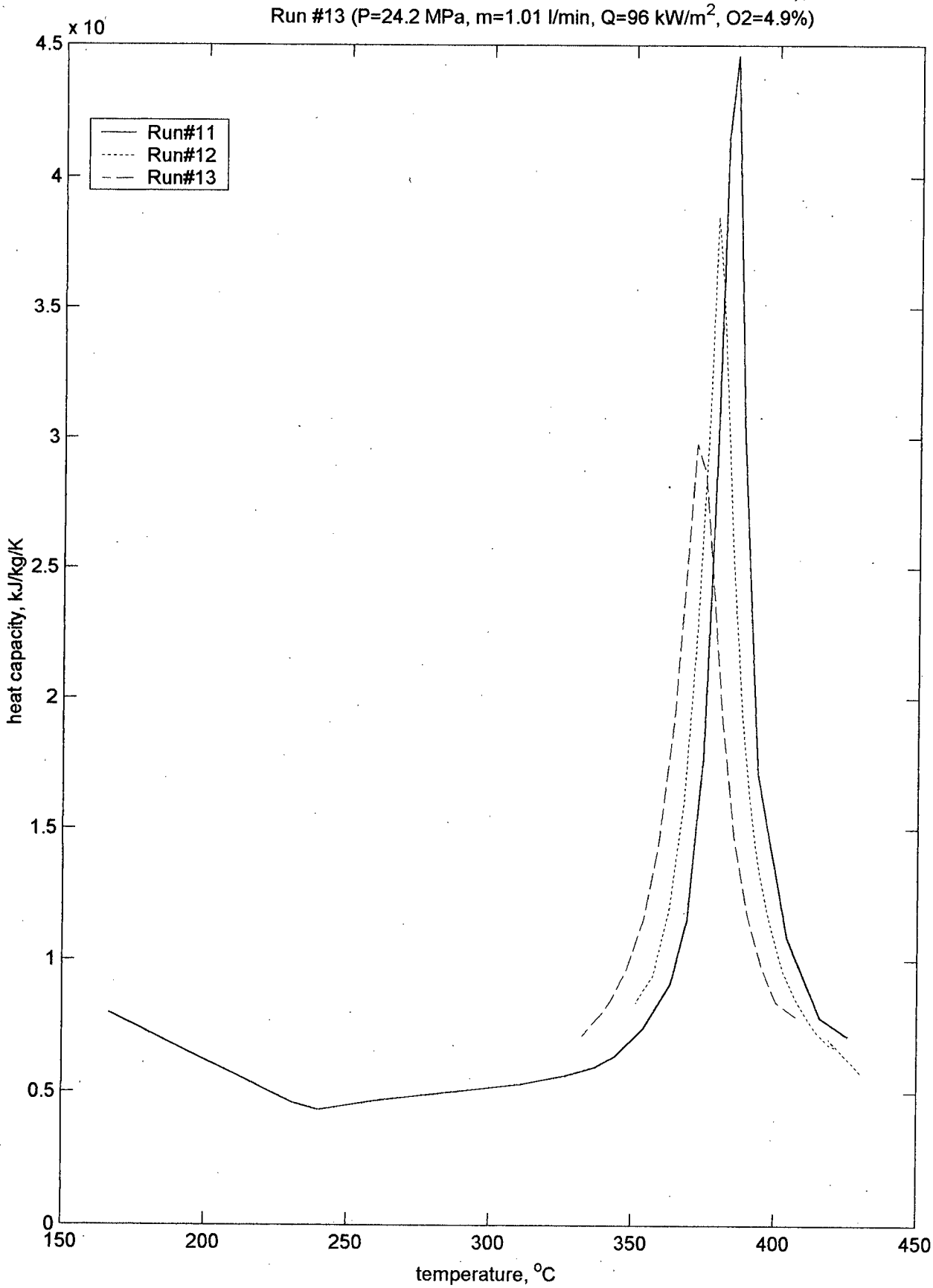

Figure 4.2b Heat transfer coefficient (bottom) for
Run #11 (P=24.2 MPa, m=1.01 l/min, Q=93 kW/m^2, O2=0),
Run #12 (P=24.5 MPa, m=1.01 l/min, Q=97 kW/m^2, O2=2%),
Run #13 (P=24.2 MPa, m=1.01 l/min, Q=96 kW/m^2, O2=4.9%)

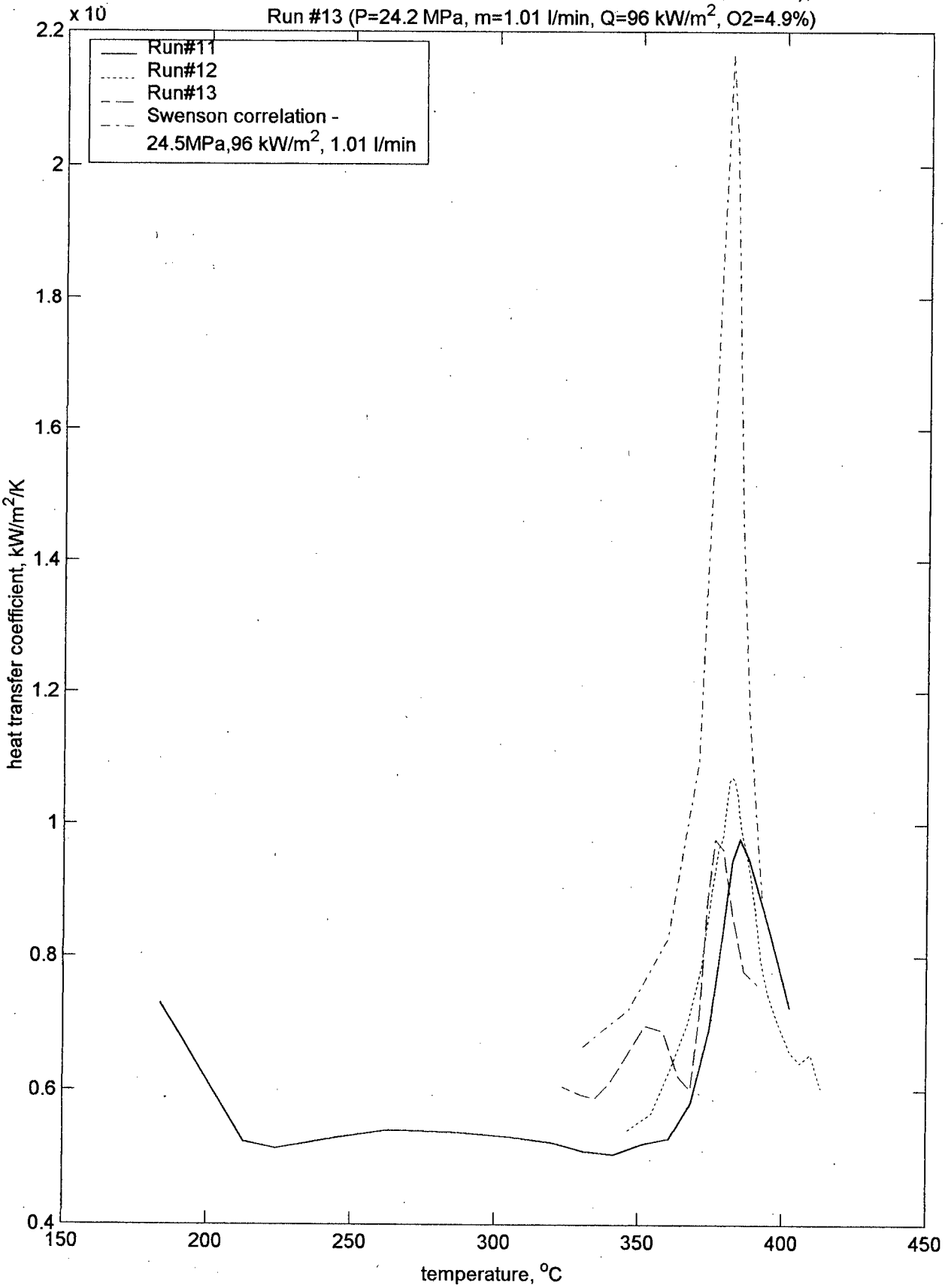

Figure 4.2c Heat transfer coefficient (top) for,
Run #11 (P=24.2 MPa, m=1.01 l/min, Q=93 kW/m^2, O2=0),
Run #12 (P=24.5 MPa, m=1.01 l/min, Q=97 kW/m^2, O2=2%),
Run #13 (P=24.2 MPa, m=1.01 l/min, Q=96 kW/m^2, O2=4.9%)

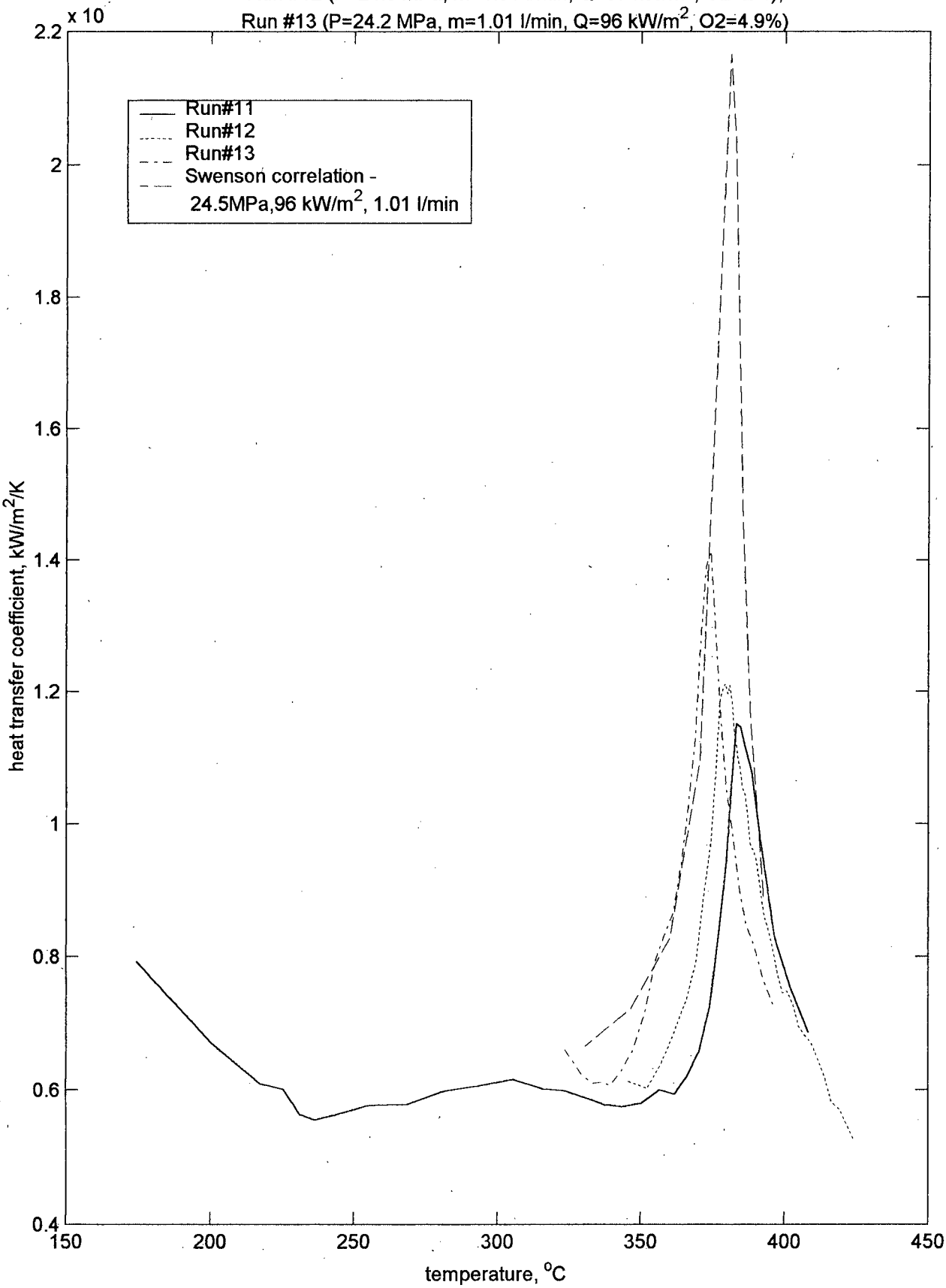

Figure 4.3a Heat transfer coefficient (bottom) for
Run #31 (P=25.3 MPa, m=1.01 l/min, Q=98 kW/m^2, O2=7.9%),
Run #32 (P=25.2 MPa, m=1.01 l/min, Q=160kW/m^2, O2=8%),
Run #33 (P=25.3 MPa, m=1.01 l/min, Q=37 kW/m^2, O2=7.6%)

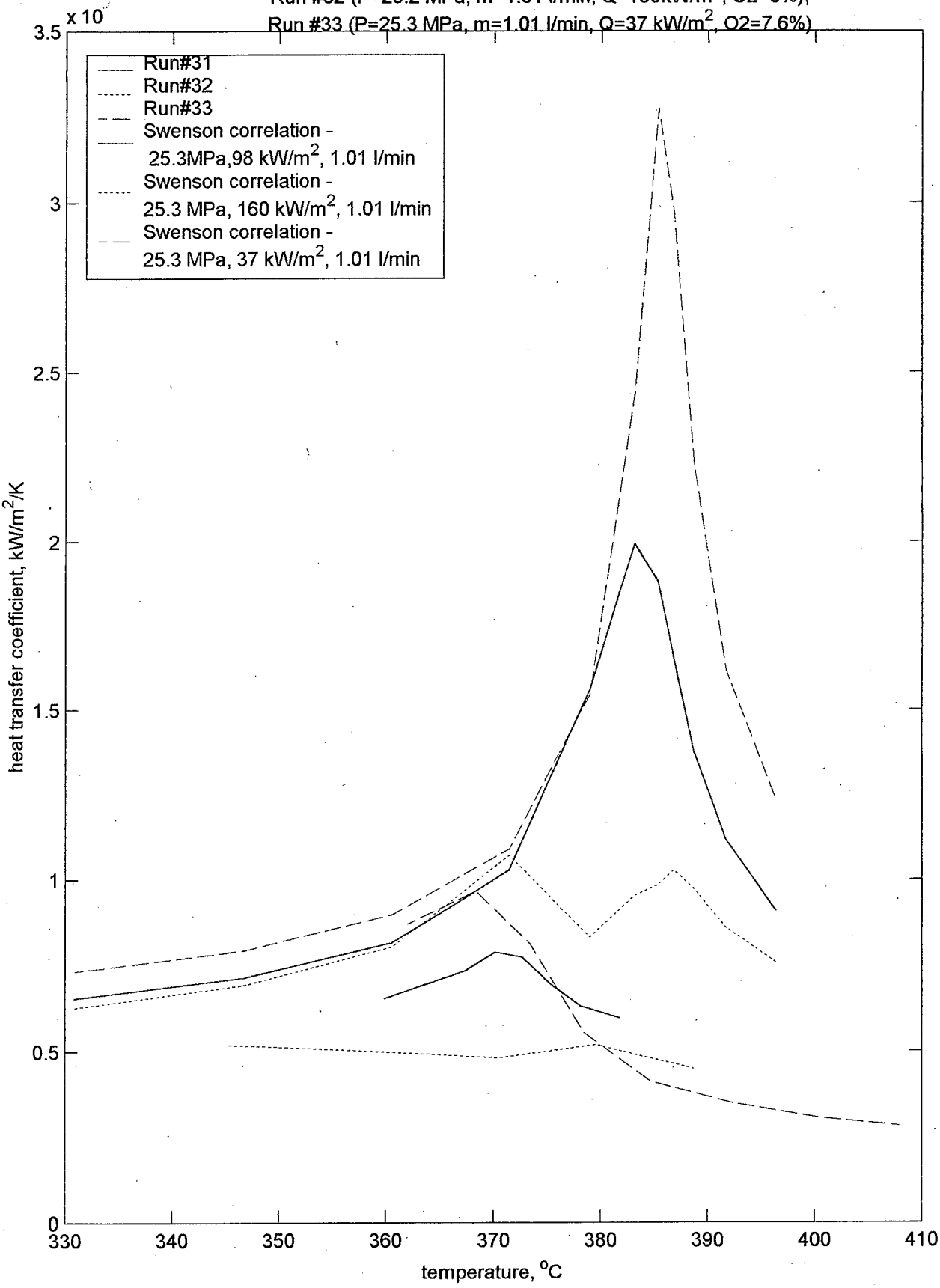

Figure 4.3b Heat transfer coefficient (top) for
Run #31 (P=25.3 MPa, m=1.01 l/min, Q=98 kW/m^2, O2=7.9%),
Run #32 (P=25.2 MPa, m=1.01 l/min, Q=160 kW/m^2, O2=8%),
Run #33 (P=25.3 MPa, m=1.01 l/min, Q=37 kW/m^2, O2=7.6%)

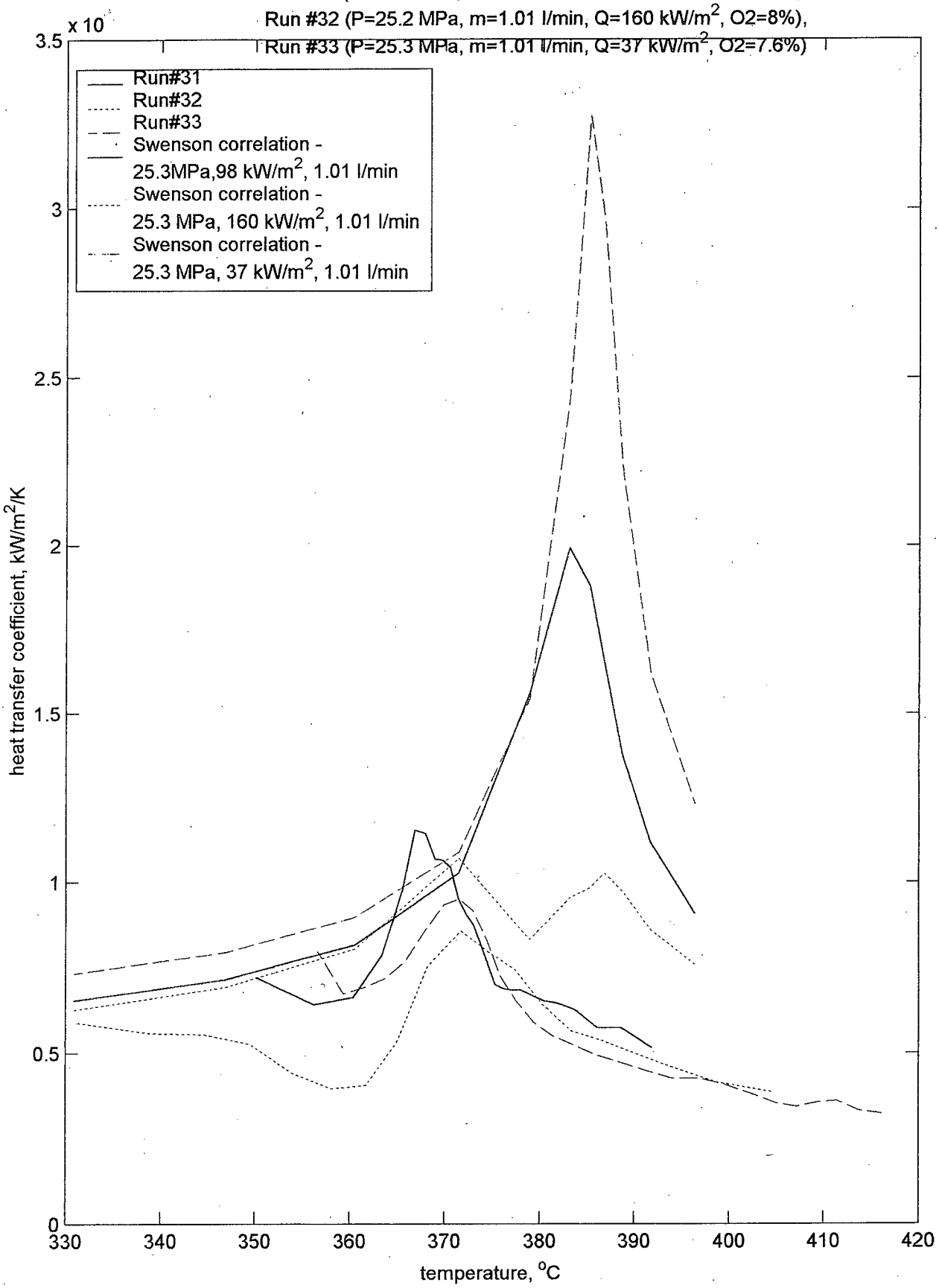

Figure 4.4a Heat transfer coefficient (bottom) for
Run #29 (P=25.1 MPa, m=1.27 l/min, Q=96 kW/m^2, O2=3%),
Run #30 (P=25.2 MPa, m=1.01 l/min, Q=95 kW/m^2, O2=3%)

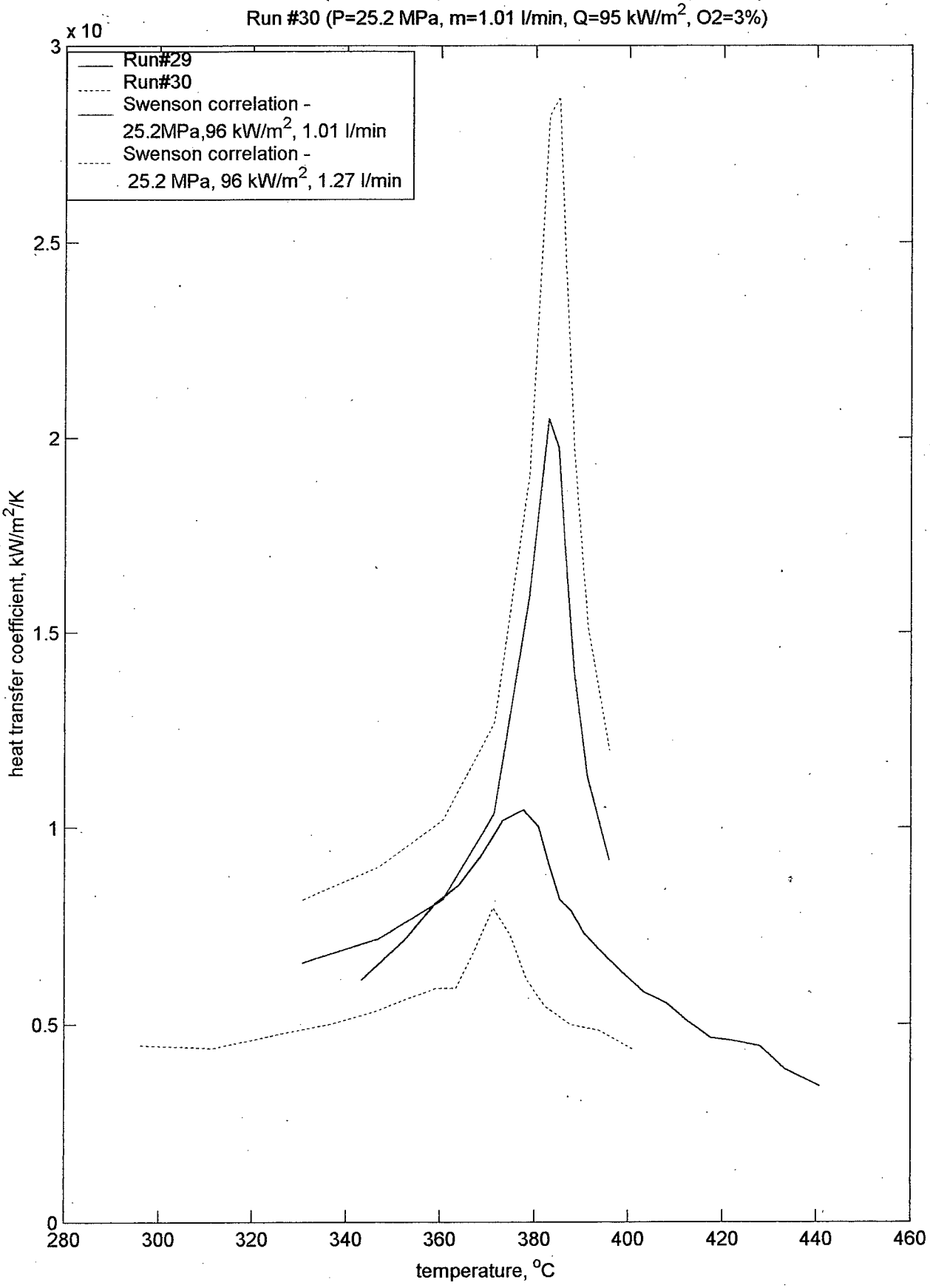

Figure 4.4b Heat transfer coefficient (top) for
Run #29 (P=25.1 MPa, m=1.27 l/min, Q=96 kW/m^2, O2=3%),
Run #30 (P=25.2 MPa, m=1.01 l/min, Q=95 kW/m^2, O2=3%)

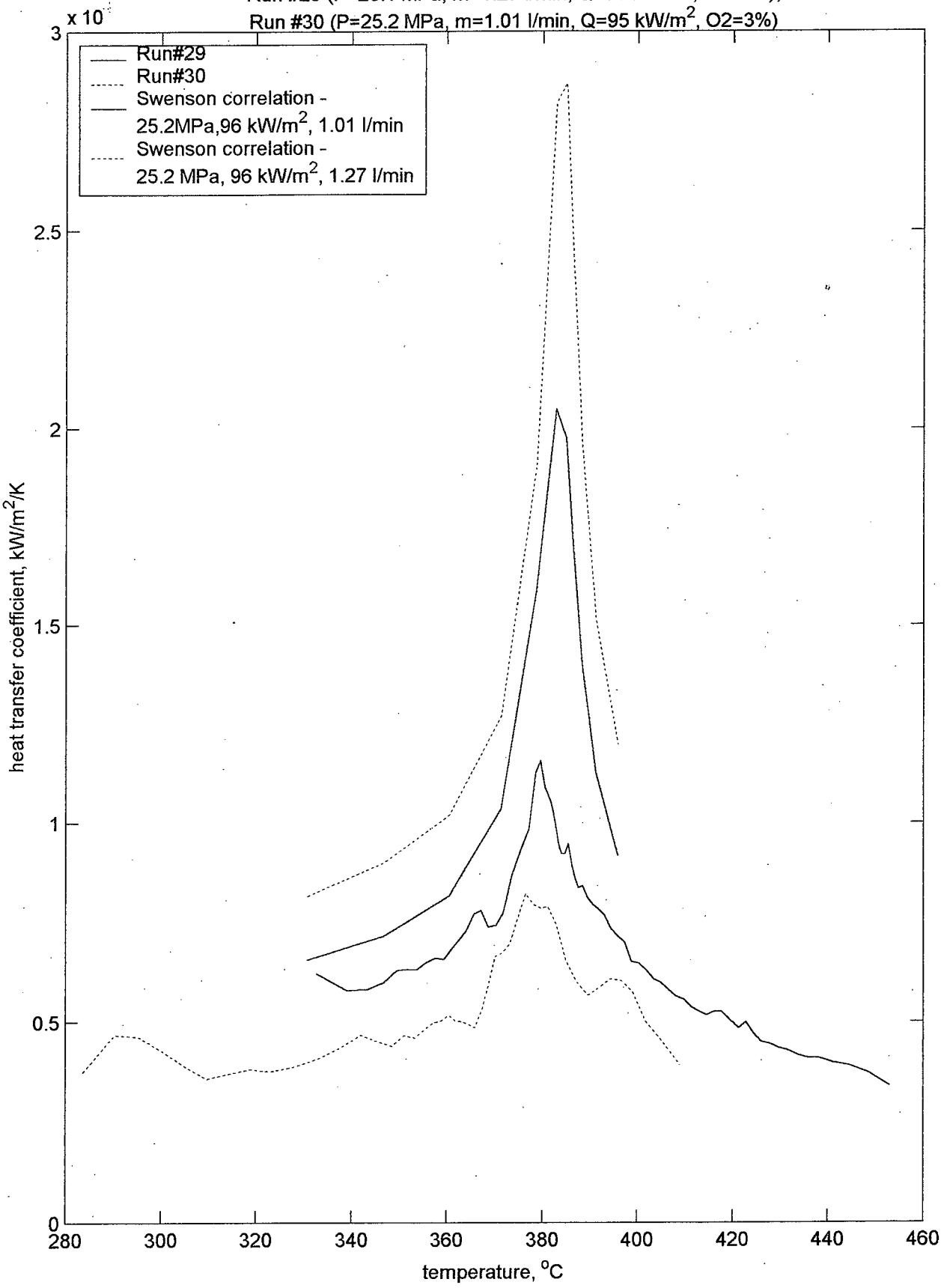

Figure 4.5 (Tpwo - Tpw) vs oxygen%

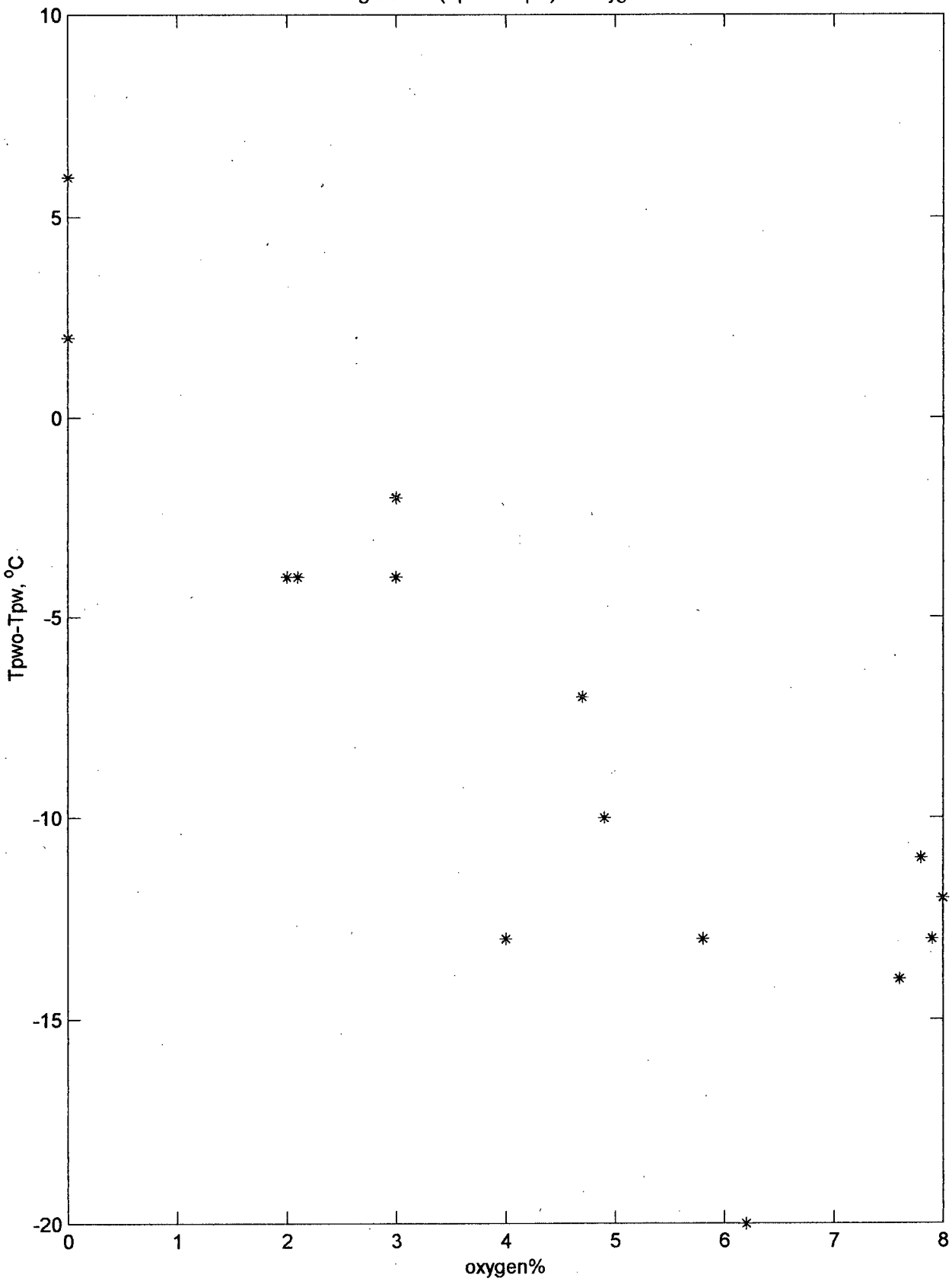

Figure 4.6 (Cpwo(P)/Cpw(P))max vs oxygen%

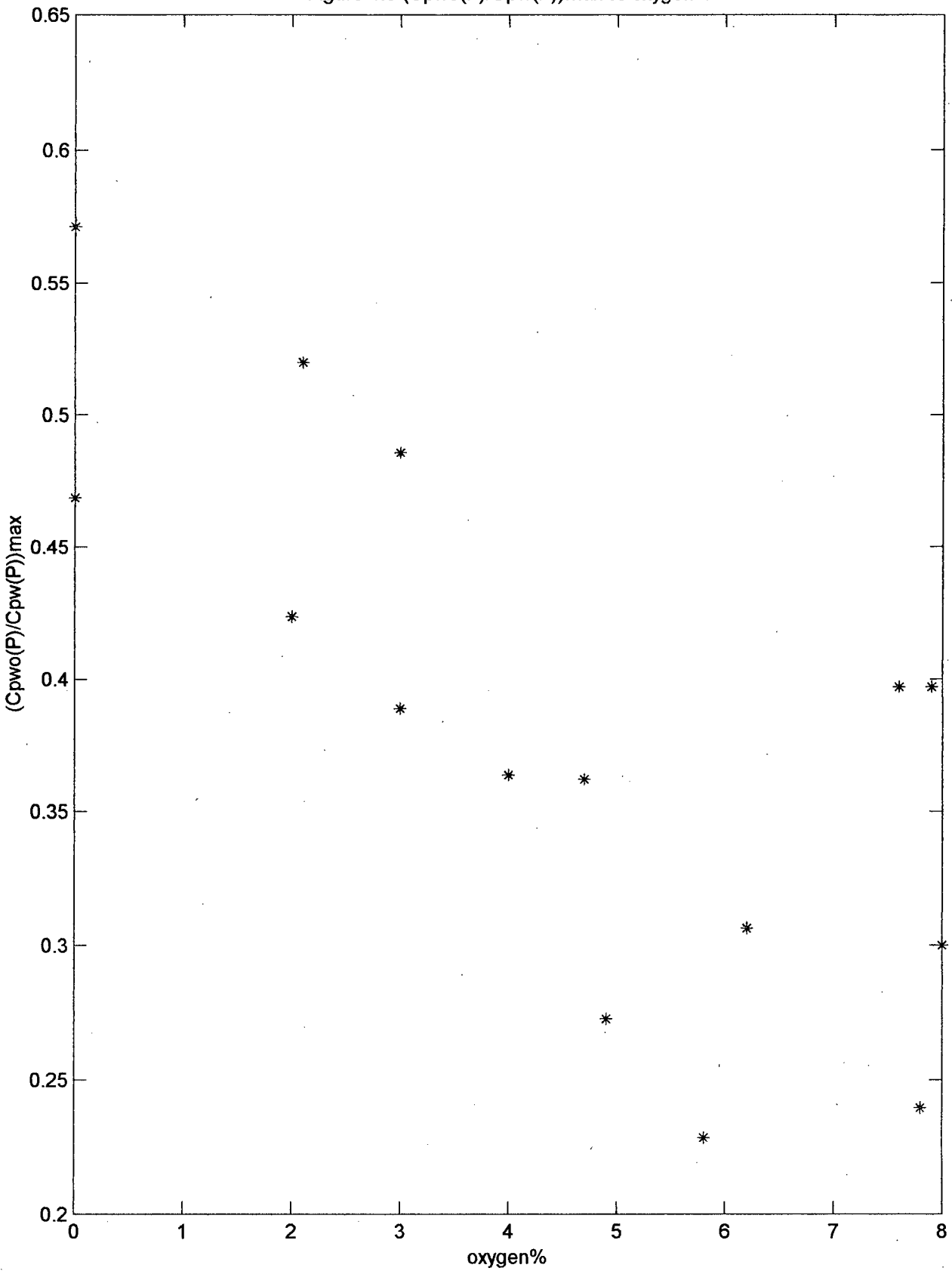

5. CONCLUSIONS

The constant-pressure heat capacity, C_p, and local forced convection heat transfer coefficient, h, for supercritical water-oxygen mixtures flowing inside horizontal smooth tubes were obtained experimentally. Data were obtained for pressures of 24 and 25 MPa; flow rates of 0.636 and 1.27 l/min, heat fluxes of 34 to 160 kW/m^2 and temperatures from 330 to 430 °C. Oxygen flow was 2 to 8 weight percentage of the total mixture flow. For a given flow and supplied heat to the mixture, C_p was determined from the bulk temperature in a heated tube. The heat transfer coefficient, h was determined from the difference in bulk and wall temperatures. Based on the measurement data it can be concluded:

1. As oxygen concentration increases heat capacity as well as heat transfer coefficient has a maximum at a lower bulk temperature
2. Introducing more oxygen reduces the magnitude of the heat capacity as well as for the heat transfer coefficient.
3. With increasing the pressure the maximum in the heat capacity and heat transfer coefficient are reduced and occur at higher temperatures.
4. The enhancement near the critical point appears to be less at high heat flux.
5. To develop any Nusselt number correlations, more accurate density measurements and an equation of state which would be suitable for thermodynamic and transport properties is needed.

6. RECOMMENDATIONS

The UBC/NORAM SCWO facility is capable of measuring the constant pressure heat capacity and heat transfer coefficient near the critical point for water-oxygen mixtures. However, during the course of this study it was shown that many improvements could be made to increase the accuracy of measurements.

Accuracy of the thermocouples should be checked for high temperature.

Accurate values of density are needed for the Nusselt number correlation.

The question of thermal conductivity and viscosity values for water-oxygen mixtures is open. Either a good measurement system or a suitable equation of state which will be able to predict those values with acceptable accuracy is needed.

REFERENCES

Bazargan, M., "Forced Convection Heat Transfer to Turbulent Flow of Supercritical Water in a Round Horizontal Tube", Ph.D. Thesis, UBC, September 2001.

Bourke, P.J., Pulling, D.J., Gill, L.E. and Denton, W.H., "Forced Convective Heat Transfer to Turbulent CO_2 in Supercritical Region", *Int. J. Heat Mass Transfer*, Vol 13, pp. 1339-1348, 1970.

Christoforakos, M. and Franck, E.U., "An Equation of State for Binary Fluid Mixtures to High Temperatures an High Pressure", *Ber. Bunsenges Phys. Chem.* Vol 90, pp. 780-788, 1986.

Croft, D.R and Lilley, D.G., *Heat Transfer Calculations Using Finite Difference Equations*, Applied Science Publishers, New York, 1977 .

Dusinberre, M.G., *Heat-Transfer Calculations by Finite Differences*, The Haddon Craftsmen Inc., New York, 1961.

Gairns, S. and Rogak, S., "UBC SCWO System Calibration Report", UBC Report, Feb. 16, 1999.

Hagen, D. K., *Heat Transfer with Applications*, Prentice-Hall Inc, London, 1999.

Hall, W.B., "Heat Transfer Near the Critical Point" in *Advances in Heat Transfer*, T.F. Irvine, Jr. and J.P. Hartnett, Eds. Academia Press, 1971.

Jackson, J.D. and Hall, W.B., "Forced Convection Heat Transfer to Fluids at Supercritical Pressure", *Turbulent Forced Convection in Channel and Bundles* , Vol 2, pp. 563 – 599, Hemisphere, New York, 1979.

Japas, M. L. and Franck, E.U., "High Pressure Equilibria and PVT-Data of the Water-Oxygen System Including Water-Air to 673 K and 250 MPa" *Ber. Bunsenges Phys. Chem.* Vol. 89, pp. 1286-1274, Munich, 1985.

Kakac, S and Yaman, *Y., Heat Conduction* , Hemisphere Publishing Corporation, New York,1985.

Kakac, S., "The Effect of Temperature-Dependent Fluid Properties on Convective Heat Transfer", in *Handbook of Single Phase Convective Heat Transfer*, S. Kakac, R.K. Shah and W. Aung eds., 1987.

Knapp, K.K. and Saberesky, R.H., "Free Convection Heat Transfer to Carbon Dioxide Near the Critical Point", *Int. J. Heat Mass Transfer*, Vol. 9, pp. 41-51, New York,1966.

Kondratev, N.S., "Heat Transfer and Hydraulic Resistance with Supercritical Water Flowing in Tubes", *Teploenergetika*, Vol. 16, No. 8, pp. 116-119, Moscow, 1967.

McCormick, M.J. and Salvadori, M.G.M., *Numerical Methods in Fortran*, Prentice-Hall Inc., London,1964.

Miropolski, L. and Shitsman, M.E., "Heat Transfer to Water and Steam at Variable Specific Heat (in Near-Critical Region), *Soviet Physics*, Vol 27, No. 10, pp. 2359 – 2372, Moscow, 1957.

Oh, C.H., Kochan, R.J. and Beller, J.M., "Numerical Analysis and Data Comparison of a Supercritical Water Oxidation Reactor", *J. AIChE*, Vol. 43, pp.1672-1636, New York, 1997.

Oka, Y., Koshizuka, S. Jevremovic, T. and Okano, Y, "System Design of Direct-Cycle Supercritical Water Cooled Fast Reactors", *Nuclear Technology*, Vol. 109, pp. 1-10, Jan. 1995.

Petukhov, B.S., Polyakov, A.F., Kuleshohov, V.A. and Sheckter, Y.L., "Turbulent Flow and Heat Transfer in Horizontal Tubes with Substantial Influence of Thermo-Gravitational Forces", in *Proc. 5th Int. Heat Transfer Conf.*, Tokyo, Paper No. NC4.8. A.S.M.E., 1974.

Pitla, S.S., Robinson, D.M., Groll, E.A. and Ramadhyani, S., "Heat Transfer from Supercritical Carbon Dioxide in Tube Flow: A Critical Review", *HVAC&R Research,* Vol 4 No. 3, pp 281, 1898.

Polyakov, A.F., "Heat Transfer under Supercritical pressures", *Advances in Heat Transfer,* Vol 21, pp. 2-51, 1991.

Robert R.C., Prausnitz J. M. and Poling E. B., The Properties of Gases and Liquids, McGraw-Hill, Inc., New York, 1980.

Rogak, S.N. and Teshima, P., "Deposition of Sodium Sulfate in Heated Flow of Supercritical Water", *AIChe Journal,* Vol 45, No. 2, February 1999.

Rogak, S., "Measurements of the Constant-Pressure Heat Capacity of Water-Oxygen Mixtures at Near-Critical Conditions" , *Proc. Of the 13th International Conference on the Properties of Water and Steam,* P.R. Tremaine, P.G. Hill, D.E. Irish and P.V. Balakrishnan, Eds. NRC Research Press, 149-156, 2000.

Sabaresky, R.H. and Hauptmann, E.G., "Forced Convection Heat Transfer to Carbon Dioxide Near the Critical Point", *Int. J. Heat Mass Transfer*, Vol. 10, pp. 1499-1508, 1967.

Saur, A.M., Behrendt, F. and Franck, E. U., "Calculation of High Pressure Counterflow Diffusion Flames up to 3000 bar", *Ber. Bunsenges Phys. Chem.*, Vol. 97, pp. 900-908, 1993.

Shaw, R.W., Brill, T.B., Clifford, A.A., Eckert, C.A. and Franck, E.U., "Supercritical Water, A Medium for Chemistry" ,*C&EN* pp. 26-39, December 1991.

Swenson, H.S., Carver, J.R. and Kakarla, C.R., "Heat Transfer to Supercritical Water in Smooth-Bore Tubes", *J. Heat Transfer*, pp. 477-484, Nov. 1965.

Teshima P., "Fouling Rates from a Sodium Sulphate – Water Solution in Supercritical Water Oxidation Reactors", M.Sc. Thesis, UBC, October 1997.

Van Wylen, G., Sonntag, R. and Borgnakke, C., *Fundamentals of Classical Thermodynamics*, John Wiley & Sons, New York, 1994.

Vargaftik, N.B., *Tables on The Thermophysical Properties of Liquids and Gases*, Hemisphere Publishing Corporation, Washington, 1975.

Wang, S., "Properties of Supercritical Water-Oxygen Mixtures", M.Sc. Thesis, UBC, September 2001.

Yamagata, K, Nishikawa, K., Hasegawa, S., Fyjii, T. and Yoshida, T., "Forced Convective Heat Transfer to Supercritical Water Flowing in Tubes", *Int. J. Heat Mass Transfer*, Vol. 15, pp. 2575-2593, 1972.

APPENDIX A Test Section 1-D Transient Heat Loss Model in Cylindrical Polar Coordinates

Introduction

The constant pressure heat capacity of a fluid (C_p) can be measured in a flow system, knowing the applied heat flux (q), the mass flux (m), and the bulk temperature difference (ΔT_b) of the flow.

$$C_p = \frac{q}{m\Delta T_b} \tag{A1}$$

The heat flux is primarily a function of applied voltage, but also depends on steady and transient heat losses to the tubing, fittings, insulation and surroundings. This Appendix describes the methods used to determine these heat losses.

The first component of the thermal model is a one-dimensional transient heat loss model, which uses measured tube wall temperatures as a boundary condition. This model is shown to reproduce transient heat fluxes quite well.

The second component is a model to predict the electrical power dissipated in the tube and transferred to the flow and the losses mentioned above.

Finally, a method for using these models in the heat capacity measurements is described.

Heat Loss Model

The heat losses were calculated applying an unsteady, one-dimensional, heat transfer model. Treating the heat transfer as one-dimensional is reasonable because of the nature of the heat penetration into the insulation and the ratio of the test section and the insulation dimensions.

As mentioned above the configuration of the test section and the insulation around it was considered as a 1-D cylindrical polar coordinate problem (shown in Fig. A1b) in which the heat transfer in the z and θ direction are insignificant. The insulation width W is 0.07125 m and the tube diameter r_{in} is 0.00475 m.

The first law of thermodynamics was applied to control volumes 1 (the insulation) and 2 (the test section pipe and fittings).

For control volume 1,

$$\frac{dE_{cv_1}}{dt} = \iiint_{V_1} \frac{dT}{dt} C_p \rho dV = \oiint_{S_1} q dA = A_{in} q_{in} - A_{out} q_{out} \qquad \text{(A2)}$$

Where:

dE_{cv1}/dt – derivative of energy for the insulation, kJ/s

C_p – insulation constant pressure heat capacity, kJ/kgK

ρ – insulation density, kg/m^3

V – insulation volume, m^3

q_{in} - inlet heat flux, kJ/ m^2

q_{out} - outlet heat flux, kJ/ m^2

A_{in} – insulation inlet area m^2

A_{out} – insulation outlet area m^2

For control volume 2 for the test section without electrical heating,

$$\frac{dE_{cv_2}}{dt} = \iiint_{V_2} \frac{dT}{dt} \rho C_p dV = -A_{in} q_{in} + mC_{p_w}(T_{bin} - T_{bout}) \qquad \text{(A3)}$$

Where:

dE_{cv2}/dt –derivative of energy for the test section, the fittings and the working fluid, kJ/s

C_p – test section, the fittings and working fluid constant pressure heat capacity, kJ/kgK

A_{in} – test section outlet area which is equal to the insulation inlet area, m^2

q_{in} - outlet heat flux which is equal to inlet flux for the insulation, kJ/ m^2

m – working fluid mass flux, kg/s

C_{pw} – working fluid constant pressure heat capacity, kJ/kgK

T_{bin} – inlet bulk temperature, °C

T_{out} – outlet bulk temperature, °C

From the Eq. A3 the heat losses are calculated as:

$$mC_{pw}(T_{bin} - T_{bout}) = Q_{losses} = \iiint_{V_2} \frac{dT}{dt} C_p dV + A_{in} q_{in} \qquad \text{(A4)}$$

The second part on the right side of the Eq. A3 was evaluated using the experimental data for the input and the output bulk temperature.

Assuming that C_p and ρ for the test section are constant, the integral on the right side of the Eq. A4 is written:

$$Cp_{tube}\rho_{tube}\iiint_{V_{tube}}\frac{dT}{dt}dV+\iiint_{V_{water}}Cp_{water}\rho_{water}\frac{dT}{dt}dV \qquad \text{(A5)}$$

The last term in Eq. A5 is neglected in the model, because the mass of the tube is much greater than the mass of the water.

C_{pw} from Equation A4 was calculated for a pressure of 25 MPa using the Steam Tables (Van Wylen *et al.*, 1994).

Evaluation of q_{in} in equations (A2) and (A3) require a transient thermal analyses of the insulation.

The energy balance for the small control volume (control cell) (Figure A2.) was obtained by Eq.A2. The relevant partial differential equation for the 1-D Transient heat transfer is:

$$k\left(\frac{\partial^2 T}{\partial r^2}+\frac{1}{r}\frac{\partial T}{\partial r}\right)=\rho Cp\frac{\partial T}{\partial t} \qquad \text{(A6)}$$

The appropriate finite differential equation for the computing cell shown on Figure A2 is

$$k\left[\frac{T_2 - 2T_1 + T_w}{(\Delta r)^2} + \frac{1}{r_1}\frac{(T_2 - T_W)}{2\Delta r}\right] = \rho Cp\frac{(T_1' - T_1)}{\Delta t} \qquad \text{(A7)}$$

for node 1, and similar expressions for each of the other nodes, except the last node and the node 0. The space step was chosen very small (0.0032m). The last node is obtained by applying the convective boundary condition.

In terms of the Fourier number Fo, where

$$Fo = \alpha\frac{\Delta t}{(\Delta r)^2} = \frac{k}{\rho Cp}\frac{\Delta t}{(\Delta r)^2}$$

equation (A7) becomes

$$T_i' = Fo\left[\left(1 - \frac{\Delta r}{2(r_0 + i\Delta r)}\right)T_{i-1} + \left(\frac{1}{Fo} - 2\right)T_i + \left(1 + \frac{\Delta r}{2(r_0 + i\Delta r)}\right)T_{i+1}\right] \qquad \text{(A8)}$$

Over a small time interval Δt, the energy balance method gives the following equation for the boundary node :

$$\rho C_p \Delta r\frac{\Delta T_n}{\Delta t} = \frac{k}{\Delta r}(T_{n-1} - T_n) + h(T_\infty - T_n) \qquad \text{(A9)}$$

where n is the number of nodes.

Eq. A9 can be rearranged and expressed in the explicit form

$$T_n' = Fo\left[T_{n-1} + BiT_\infty + T_n\left(\frac{1}{Fo} - Bi - 1\right)\right] \qquad \text{(A10)}$$

where

$$Fo = \frac{k\Delta t}{\rho Cp(\Delta r)^2}$$

and

$$B_i = \frac{h\Delta r}{k}$$

For stability there is a restriction on the value of Fo and from Eqs. (A8) and (A10) the criteria are (Croft *et al.*, 1977):

$$\frac{2}{Fo} - 4 \geq 0 \qquad \text{(interior nodes)}$$
$$Fo \leq 0.5$$

(A11)

$$\frac{1}{Fo} - 1 - Bi \geq 0 \qquad \text{(boundary nodes)}$$
$$Fo \leq \frac{1}{2(1+Bi)}$$

Ambient temperature was 20 °C and the heat transfer coefficient for the surrounding air was assumed to be 7 W/m^{2}K. The left boundary condition was wall

temperature, which was measured. The heat losses were calculated for a 3.00 m long test section.

Figure A3 shows the heat loss as a function of the different time steps and the same thermal conductivity coefficient 0.35 W/mK, density 480 kg/m^3 , specific heat 710 J/kgK and radial step 0.0032 m. The losses are almost independent of the time step.
The heat losses predicted by the model have the same trend as has the experimental ones (Figures A6, A7 and A8). Figure A4 shows the heat losses for two different insulation densities (480 and 600 kg/m^3) and thermal conductivity coefficient 0.5 W/mK. With increasing density, the heat losses increased.

Figure A5 shows the effect of different assumed values of insulation thermal conductivity. It is clear that heat losses increased with an increase in the thermal conductivity.

The model with thermal conductivity 0.35 W/mK predicts the heat losses fairly well (Fig.A6). The presented experimental data are for the slow heating case with average heating rate of about 0.3 °C/s and a flow rate 0.636 kg/min. The agreement between model and experiment is acceptable in the temperature range below the critical temperature. When $T<T_C$ the difference is about 0.3 kW.

An experiment was done also for the cooling case with an average cooling rate of 0.23 °C/s and a flow rate 0.636 kg/min and with cooling rate 0.25 °C/s and flow rate 1.269 kg/min. Figures A7 and A8 present the model prediction and the experimental values. The agreement is acceptable for all of the temperature range including the critical temperature.

Electrical Power Dissipation Model

The heat flux supplied to the working fluid was calculated by subtracting heat losses from the power supplied to the test section. The power supplied to the test section was calculated using the data from the calibration test (UBC SCWO System Calibration Review, pp 14) and resistivity as a function of wall temperature. Figure A9 shows the resistivity as function of wall temperatures. Figure A10 shows the correlation between the SCR voltages and R.M.S. voltages. The correlations for the resistivity and voltages are:

$$\rho = \left(10^{-9}T_w^3 - 10^{-6}T_w^2 + 0.0004T_w + 1.288\right) * 10^{-6}, \text{ ohms*m} \qquad \text{(A12)}$$

$$\text{RMS voltage} = 0.0491\text{CRvoltage} - 1.2564, \text{ volt} \qquad \text{(A13)}$$

Power was calculated from:

$$Q_{elec} = V^2 / R$$
$$R = \rho l / A \qquad \text{(A14)}$$

where R is resistivity in ohms and A is area:

$$A = \pi\left(R_0^2 - R_i^2\right) = 3.14(0.0048^2 - 0.003137^2) = 41.486 \text{ mm}^2$$

$l = 1.473$ m

Where R_o and R_i are the outside and the inside tube radius respectively.

The heat supplied to the working fluid was obtained from:

$$Q_f = Q_{elec} - Q_{losses} \tag{A15}$$

The Evaluation of the Power Dissipation Model:

Pure water measurements were used to evaluate the power dissipation model. Heat flux supplied to the working fluid was calculated using:

$$Q_f = mC_p\,(T_{bout} - T_{bin}) \tag{A16}$$

For the constant pressure heat capacity values from the steam tables were used (Van Wylen et al., 1994).

Figure A11 shows the heat supplied to the first part of the test section for the measurements and for the model. The predictions of the model are acceptable.

This model was used to predict the heat supplied to the working fluid in the case when the working fluid was a water-oxygen mixture. Figure A12 shows C_p as a function of temperature. The experiment was done for a 2% O_2 weight concentration, water flow rate = 1kg/min and pressure = 25 MPa (Run#17). C_p was calculated in two different ways:

- applying the present model and
- assuming constant heat flux

The constant heat flux assumption is acceptable. This agreement occurred when the heating rate was about 0.1 °C/s.

Figure A13 shows C_p for 5% O_2 by weight, water flow rate = 1kg/min and pressure = 23.9 MPa (Run #13). The heating rate was the same as in the previous case 0.1 °C/s. The constant heat flux assumption is acceptable for heating rate in the range 0.1 – 0.3 °C/s. This conclusion was used for the heating strategy in the experiments.

Electric power has to be corrected by a factor F. Factor F was found from a low temperature, low flow rate test for pure water. Under these conditions the temperature difference is large, losses are low and the heat capacity is well known.

$$mCp\Delta T = F\frac{V^2}{R}$$
$$F = \frac{mCp\Delta TR}{V^2} \qquad \text{(A17)}$$

Table A1 shows values for the coefficient F for Runs 36, 37 and 38. For the calculations F equals 0.789 was used. Temperature does not have significant effect on the coefficient F (Figure A14 and A 15).

Table A1. Value of coefficient F for Runs 36,37 and 38

Run#	mass flow, l/min	Heat flux, V	bulk temperature interval, C		average coefficient F = mCpΔT/(V^2/R(T))	
			TS1	TS2	TS2	TS1
36	1.068	300	162-165	180-183	0.845	0.799
37	1.068	300	185-208	227-246	0.795	0.764
38	1.068	300	223-301	253-331	0.785	0.742
			Average value		**0.81**	**0.768**

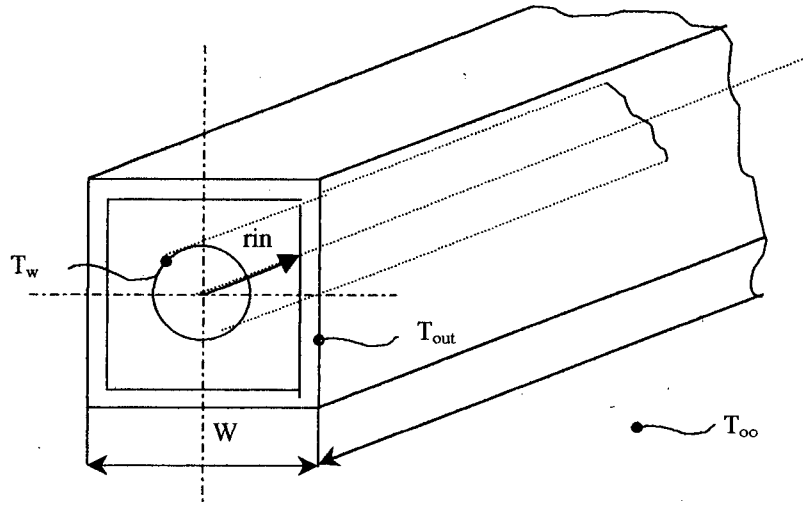

Figure A1. (a) Test section with insulation – real configuration

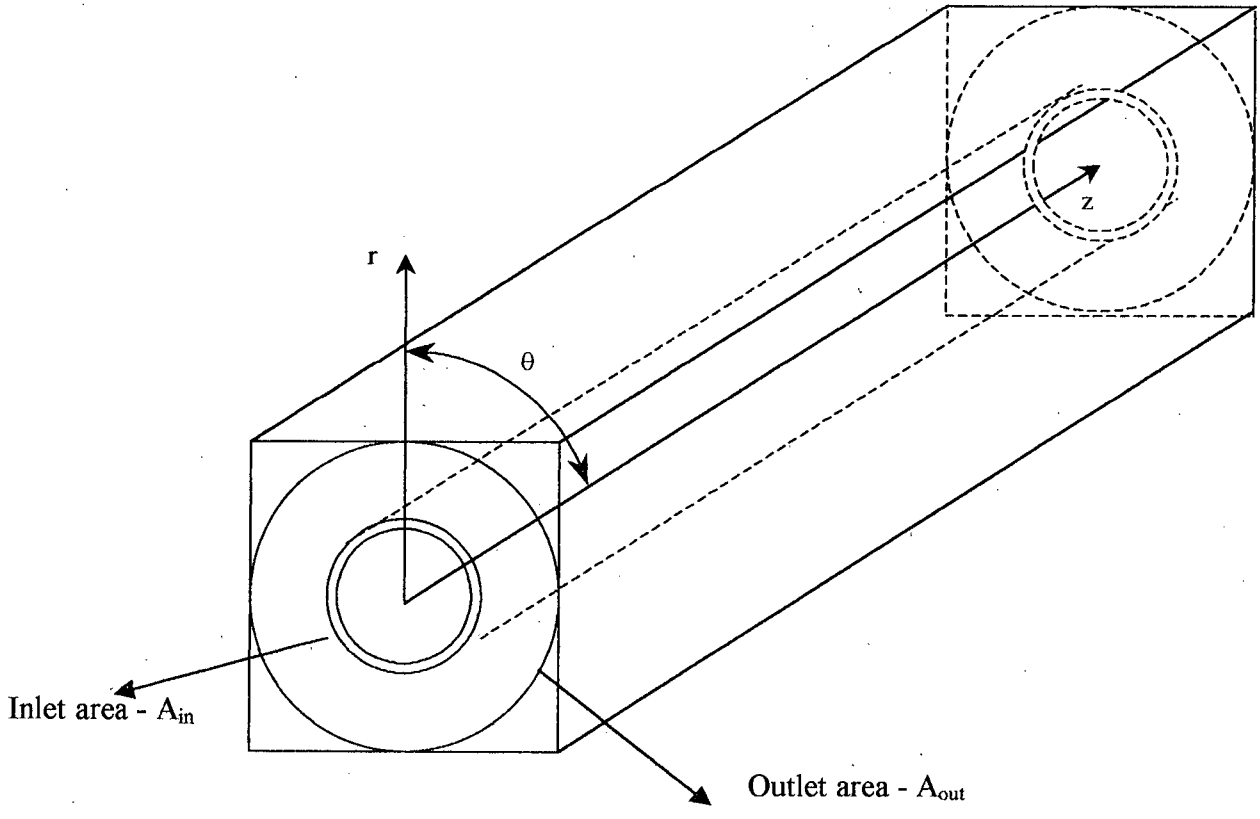

Figure A1. (b) Insulation – control volume V_1

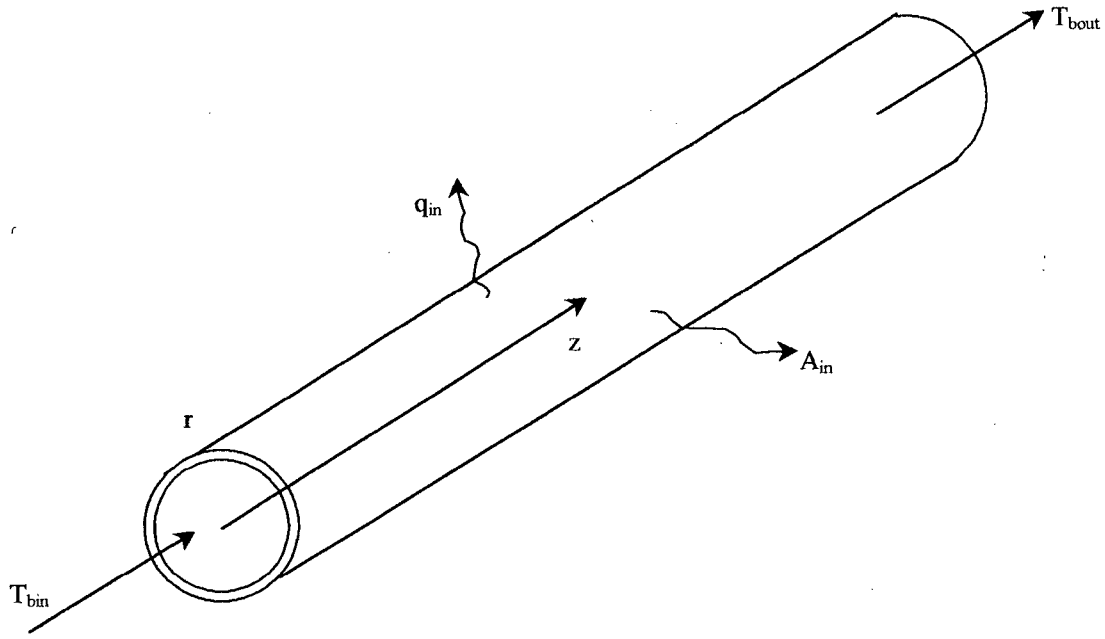

Figure A1. (c) Test section tube – control volume V_2

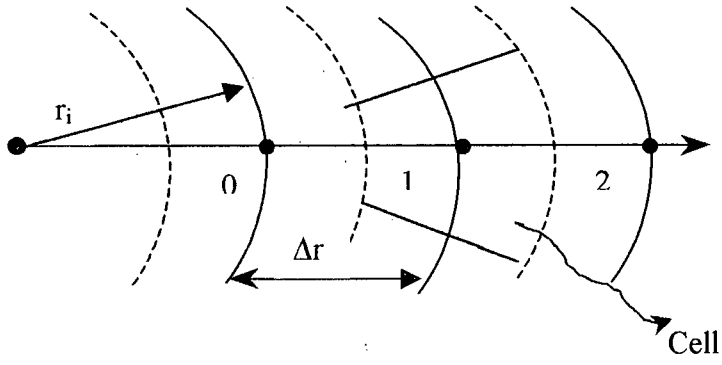

Figure A2. Computing cell

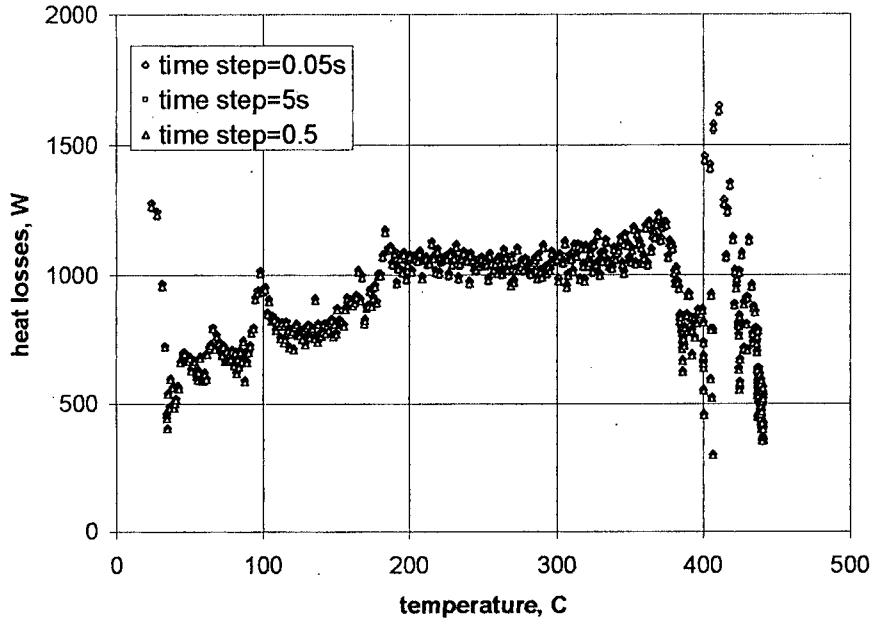

Figure A3. Heat losses as a function of time step for assumed insulation density of 480 kg/m^3, conductivity 0.35 W/m, Run #19

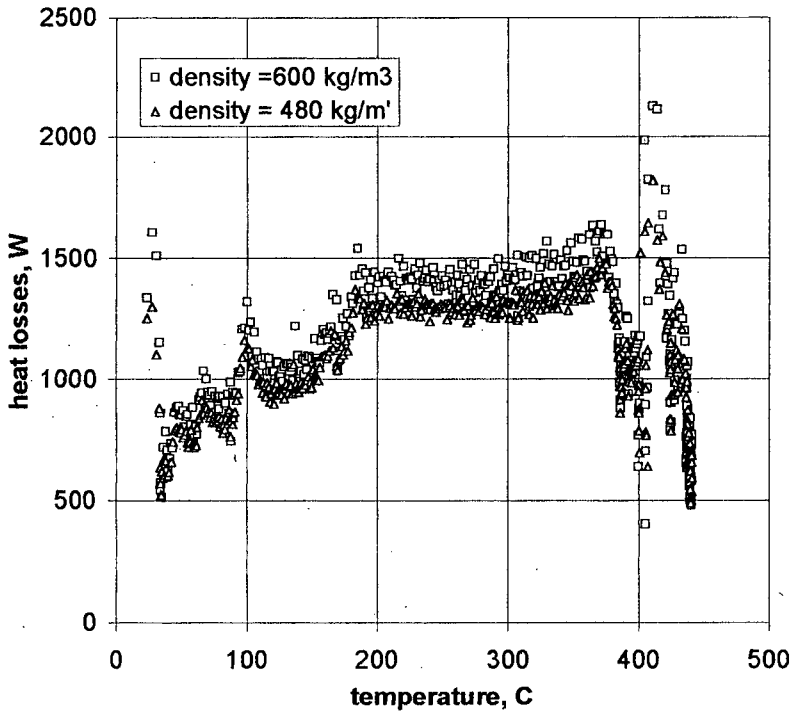

Figure A4. Heat losses as a function of density for assumed insulation conductivity 0.5 W/mK, Run #19

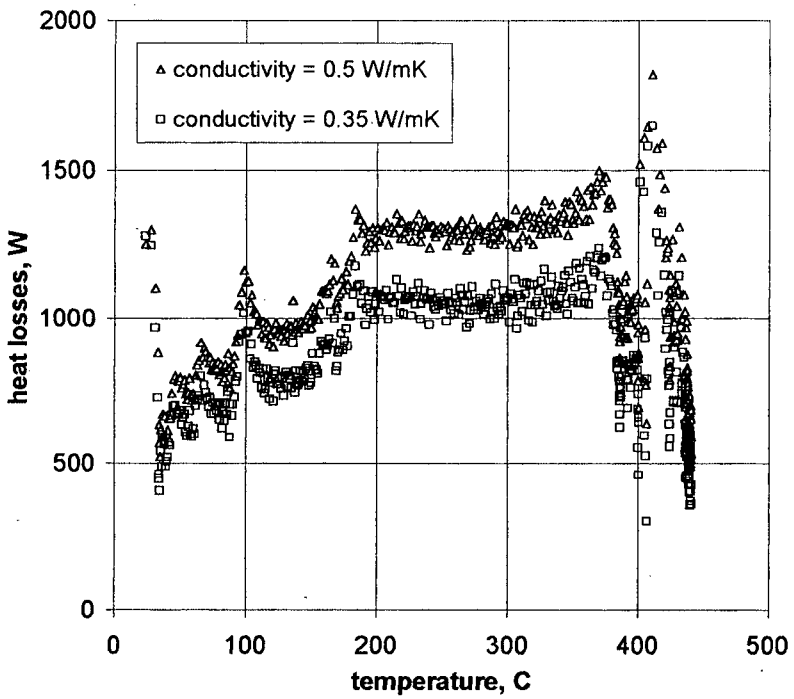

Figure A5. Heat losses as a function of thermal conductivity for assumed density 480 kg/m^3, Run #19

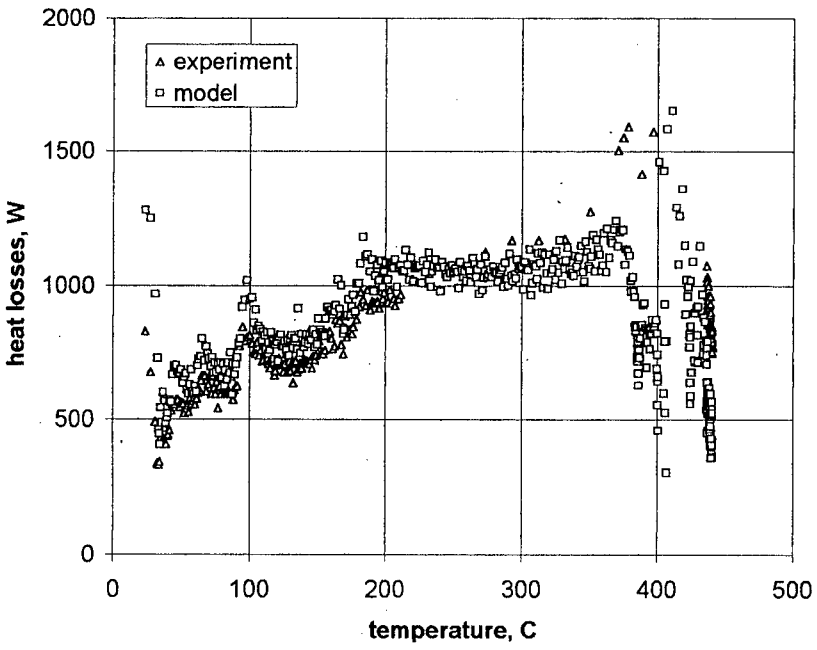

Figure A6. Heat losses as a function of a wall temperature, Run #19

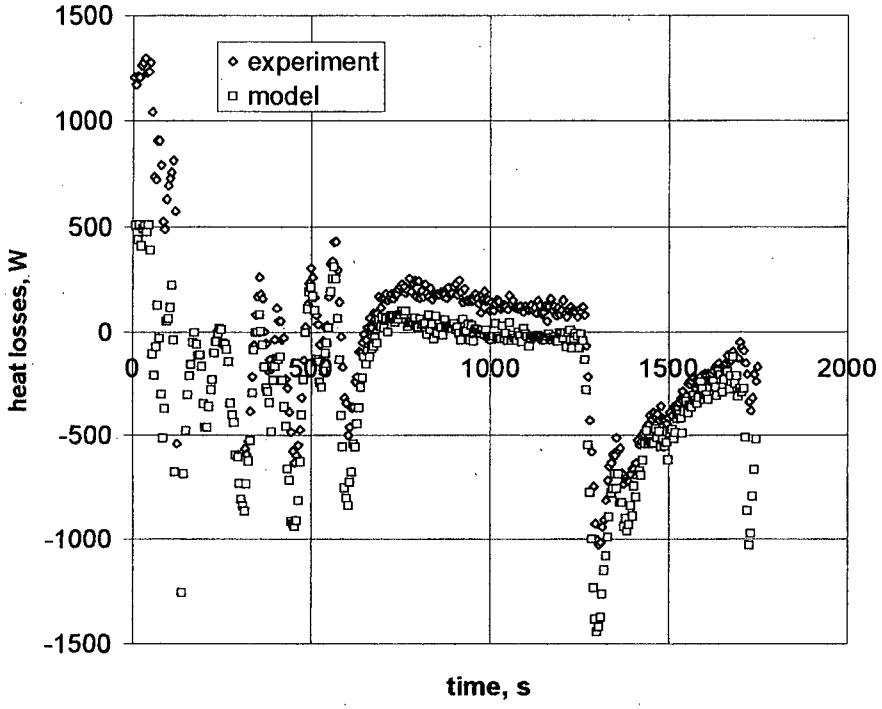

Figure A7. Heat losses for assumed insulation density 480 kg/m^3 and conductivity 0.35 W/mK and for the experiment with flow rate 0.636 kg/min, Run #21

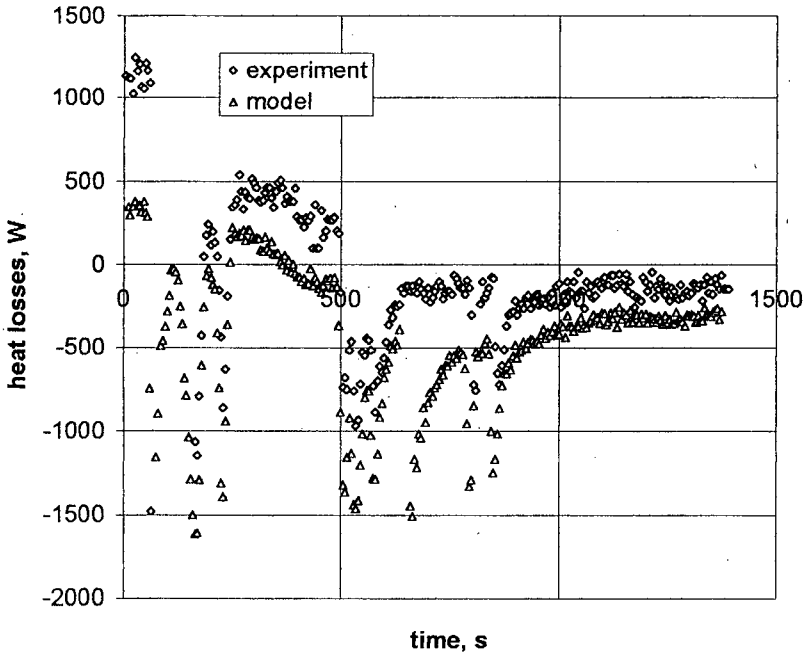

Figure A8. Heat losses for assumed insulation density 480 kg/m^3 and conductivity 0.35 W/mK and for the experiment with flow rate 1.296 kg/min, Run #21

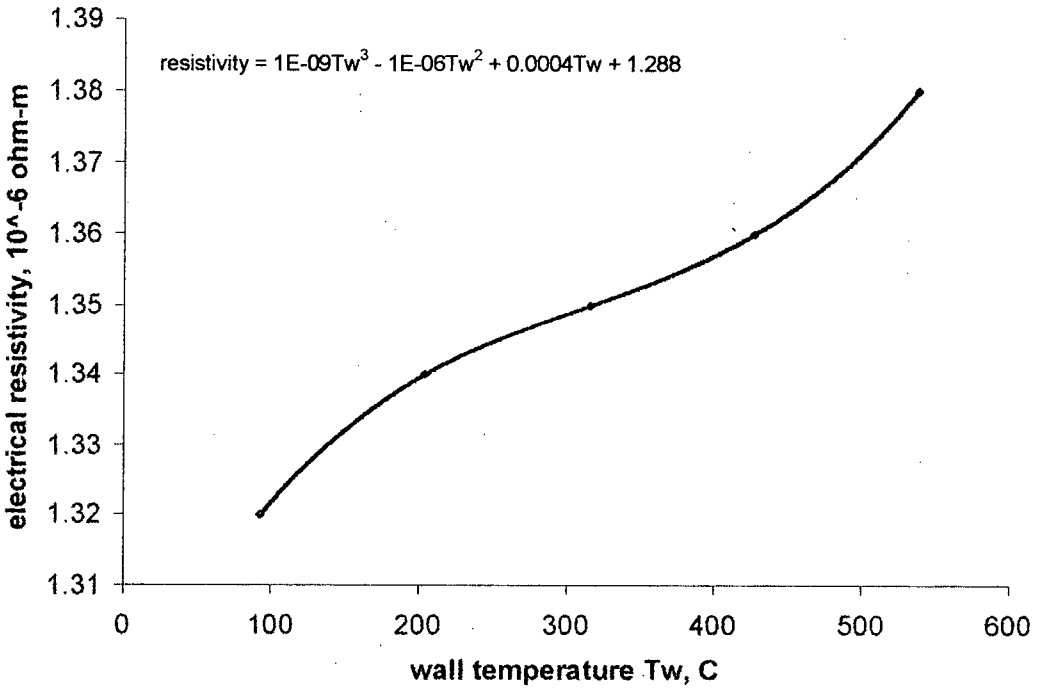

Figure A9. Resistivity as a function of the wall temperature

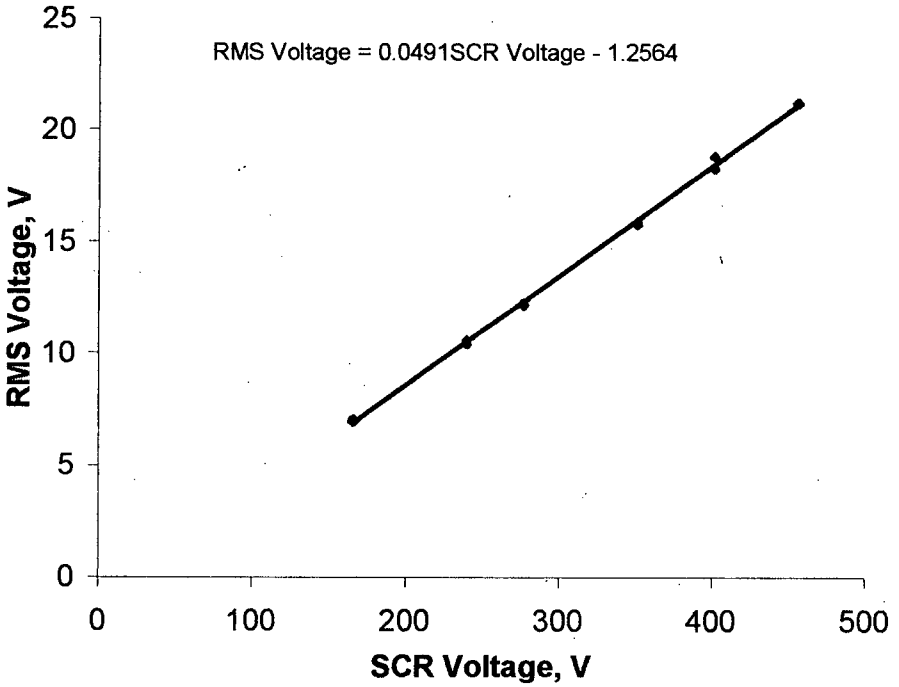

Figure A10. RMS voltage as à function of SCR voltage panel reading

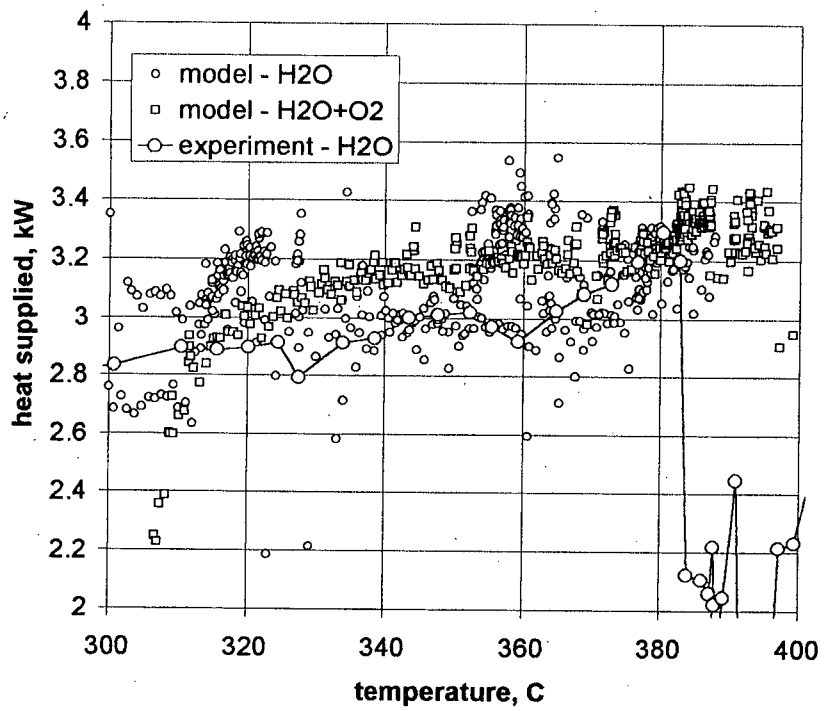

Figure A11. Heat supplied to the working fluid for the model and the experiment, Run #19 (P = 24.5 MPa, m = 0.636 l/min)

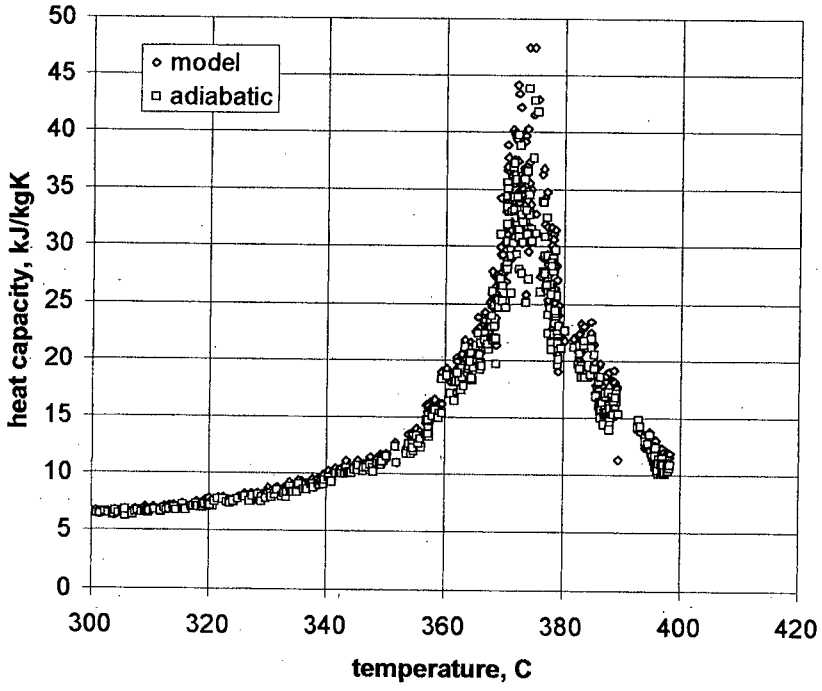

Figure A12. Heat capacity for water-oxygen mixture – Run #17 (P = 25.4 MPa, m = 1.05 l/min, Q = 95 kW/m^2, O2 = 4%)

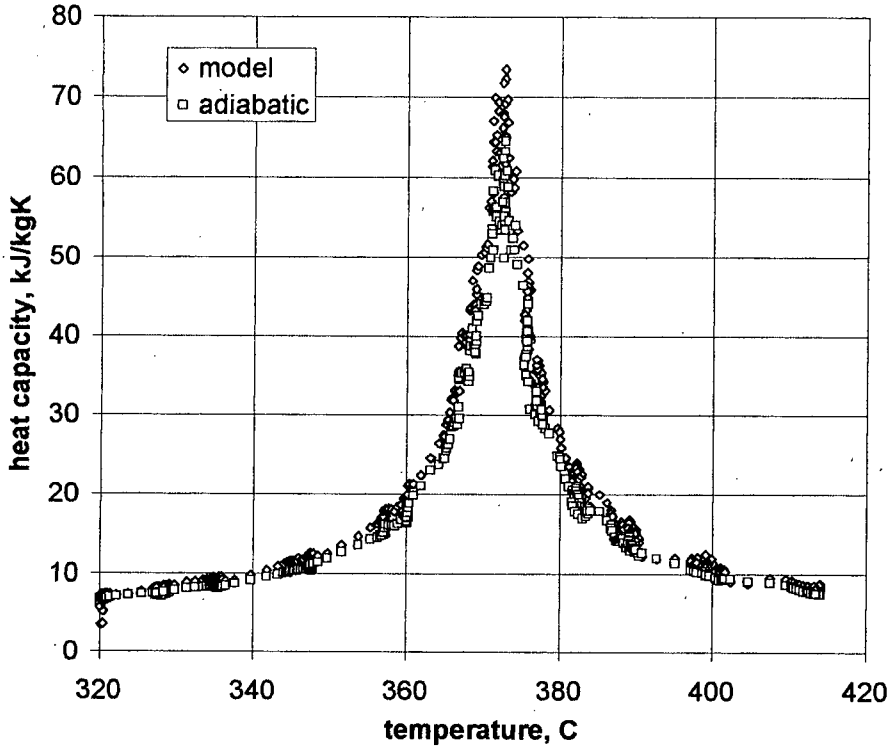

Figure A13. Heat capacity for water-oxygen mixture –Run #13 (P =24.2 MPa, m = 1.01 l/min, Q = 96 kW/m^2, O2 = 4.9%)

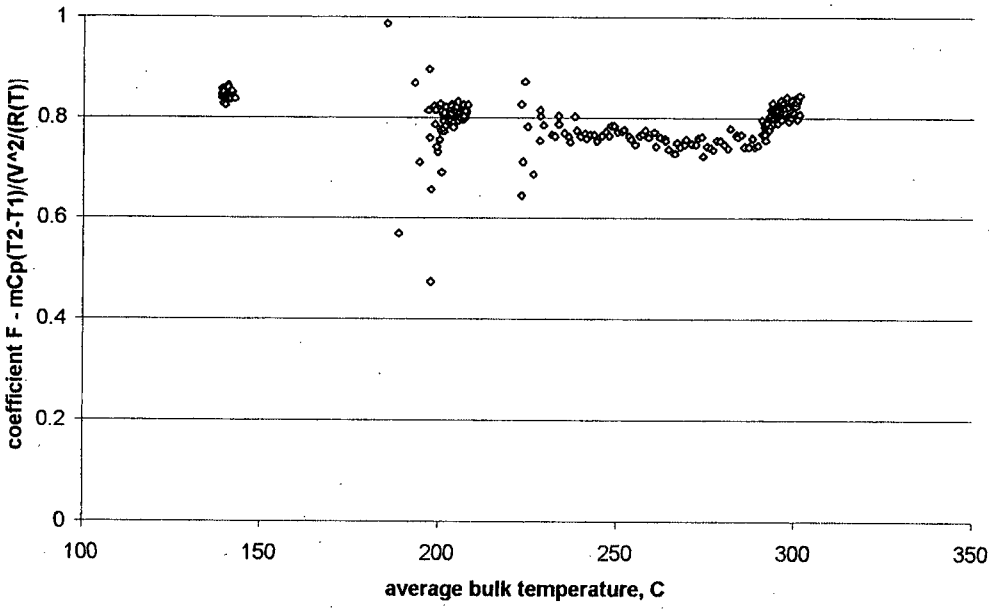

Figure A14 Coefficient F as a function of bulk temperature for part 1 of test section and Run # 36 - 38

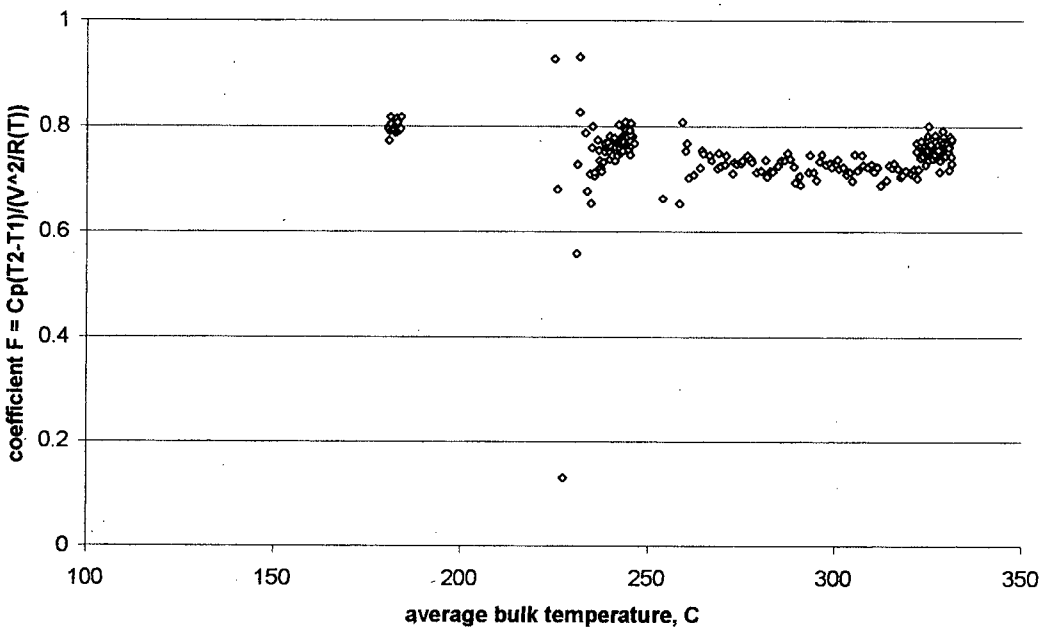

Figure A14 Coefficient F as a function of bulk temperature for part 2 of test section and Run # 36 - 38

APPENDIX B Thermodynamic and transport properties

A complete set of thermodynamic properties for supercritical water-oxygen mixtures is not available in the literature. From data provided by Christoforakos and Franck (1986), phase equilibria were calculated and P-V-T-x relations for water-oxygen developed. They developed an Equation of State (EOS) for mixtures based on a Caranhan-Starling repulsive term with a temperature dependent sphere diameter (σ) and square well potential as a basis for the attraction coefficient.

$$p(T,V_m,x)=\frac{RT}{V_m}\frac{V_m^3+V_m^2\beta(T,x)+V_m\beta^2(T,x)-\beta^3(T,x)}{\left(V_m-\beta(T,x)\right)^3}-\frac{4RT}{V_m^2}\beta(T,x)(\lambda_{ij}{}^3-1)\left(\exp\left(\frac{\varepsilon_{ij}}{kT}\right)-1\right) \tag{B1}$$

with mixing rules:

$$\beta(T,x)=\sum_{i,j=A,B}x_i x_j\beta_{ij}(T) \tag{B2}$$

$$\begin{aligned}\beta_{ij}(T)&=\frac{4\pi}{3}N_0\sigma_{ij}^3(T)\\ \sigma_{ij}(T)&=\frac{\sigma_i+\sigma_j}{2}\zeta\\ \varepsilon_{ij}&=\left(\varepsilon_i\varepsilon_j\right)^{1/2}\xi\end{aligned} \tag{B3}$$

where β, ε are temperature dependent parameters defined by:

$$\beta(T) = \beta(T_c)(T_c / T)^{3/m}$$
$$\beta(T_c) = 0.04682 \frac{RT_c}{p_c} \qquad \text{(B4)}$$
$$\varepsilon / k = T_c \ln\left(1 + \frac{2.6503}{(\lambda^3 - 1)}\right)$$

T_c, p_c are the critical temperature and pressure, k is the Boltzman constant. The parameter m can take values 9.5 or 10, while λ depends on molecular polarity and, for example, for water it is 1.199. As a first aproximation ξ and ζ can be taken as equal to one. Christoforakos and Franck (1986) applied this equation of state to water-nitrogen, water-methane, water-xenon and water-carbon-dioxide mixtures.

With this EOS density and mixture heat capacity were calculated (Saur *et al.*, 1993). Viscosity and thermal conductivity were obtained as deviations from values for low density gases. Van der Waals "one fluid theory" was used for mixture rules. Expressions for viscosity and thermal conductivity with mixture rules are as follow:

$$\frac{\mu}{\mu_0} = \frac{1}{\chi}\left[1 + \frac{8}{15}\pi n\sigma^3\chi + 0.761\left((2/3)\pi n\sigma^3\chi\right)^2\right]$$
$$k = \frac{1}{\chi}\left[k_0 + k_{mono}\left(\frac{4}{5}\pi n\sigma^3\chi + 0.757\left((2/3)\pi n\sigma^3\chi\right)^2\right)\right] \qquad \text{(B5)}$$

If a gas consists of polyatomic molecules, the "monatomic" part has to be separated to calculate the high-density collision contribution to the thermal conductivity. n is the density N/V. The hard sphere equation of Caranhan-Starling was used to defined

the χ, where n is the density (number of mols per cubic meter) and σ is the sphere diameter:

$$\chi = \frac{1 - \frac{\pi}{12} n\sigma^3}{\left(1 - \frac{\pi}{6} n\sigma^3\right)^3} \tag{B6}$$

The mixing rules are defined by combination of the parameters of the pure components according to their relative mole fractions:

$$\sigma^3 = \sum_i \sum_j x_i x_j \sigma_{ij}^3 \tag{B7}$$

Wang (2001) in her thesis applied the Redlich-Kwong-Soave equation of state (RKS EOS). This equation was improved for both liquids and gases, polar and non-polar compounds.

$$P = \frac{RT}{v - b} - \frac{a}{v(v + b)} \tag{B8}$$

where:

P- pressure, Pa

T – temperature, K

v – specific volume, m^3/kg

a – coefficient depends on the attractive force between molecules

b - coefficient depends on the repulsive force between molecules

Coefficients a and b are given by:

$$a = 0.042748\frac{R^2T_c^2}{P_c}\left(f(T_r)\right)^2$$
$$b = 0.08664\frac{RT_c}{P_c} \qquad \text{(B9)}$$

where:

T_c – critical temperature, K

P_c – critical pressure, Pa

T_r –reduced temperature T/T_c

Function f is given with:

$$f(T_r) = \begin{cases} 1 + C_1 y + C_2 y^2 + C_3 y^3 & T_r \le 1 \\ 1 + C_1 y & T_r > 1 \end{cases} \qquad \text{(B10)}$$

where:

$$y = -\sqrt{T_r} + 1$$

The coefficients C_1, C_2 and C_3 are given below (Dahl *et al.*, 1991):

For water, C_1= 1.0873, C_2 = -0.6377 and C_3 = 0.6345

For oxygen, C_1= 0.8252, C_2 = 0.2515 and C_3 = -0.7039.

Wang (2001) calculated the phase boundary applying both equation of states and compared it with the experimental data from Christoforakos and Franck (1986) . The phase boundary predicted by RKS EOS and Hard Sphere EOS at 25 MPa agreed well with experimental data (Fig. B1). Heat capacity values calculated with the Hard Sphere EOS are higher than experimental data in the sub-critical region and lower in the supercritical region (Fig B2, B3). Better prediction is given by the RKS EOS (Fig. B4). To validate the equation of state specific volume experimental data was used, which were obtained, by using a venturi. Density is calculated applying only the RKS EOS. It has shown a significant difference in the subcritical and critical region. Better agreement was seen in the higher temperature region.

Oh *et al.* (1997) calculated thermodynamic and transport properties for SCWO fluids (water, ethanol, isopropyl alcohol, nitrogen, oxygen and carbon dioxide). They applied the Redlich-Kwong cubic equation of state, which is recommended for highly nonideal systems at high pressures and temperatures. The mixture properties were computed based on mass fractions. These are ideal mixing assumptions and may not be strictly accurate at supercritical conditions.

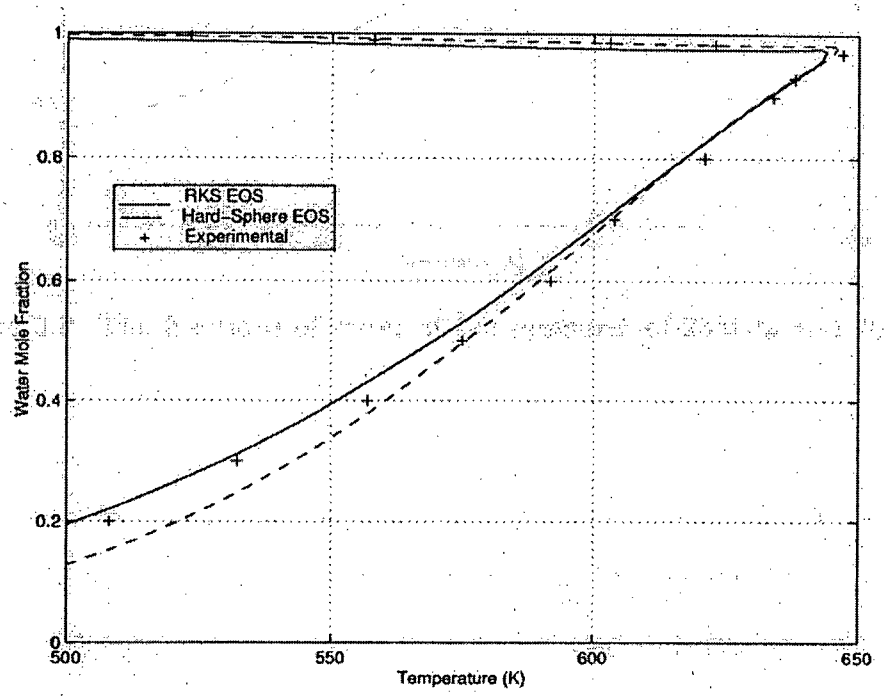

Figure B1. The boundary phase for water-oxygen mixtures at 25 MPa

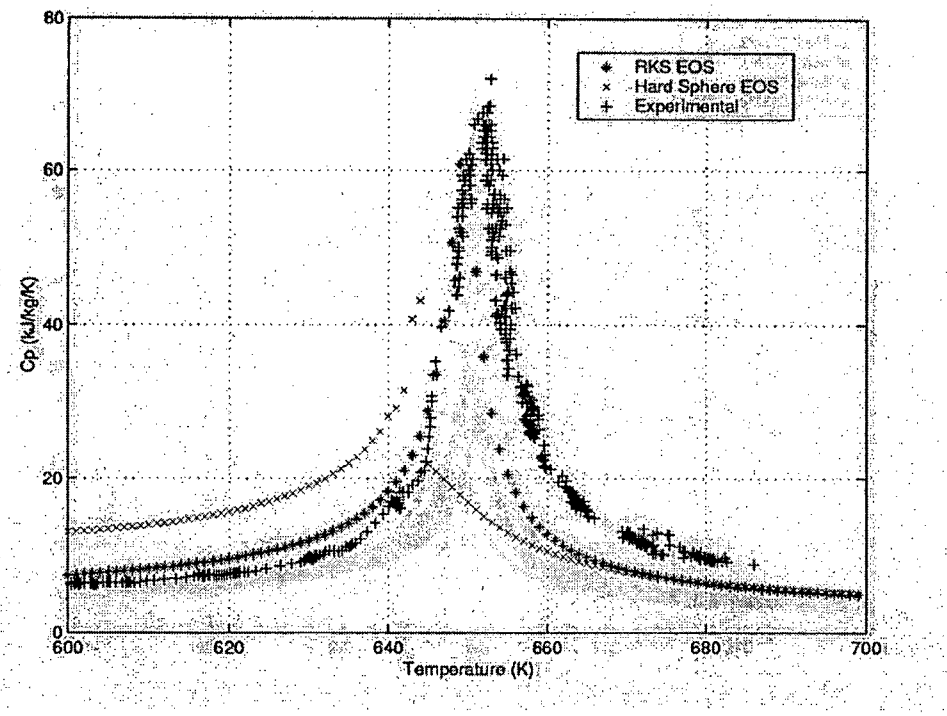

Figure B2. Heat capacity for 2% oxygen at 26 MPa (Run #12)

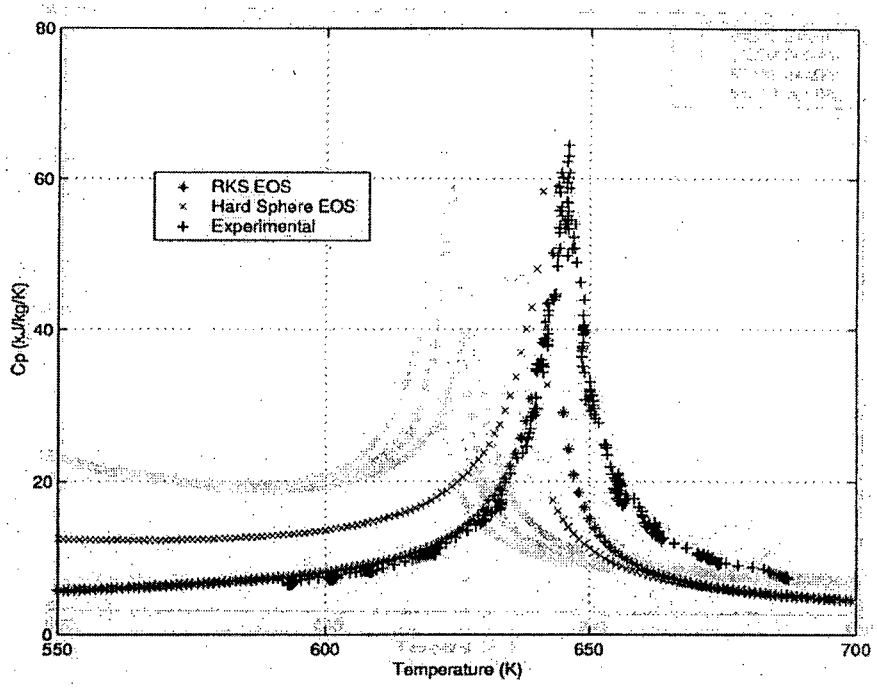

Figure B3. Heat capacity for 5% oxygen at 24 MPa (Run #13)

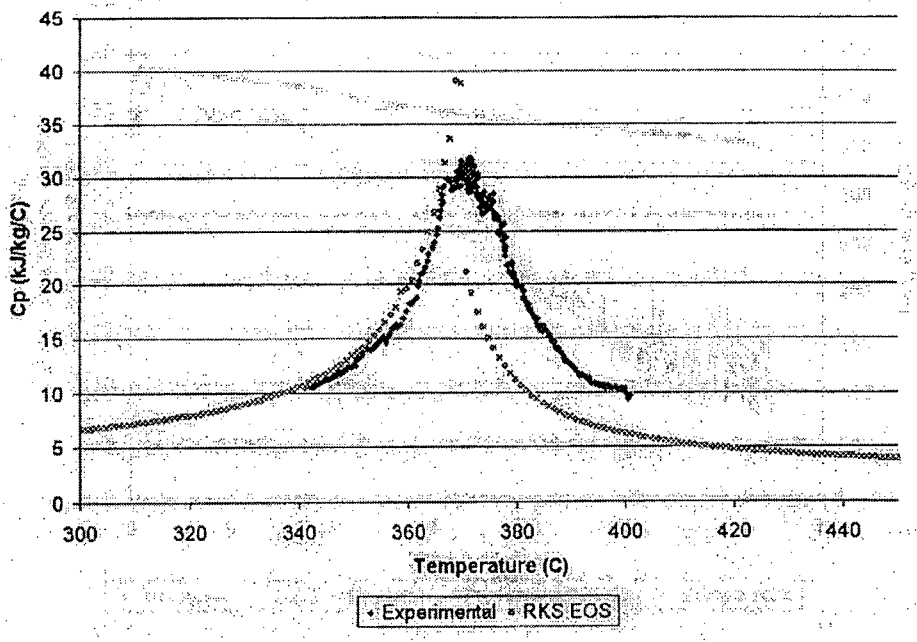

Figure B4. Heat capacity for 8% oxygen at 25 MPa (Run #31)

APPENDIX C Oxygen flow calibrations

A Foxboro E13DH-ISAM2 Transmitter was used for oxygen flow rate measurements. It contains a orifice (0.86 mm) and pressure differential measurement across the orifice. The output signal has a range 4 – 20 mA. Since the data acquisition system has a 0-10 V signal, a 500 Ohm resistor is used to get 2-10 V output from the transmitter. A 24 V power supplier was used to provide the power for the transmitter.

A correlation between mass flow rate and output signal was obtained by applying Bernoulli's equation and a lineer correlation between pressure and output signal:

$$\frac{m^2}{\rho} = k\Delta P$$
$$\frac{m^2}{\rho} = k'(V - V_0) \qquad \text{(C1)}$$

where:

V - voltage signal, V

V_0 - zero offget, V

k, k' – coefficient

m – mass flow rate, kg/h

ρ - density, kg/m^3

P – pressure, Pa

The transmitter was calibrated at three different pressures 101.3 kPa, 22.06 MPa and 27.23 MPa.

At 101.3 kPa and 27.23 MPa, a bubble meter was used to measure the outlet flow rate. Nitrogen was used as the working fluid. Oxygen as the working fluid was used at 27.23MPa. At 22.06 MPa, the mass flow rate was measured by an Omega mass flow meter (range 0-5 V) and nitrogen was used as a working fluid.

The calibration data are listed in Tables 1 to 3. At each pressure, the coefficient k was found. It changes from 0.0627 at 101.3 kPa to 0.047 at 22.06 MPa and to 0.048 at 327.23 MPa. The mass flow rate for 27.23 MPa is claculated by:

$$m = 4.16\left(V - V_o\right)^{\frac{1}{2}} \qquad \text{(C2)}$$

where:

m – mass flow rate, kg/h

V – output voltages, V

V_o – zero offset of the transmiter

Table C1 Calibration data for oxygen flow rate at 101.3 kPa

Output of the transmitter, V	Bubble flow meter, l/min	Flow rate, kg/h	$V-V_o$	m^2/ρ
1.997	0.0	0.0	0.0	0.0
2.0584	0.8384	0.0780	0.0614	0.0039
2.1557	1.261	0.1172	0.1587	0.0089
2.2173	1.531	0.1424	0.2203	0.0131
2.2482	1.638	0.1523	0.2512	0.0150
2.3131	2.833	0.1705	0.3161	0.0187
2.4190	2.100	0.1953	0.4220	0.0246
2.5363	2.415	0.2246	0.5393	0.0325
2.7376	2.852	0.2652	0.7406	0.0454
2.8764	3.122	0.2903	0.8794	0.0544
3.0491	3.408	0.3169	1.0521	0.0648
3.2181	3.696	0.3437	1.2211	0.0762
3.6250	4.227	0.3931	1.6280	0.0997
3.9624	4.701	0.4372	1.9654	0.1233
4.3432	5.160	0.4799	2.3462	0.1486
4.9134	5.752	0.5349	2.9164	0.1846
5.0370	5.896	0.5483	3.0400	0.1940

Table C2 Calibration data for oxygen flow rate at 22.06 MPa

Output of the transmitter, V	Bubble flow meter, l/min	Flow rate, kg/h	$V-V_o$	m^2/ρ
2.0600	0.0	0.0	0.0	0.0
2.0756	0.203	0.5891	0.0156	0.0015
2.1277	0.310	0.8996	0.0677	0.0035
2.1827	0.409	1.1869	0.1227	0.0061
2.2660	0.512	1.4858	0.2060	0.0096
2.3122	0.602	1.747	0.2522	0.0132
2.3977	0.701	2.0343	0.3377	0.0179
2.5503	0.805	2.3361	0.4903	0.0236
2.6796	0.912	2.6466	0.6196	0.0303
2.7766	1.010	2.931	0.7166	0.0372
2.9467	1.117	3.2415	0.8867	0.0455
3.1009	1.215	3.5259	1.0409	0.0538
3.2585	1.297	3.7639	1.1985	0.0613
3.5547	1.454	4.2195	1.4947	0.0771
3.9368	1.589	4.6113	1.8768	0.0920
4.4958	1.795	5.2091	2.4358	0.1175
5.0186	1.972	5.7227	2.9586	0.1418
5.8211	2.214	6.425	3.7611	0.1787
6.5829	2.417	7.0141	4.5229	0.213
7.5668	2.695	7.8209	5.5068	0.2648
8. 3414	2.823	8.1923	6.2184	0.2905
9.3874	3.038	8.8163	7.3274	0.3365

Table C3 Calibration data for oxygen flow rate at 27.23 MPa

Output of the transmitter, V	Bubble flow meter, l/min	Flow rate, kg/h	$V-V_o$	m^2/ρ
1.9945	0.0	0.0	0	0
2.0035	6.203	0.4943	0.0009	0.0007
2.0213	8.902	0.7093	0.0268	0.0014
2.0494	12.40	0.9880	0.0549	0.0027
2.0753	14.84	1.1825	0.0808	0.0039
2.0822	15.28	1.2175	0.0877	0.0041
2.0912	15.99	1.2741	0.0967	0.0045
2.1093	16.99	1.3538	0.1148	0.0051
2.1315	18.21	1.4510	0.137	0.0058
2.1346	19.64	1.56498	0.1401	0.0068
2.1461	20.29	1.6167	0.1516	0.0072
2.1709	22.34	1.7801	0.1764	0.0088
2.1958	23.86	1.9012	0.2013	0.0100
2.2229	23.21	2.0087	0.2284	0.0129
2.2638	27.13	2.1617	0.2693	0.0175

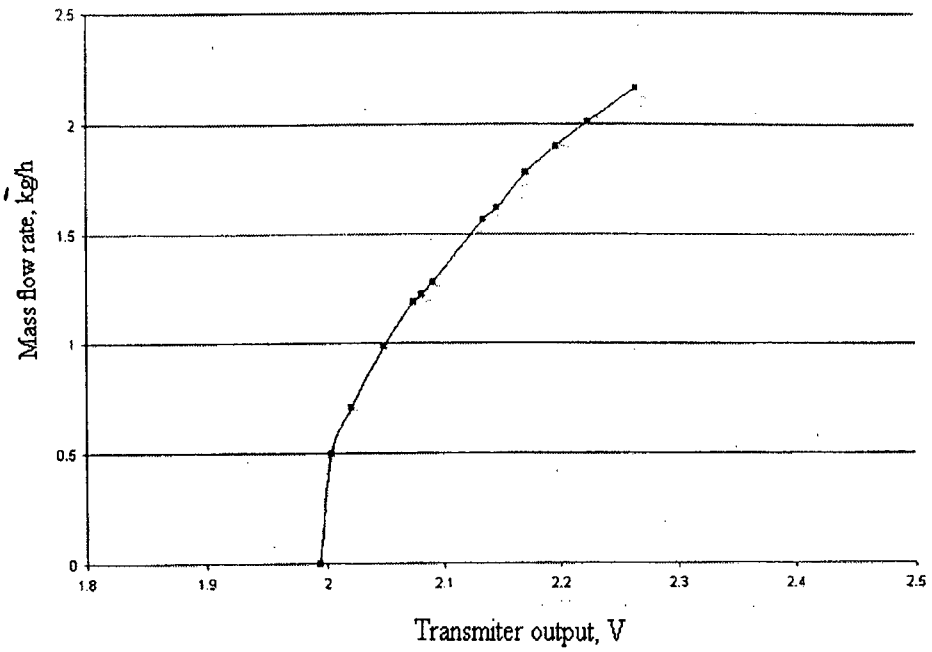

Figure C1. Calibration data (kg/hour vs voltage) for oxygen flow rate transmitter

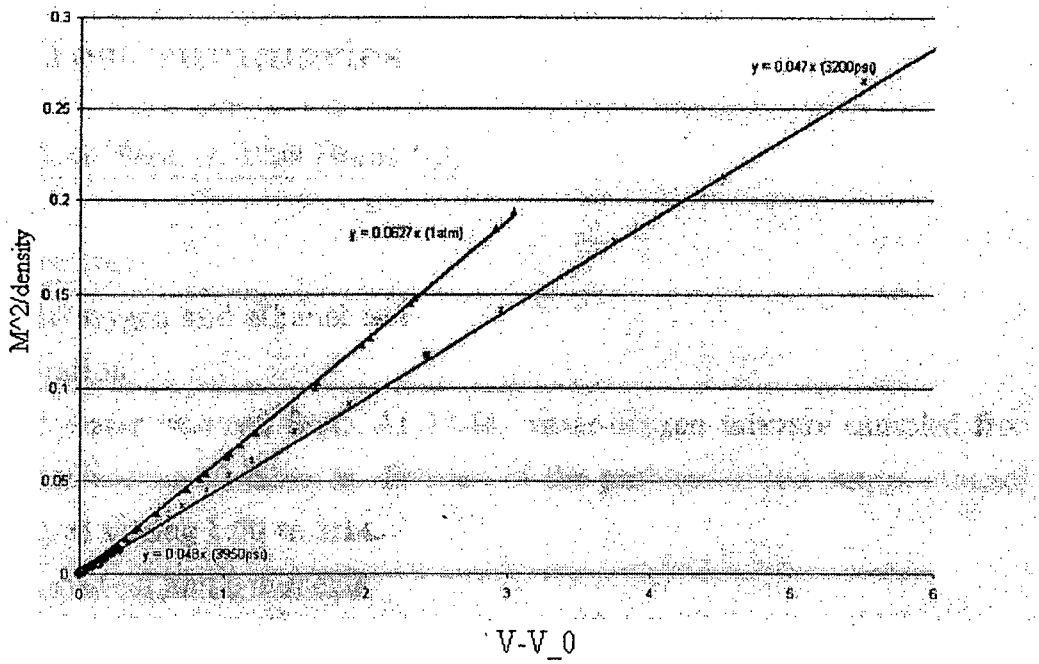

Figure C2. Oxygen flow rate (m^2/ρ) versus output voltage reading (V-V_0)

APPENDIX D Test summaries

1. Date: September 2, 1998 (Runs 1-6)

Objectives:

Water –oxygen and ethanol tests

Operation:

The first run was for pure water. At 12:44 pm., the water oxygen mixture was sampled from the intermediate sample point for 10 minutes. Ethanol was stopped in the period from 13:00 to 13:14, because the pump did not work properly.

Observation and comments

Surface temperatures for test section and reactors were around 10 °C lower than bulk temperatures.

2. Date: March 10, 1999 (Runs 7-10)

Objectives:

Pure water and water-oxygen heat capacity test

Operation:

Different heat fluxes applied to the test section.

Observation and comments:

Steam leaking was observed. Oxygen pressure was 19.3 MPa.. Booster was running 1 cycle/min.

3. Date: June 17, 1999 (Runs 11-16)

Objectives:

Water-oxygen heat capacity tests.

4. Date: December 8, 1999 (Runs 17-18)

Objectives:

Water-oxygen heat capacity tests.

Operation:

Heater voltage for the test section was 300 V. Heater voltage for the preheater 1 was 300V and for the preheater 2 was set on automatic control.

Observation and comments:

The test was interrupted by oxygen flow rate fluctuation.

5. Date: June 19, 2000 (Runs 19-22)

Objectives:

Heat losses test – pure water

Operation:

No heat flux applied to the test section

Observation and comments:

At 13:03, the surface temperature tripped the alarm. Pump speed was increased to cool down the system.

6. Date: May 24, 2001 (Run 23)

Objectives:

Pure water test for the venturi calibration at 25 MPa and 450 °C.

Operation:

The flow rate was initially set with the pump speed of 1600 rpm. Power supply to the preheater 2 was broken. Pump speed was reduced to 12000 rpm at 12:53. At 13:02, flow was reduced to 1000 rpm. The experiment was finished at 14:49. The system pressure was set at 27.5 MPa. Full power was supplied to the preheater 1, test section and the reactor.

Observation and comments:

The offset of the transducer for pressure drop across the venturi was different for low and high pressure. The fluctuation of the flow effected the pressure differential reading. Valve 9 was closed to reduce the fluctuation. The outlet temperature from the test section was lower then desired. Pump speed was decreased from 1200 rpm to 1000 rpm.

7. Date: June 5, 2001 (Runs 24-27)

Objectives:

Pure water and water-oxygen density and heat capacity test

Operation:

The pump was set at 800 rpm and 1600 rpm. The power applied on the test section was 300 V. The preheater 2 temperature was ramped.

Observation and comments:

File 1600wo.txt uses a constant test section voltage of 289 V. From 13:32:29 (logbook and file time), the pump ran at 1600 RPM. Power slowly decreased in Preheater 2 as the temperature dropped. At 14:05, near the temperature minimum, pump RPM changed to 800 RPM. At 15:00, the oxygen was turned off.

The bypass valve of DPT 429 leaked. A thermocouple was attached at the surface of the pressure tap at the inlet of the venturi. It was observed that the temperature increased very slowly. The oxygen flow rates from gas flow meter were also recorded. The zero offset of the transmitter for oxygen flow rate changed from 2 V to 1.9033 V.

8. Date: June 20, 2001 (Run 28-35)

Objectives:

The test was performed to get heat capacity, heat transfer coefficient and density of pure water and water-oxygen mixtures at different pressures, flow rates and oxygen concentrations.

Operation:

In the test section, heat flux were kept constant for each run. Different heat (10.184, 6.122 and 2.315 kW) fluxes were applied to observe the heat transfer effect on the heat capacity for a water-oxygen mixture with 8% oxygen. The range of temperature was between 340 and 400 °C. The ramping time was 30 or 40 minutes.

Observation and comments:

Water feed valve V9 had leakage. This gave a higher oxygen percentage than was expected. The zero offset of the transmitter for oxygen flow rate changed from 2V at the

start to 1.8V when it was stopped. The oxygen flow rates from gas flow meter were also recorded. The pressure gauge near V15 was reading 200 psi higher than the real pressure was. Calibration of the system pressure was done after the experiment. The bulk thermocouple in the middle of the test section was broken.

9. Date: November 25, 1999 (Run 36-38)

Objectives:

Heat capacity test for pure water

Operation:

Heat flux was 6.122 kW. Temperature ramping was applied on Preheater 2. There were three data files with temperature set points of 120, 200 and 300 ° C.

APPENDIX E Data files for experimental runs

Run	File (.txt)	Date	Pressure (MPa)	Running conditions								Chan. conf.
				Water flow rate		Heat flux in test section		Oxygen flow rate (kg/h)		Fraction of oxygen (%)	Ramping	
				rpm	l/min	Volts	kW	Gas meter	Orifice		Temperature range(°C)	Time (min)	
1	sept2a	02-Sep-98	25.0	900	1.2	Varies			0	0			1
2	sept2b	02-Sep-98	25.0	900	1.2	Varies			0	0			1
3	sept2c	02-Sep-98	25.0	900	1.2	299	6.072		0	0			1
4	sept2d	02-Sep-98	25.0	900	1.2	299	6.072		0	0			1
5	sept2e	02-Sep-98	25.0	900	1.2	299	6.072		2.7	3.6			1
6	sept2e[a]	02-Sep-98	25.0	900	1.2	298	6.072		2.7	3.6			1
7	qhfmtal1	10-Mar-99							0	0			2
8	qhfmtal2	10-Mar-99							0	0			2
9	qhfitall	10-Mar-99			0.94	Varies[b]			0	0			2
10	mar10Cp[c]	10-Mar-99	24.4		1.2	300	6.122						2
11	T1june17	17-Jun-99	24.4		1.01	300	6.122		0	0	310-430		3
12	T2june17	17-Jun-99	24.5		1.01	300	6.122		1.22	2	430-310		3
13	T3june17	17-Jun-99	24.2		1.01	300	6.122		3.83	4.9	310-430		3
14	T4june17	17-Jun-99	25.8		1.01	300	6.122		3.83	4.7	430-310		3
15	T5june17	17-Jun-99	26.4		1.01	300	6.122		1.22	2.1	310-430		3
16	T6june17	17-Jun-99	26.1		1.01	300	6.122		0	0	430-310		3
17	O1Tall	08-Dec-99	25.4	800	1.05	300	6.122		4.839+/-0.42	4	to 250	25	4
18	O2Tall	08-Dec-99	25.9	800	1.05	300	6.122		3.471+/-0.41	6.2	250-415	25	4
19	Jun19a	19-Jun-00	24.5	500	0.636	0	0		0	0			5
20	Jun19b	19-Jun-00	24.9	500	0.636	0	0		0	0			5
21	Jun19c	19-Jun-00	24.5	1100	1.296	0	0		0	0			5
22[g]	Jun19d	19-Jun-00	25.0	1100	1.296	0	0		0	0			5
23	May24	24-May-01	25.48+/-0.38	1000	1.365	Varies[e]			0	0			6
24	800w	05-Jun-01	25.0	800	1.028	300	6.122		0	0	400		7
25[a]	800w	05-Jun-01	25.0	800	1.028	300	6.122	2.772	3.16		350-410	40	7
26	1600w	05-Jun-01	25.11+/-0.1	1600	2.117	Varies[f]			0	0			7
27	1600awo	05-Jun-01	25.2	800	1.026	289	6.122	2.576	3.04+/-0.15	5.8	350-410	40	7
28	14water	20-Jun-01	25.2	1400	1.269	300	6.122		0	0	350-400	30	8
29	14wo	20-Jun-01	25.1	1400	1.269	300	6.122		2.3+/-0.15	3	400-350	30	8
30	12wo	20-Jun-01	25.2	1200	1.007	300	6.122	1.624	1.87+/-0.07	3	350-400	30	8
31	12wo-5-300	20-Jun-01	25.3	1200	1.007	300	6.122		5.16+/-0.19	7.9	400-350	30	8
32	12wo-5-370	20-Jun-01	25.2	1200	1.007	370	10.184	Unstable		8	350-400	30	8
33	12wo-5-200	20-Jun-01	25.3	1200	1.007	200	2.315	4.6	4.97+/-0.22	7.6	400-350	30	8
34	12wo-534	20-Jun-01	24.0	1200	1.007	200	2.315	4.95	5.17+/-0.11	7.8	350-400	30	8
35	12water	20-Jun-01	23.92+/-.21	1200	1.007	0	0		0	0			8
36[h]	O0T120	25-Nov-99	25.0	800	1.068	300	6.122		0	0	120		4
37	O0T200	25-Nov-99	25.0	800	1.068	300	6.122		0	0	200		4
38	O0T300	25-Nov-99	25.0	800	1.068	300	6.122		0	0	300		4

[a]Ethanol is included, channel 2 to 5 were replaced by reactor surface temperature

[b]150V to 15:33, 300V from 15:33 to 15:34, 457V from 15:37 to 16:26, 393 from 16:26 to 16:31, 348 from 16:31 to 16:32, 300v from 16:32 to 16:34, 250V from 16:34 to 16:36, 0V after 16:36

[c]Files sept21 to mar10Cp are missing

[d]It is adjusted according to the temperature in the test section

[e]Graphs for Runs # 24, # 25 and #26 are not listed because the running conditions are unstable

[f]298V after 1:22 pm

[g]Run #22 is not listed because of the unstable pressure

[h]Runs #36,37,38 are not listed because temperature interval was small

Table E1 List of the runs for water and water-oxygen mixtures

Table E2. Channel configuration (Wang, 2001)

cha-nnel	Channel configuration number															
	1		2		3		4		5		6		7		8	
	Code	Axial Position (m)	Code	Axial Position (m)	Code	Axial Position (m)	Code	Axial Position (m)	Code	Axial Position (m)	Code	Axial Position (m)	Code	Axial Position (m)	Code	Axial Position (m)
1	B2[a]	0.0	B2	0.0	Ph2in	PH 2 inlet	DT	PH 2 inlet & outlet	Ph2in	PH 2 inlet	Ph2in	PH 2 inlet	Ph2in	PH 2 inlet	Ph2in	PH 2 inlet
2	B3	1.473	B3	1.473	Ph2out	PH 2 outlet	B2	0	Ph2out	PH 2 outlet	Ph2out	PH 2 outlet	Ph2out	PH 2 outlet	Ph2out	PH 2 outlet
3	B4	2.946	B4	2.946	B2	0	B4	2.946	B2	0	B2	0	B2	0	B2	0
4	S2	0.247	S5	0.749	SB1	0.148	B3	1.473	B3	1.473	B3	1.473	B3	1.473	B3	1.473
5	S3	0.442	S7	0.969	SB3	0.521	S4	0.612	B4	2.946	RL2IN	RL2 inlet	RL2IN	RL2 inlet	B5	3.259
6	S5	0.749	SB20	2.822	SB5	0.776	SB4	0.691	S4	0.612	SB1	1.325	SB1	1.325	SB1	1.325
7	S6	0.837	SB6	0.861	SB7	1.03	S5	0.749	SB4	0.691	S3	1.031	S3	1.031	S3	1.031
8	S7	0.969	SB7	1.03	SB8	1.179	S6	0.837	S5	0.749	S4	0.861	S4	0.861	S4	0.861
9	S9	1.25	SB8	1.179	SB9	1.329	SB6	0.861	S6	0.837	SB6	0.612	SB6	0.612	SB6	0.612
10	S11	1.551	SB9	1.329	S2	0.247	S7	0.969	SB6	0.861	S7	0.504	S7	0.504	S7	0.504
11	S12	1.721	SB3	0.521	S4	0.612	SB7	1.03	SB7	1.03	S10	0.063	S10	0.063	S10	0.063
12	S14	2.024	S14	2.024	S6	0.837	S8	1.123	SB8	1.179	S11	1.551	S11	1.551	S11	1.551
13	S16	2.278	S6	0.837	S8	1.123	SB8	1.179	SB9	1.329	S12	1.721	S12	1.721	S12	1.721
14	S17	2.414	S8	1.123	S9	1.25	S9	1.25	S10	1.41	S15	2.151	S15	2.151	S15	2.151
15	S20	2.822	SB5	0.776	S10	1.41	SB9	1.329	S12	1.721	S18	2.551	S18	2.551	S18	2.551
16	B5	3.259	S9	1.25	B3	1.473	S10	1.41	S14	2.024	S20	2.822	S20	2.822	S20	2.822
17	Conductivity meter		Conductivity meter		Conductivity meter		S12	1.721	S16	2.278	SB20	2.822	SB20	2.822	SB20	2.822
18	PT431	System pressure	PT431	System pressure	PT431	System pressure	S16	2.278	S18	2.822	RL6IN	Reactor 6 inlet	RL6IN	Reator 6 inlet	RL6IN	Reactor 6 inlet
19	DPT429	test section DP	DPT429	test section DP	DPT429	test section DP	SB20	2.822	SB20	2.822	R15B	RL15	R15B	RL15	R15B	RL15
20	DP(O_2)	O_2 flow rate	DP(O_2)	O_2 flow rate	DP(O_2)	O_2 flow rate	S20	2.822	S20	2.874	RL10IN	RL10 inlet	Surface temperature (DPT429)		RL2-IN	RL2 inlet
21	PH2IN	PH2 inlet	S20	2.822	S11	1.551										
22	PH2OUT	PH2 inlet	S17	2.414	S20	2.822	PT431	System pressure	PT431	System pressure	PT431	System pressure	PT431	System pressure	PT431	System pressure
23	RL2IN	RL2 inlet	S3	0.442	B4	2.946	DPT429	Test section DP	DPT429	Test section DP	DPT429	Test section DP	DPT429	Test section DP	DPT429	Test section DP
24	RL6OUT	RL6 outlet	S10	1.41	B5	3.259	DP(O_2)	O_2 flow rate	DP(O_2)	O_2 flow rate	DP(O_2)	O_2 flow rate	DP(O_2)	O_2 flow rate	DP(O_2)	O_2 flow rate

: Channel configuration

[a]Top thermocouples's angular positions are 0°. Bottom thermocouple's angular positions are 180°.

APPENDIX E1 Results of Experiments

Results of each of the experiments were presented by five different graphs. The first graph shows inlet and outlet temperature, pressure and oxygen distribution in function of time. The second graph presents constant pressure heat capacity and heat loss distribution in function of bulk temperature. The third and fourth graphs show heat transfer coefficient for different thermocouples for top and bottom surfaces in function of bulk temperature. The last graph presents the average values for heat transfer coefficient for top and bottom surfaces in function of bulk temperature.

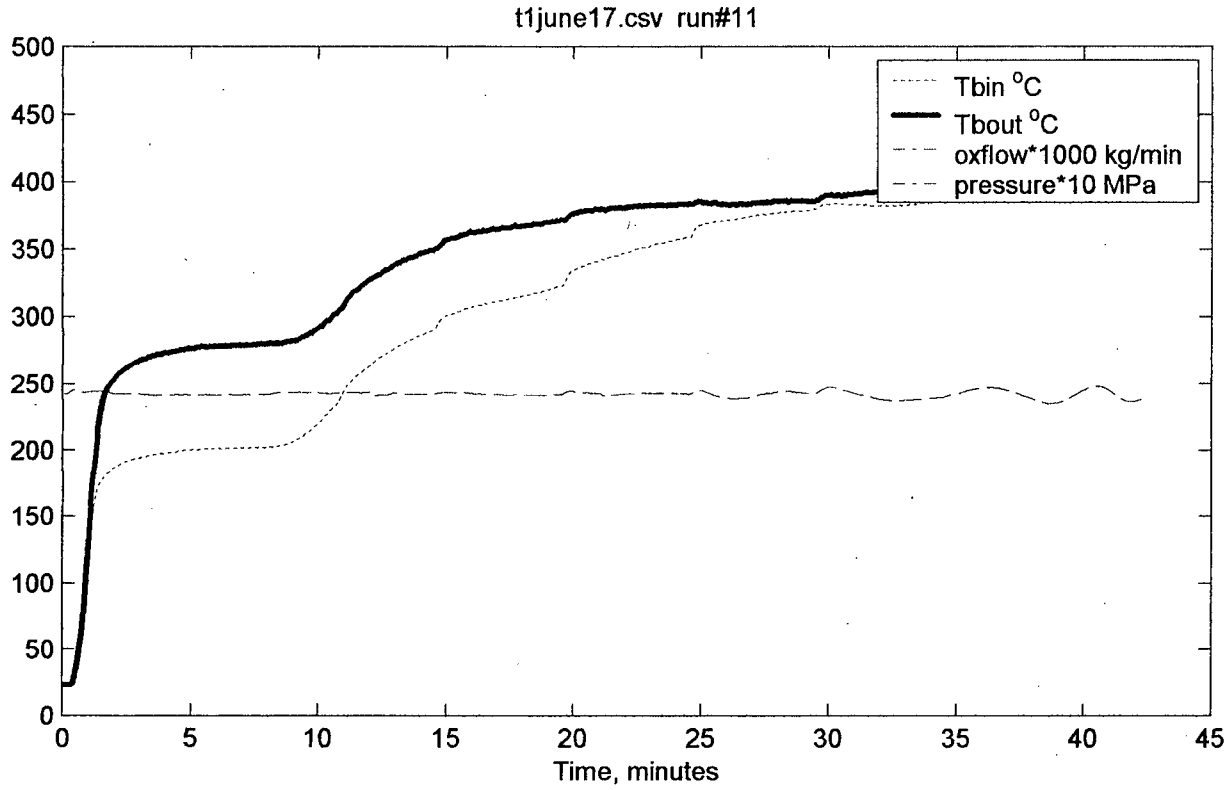

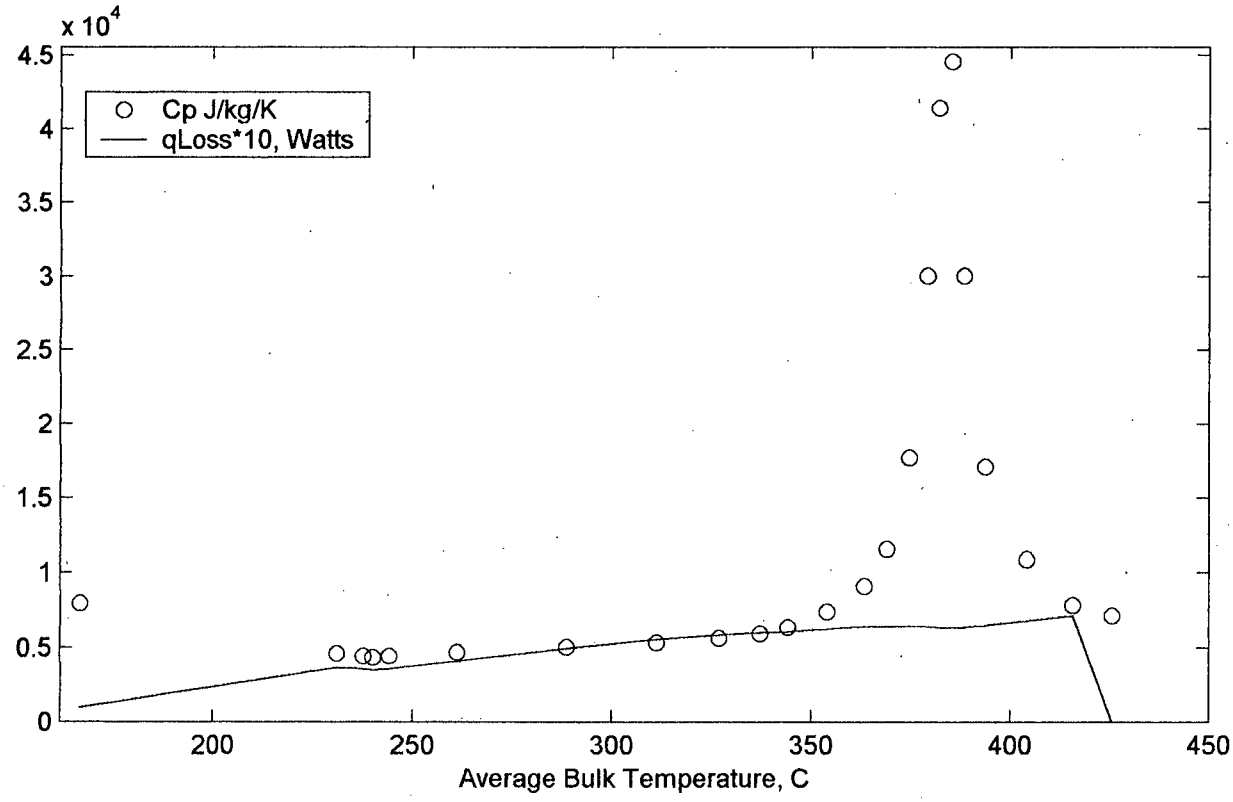

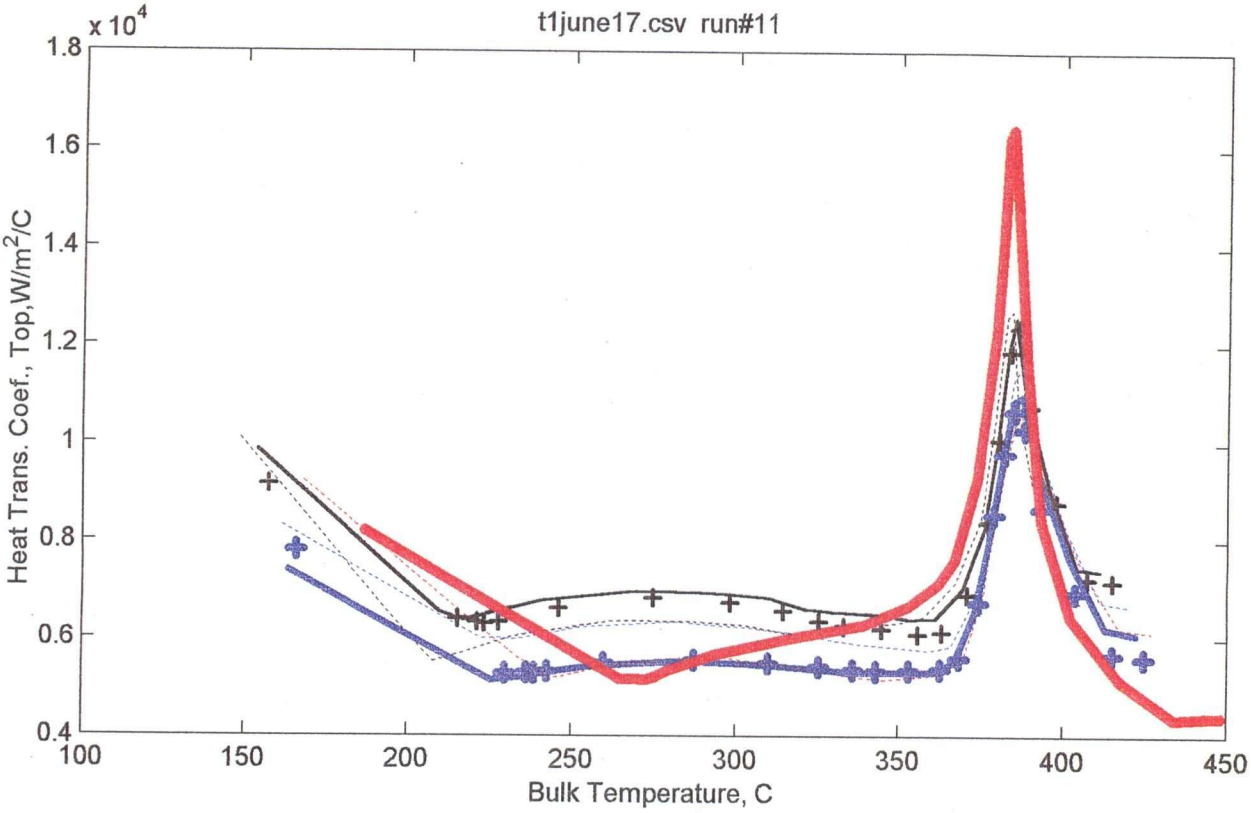

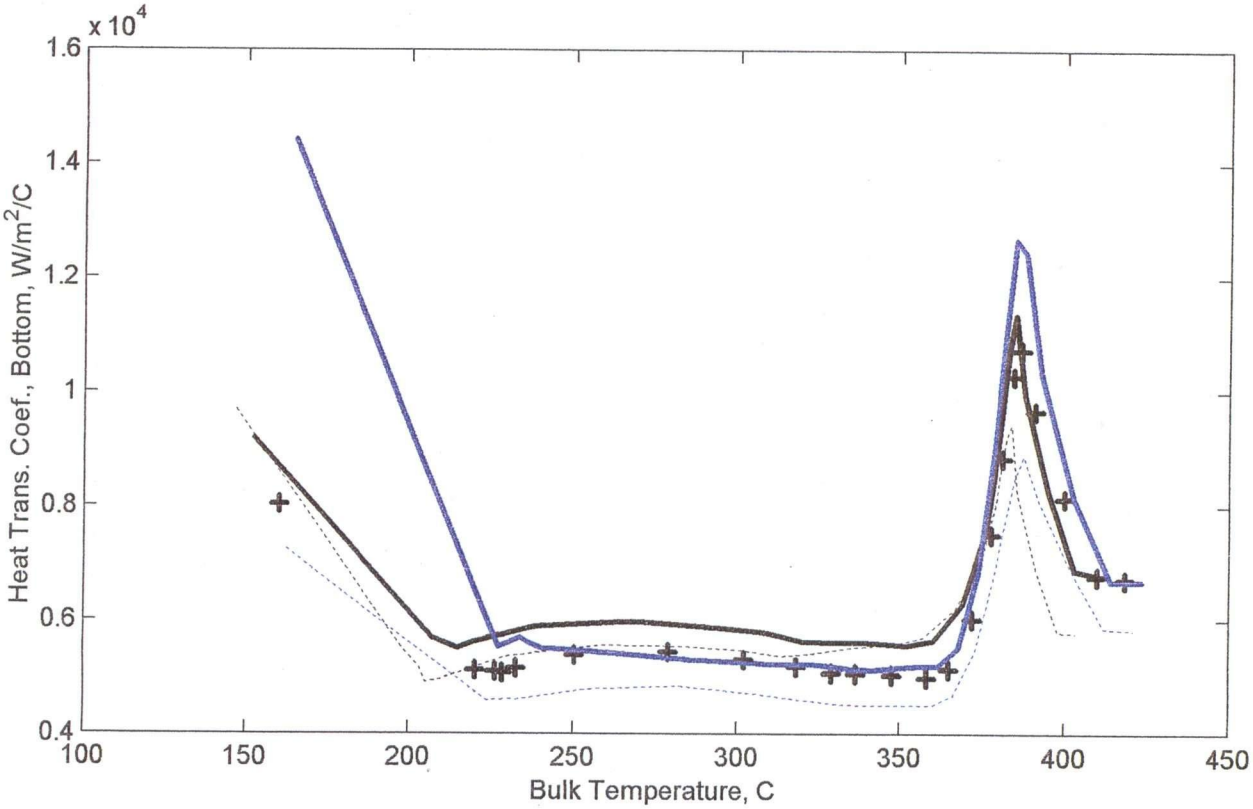

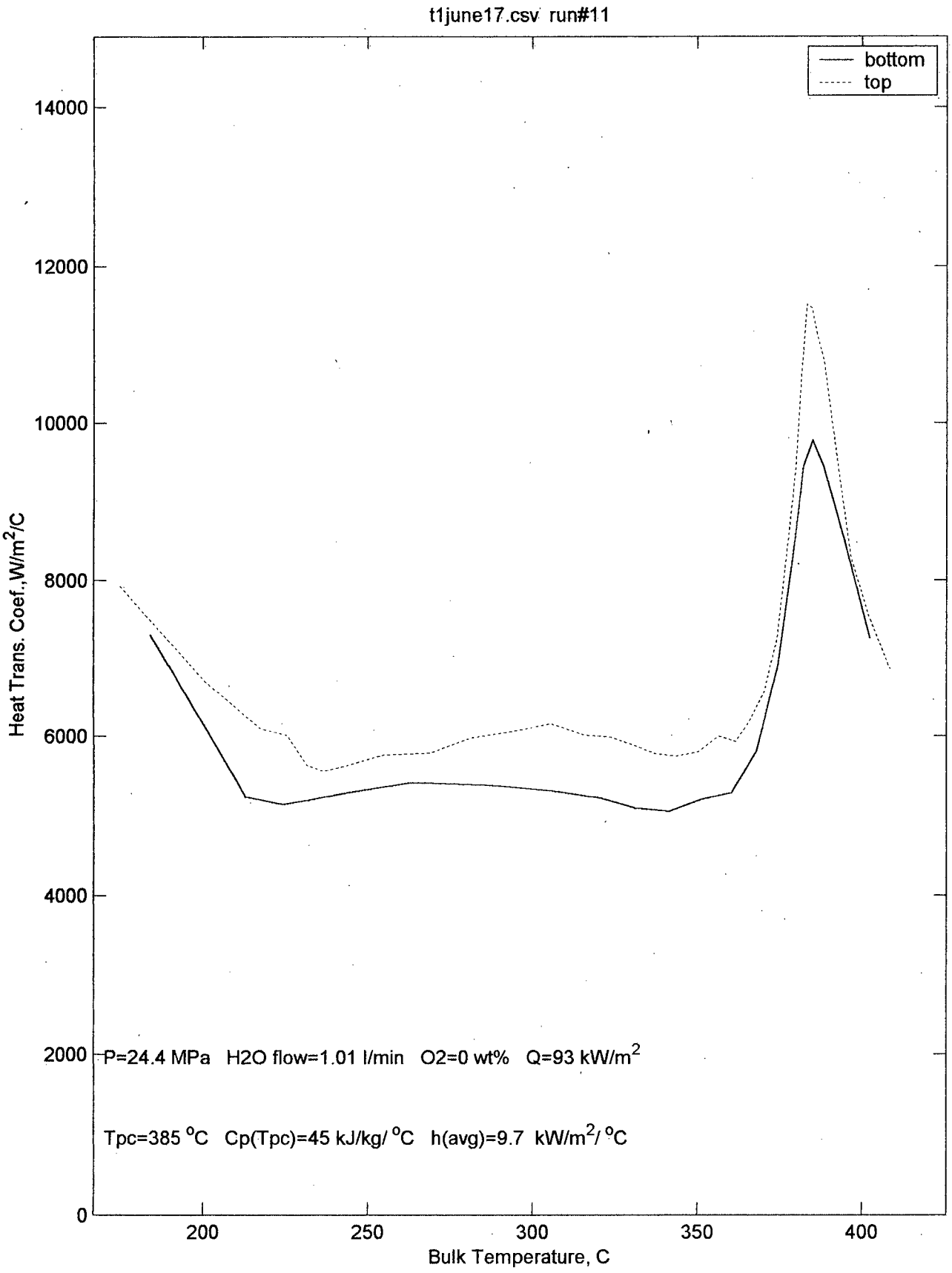

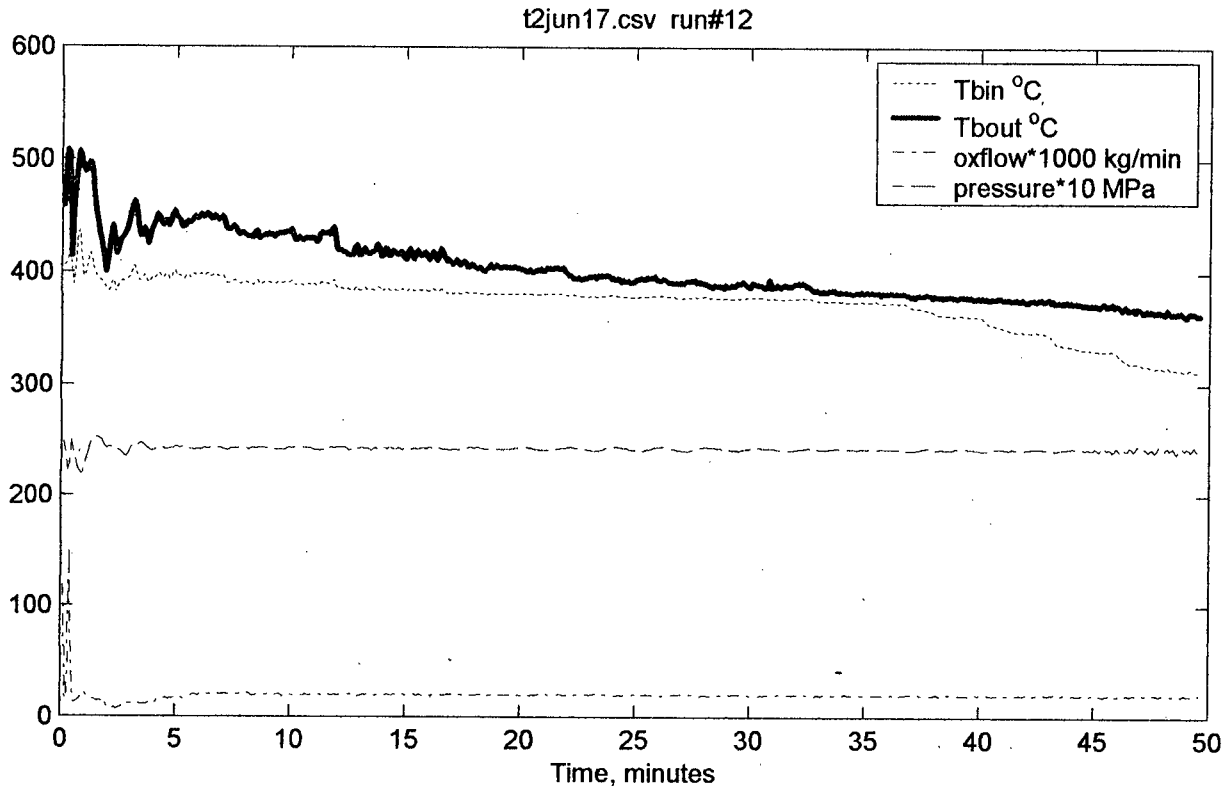

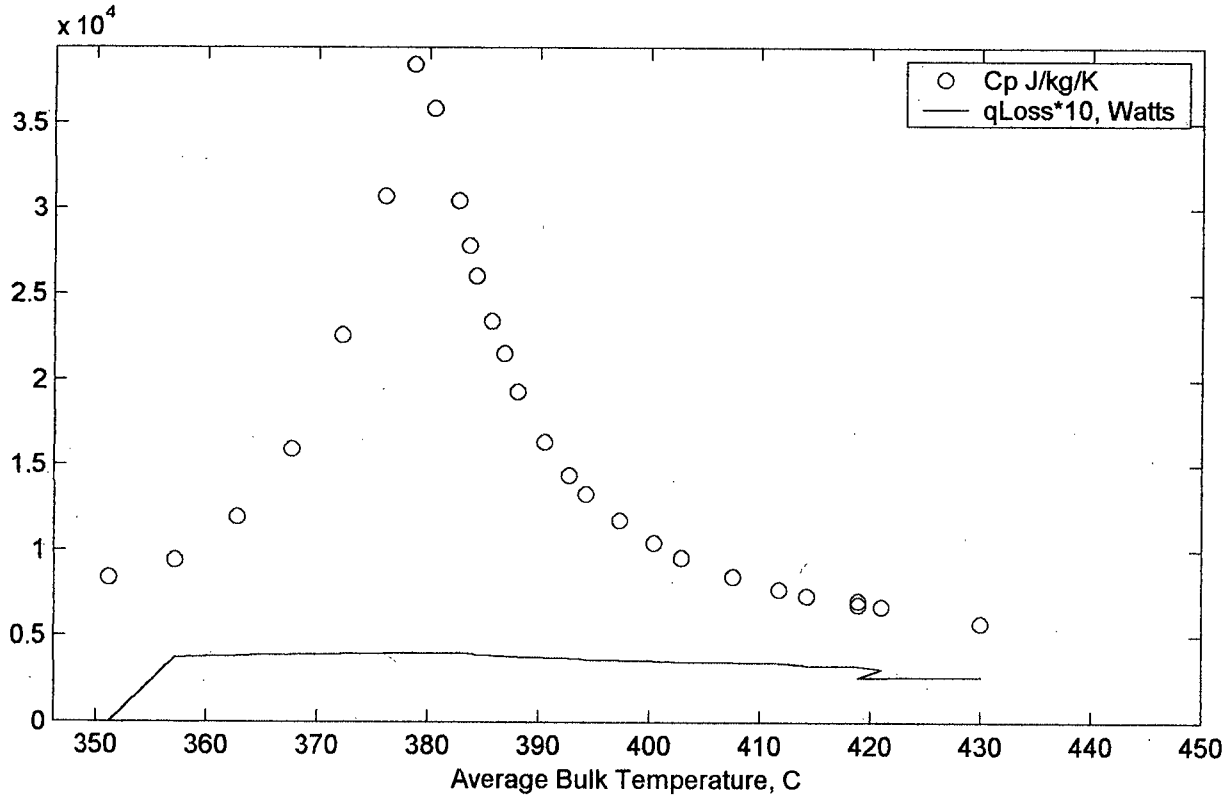

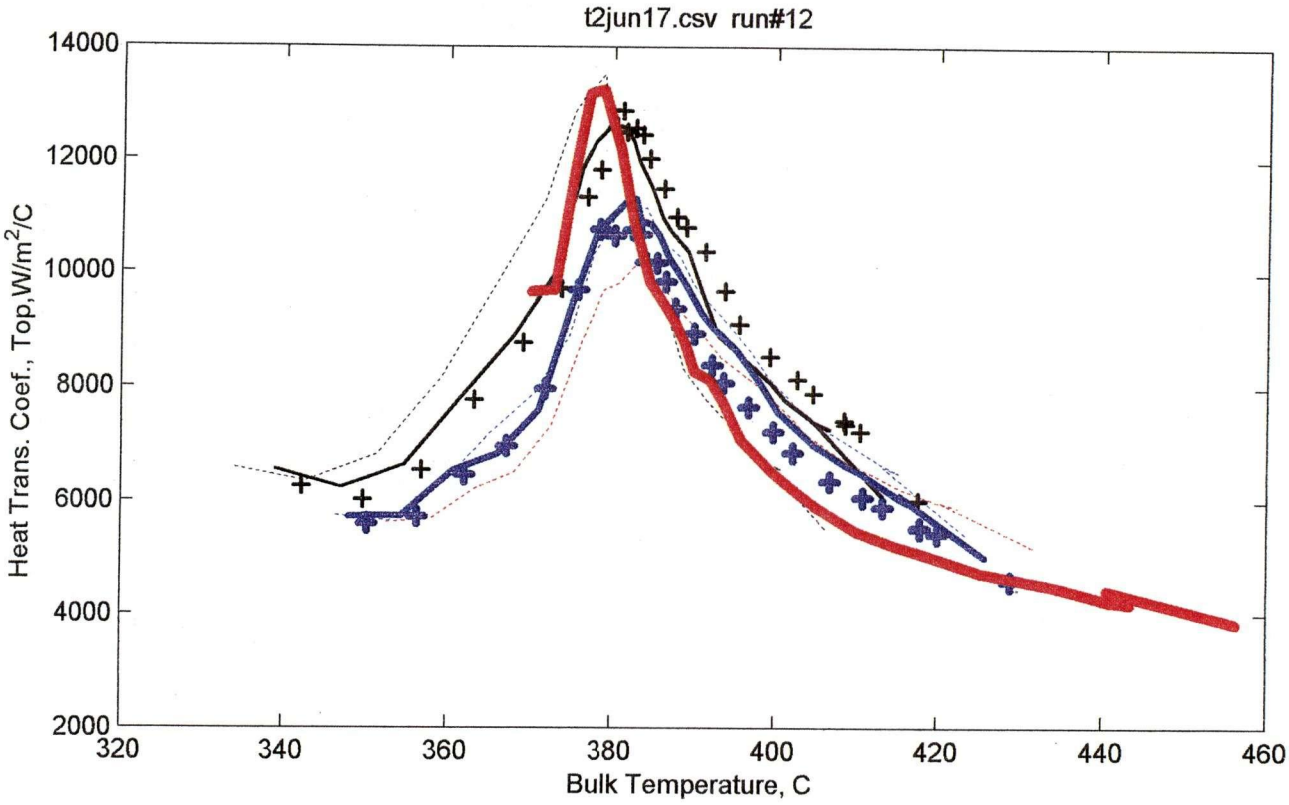

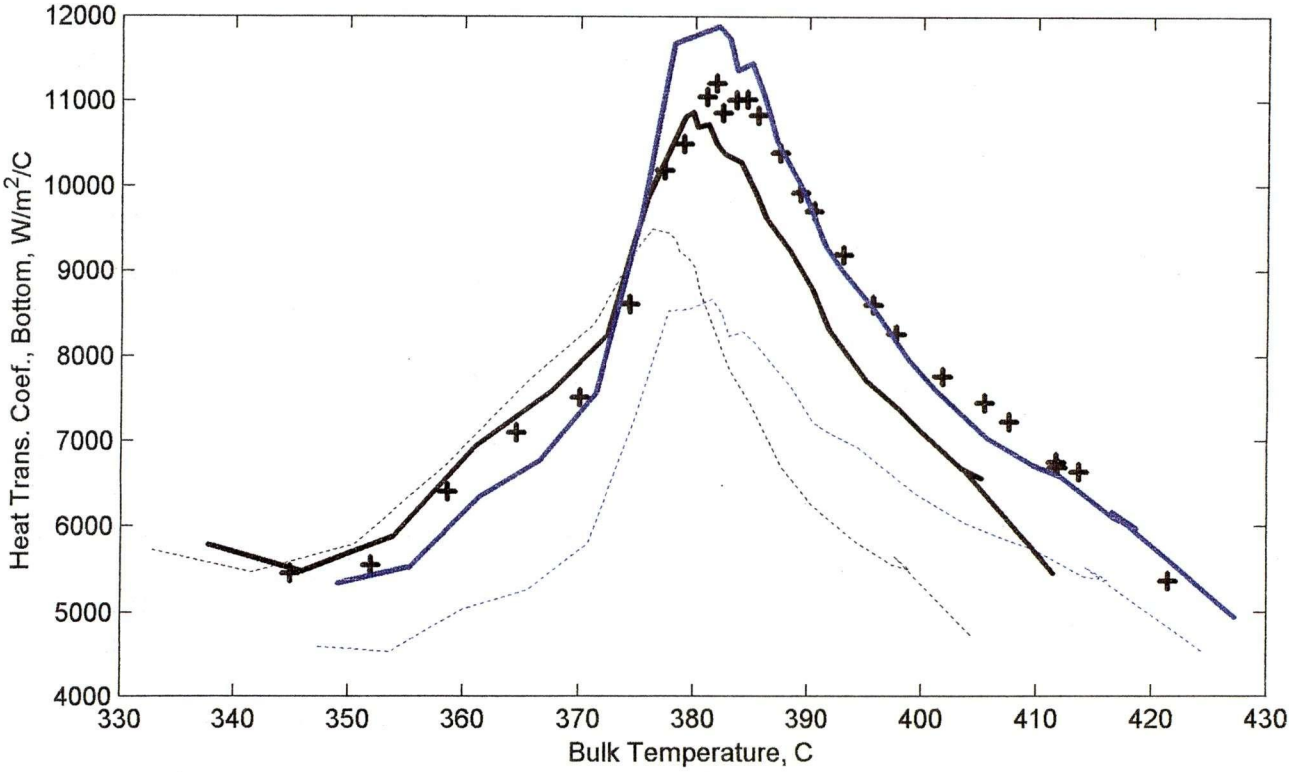

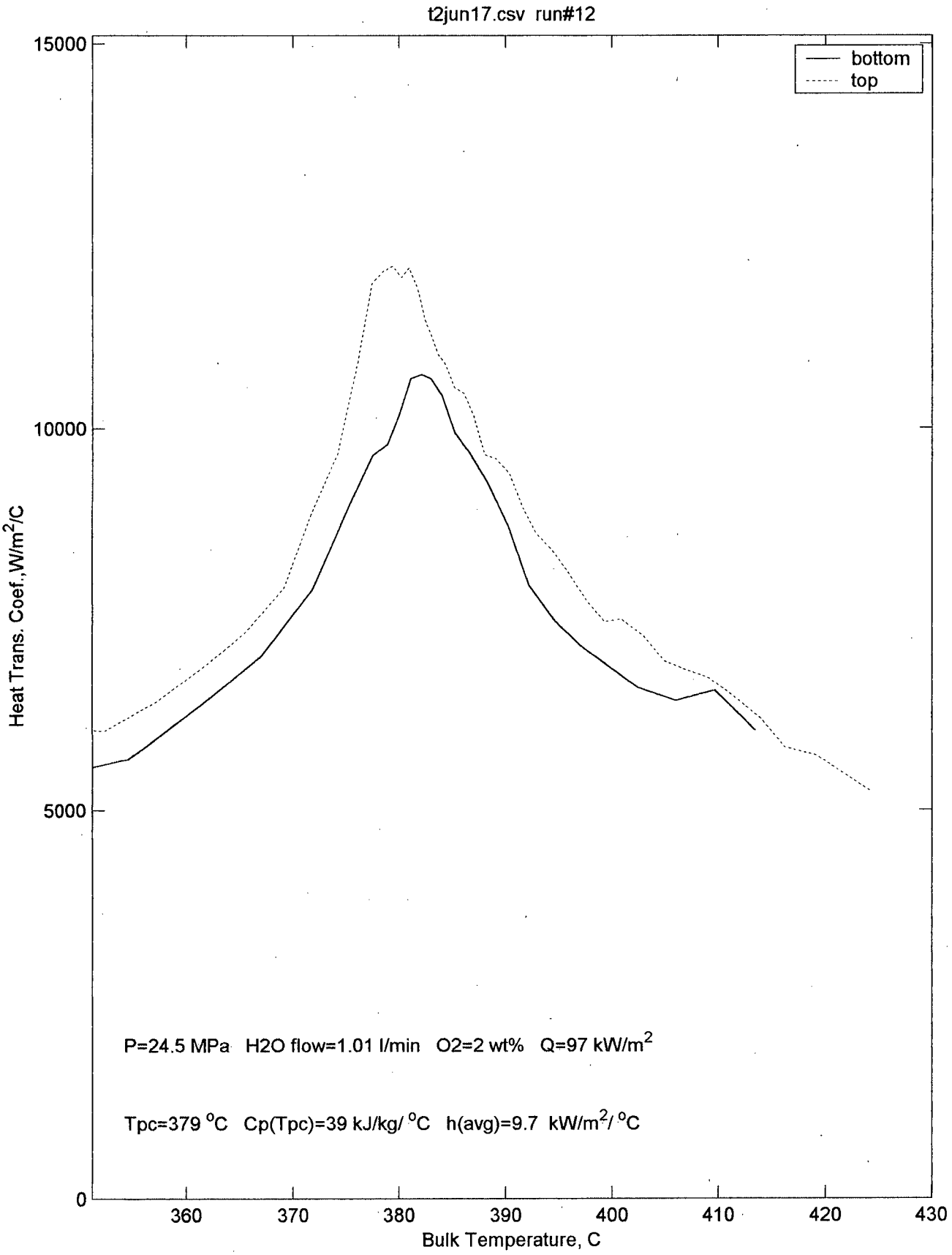

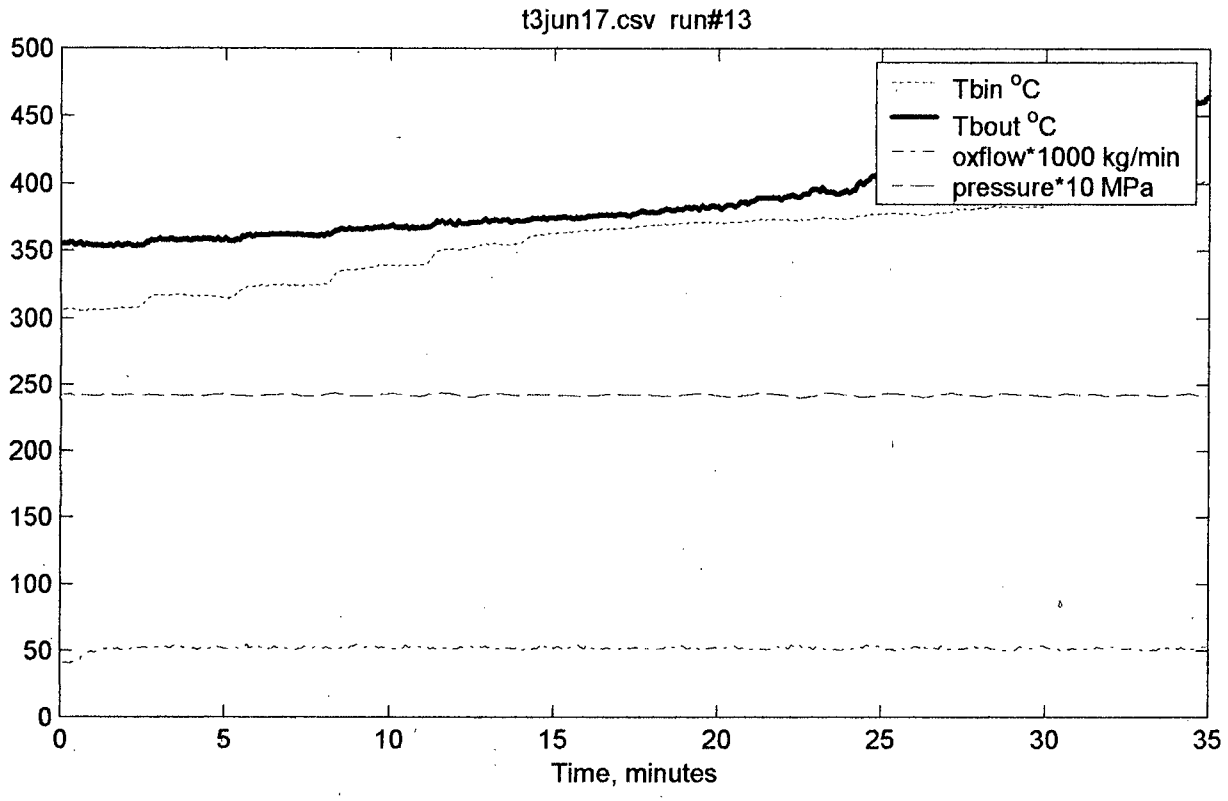

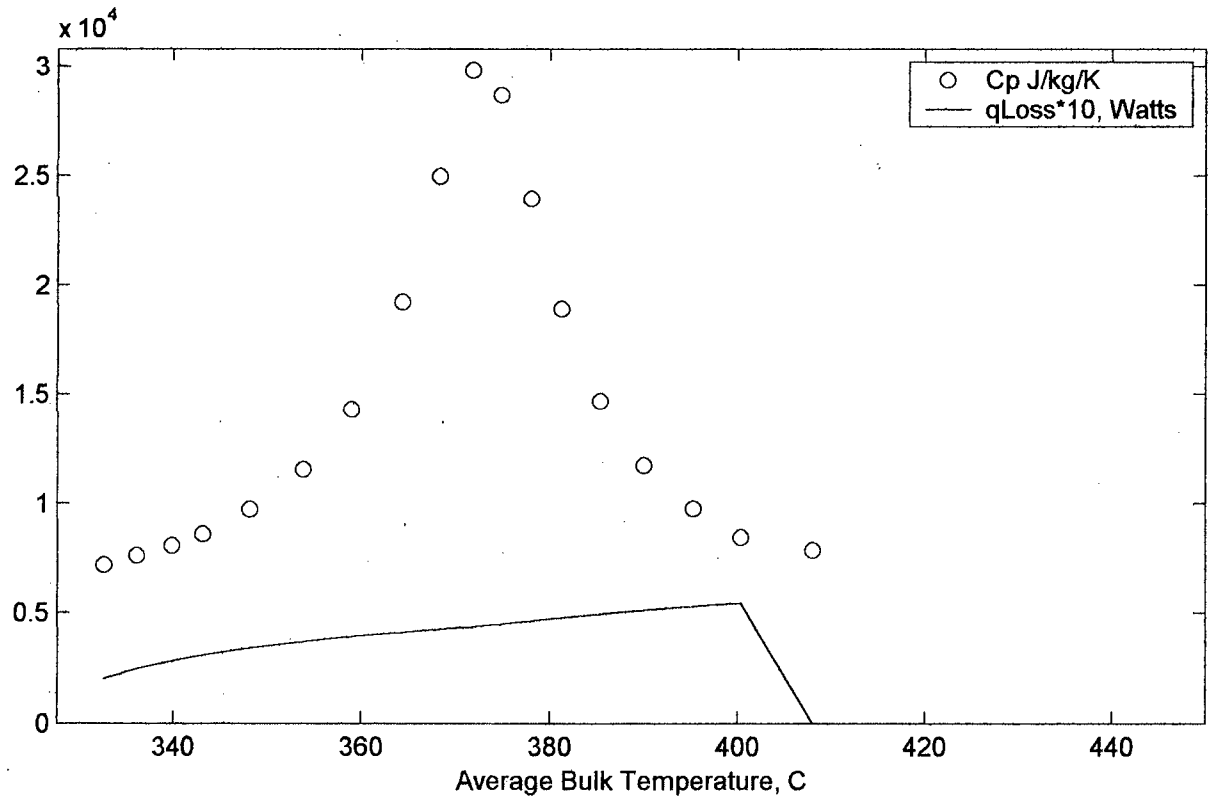

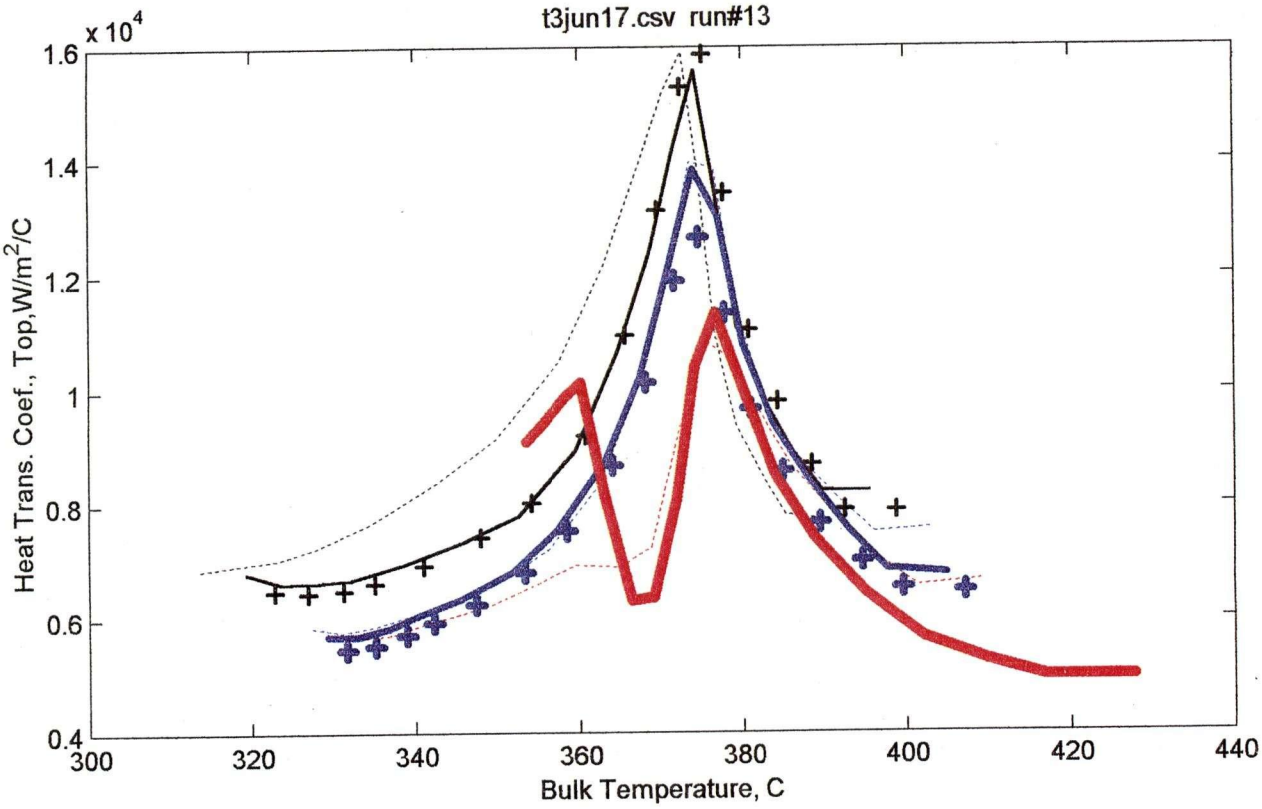

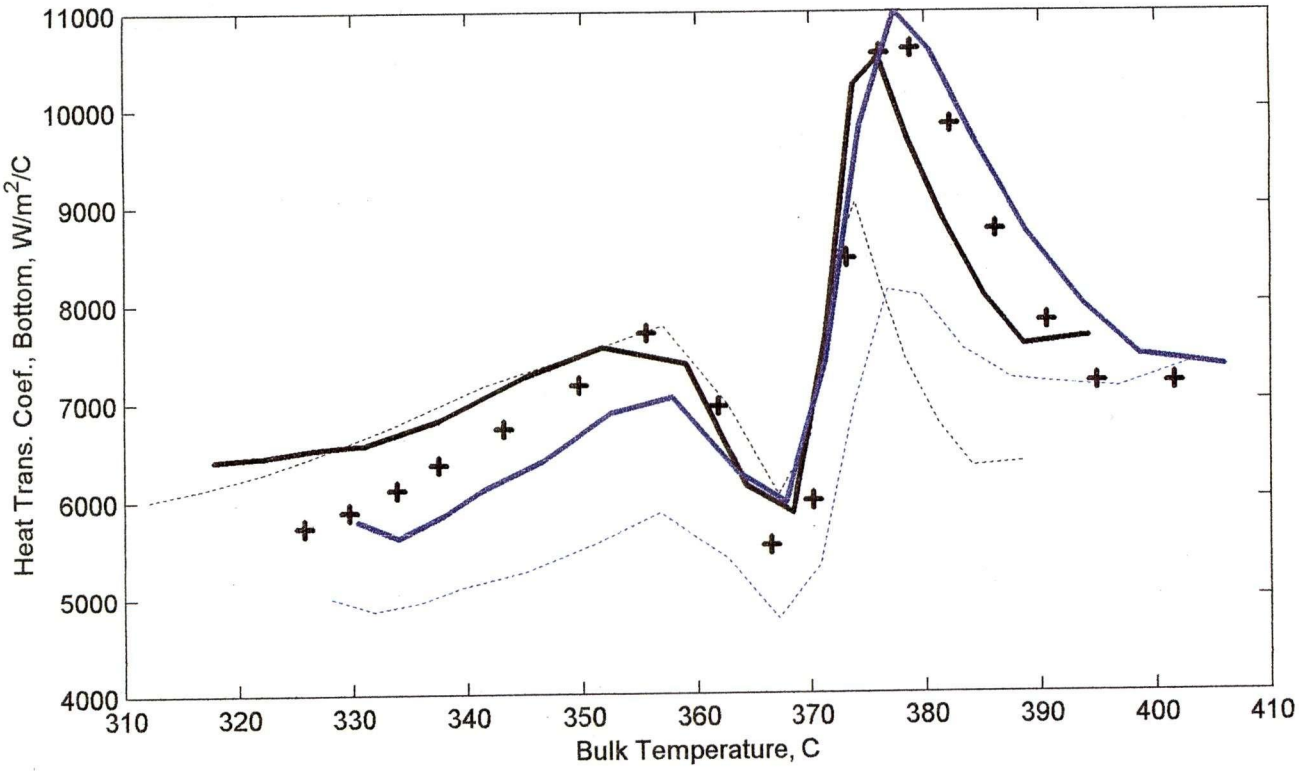

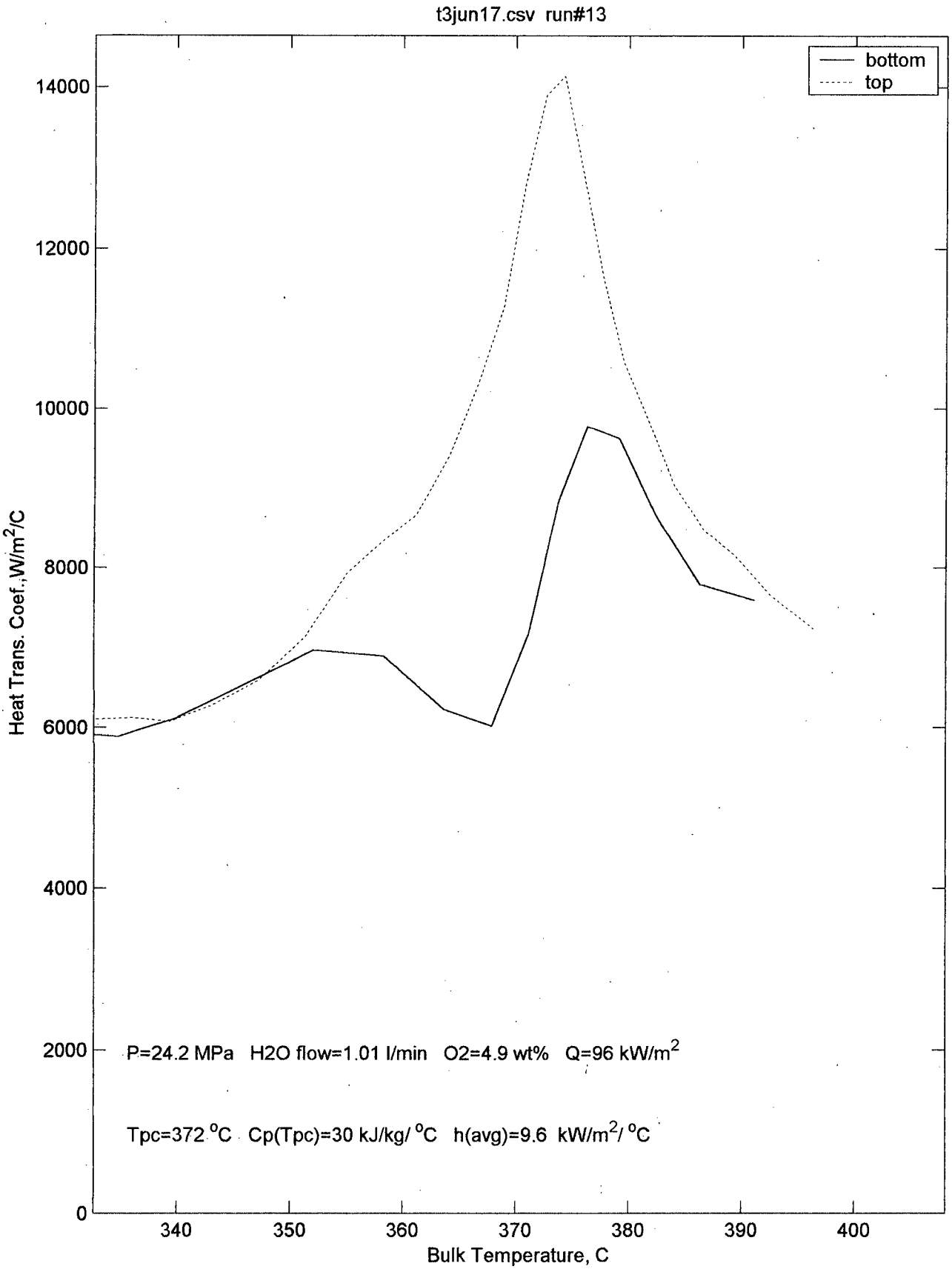

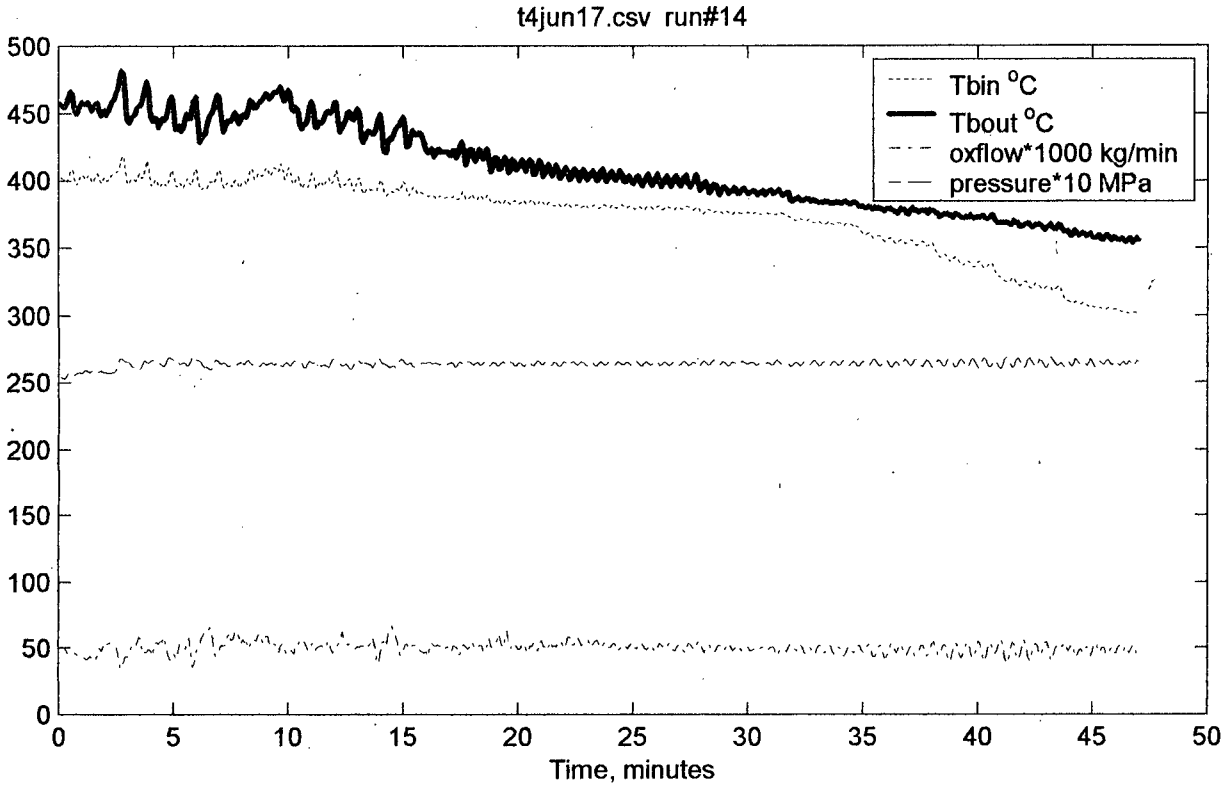

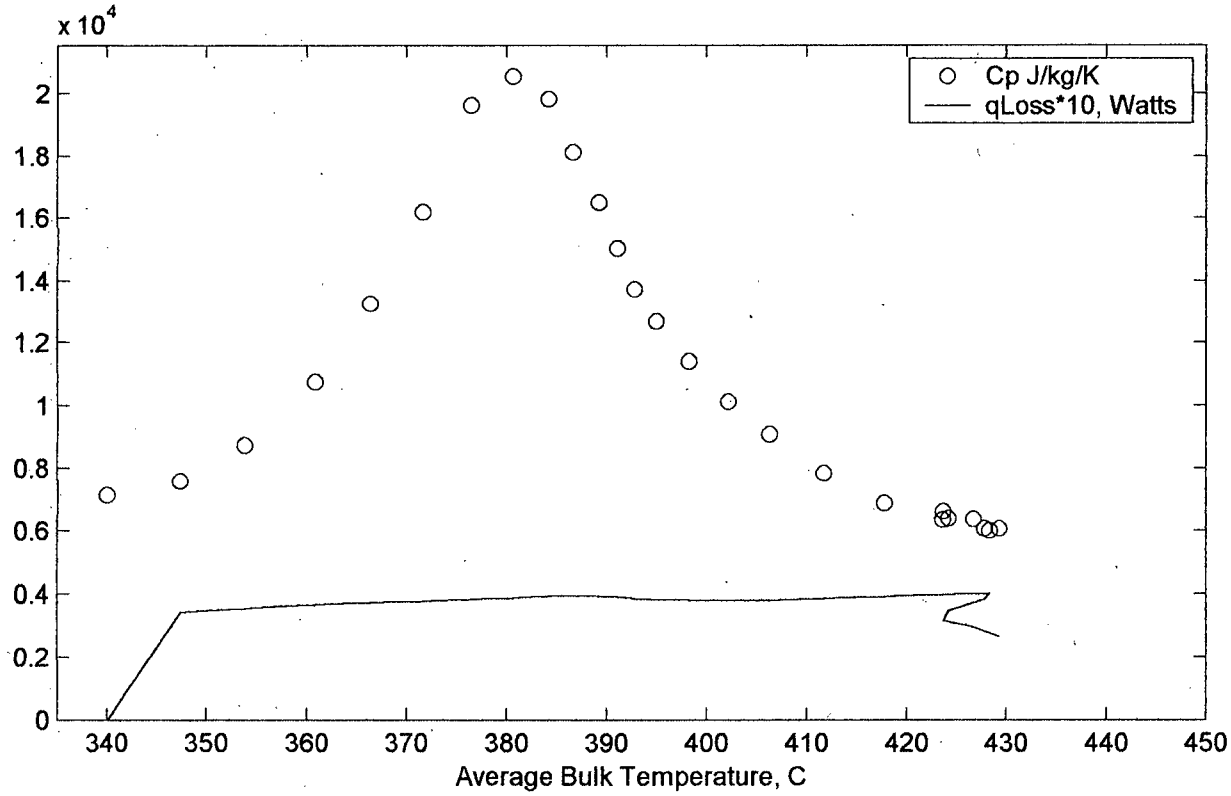

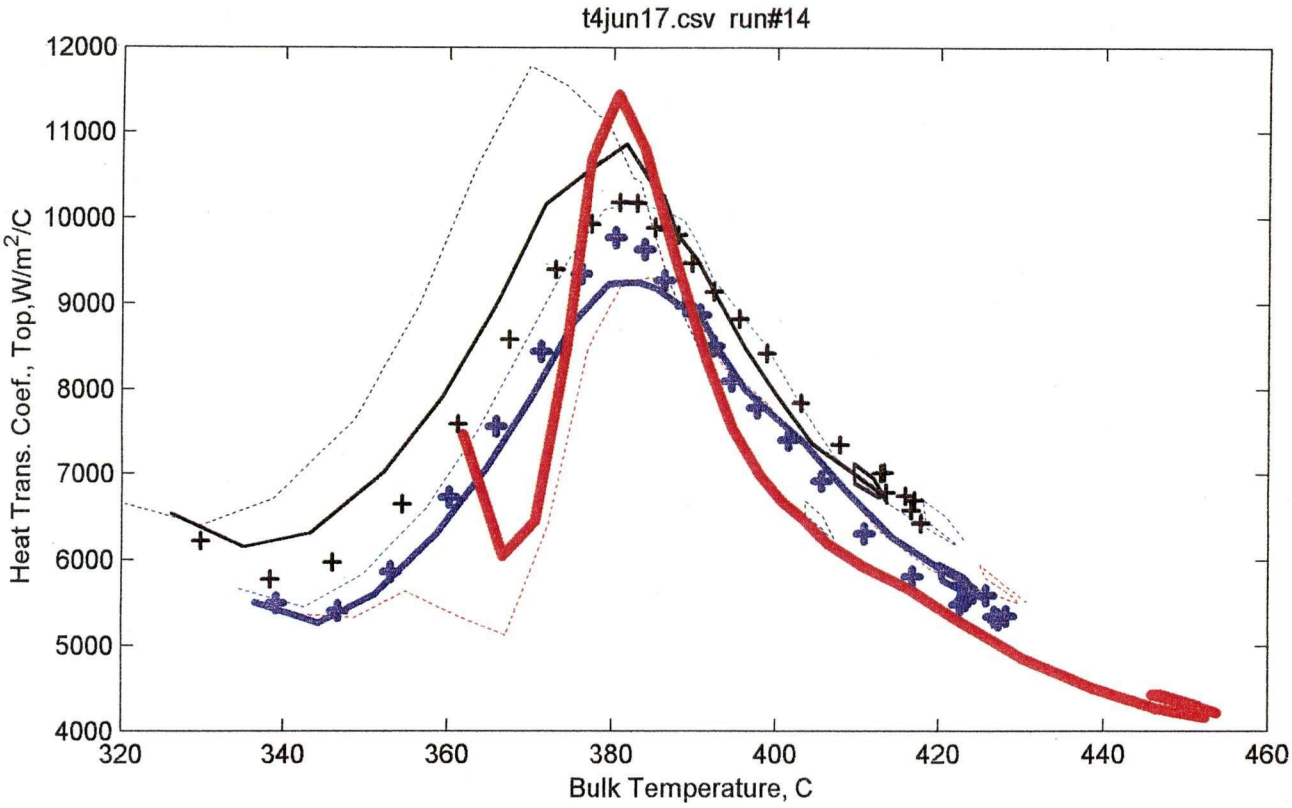

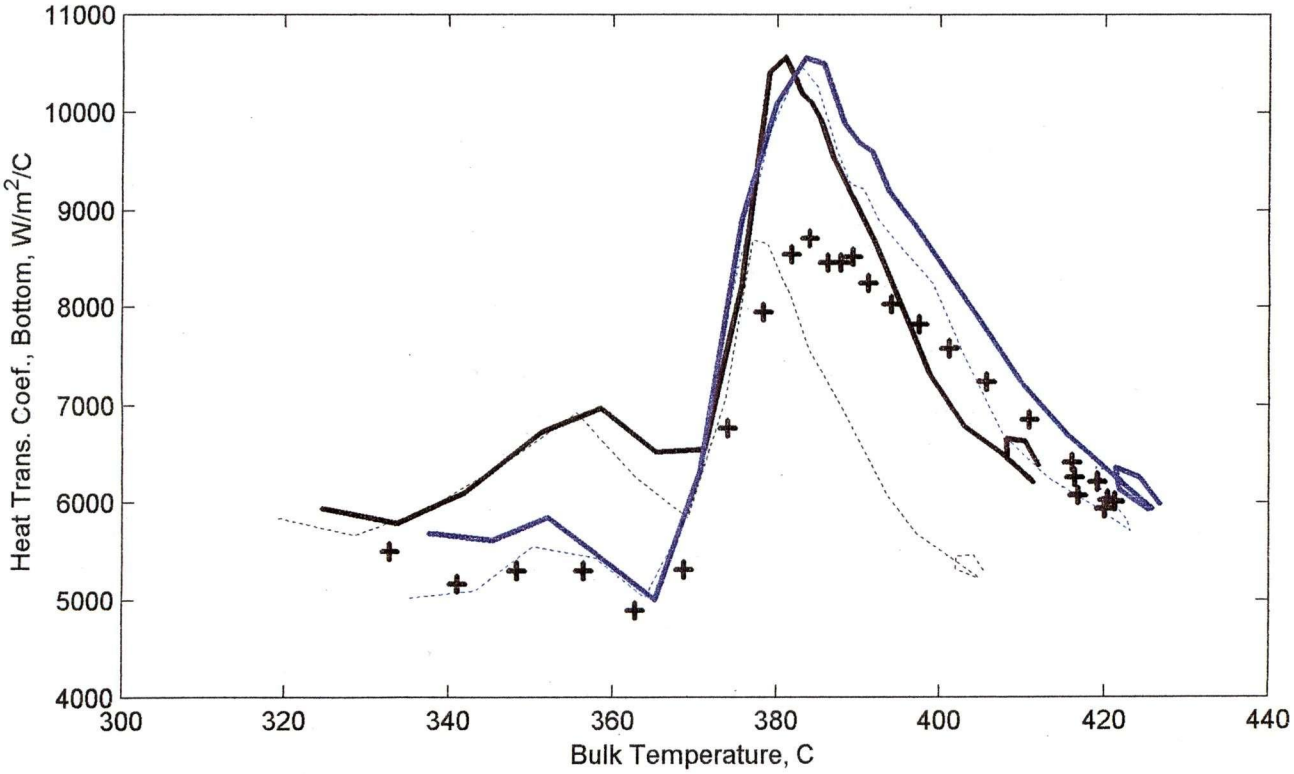

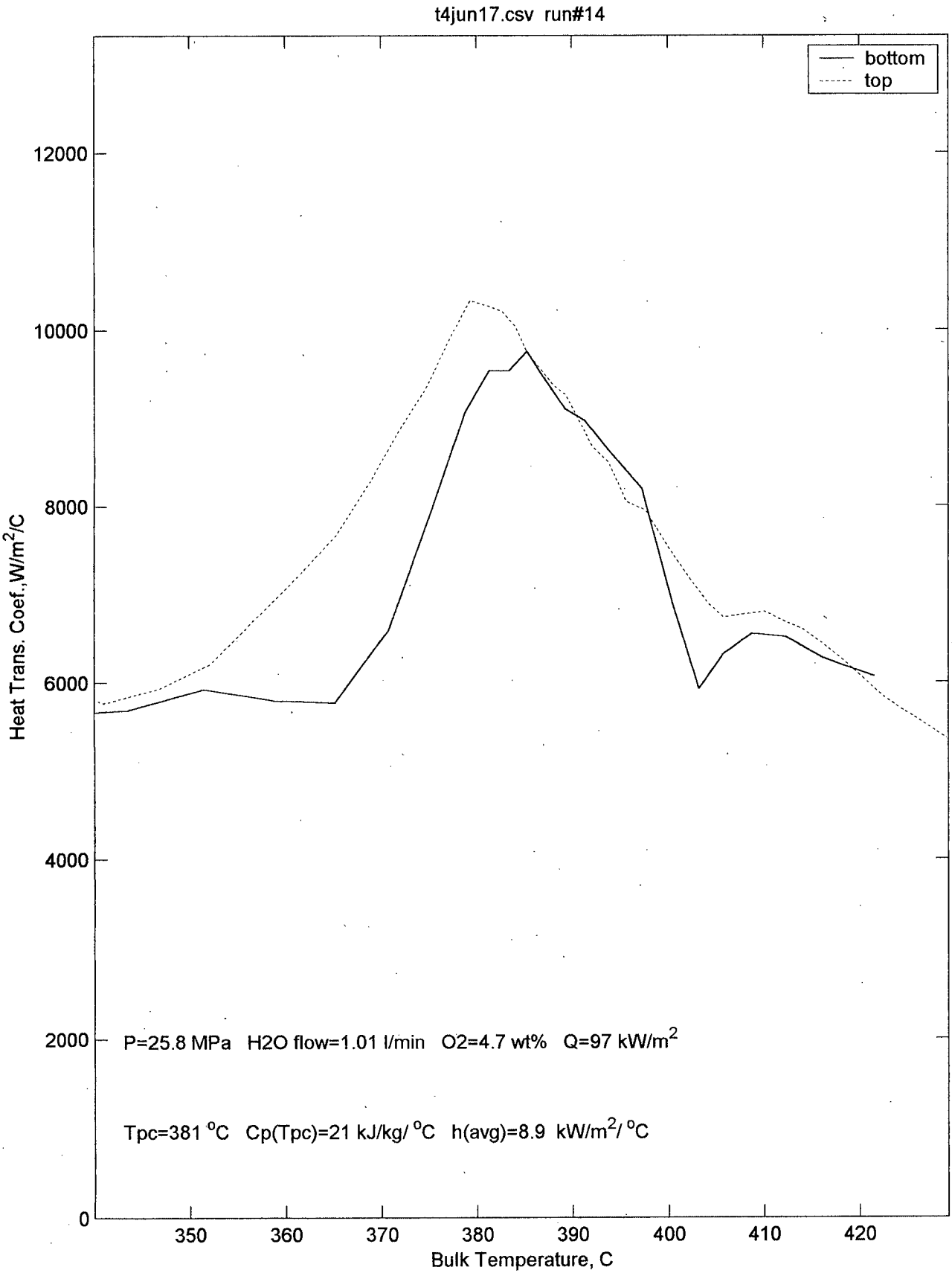

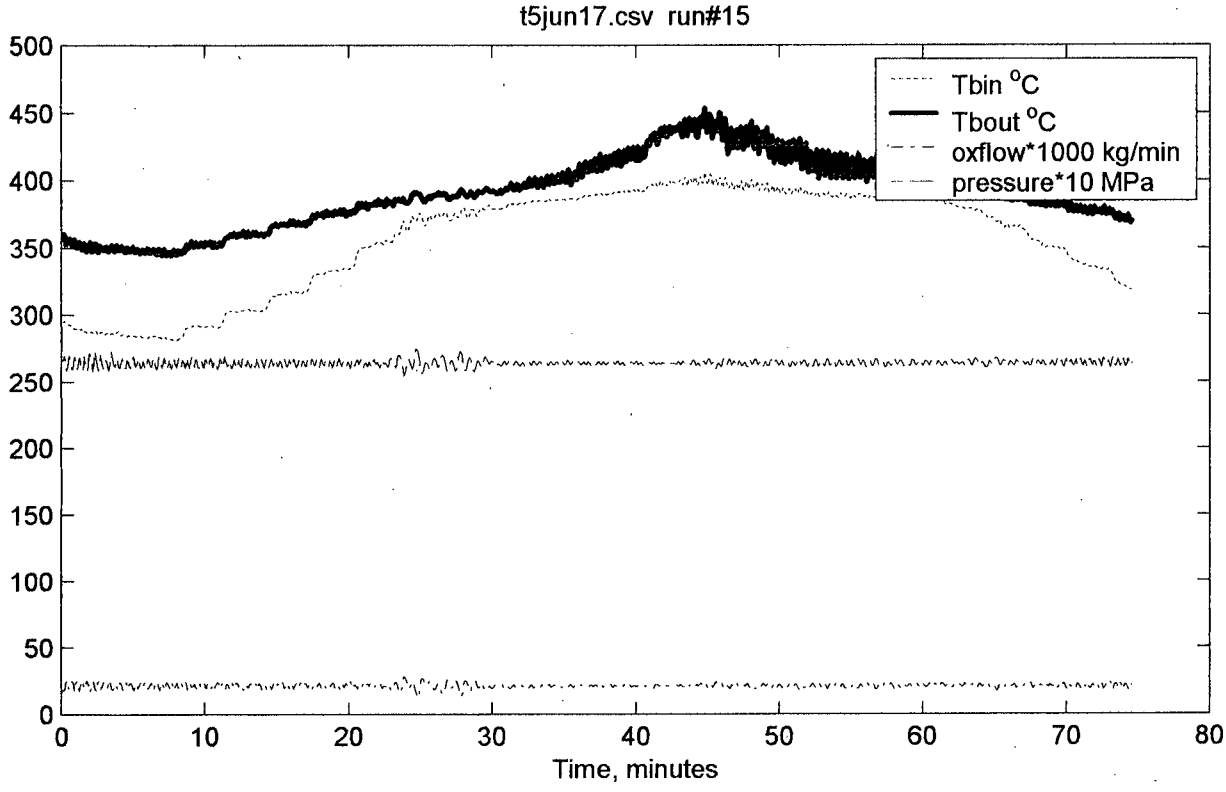

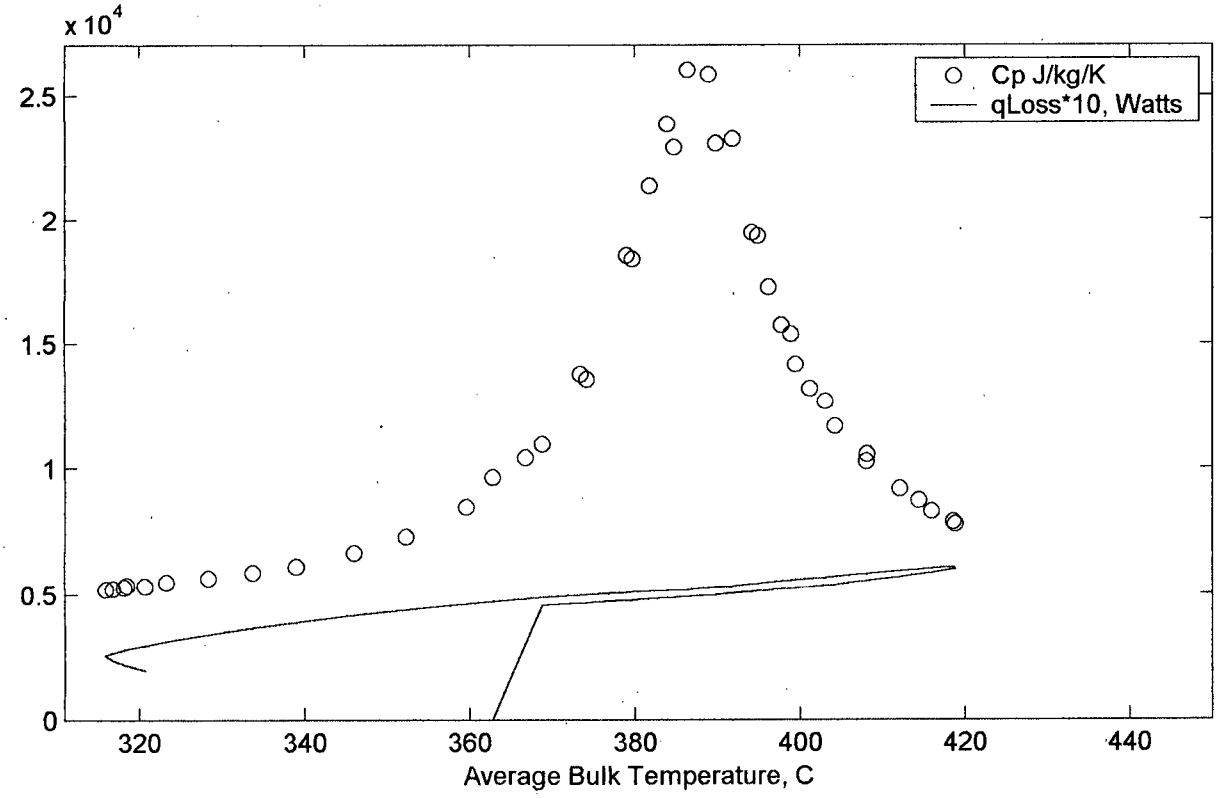

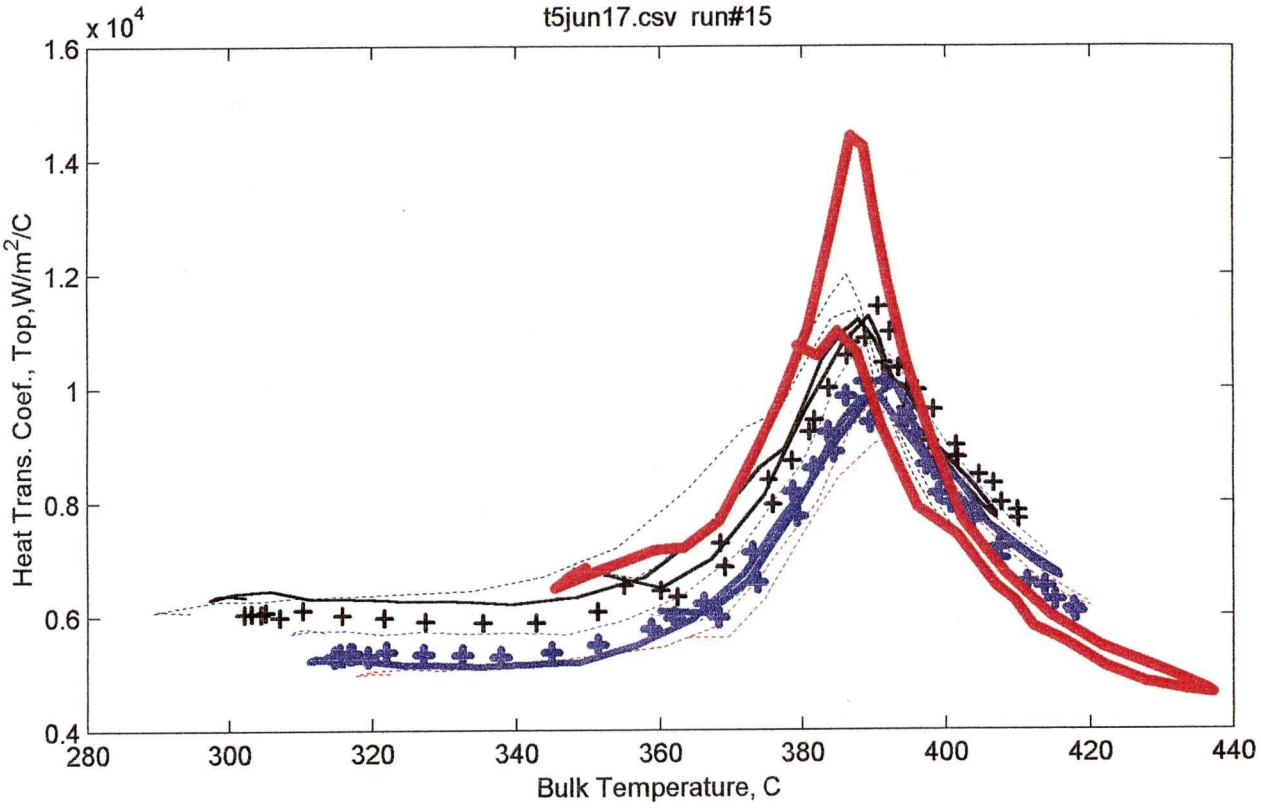

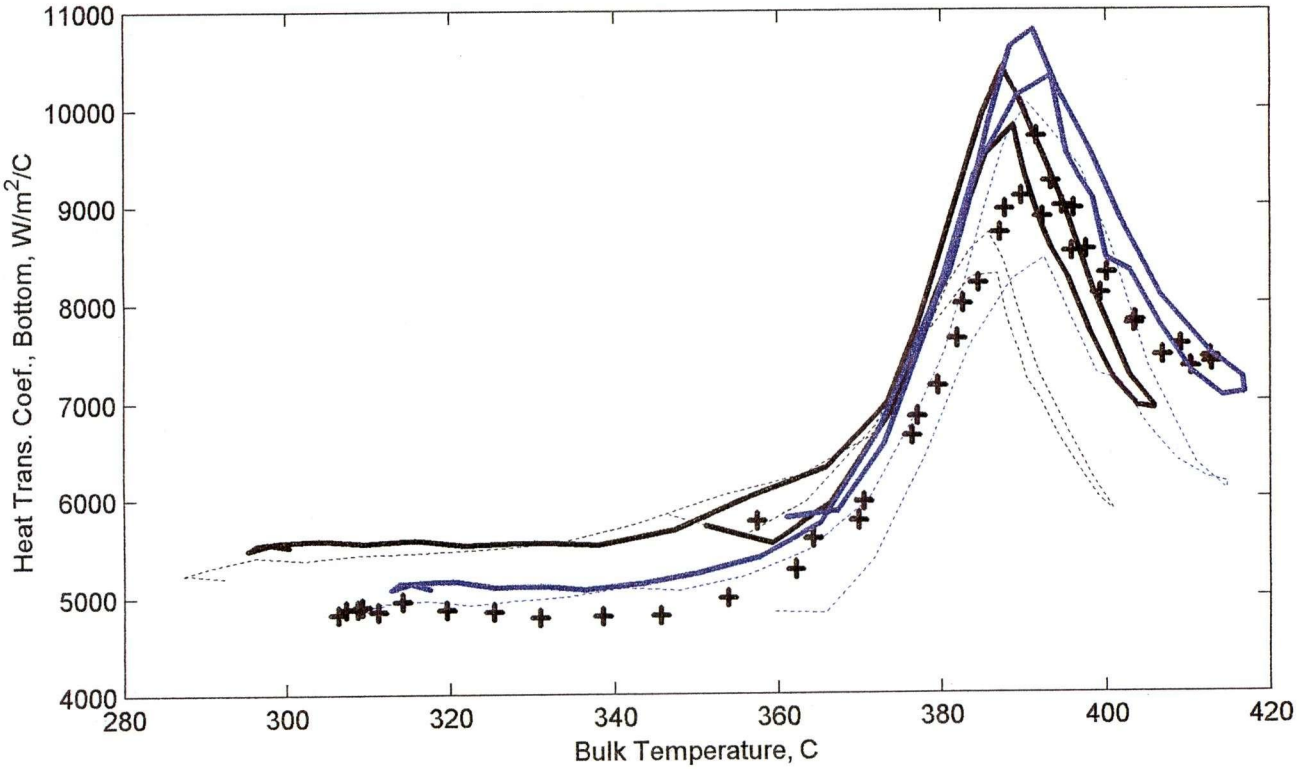

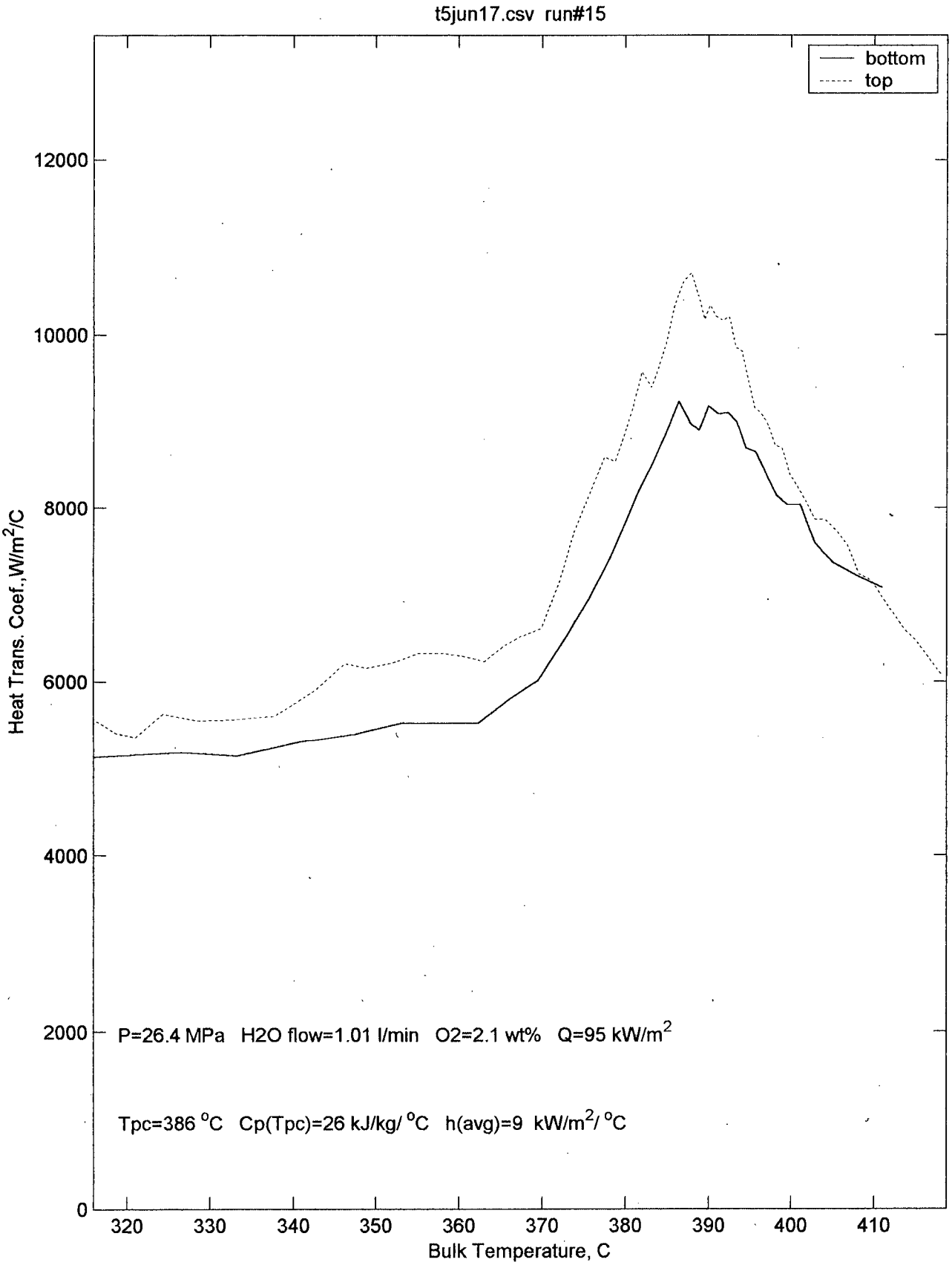

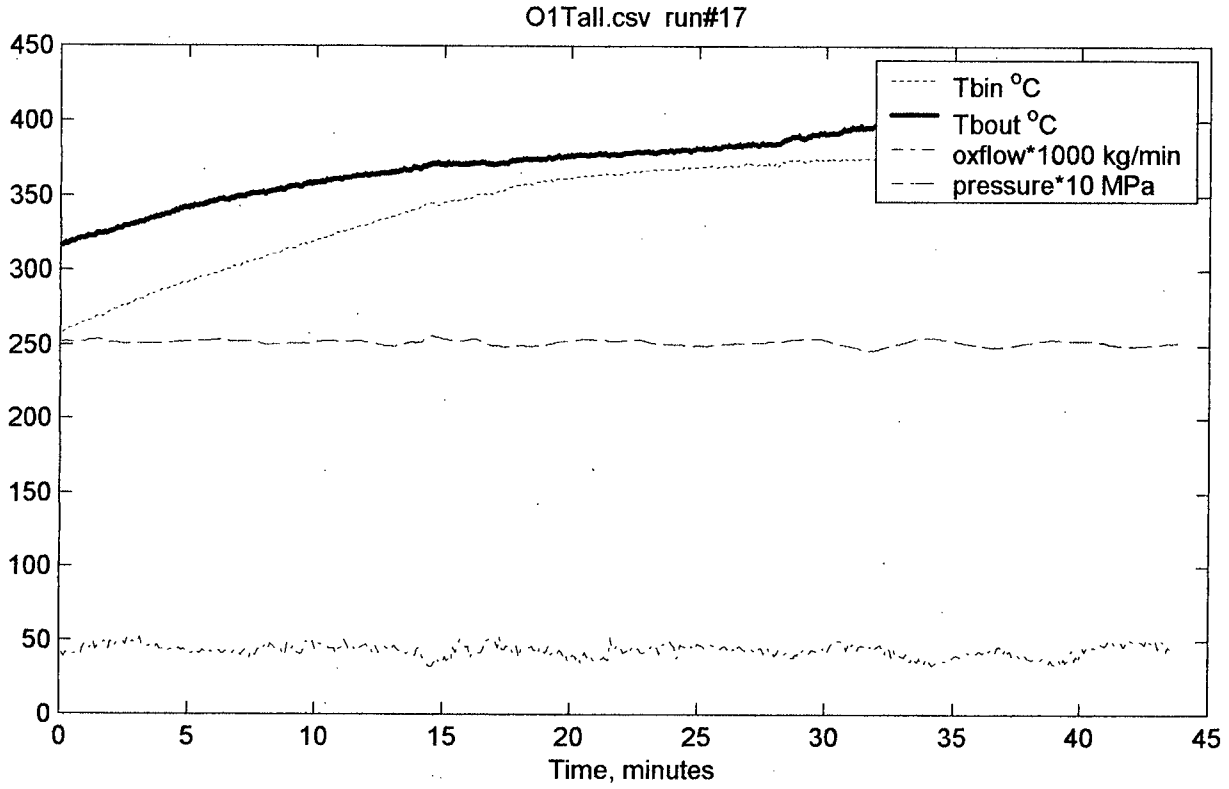

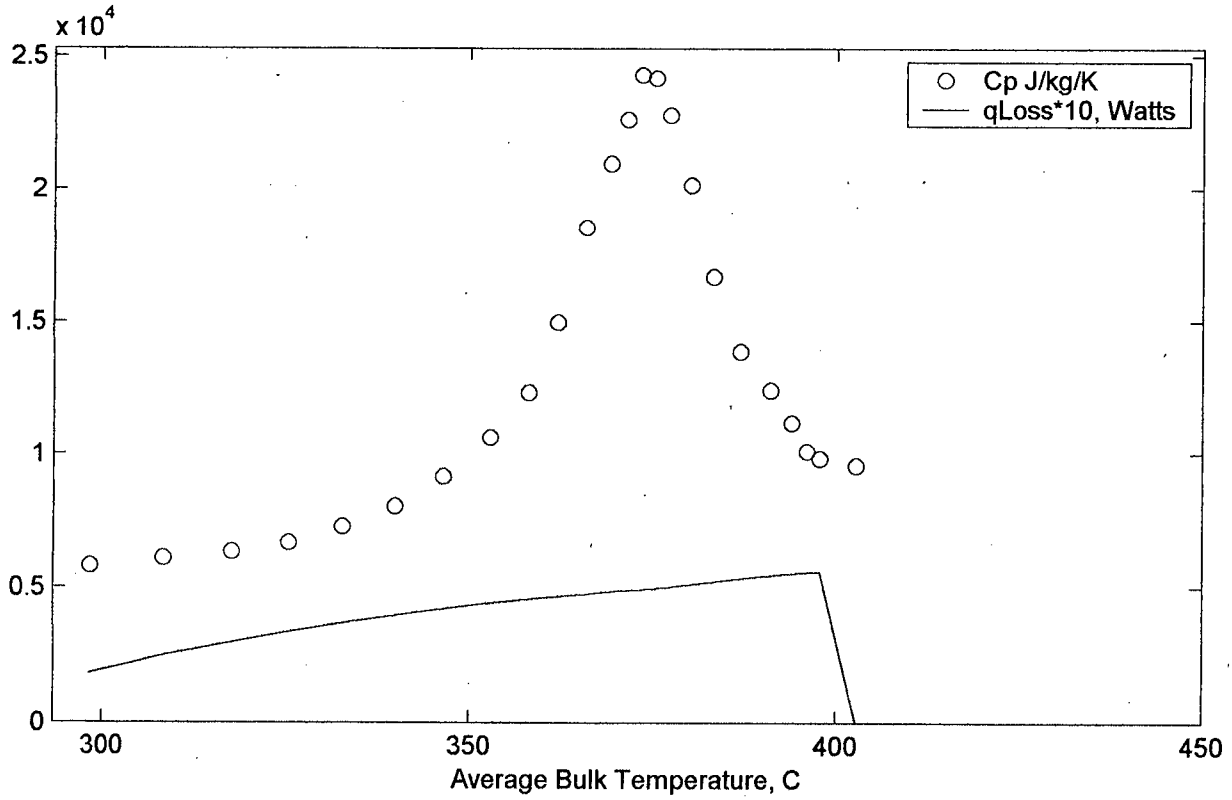

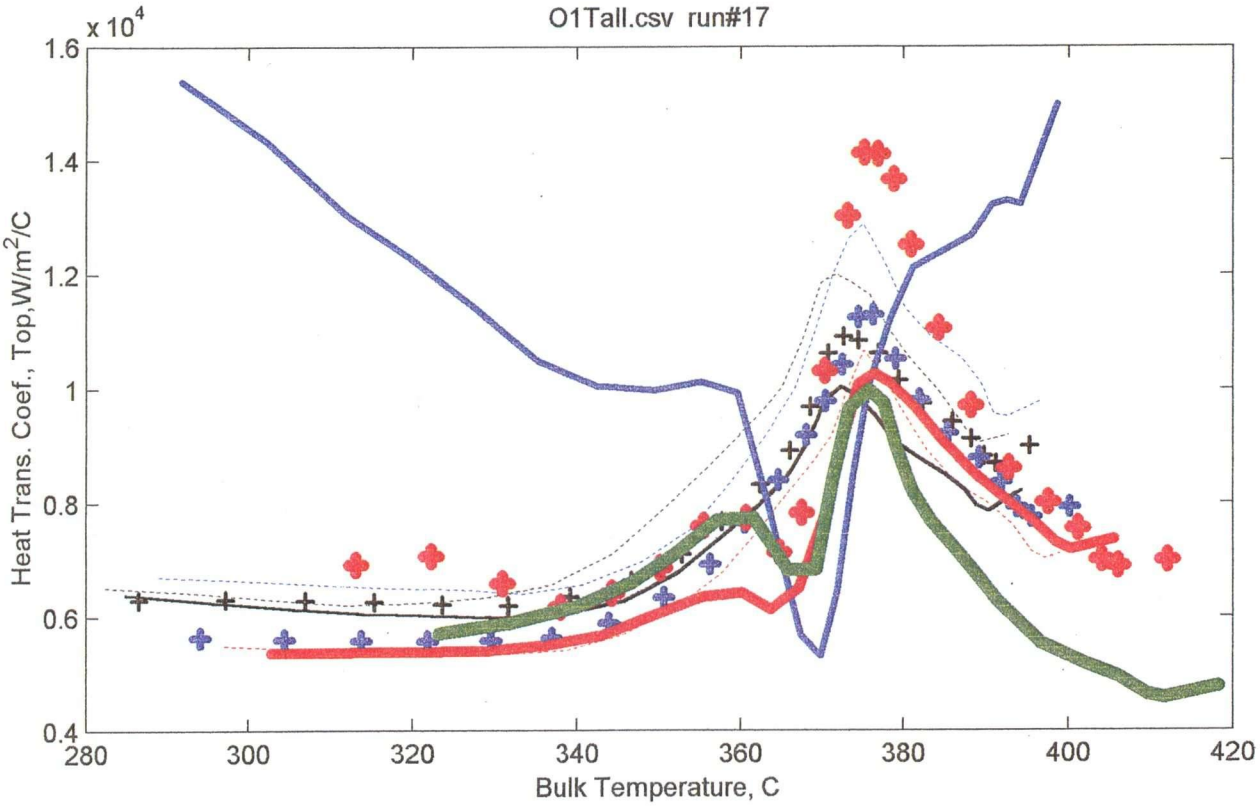

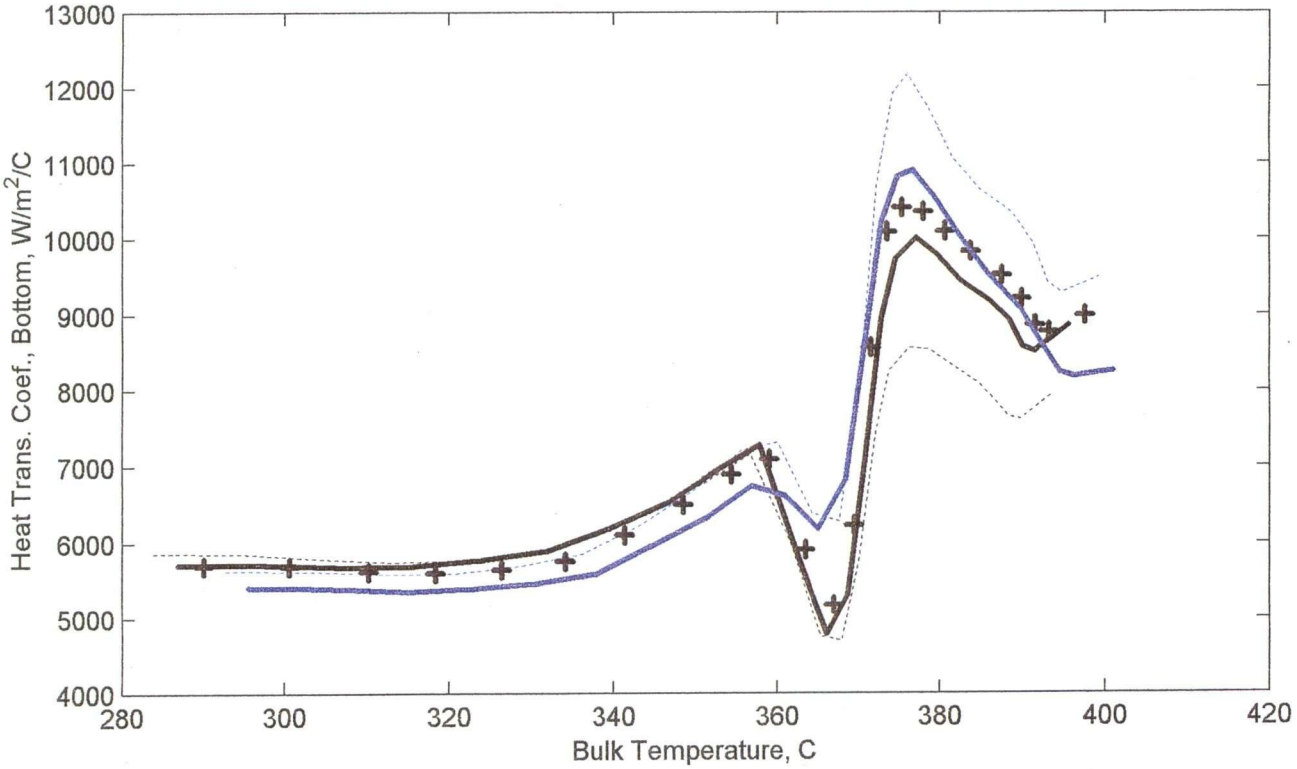

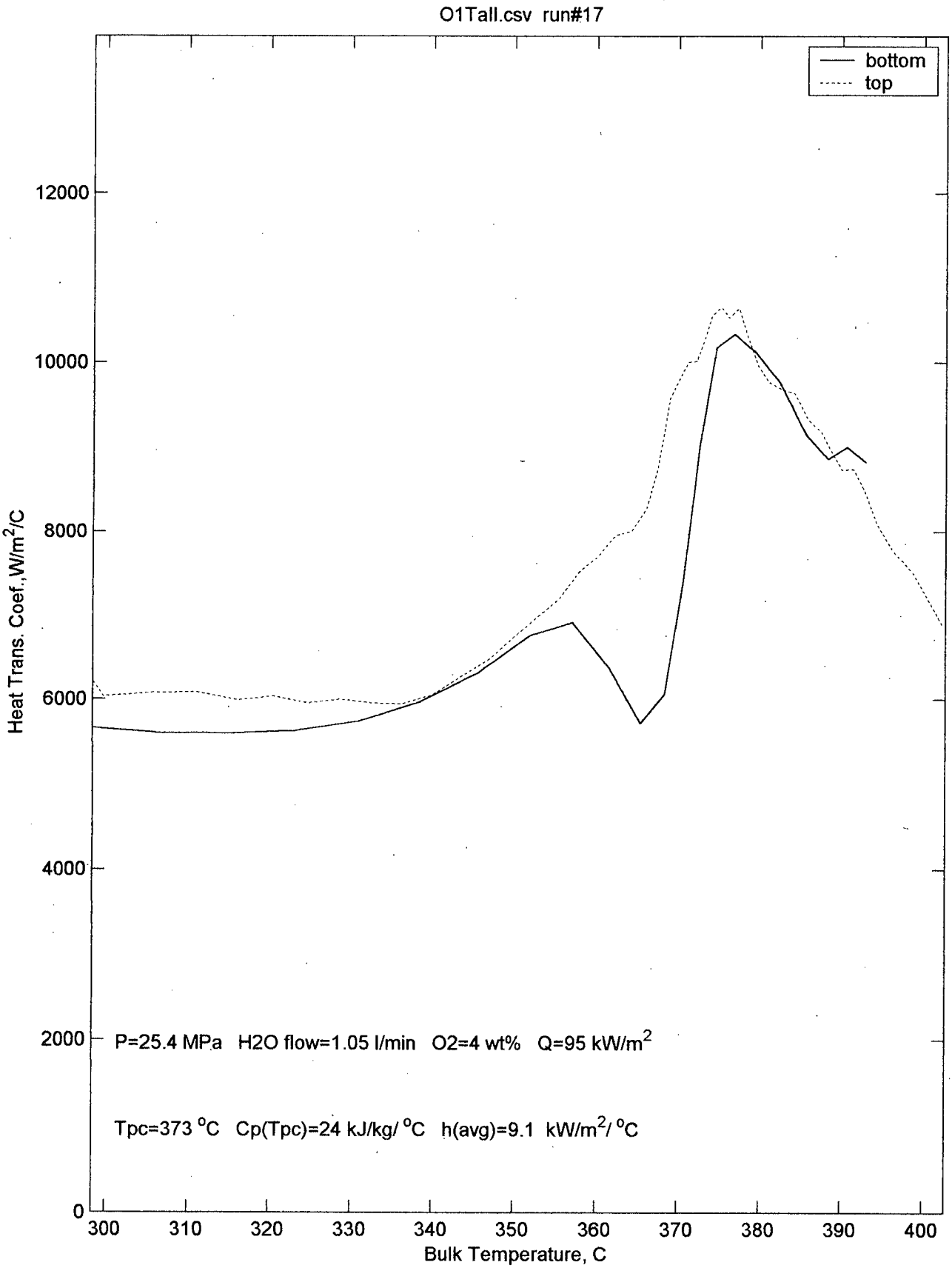

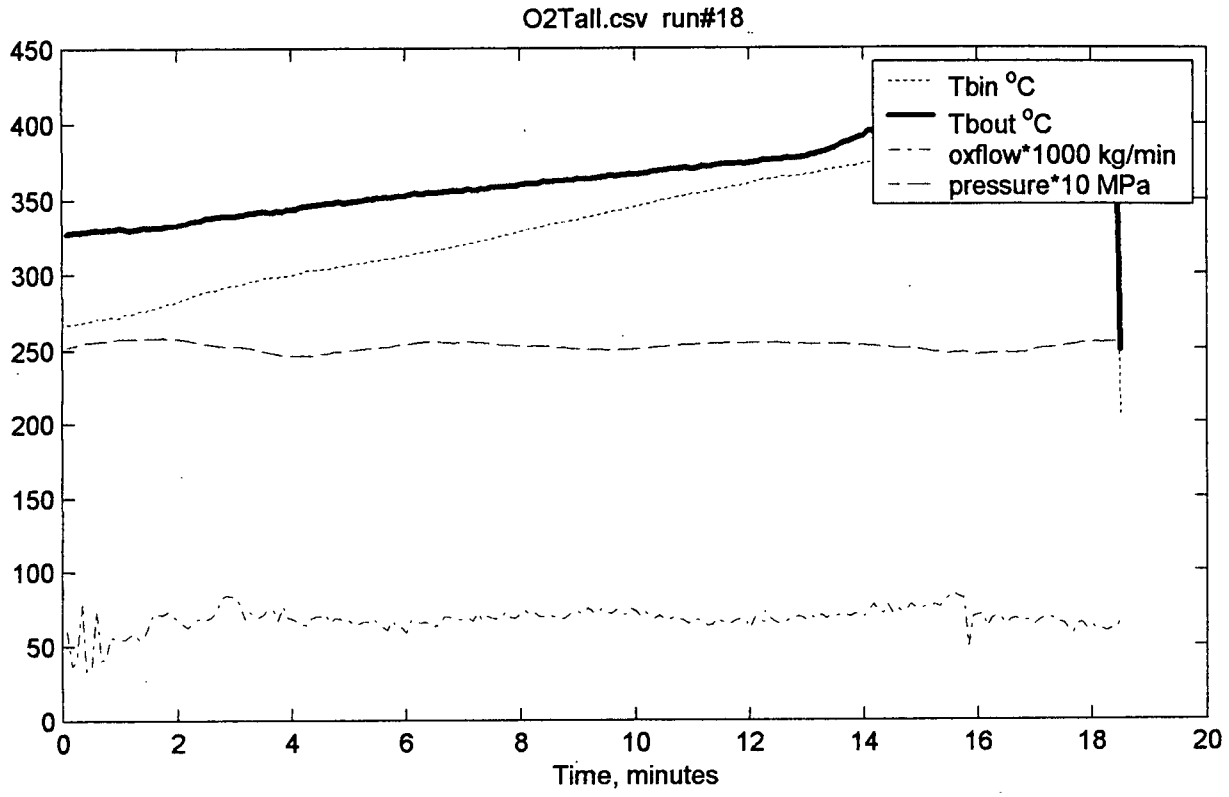
O2Tall.csv run#18
Tbin °C
Tbout °C
oxflow*1000 kg/min
pressure*10 MPa
Time, minutes

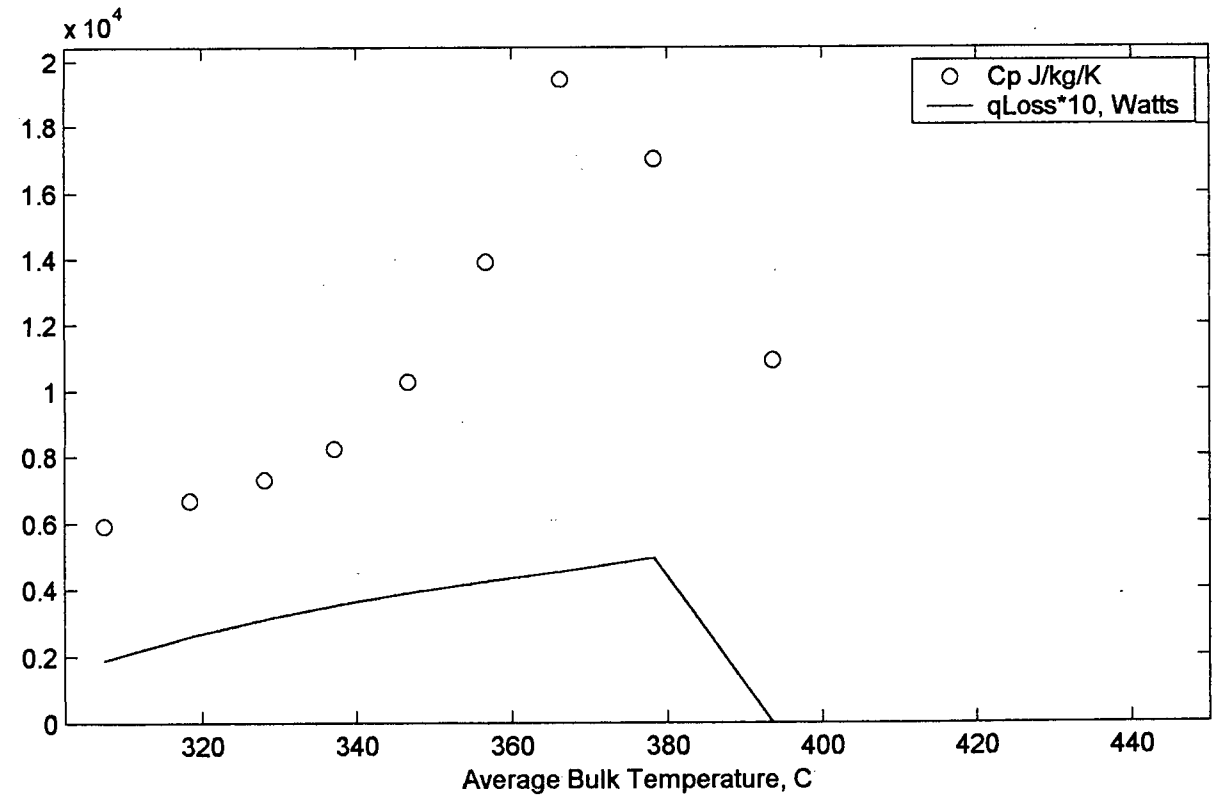
x 10^4
Cp J/kg/K
qLoss*10, Watts
Average Bulk Temperature, C

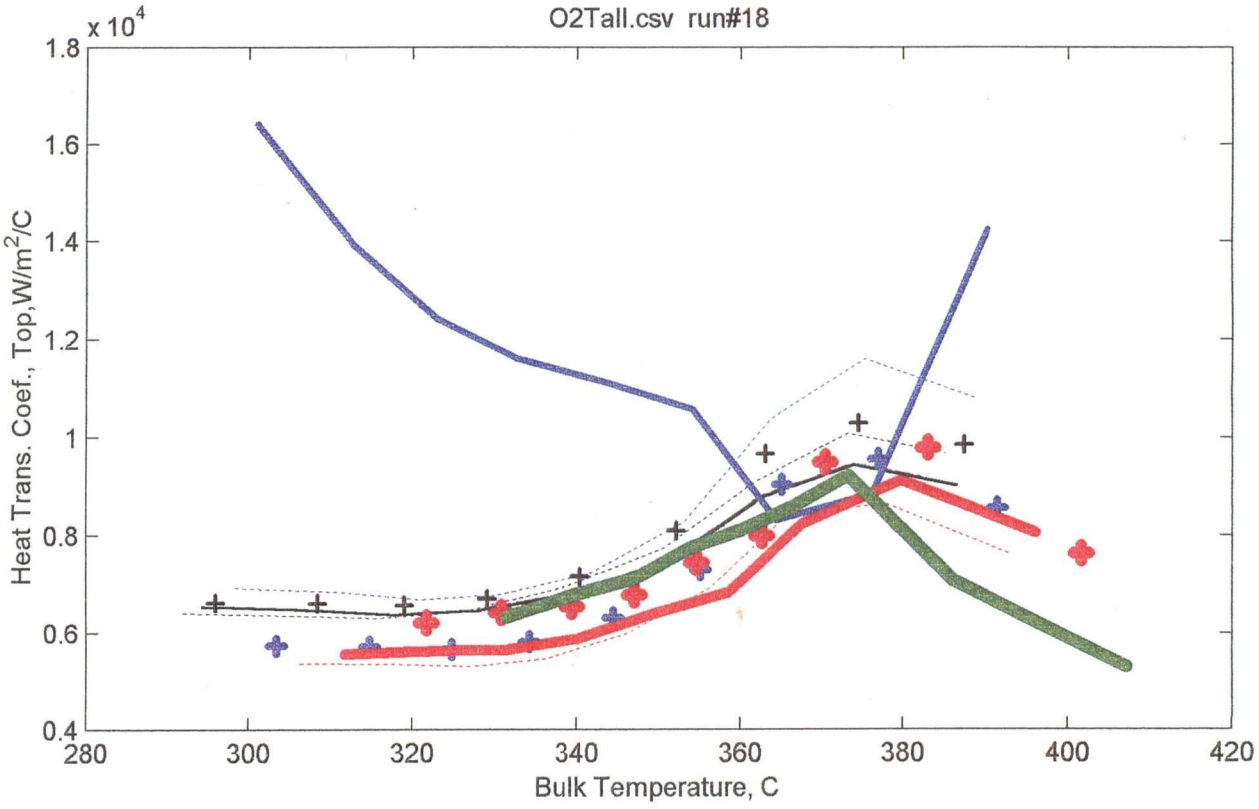

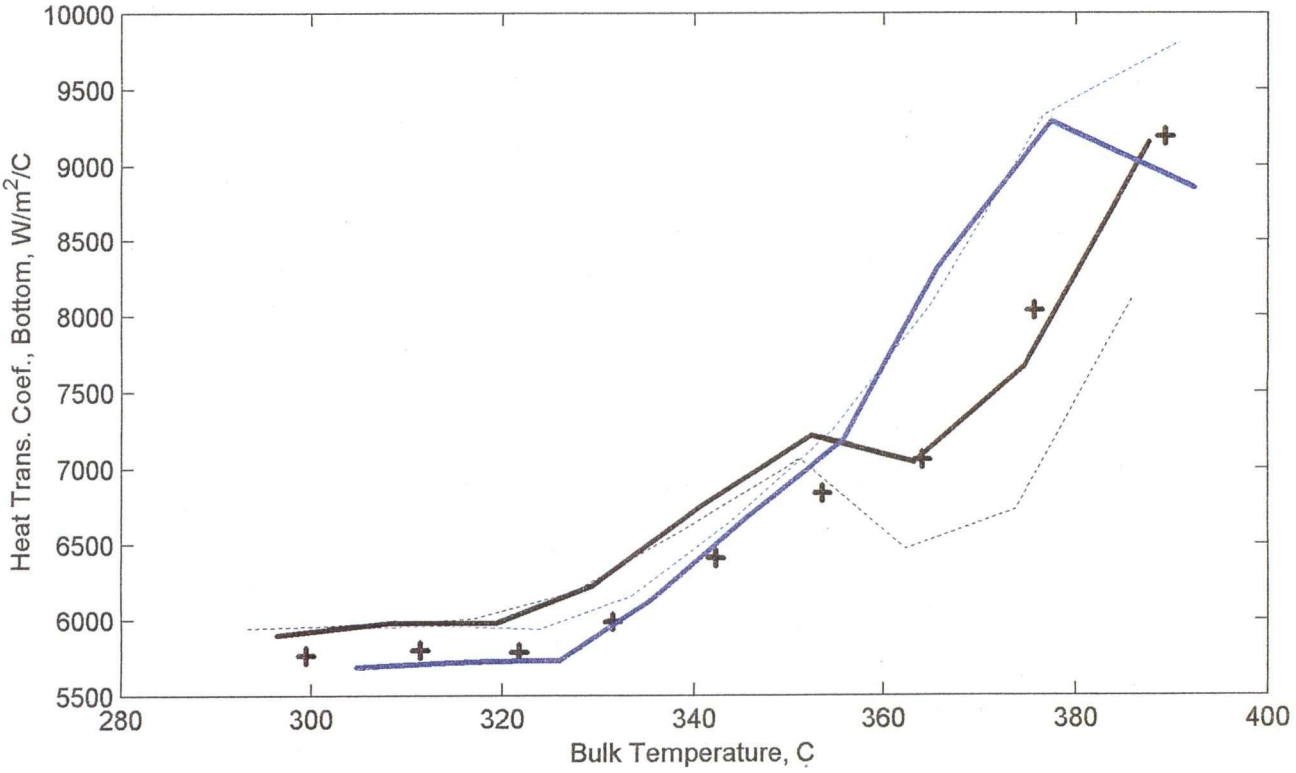

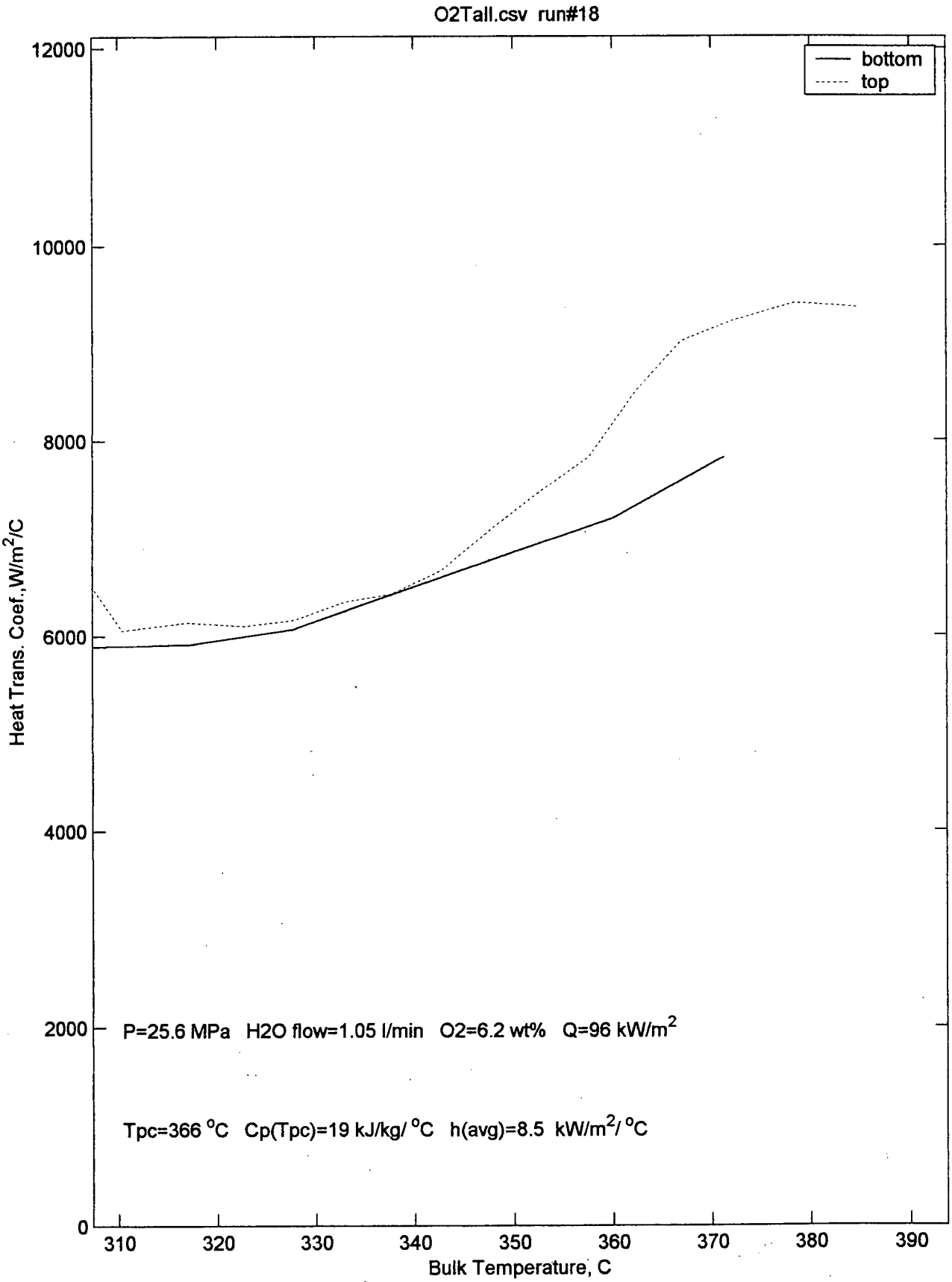

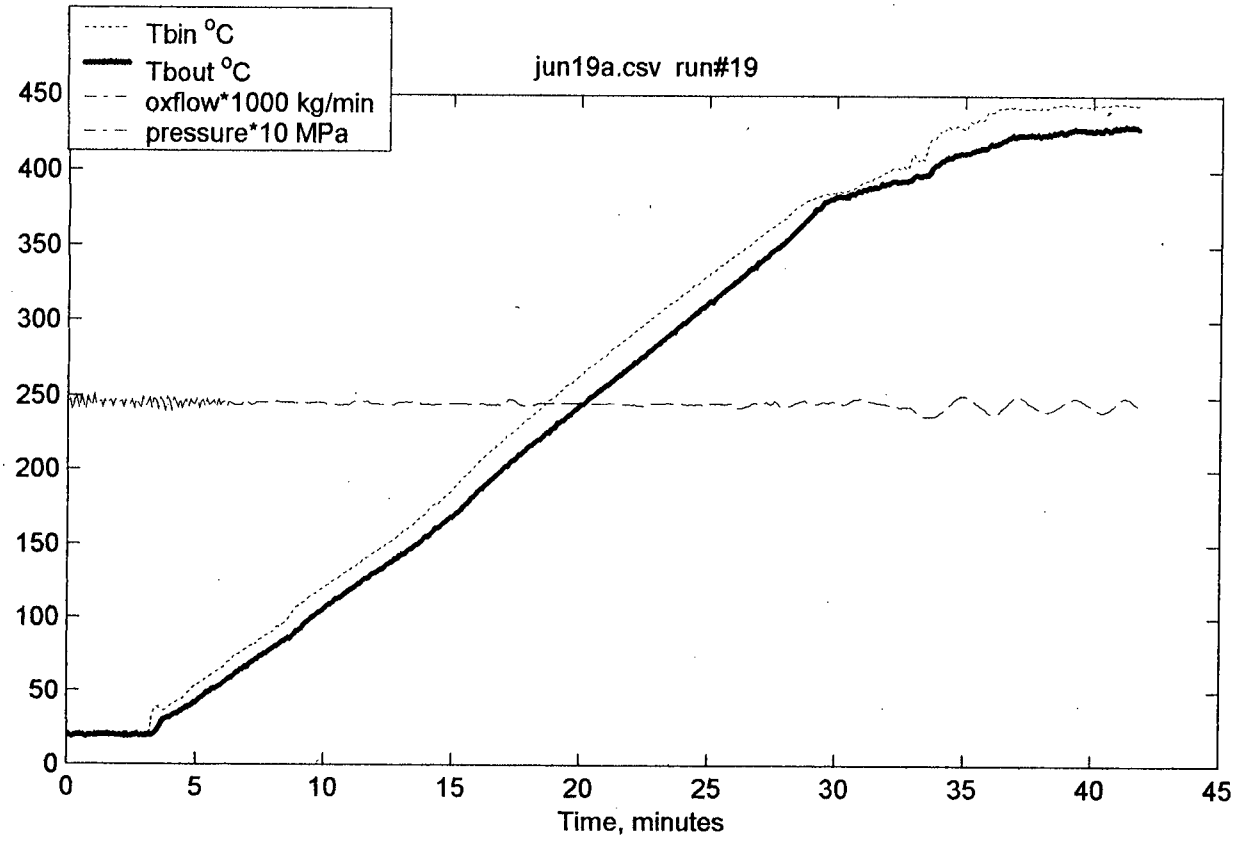

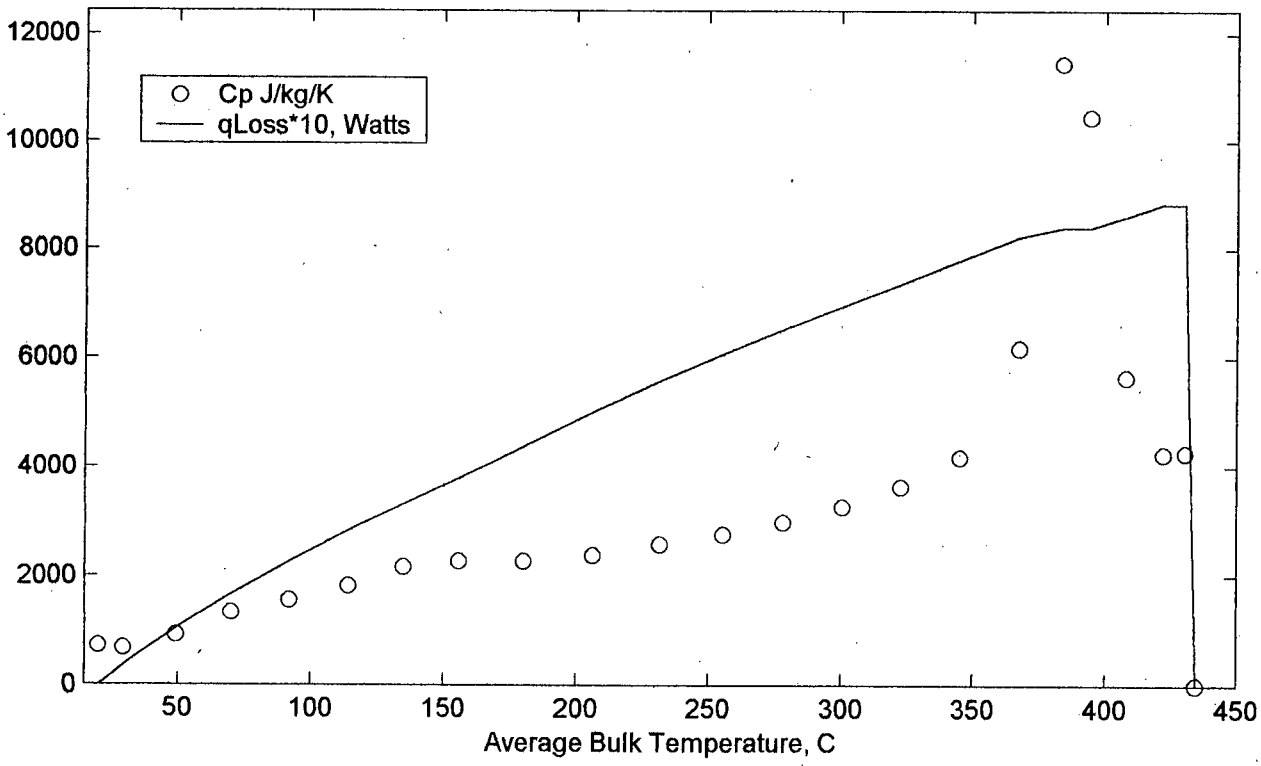

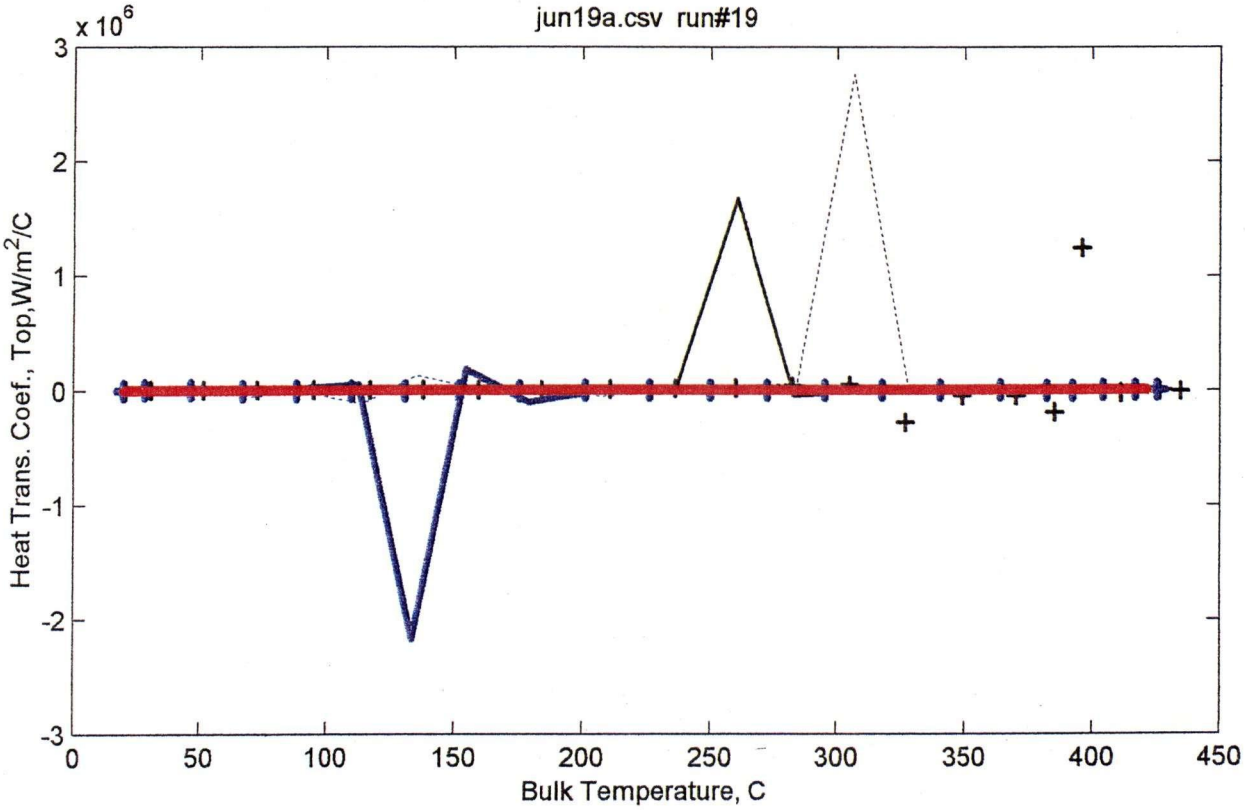

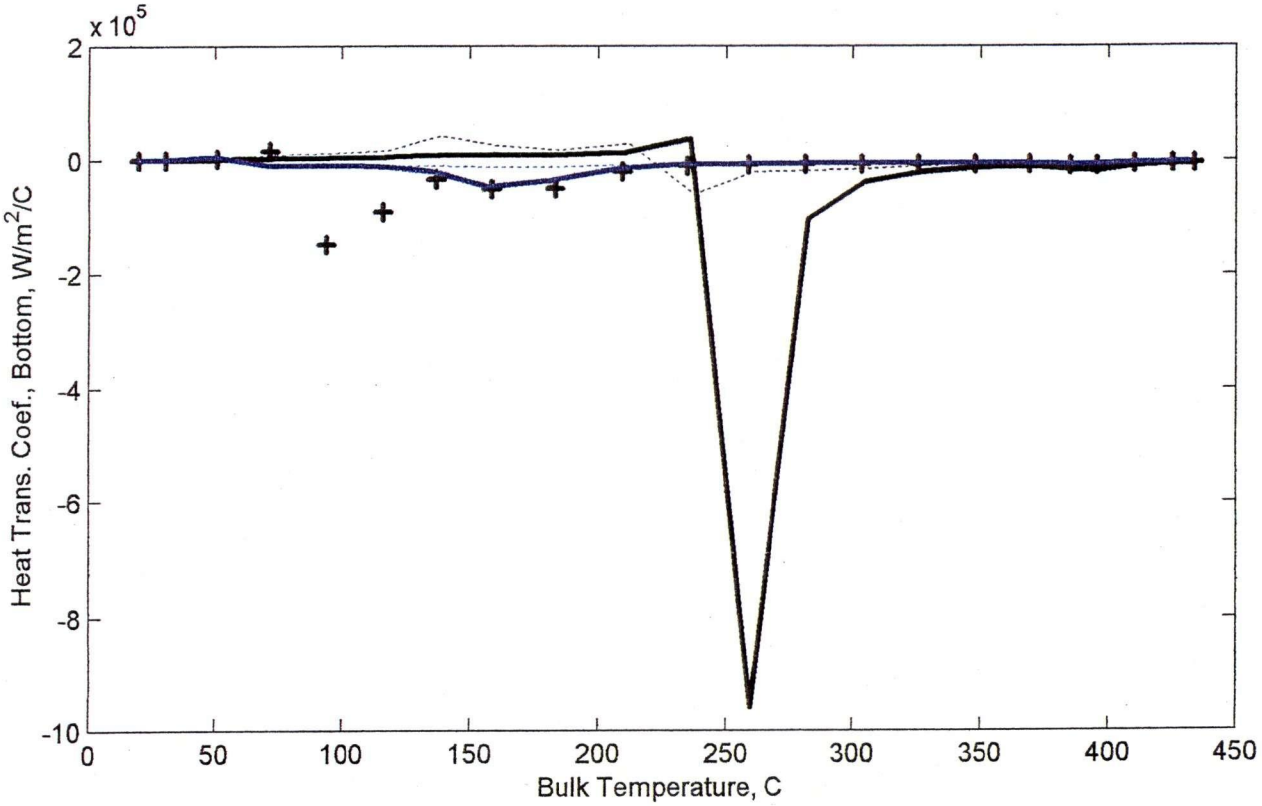

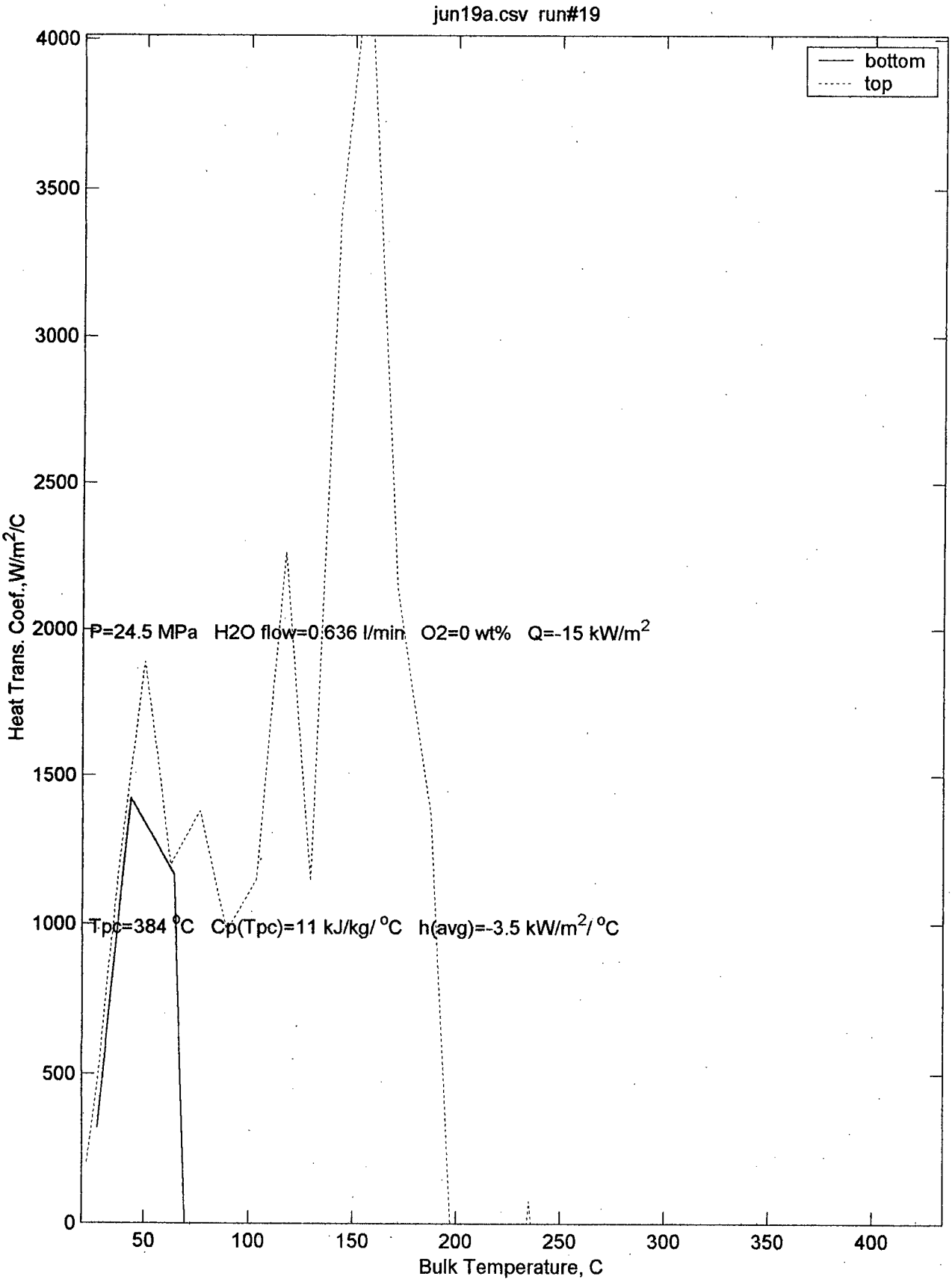

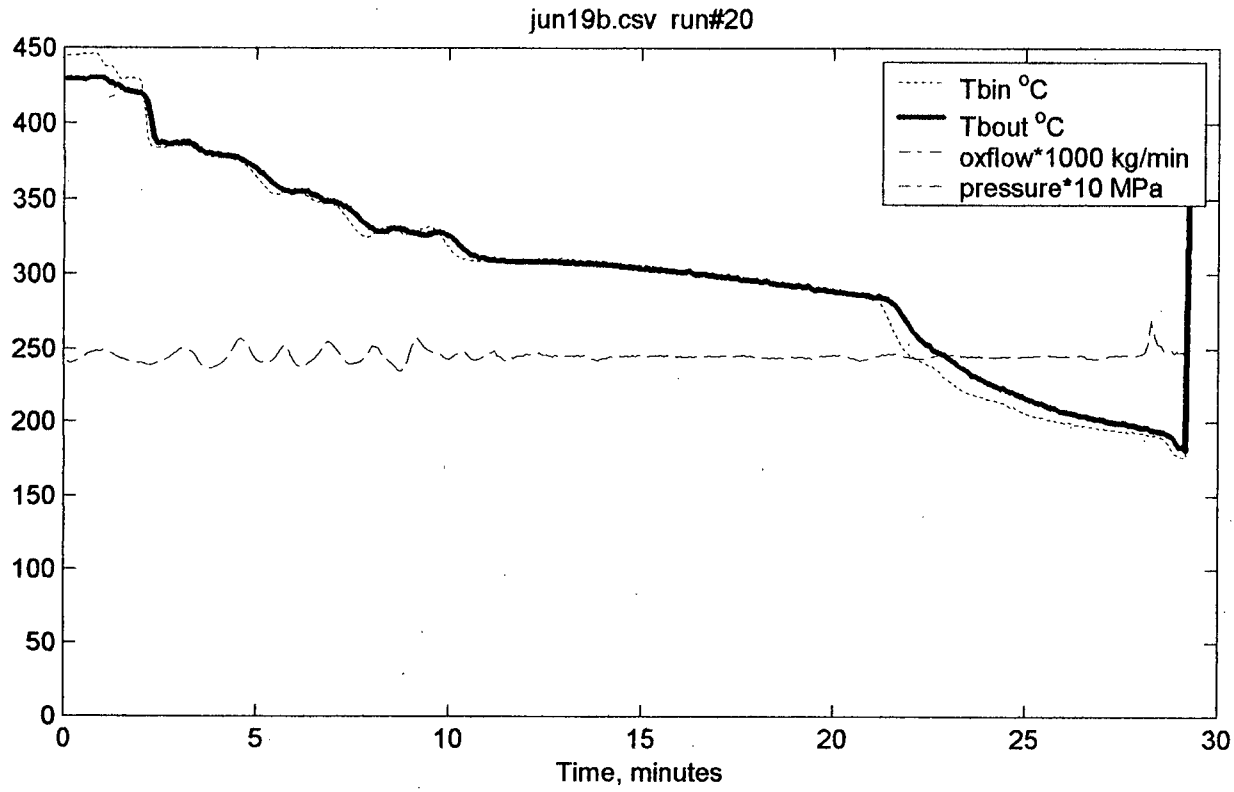

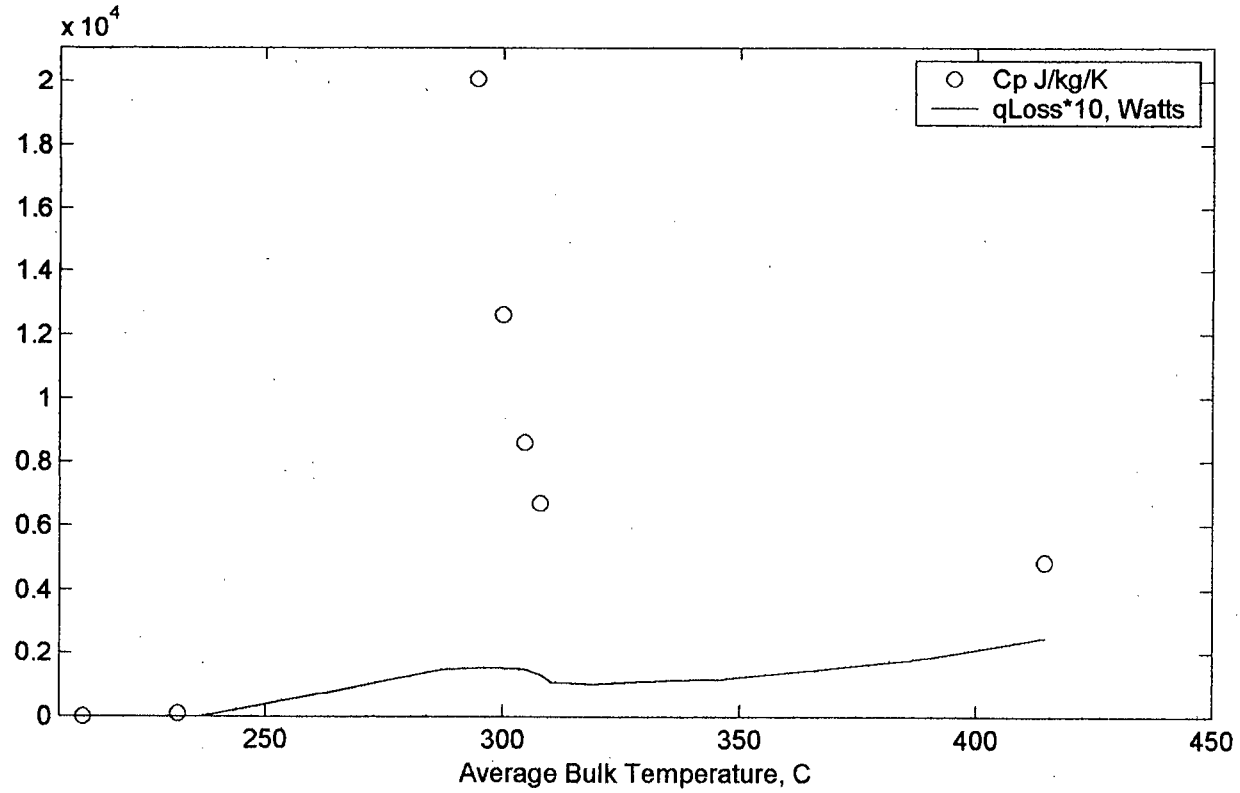

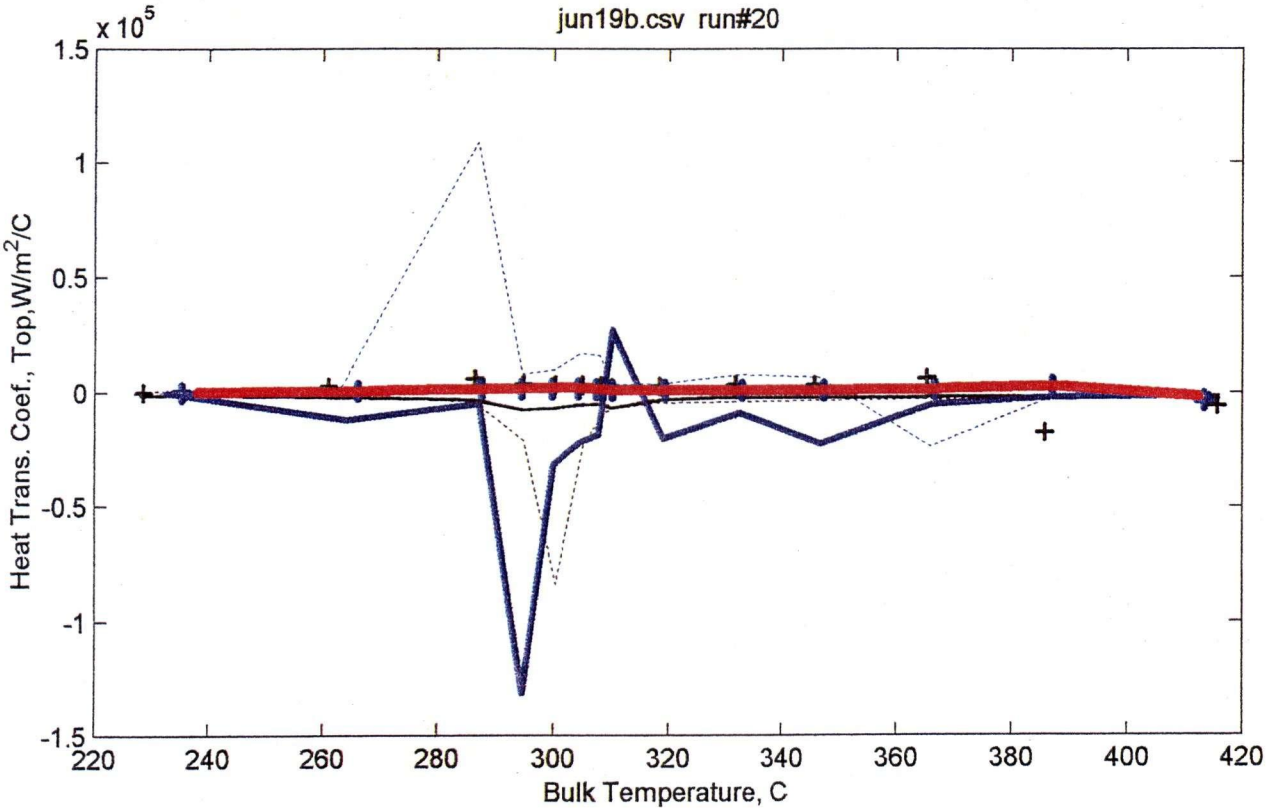

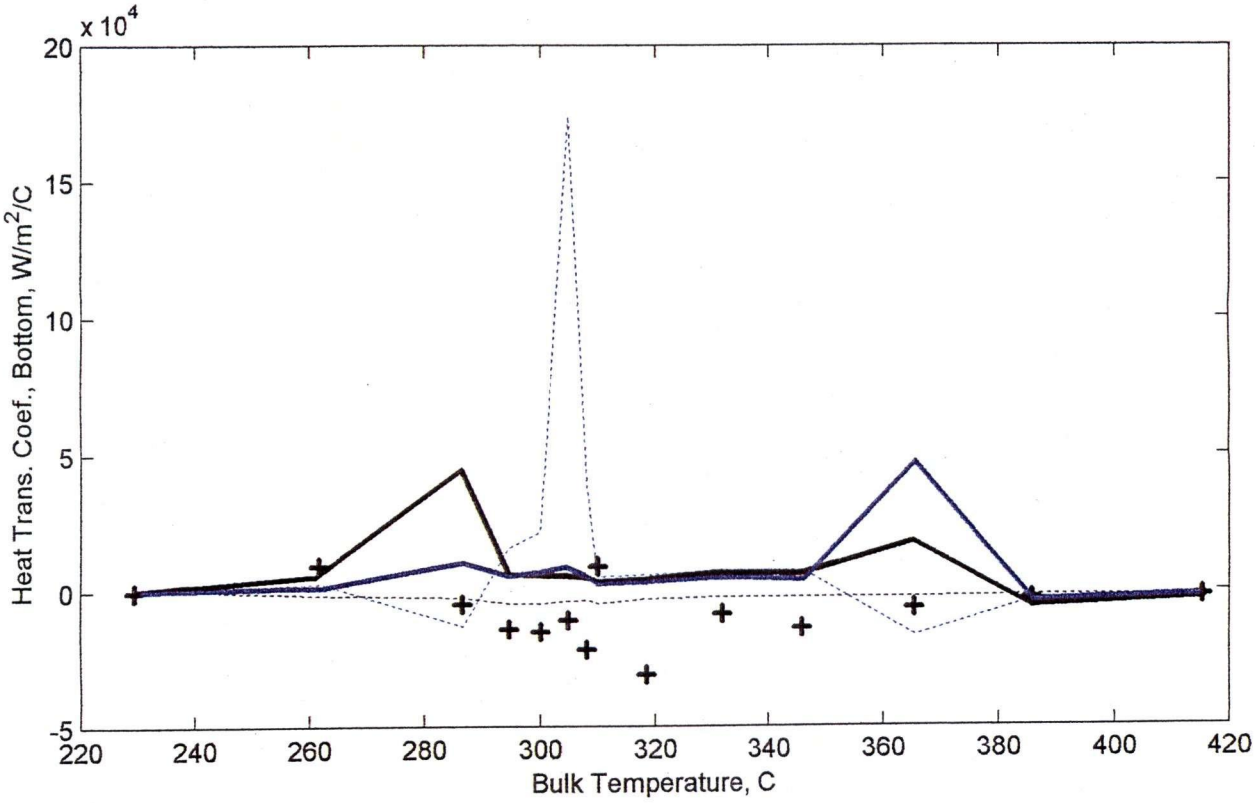

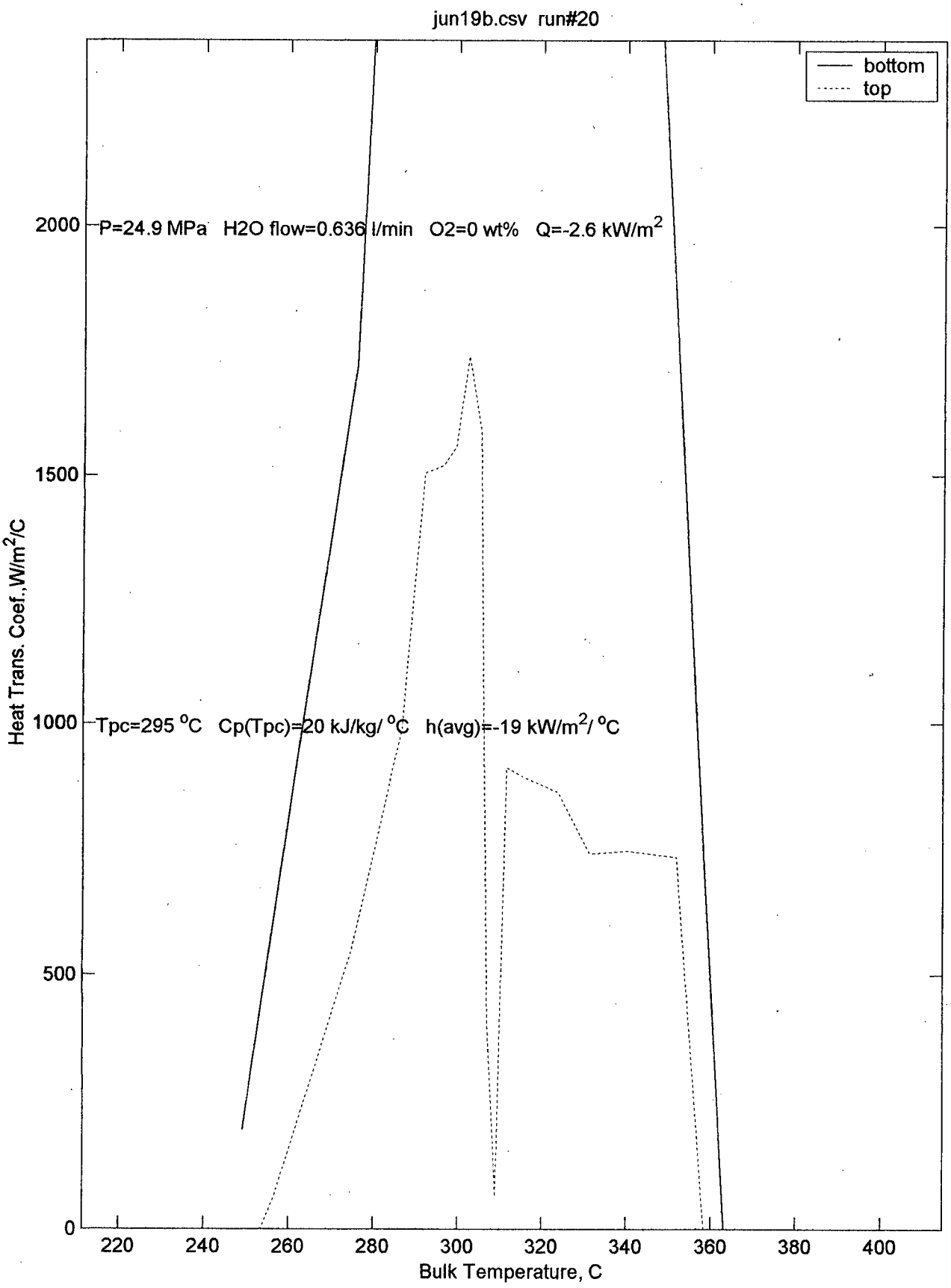

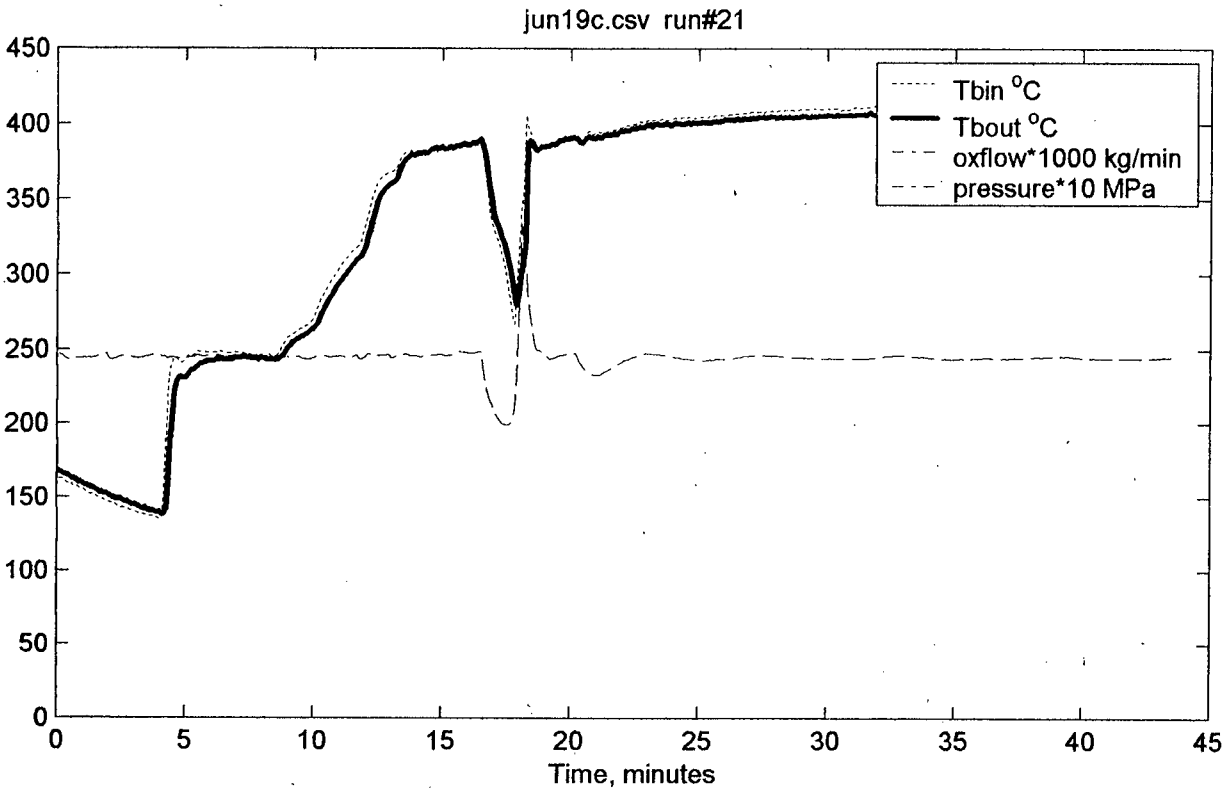

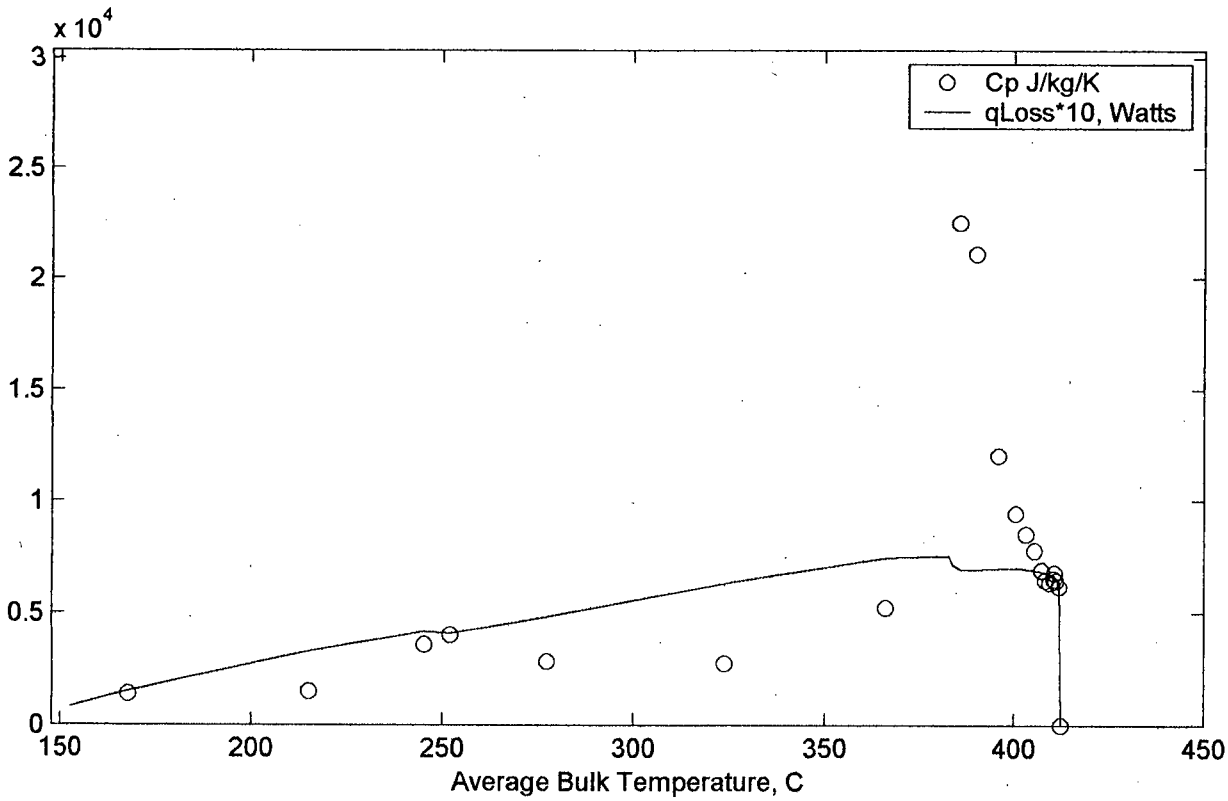

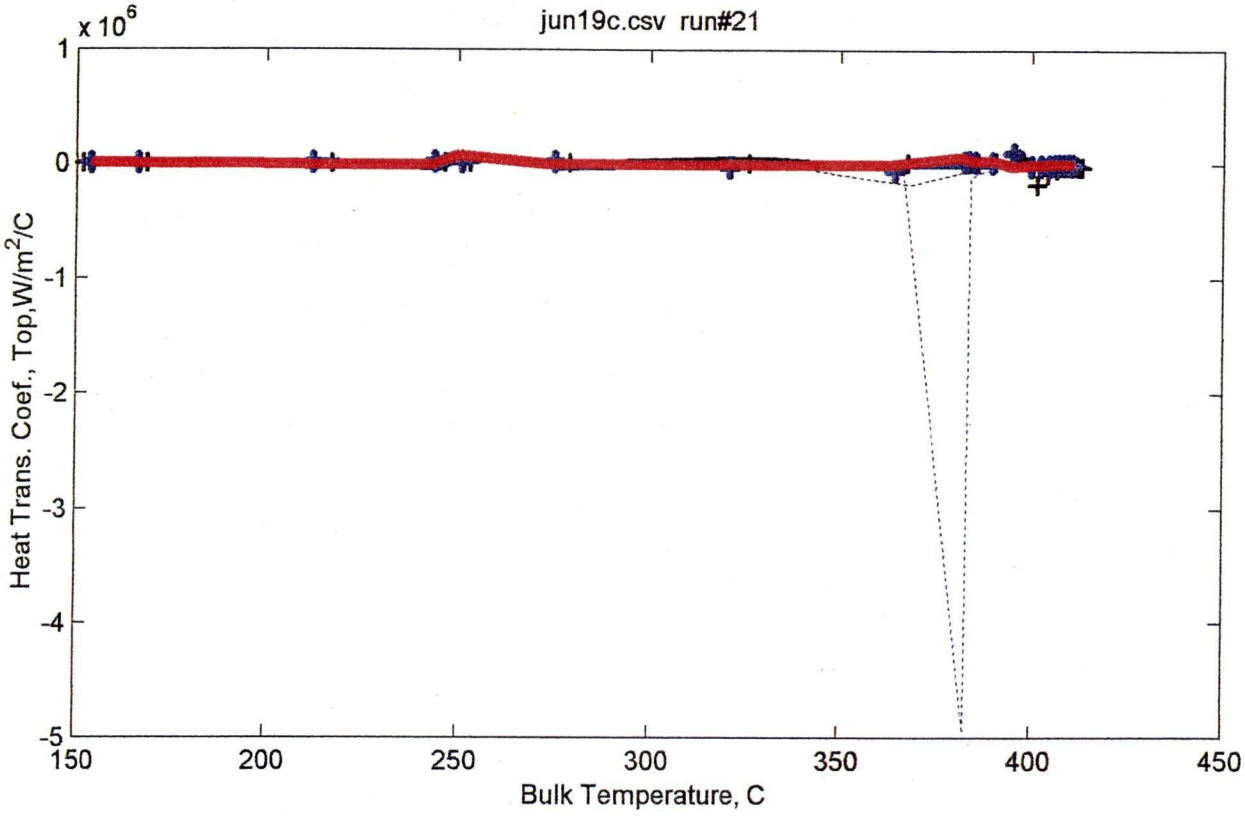

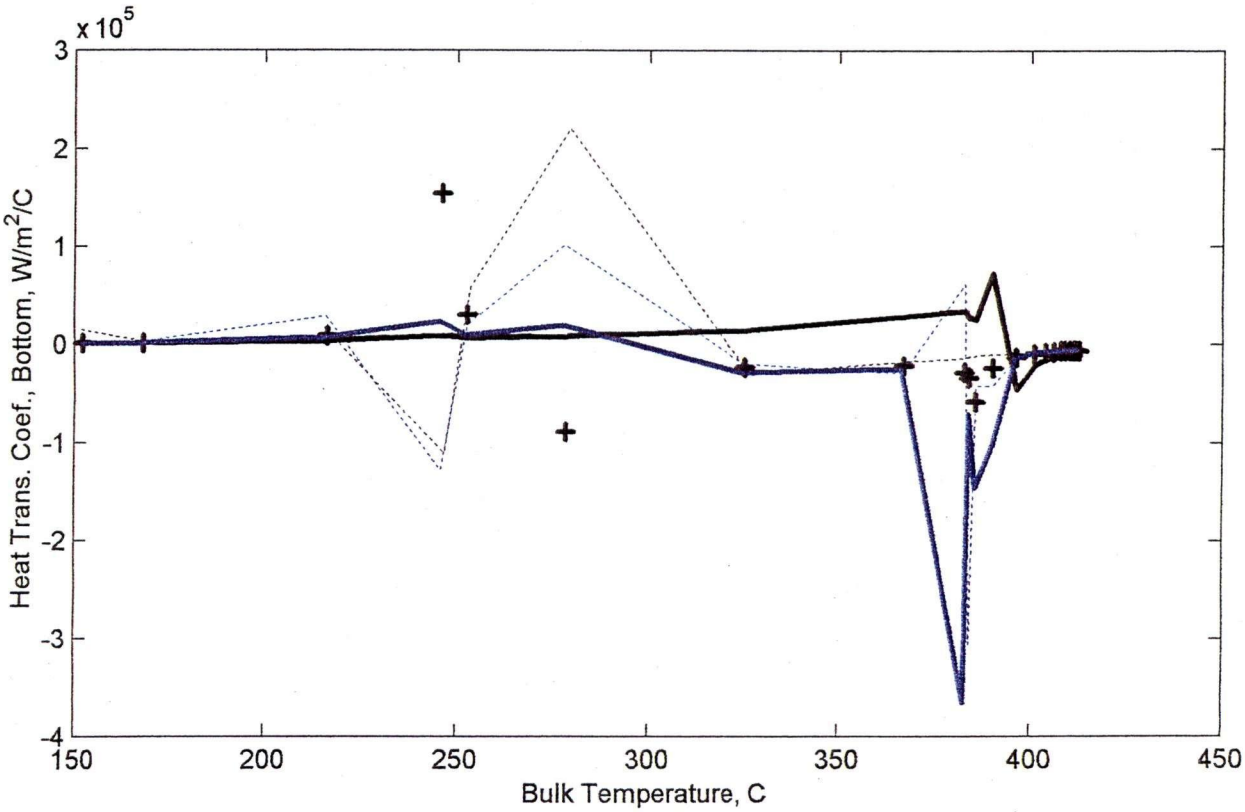

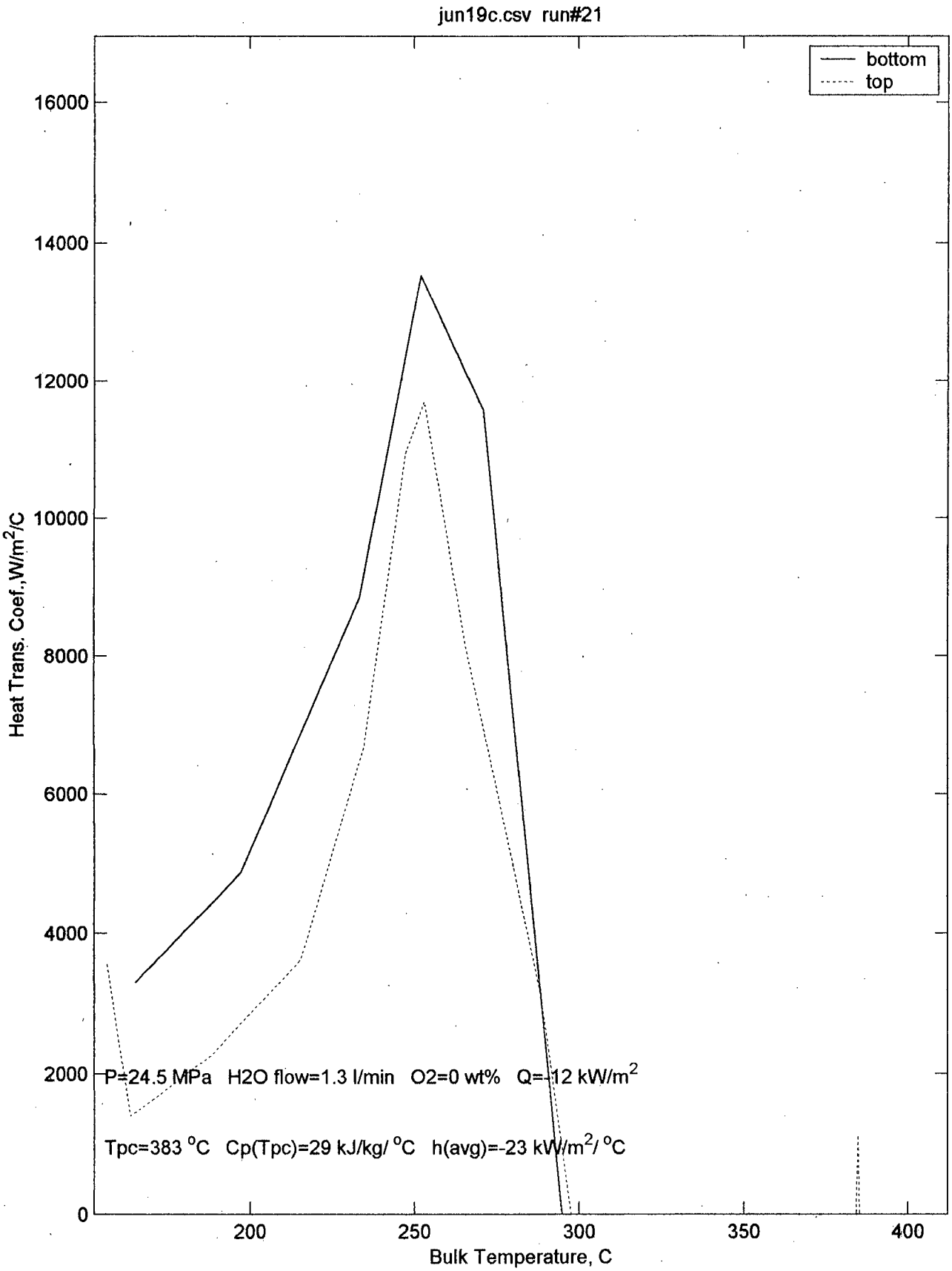

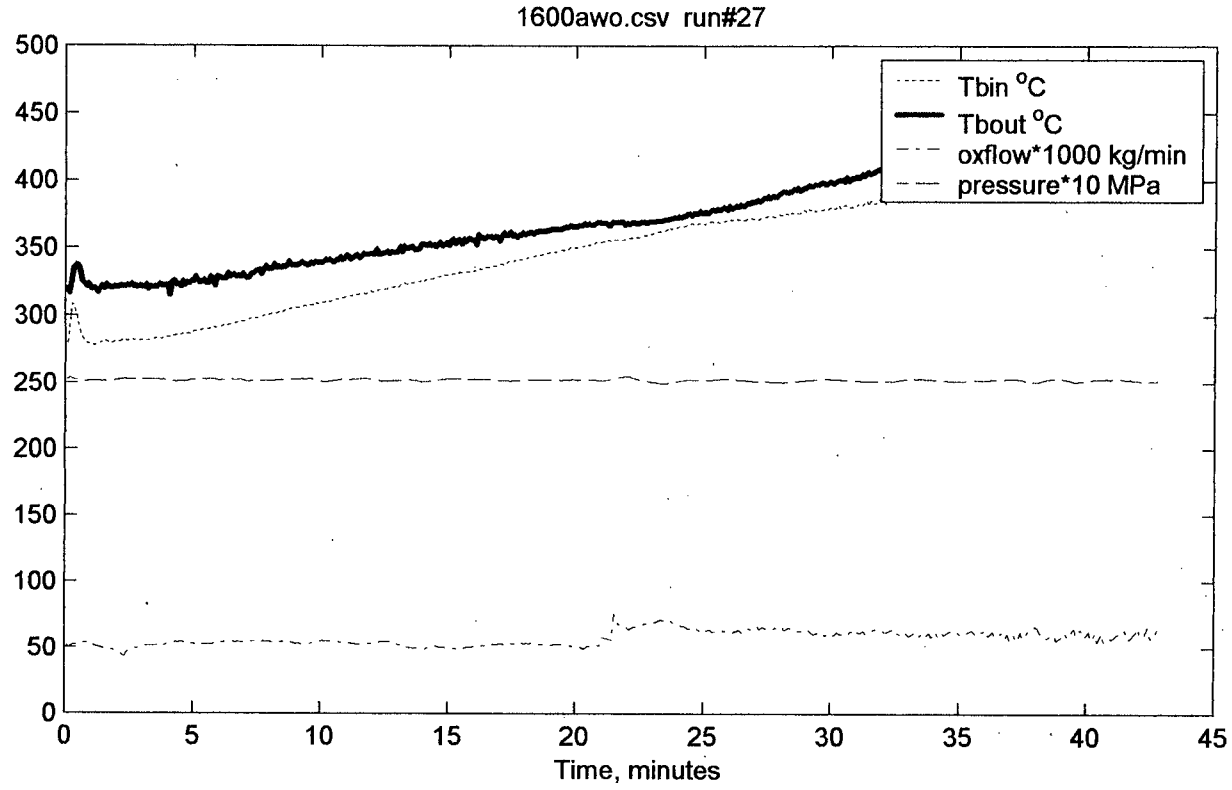

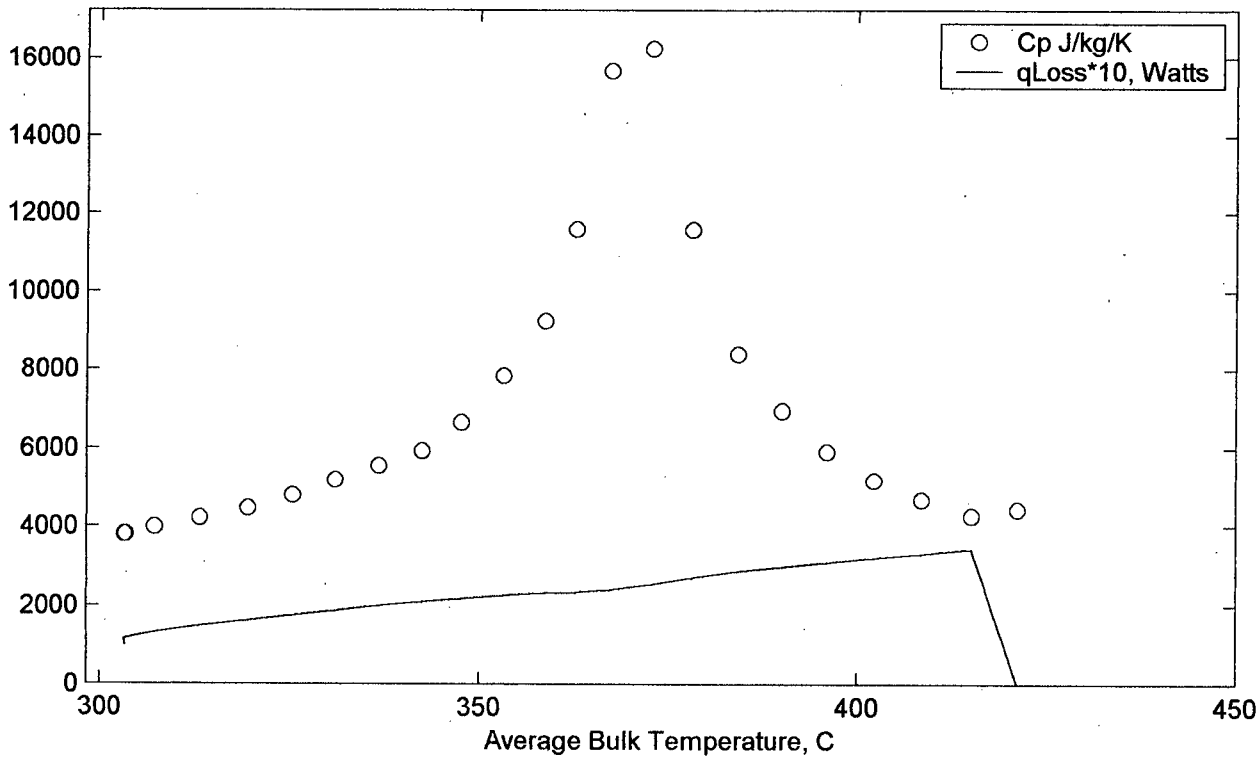

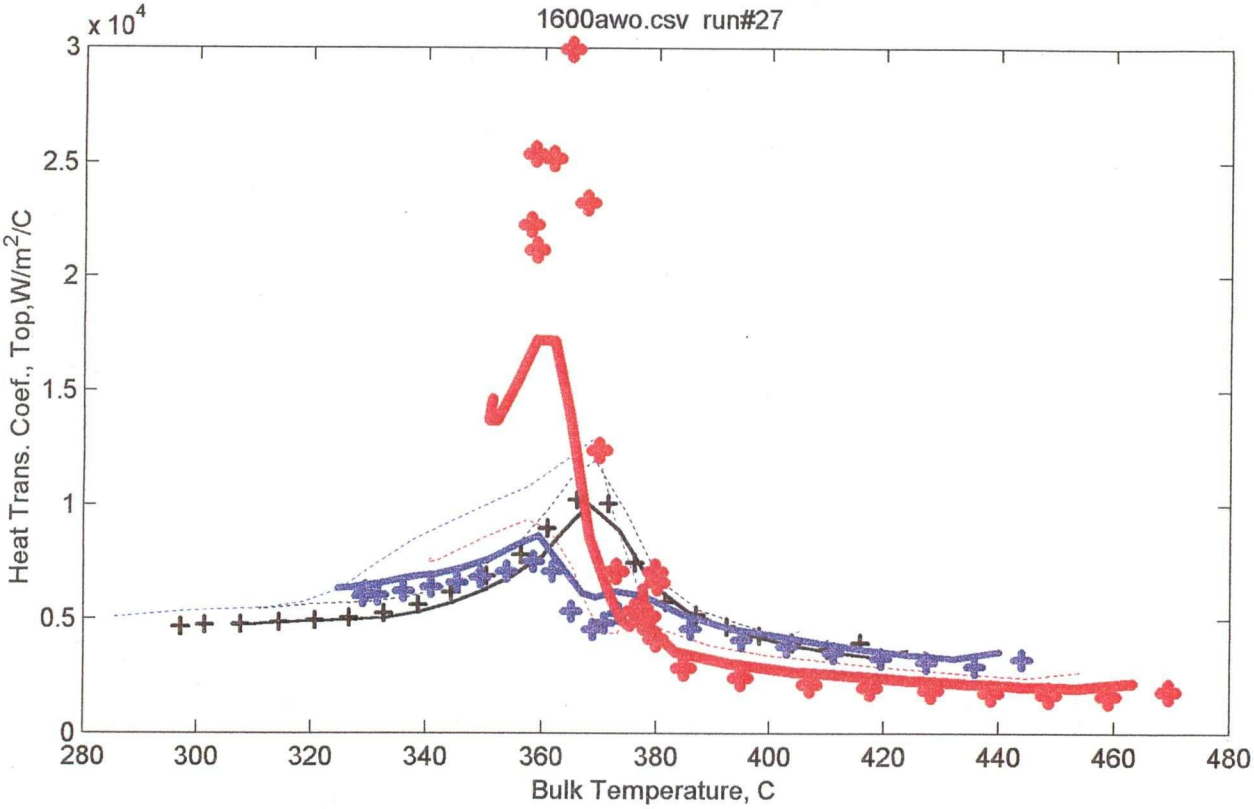

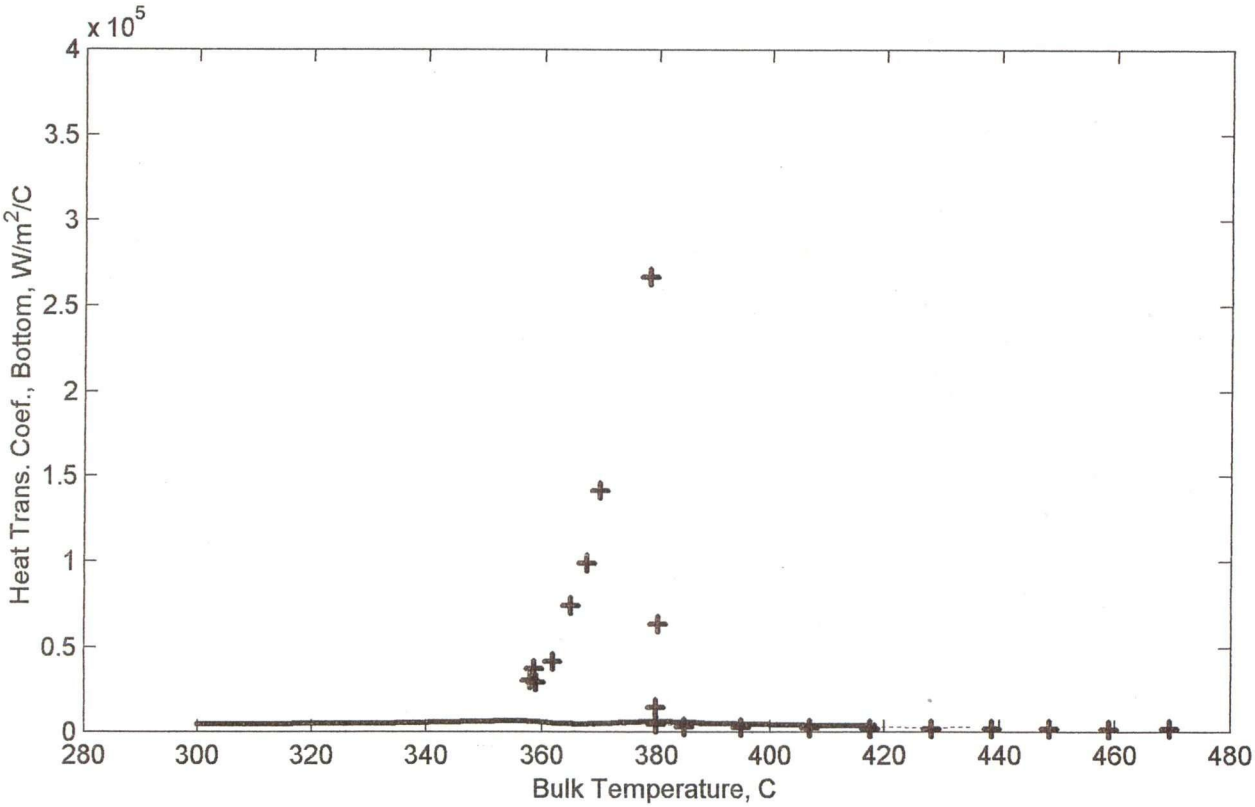

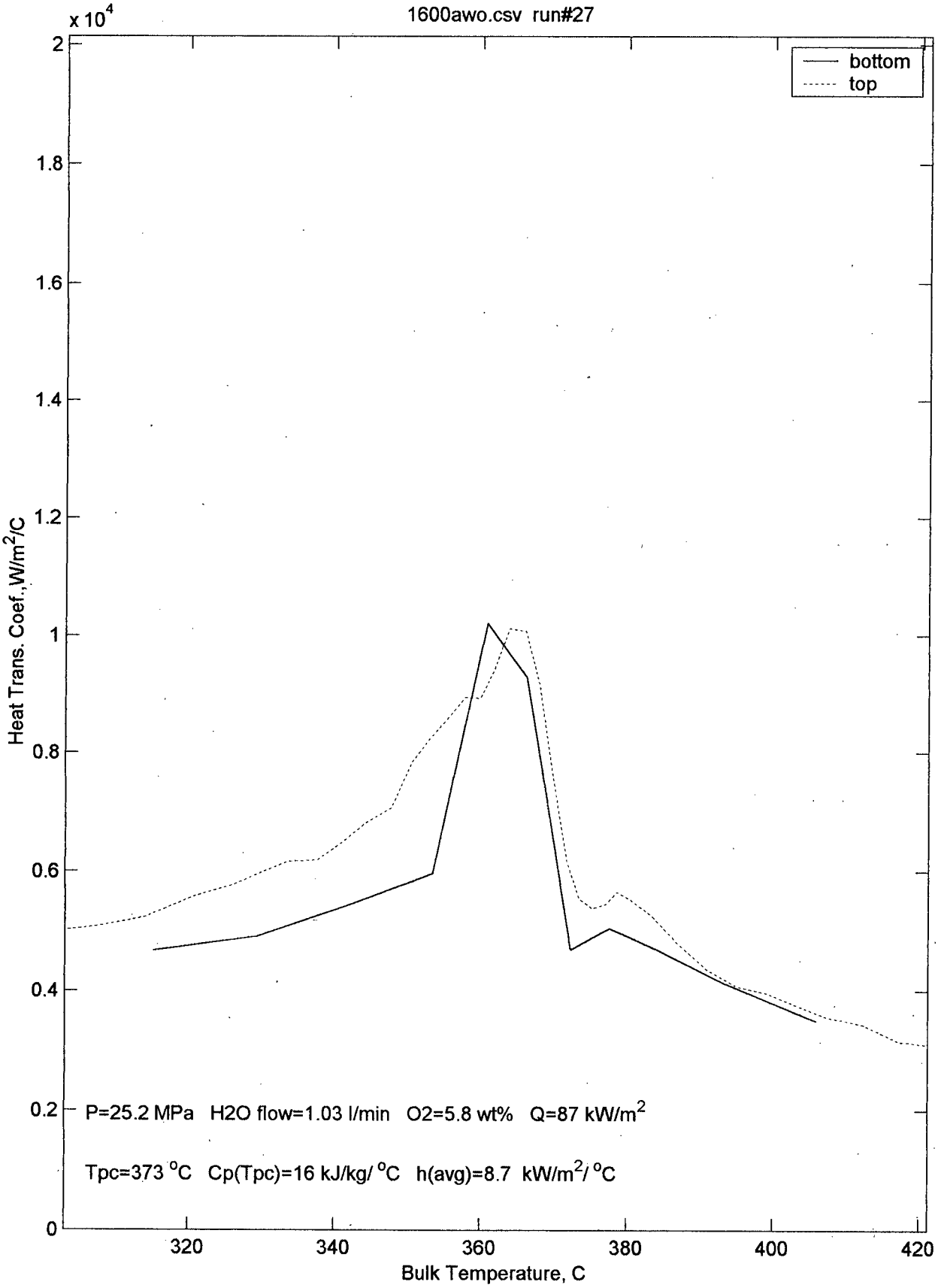

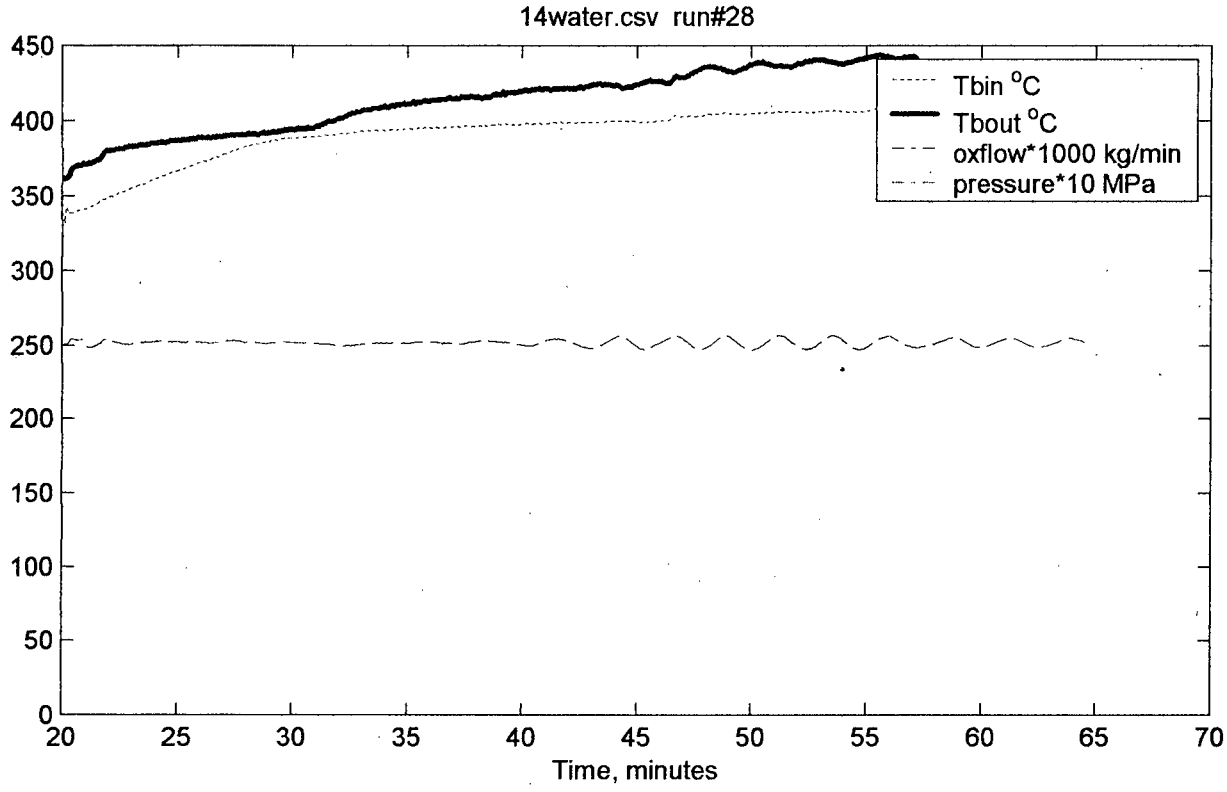

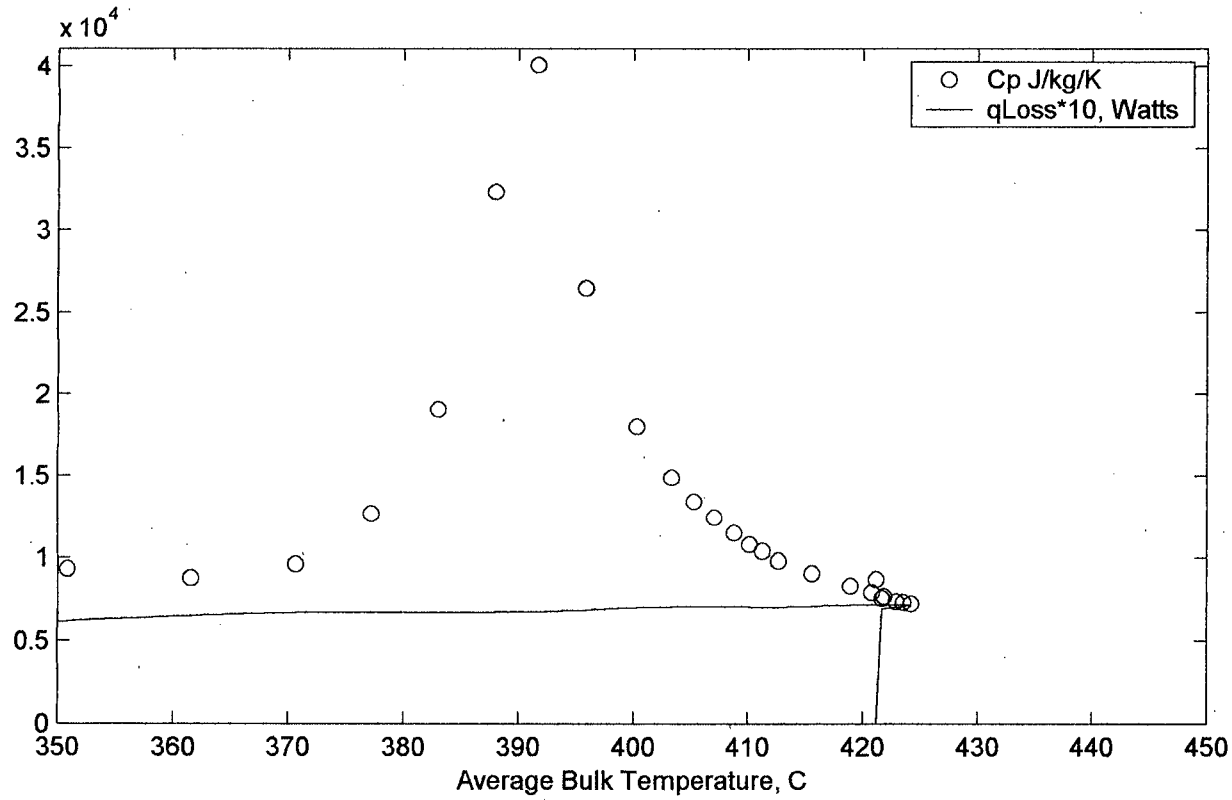

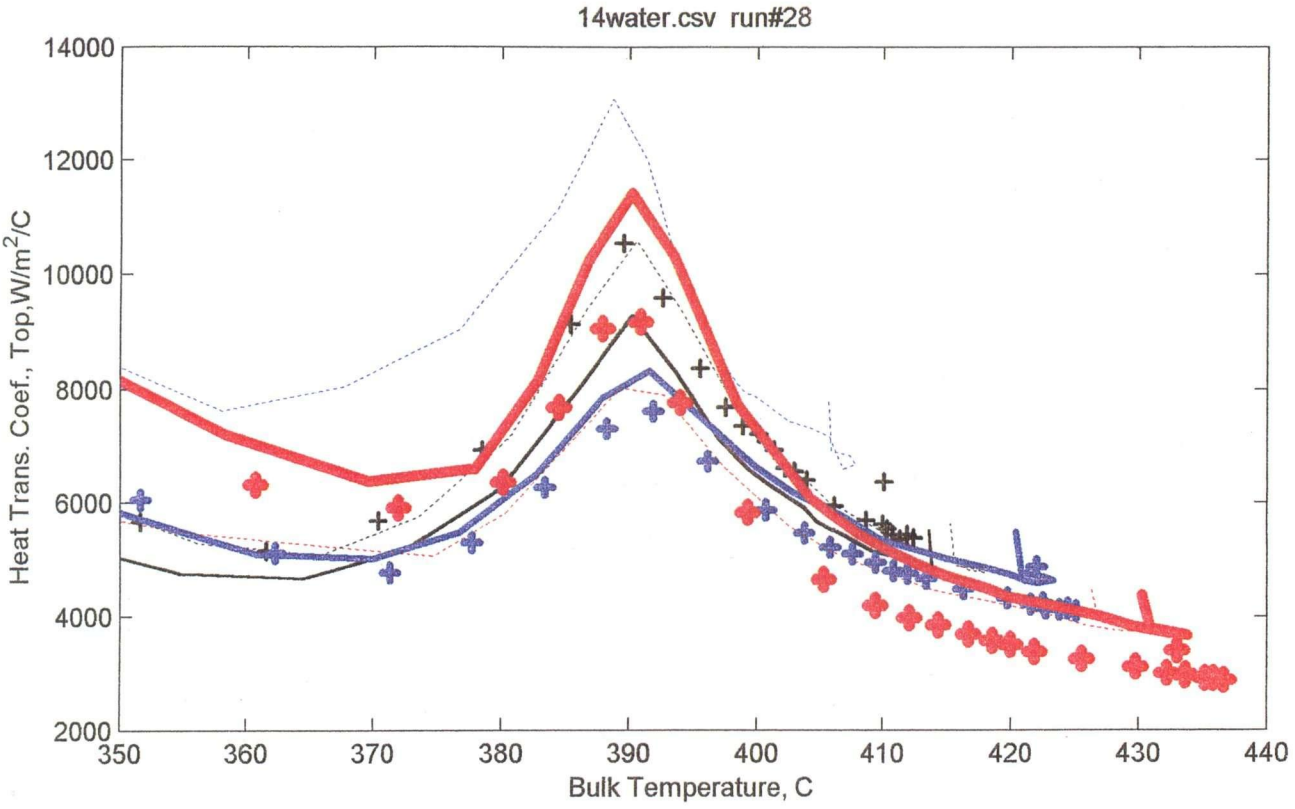

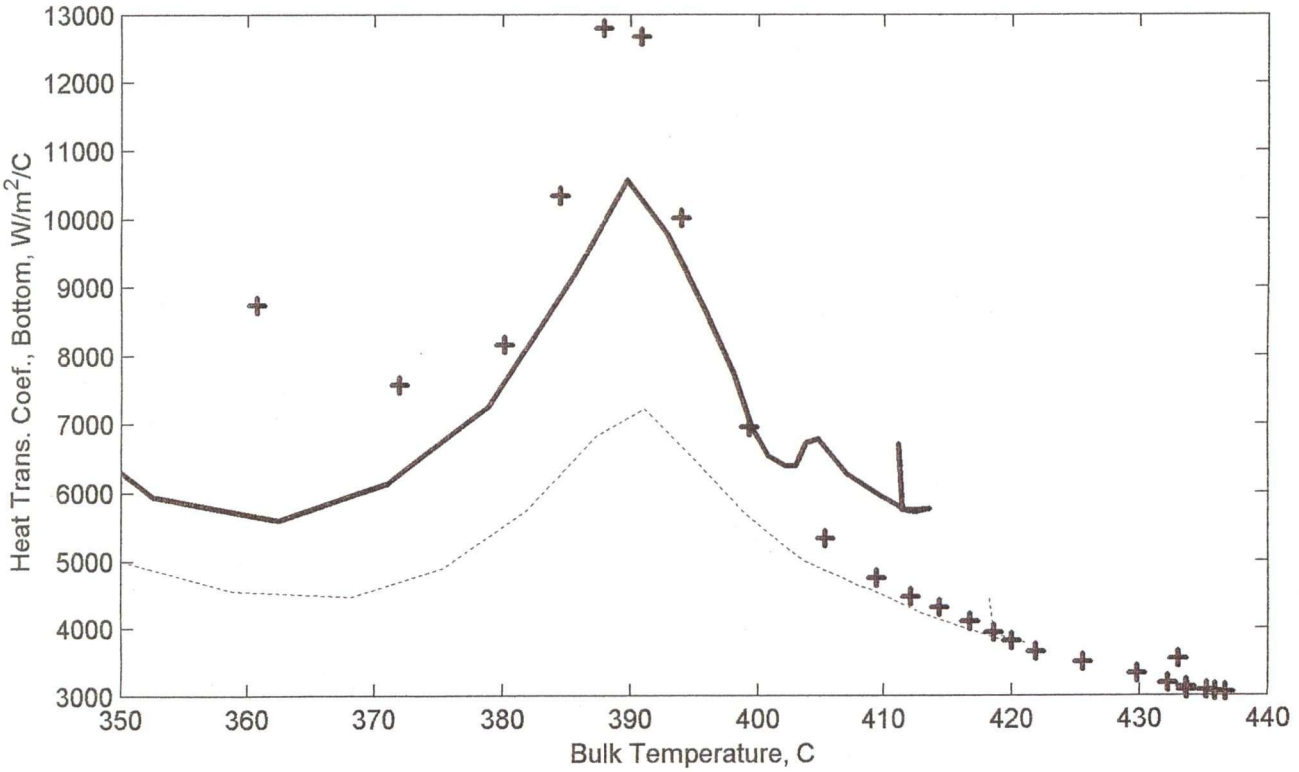

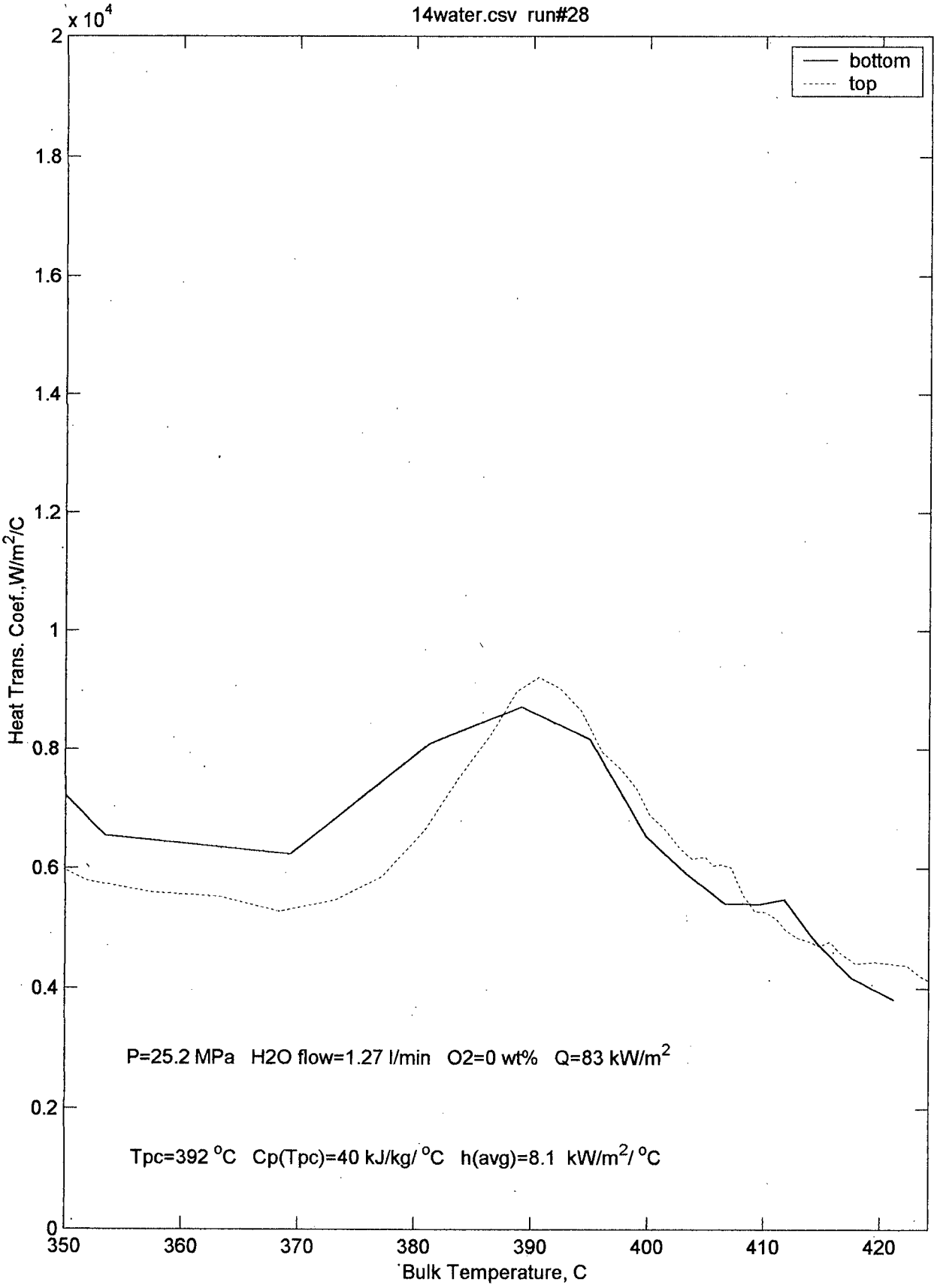

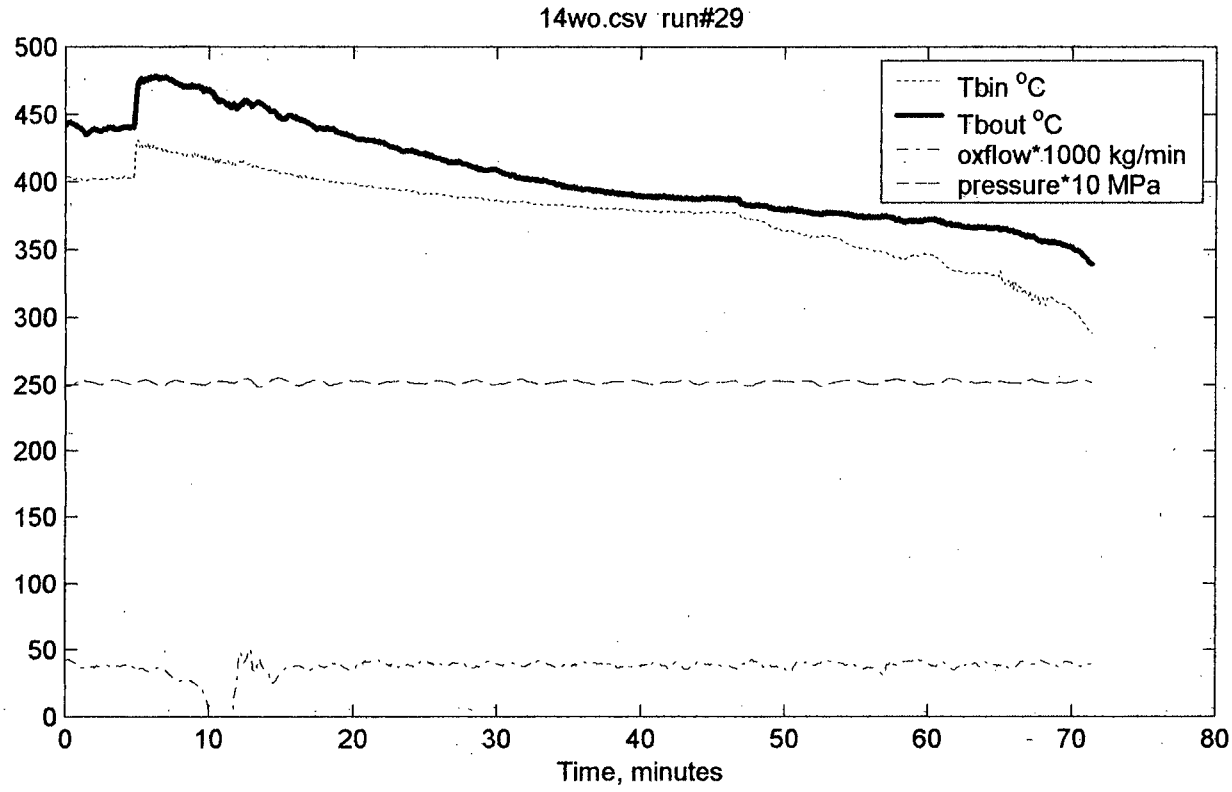

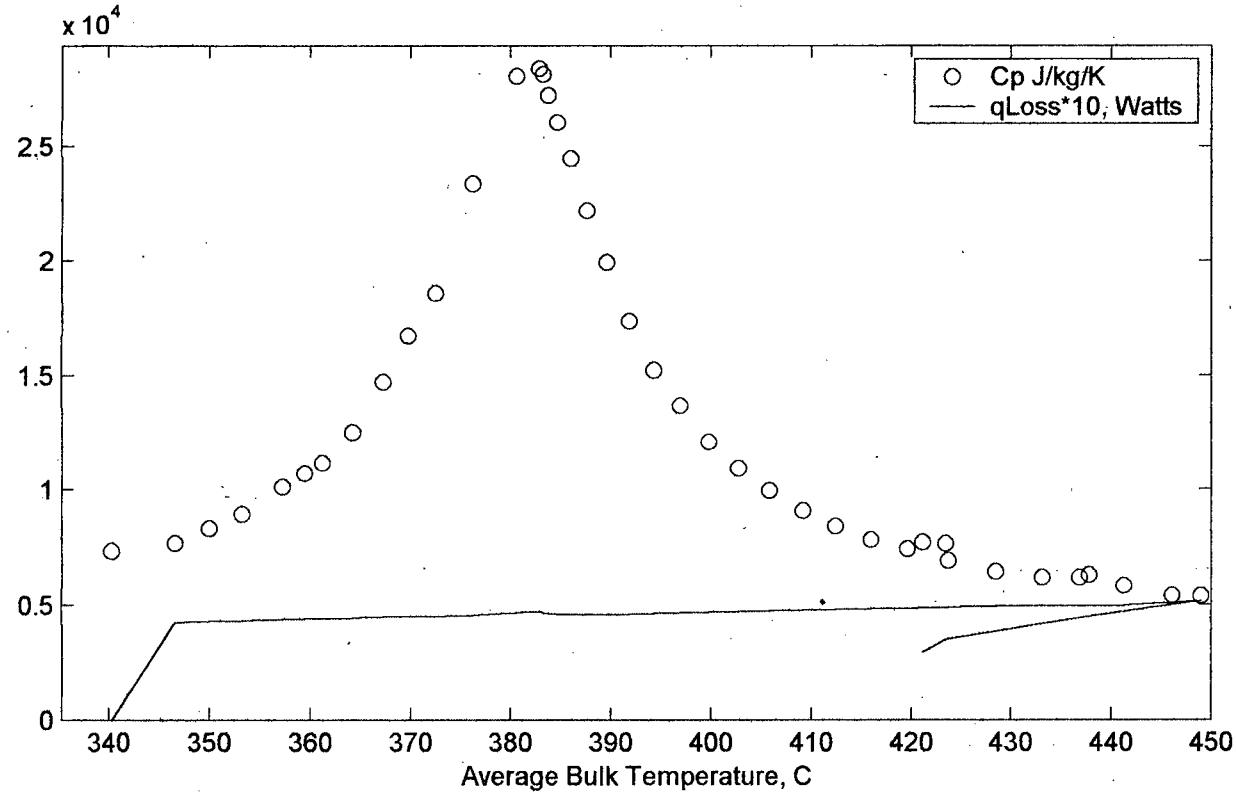

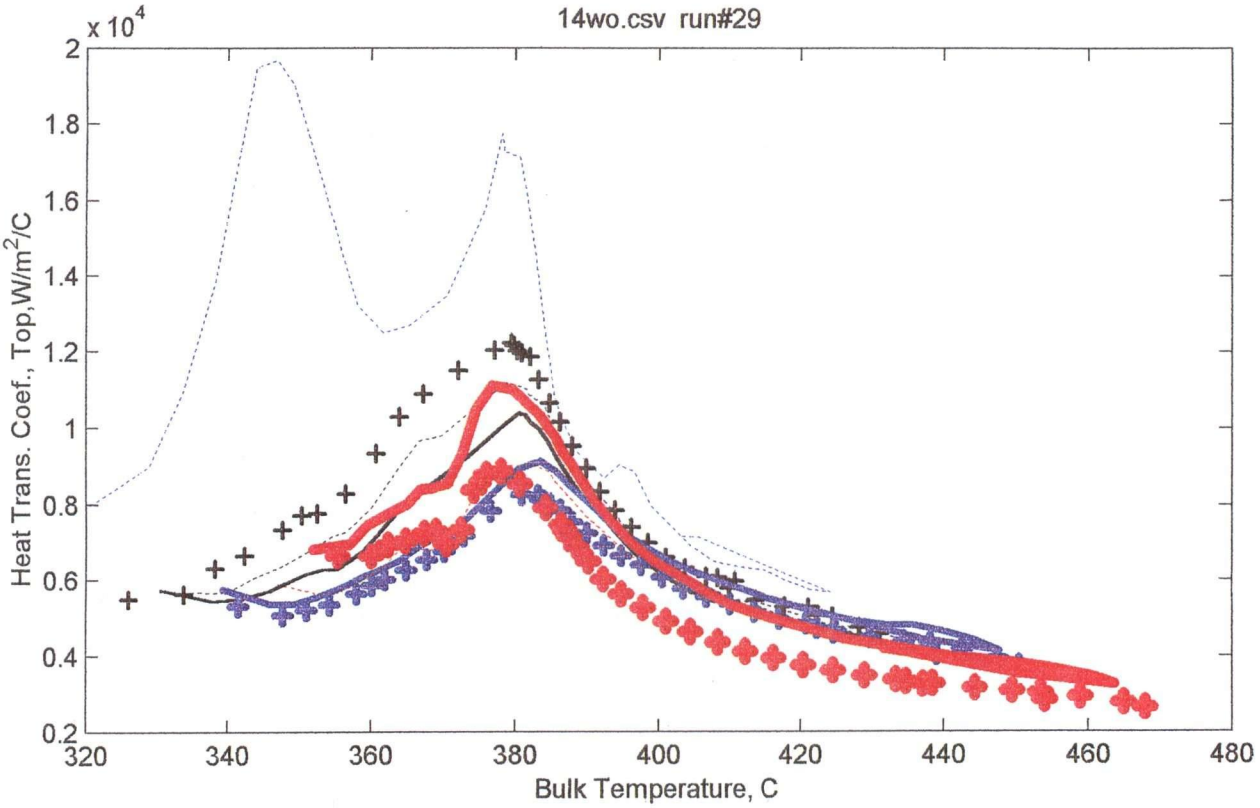

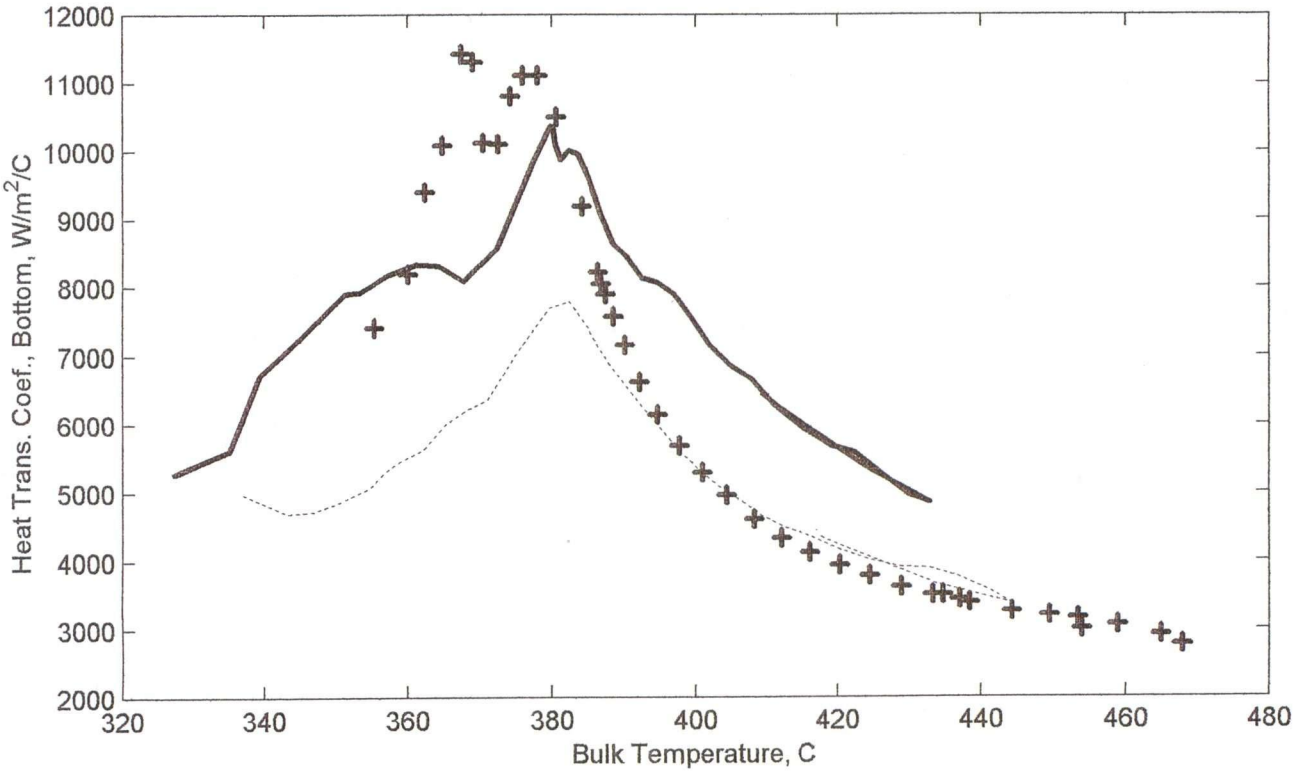

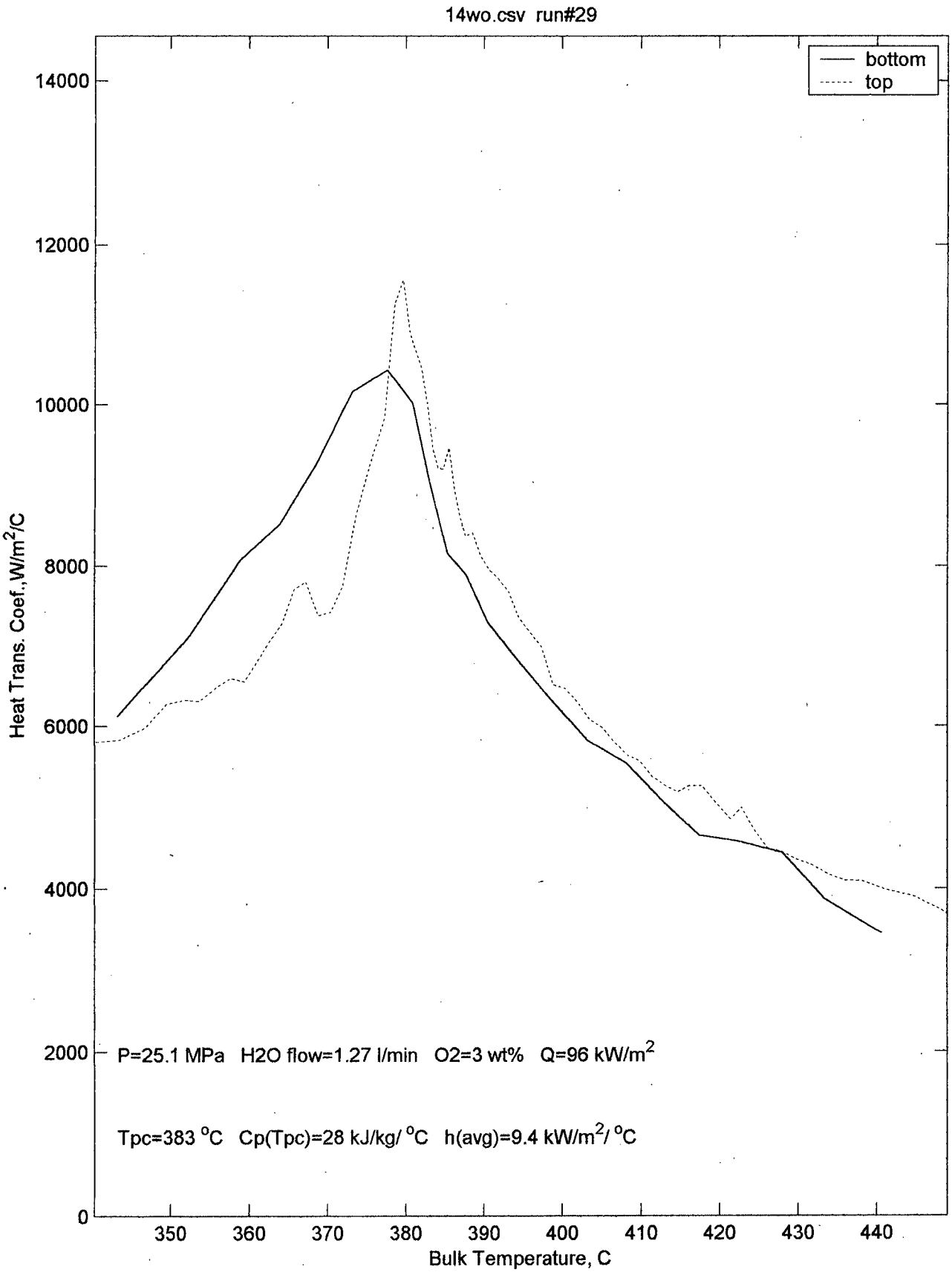

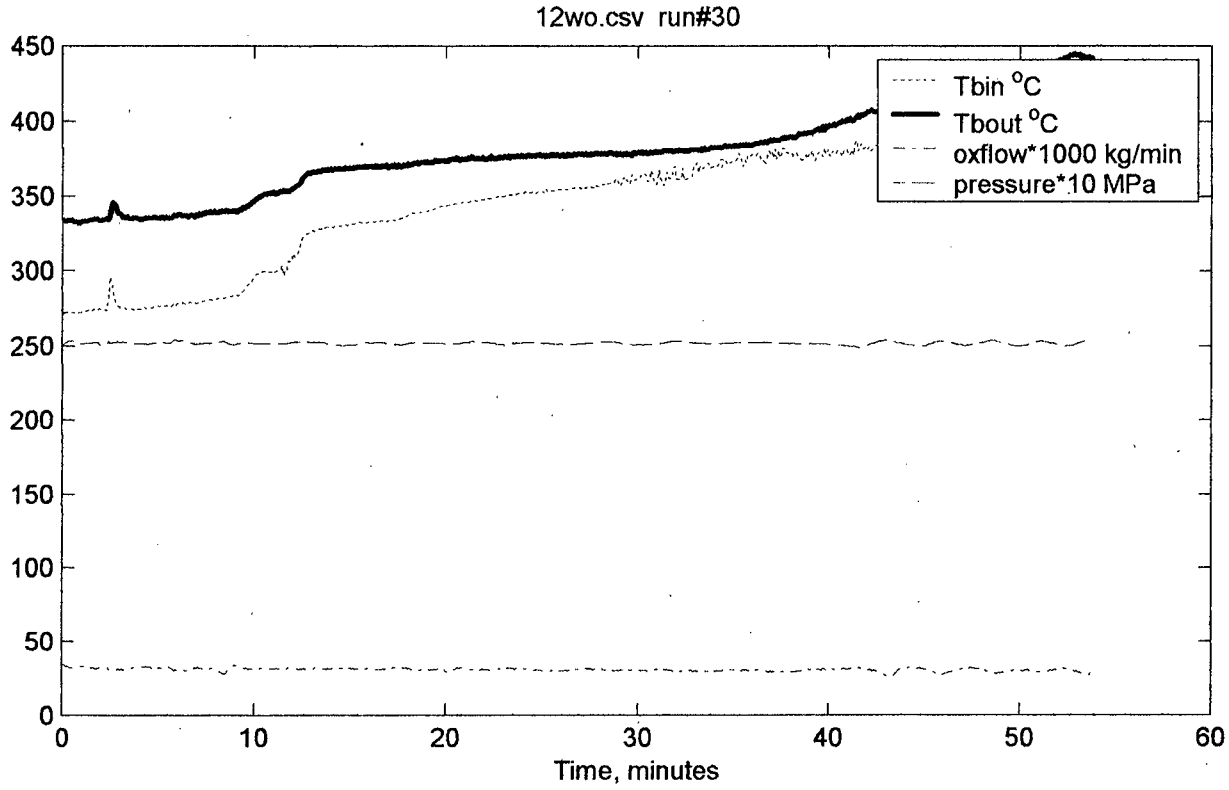

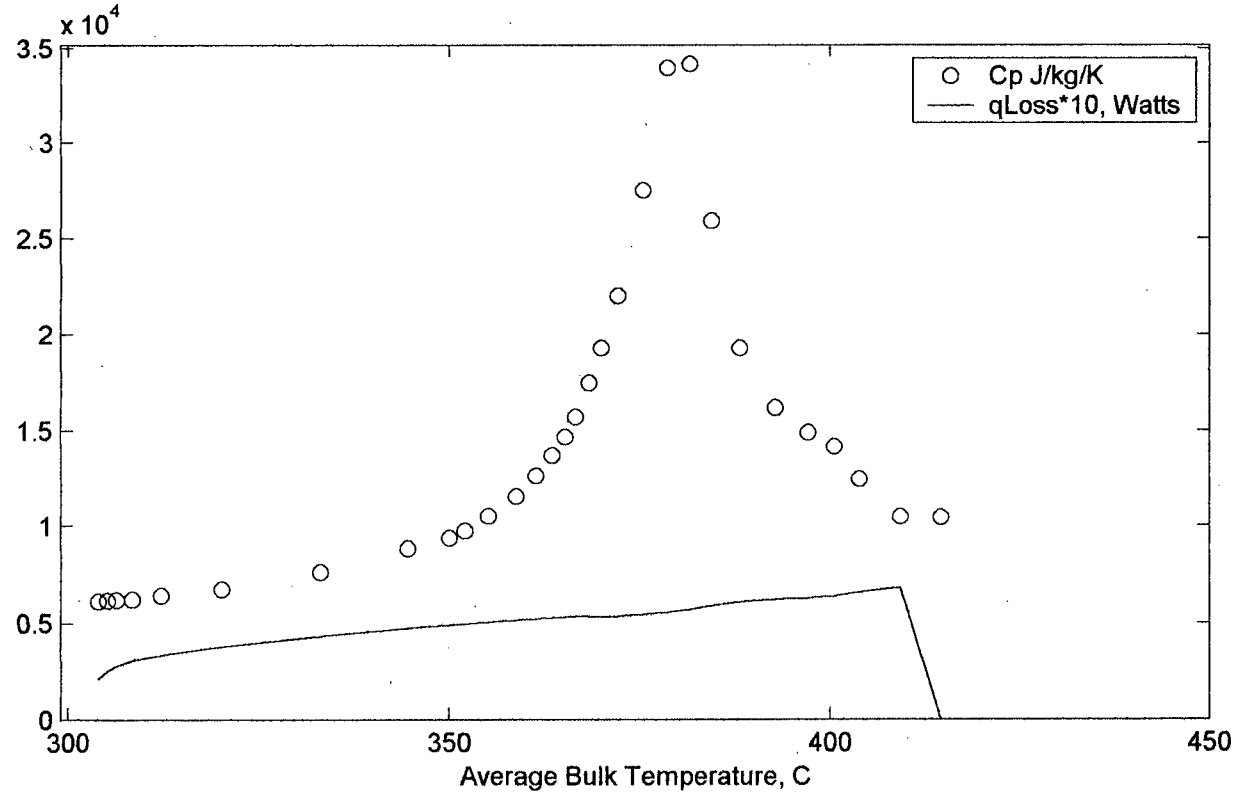

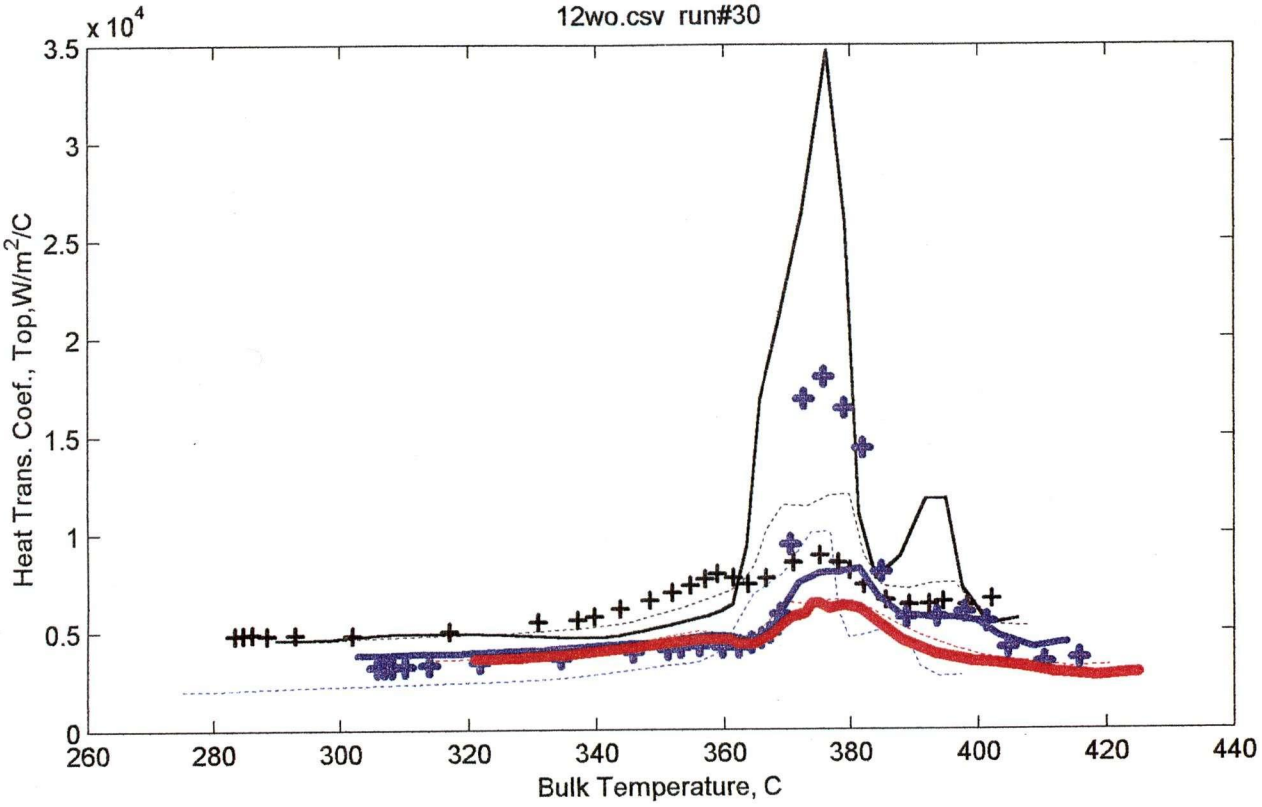

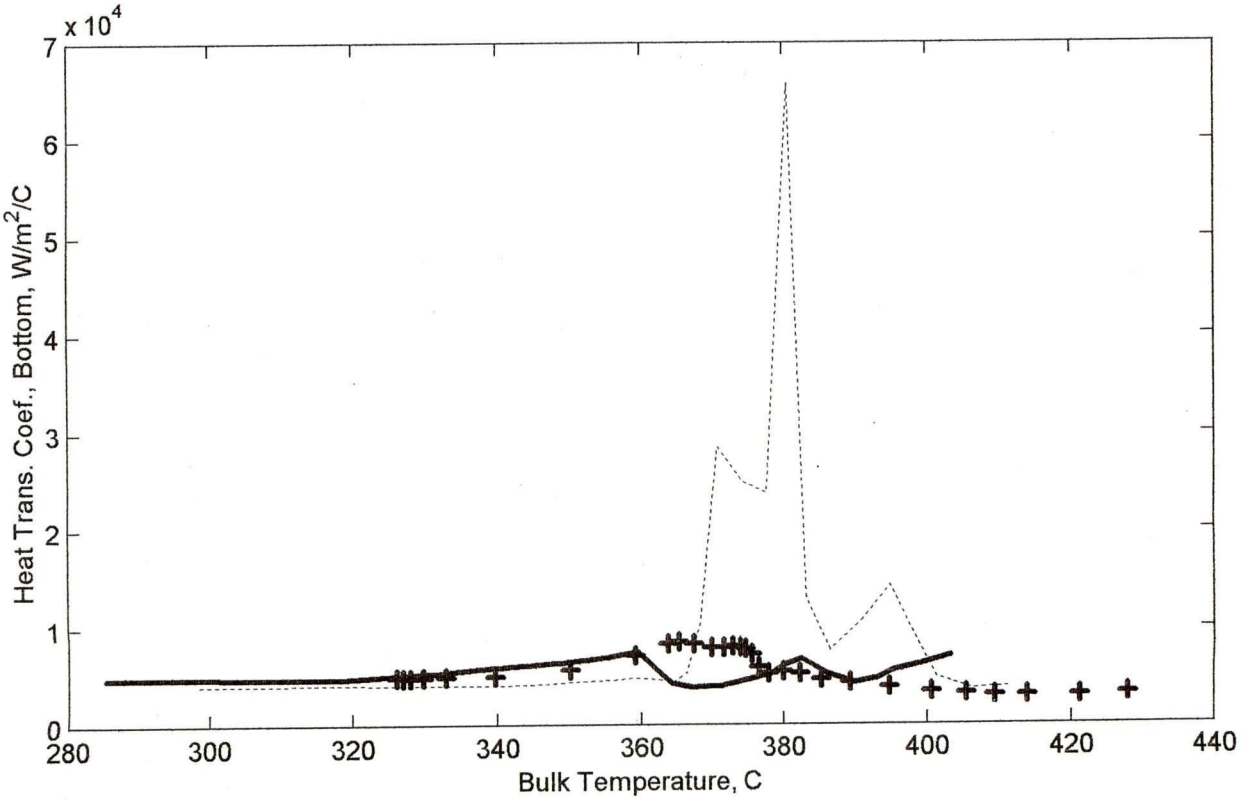

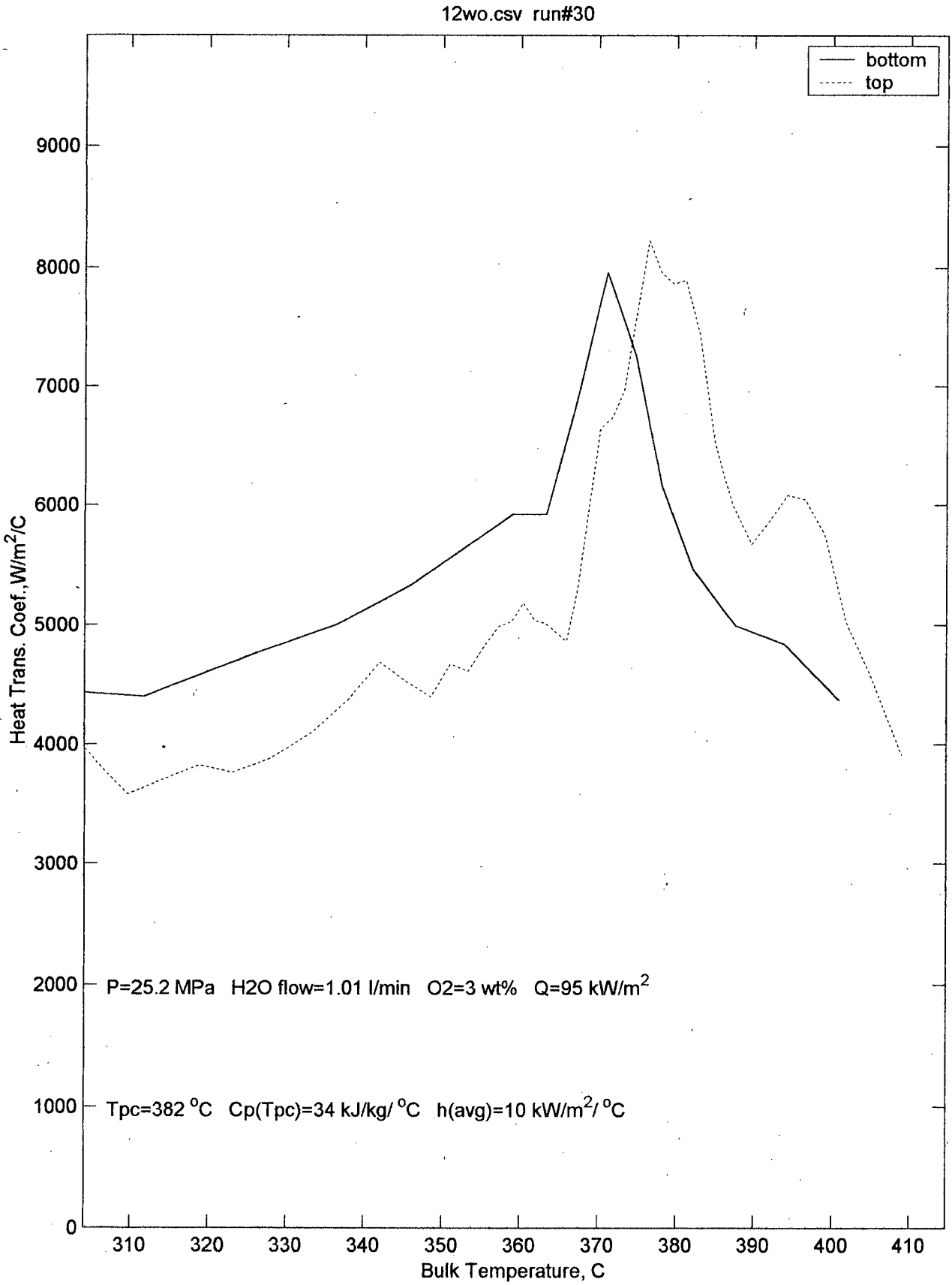

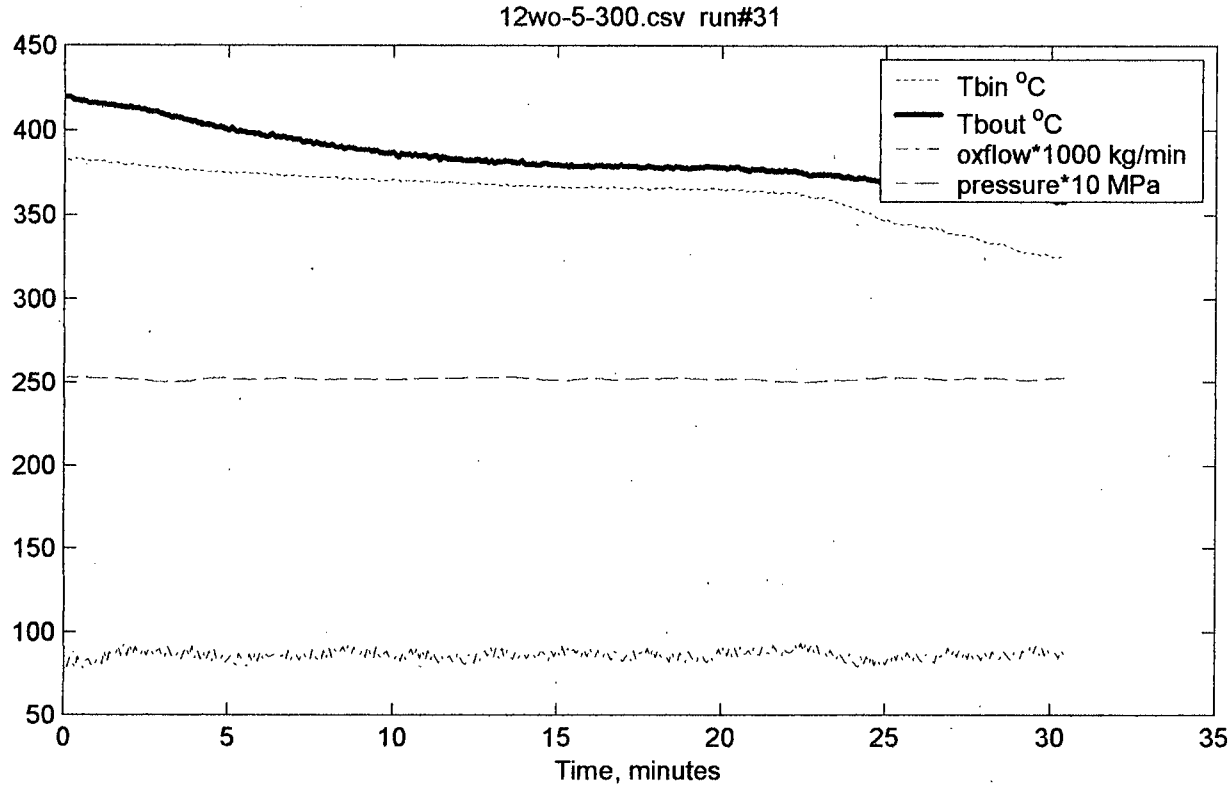

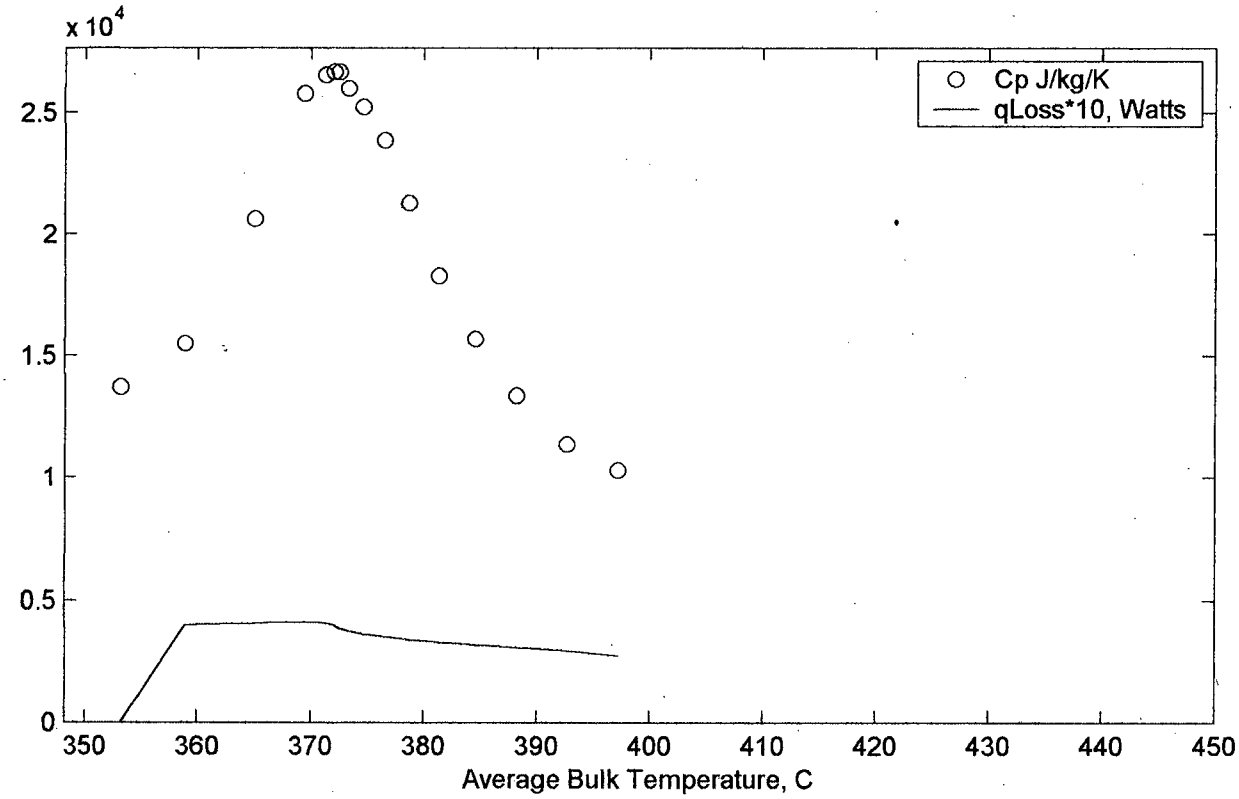

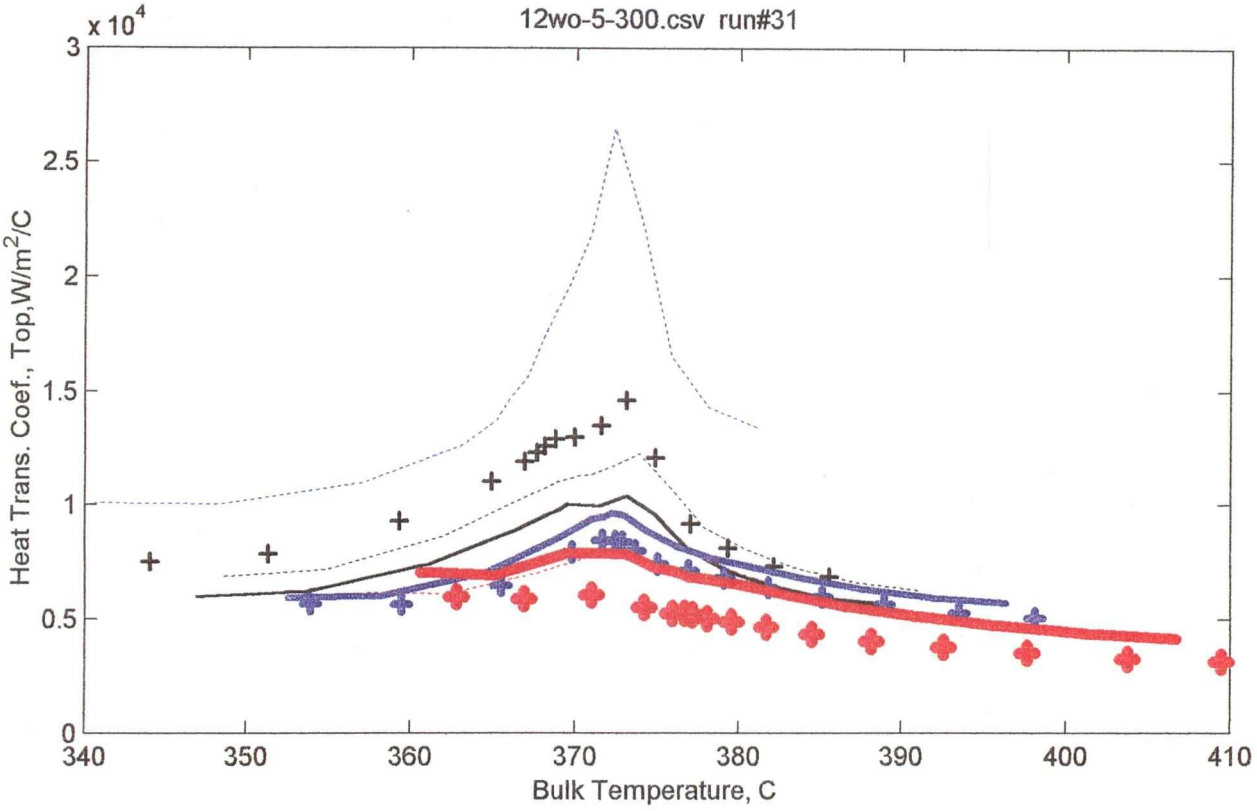

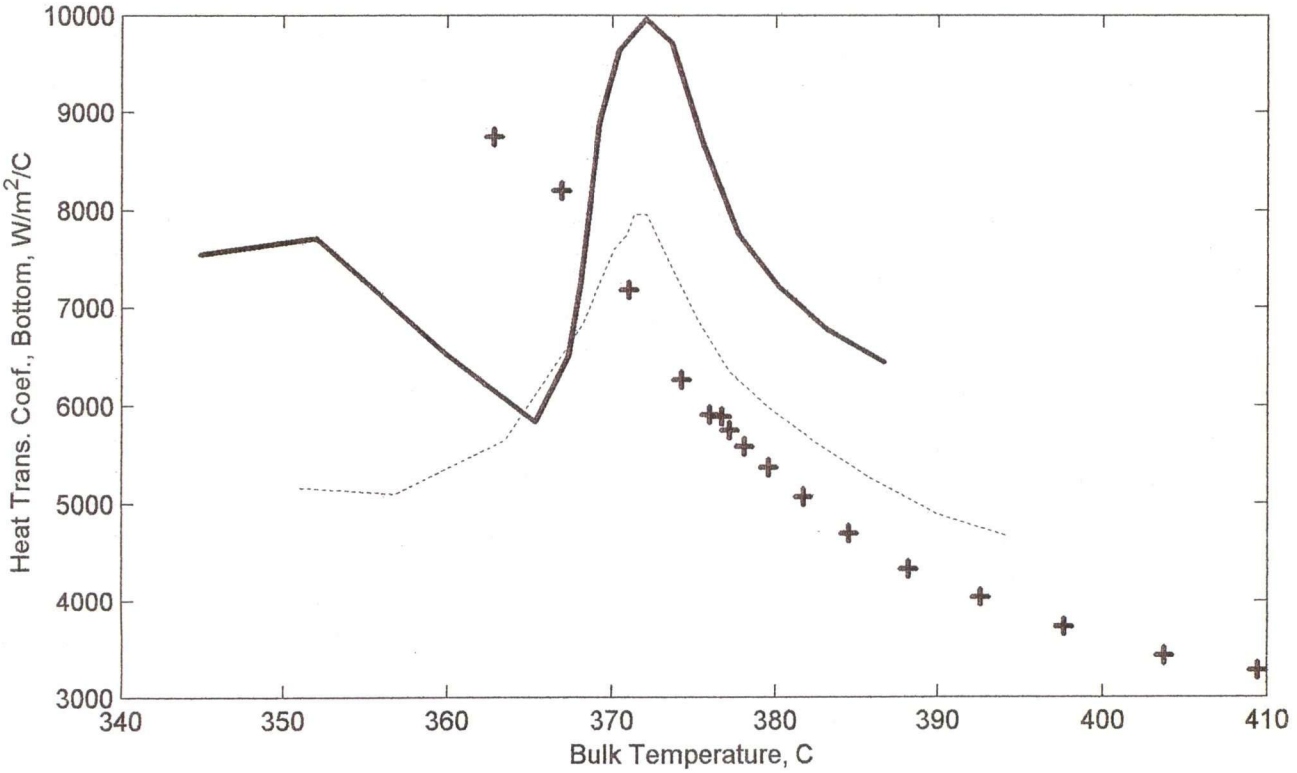

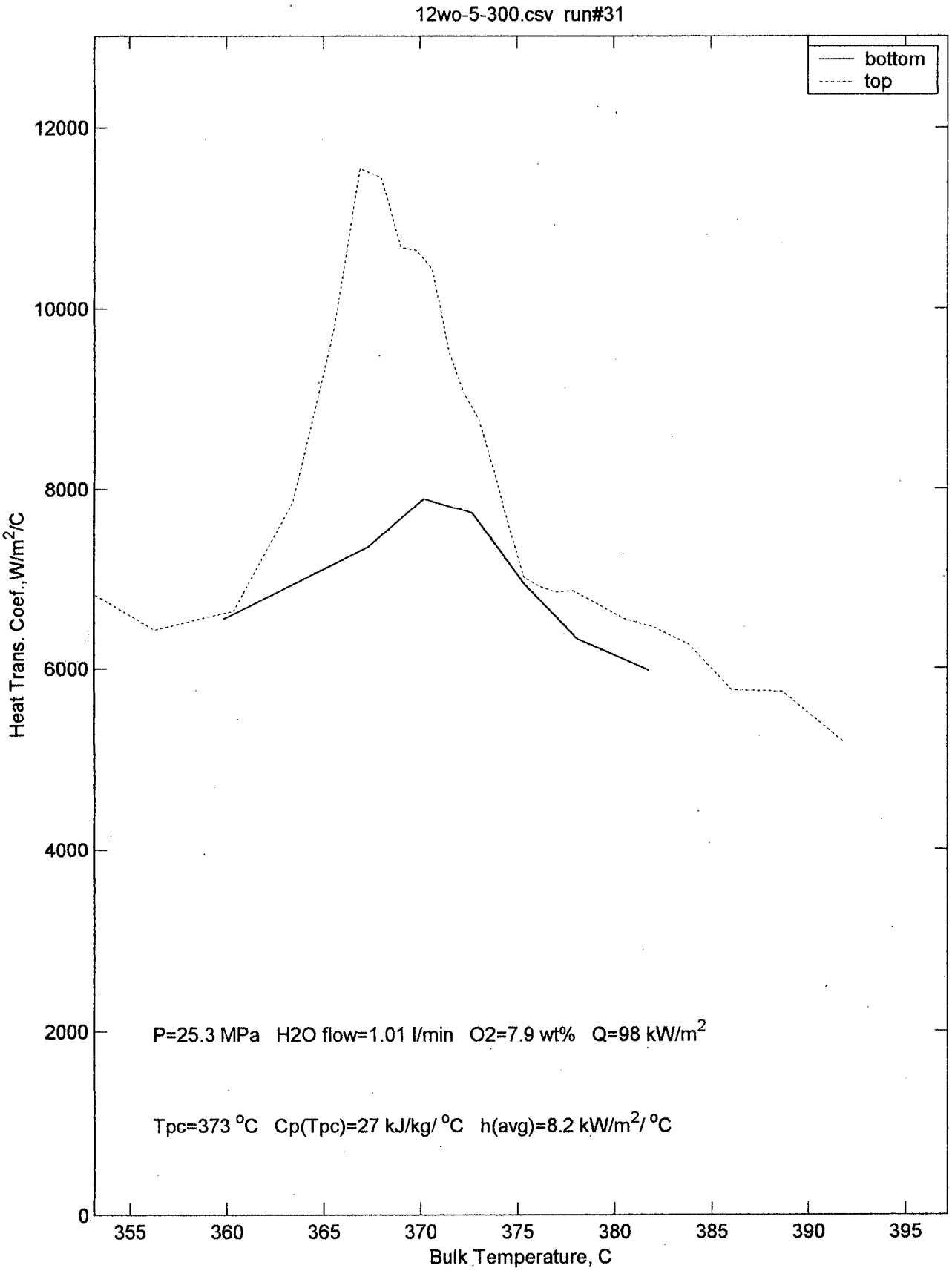

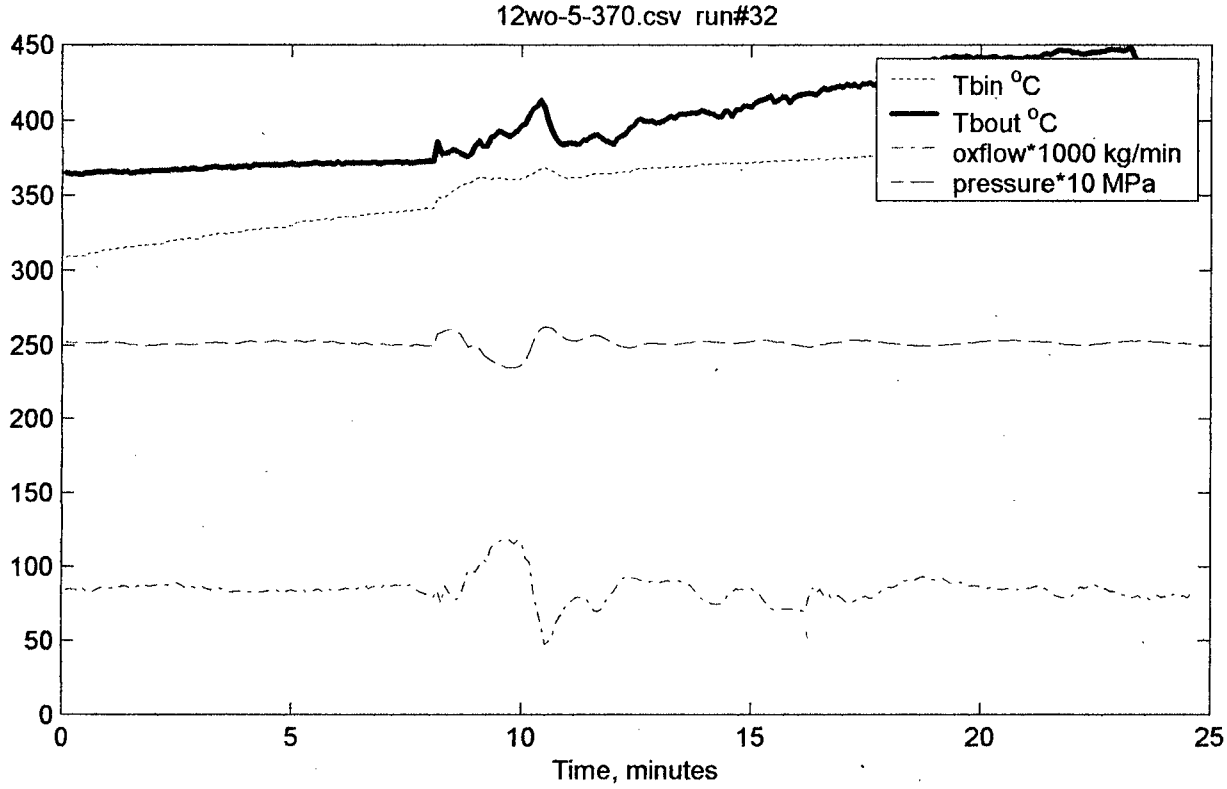

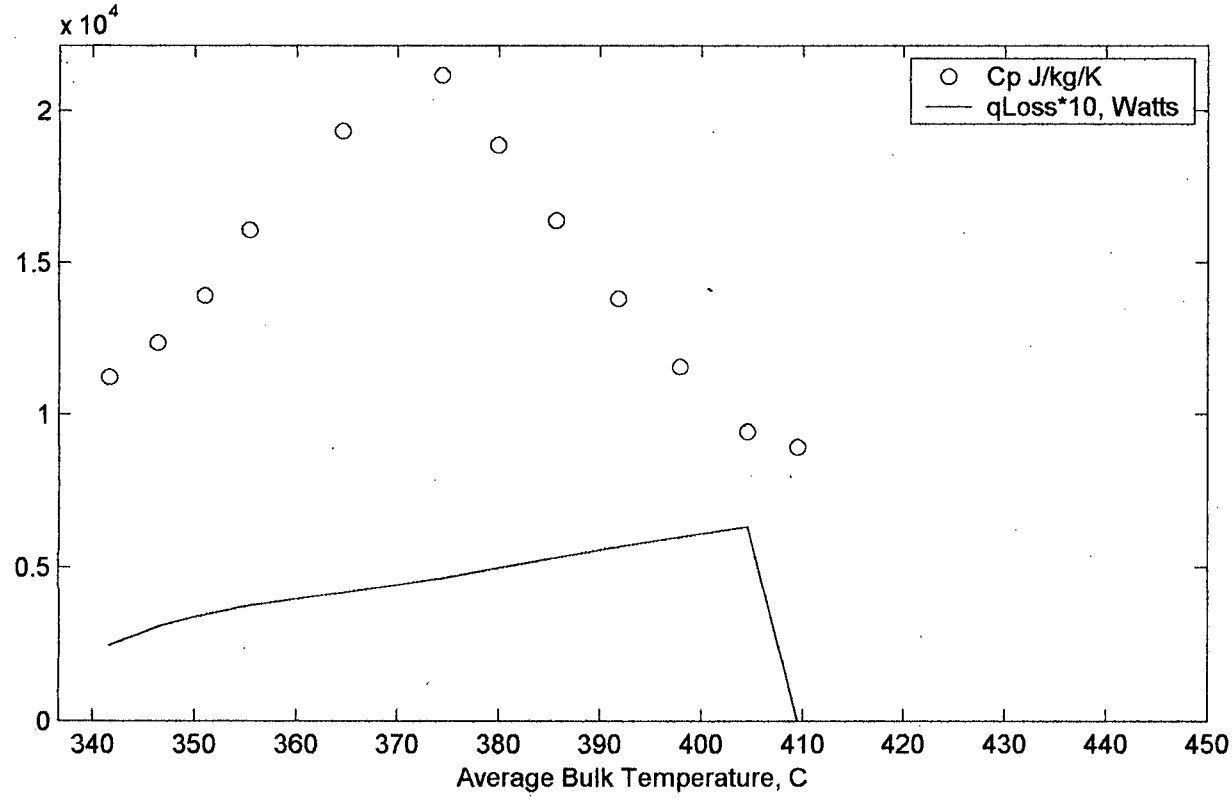

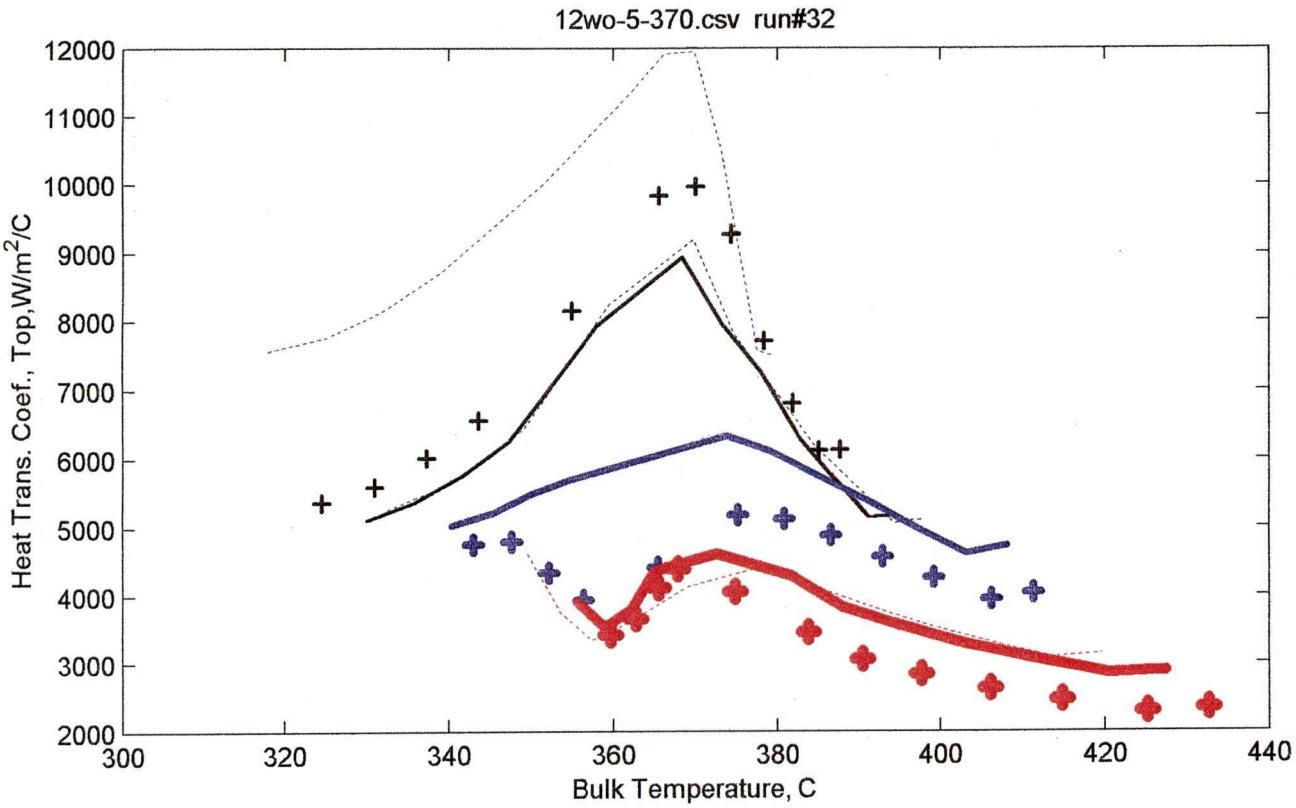

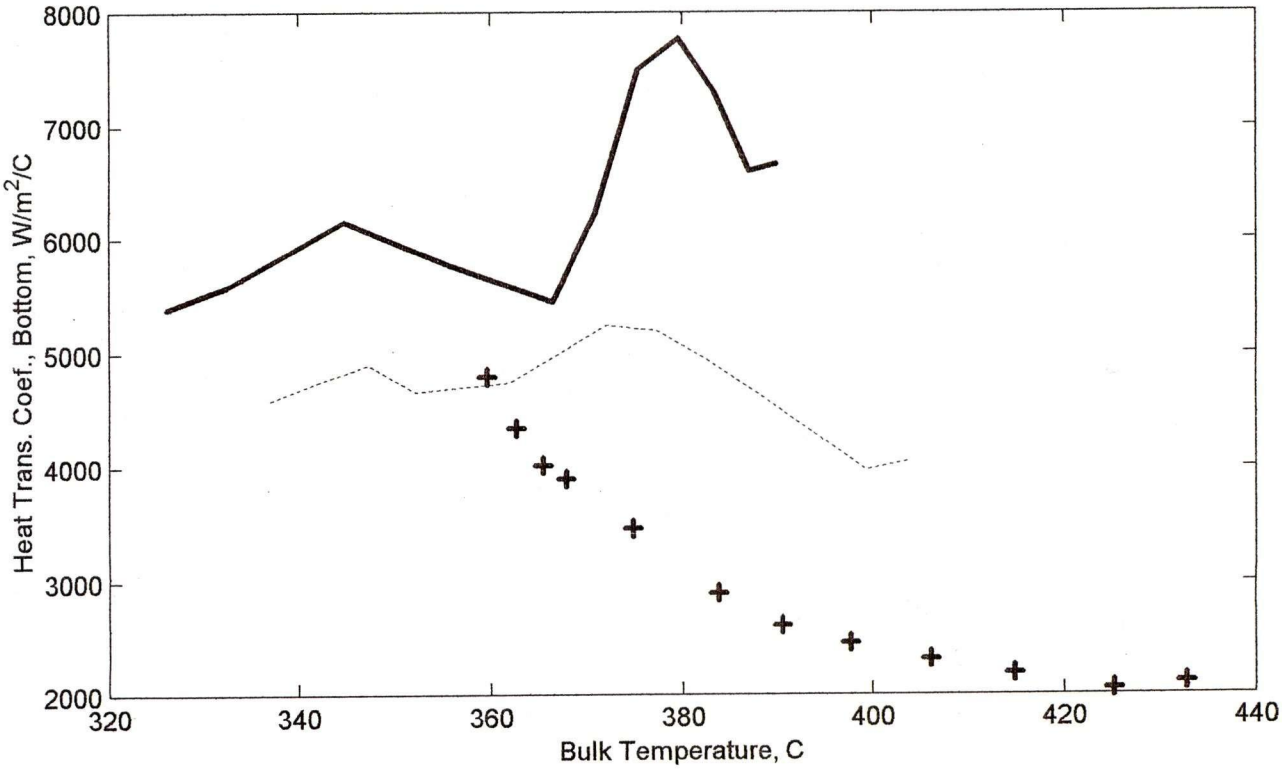

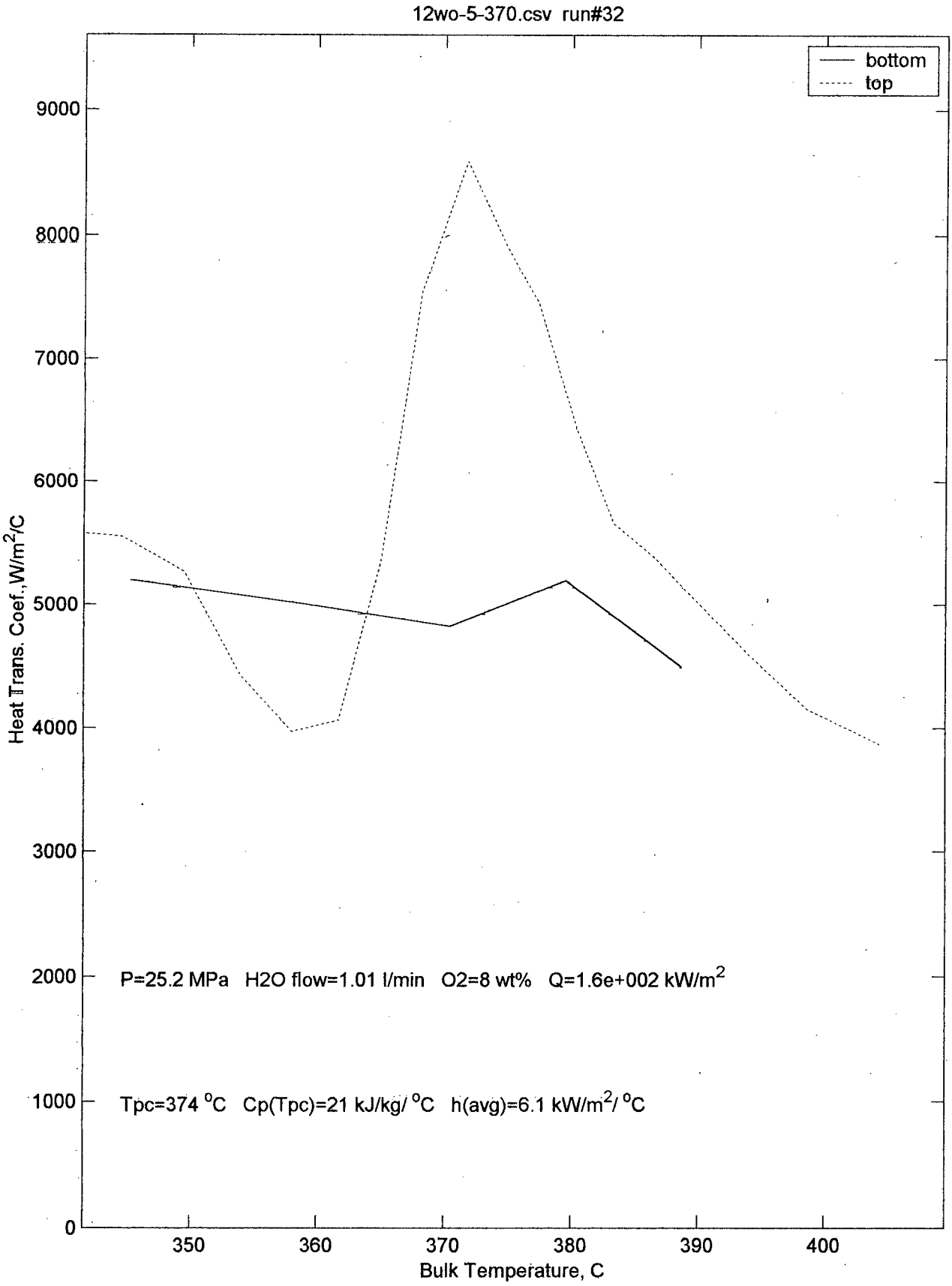

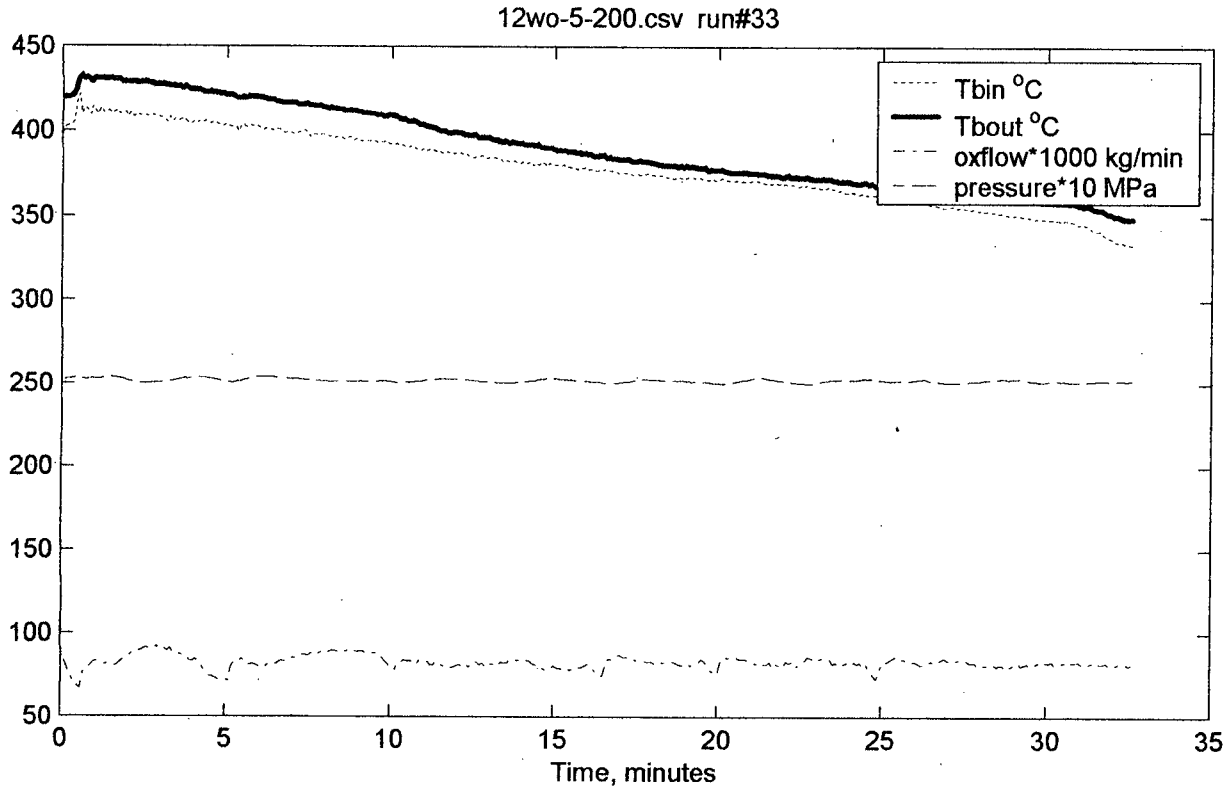

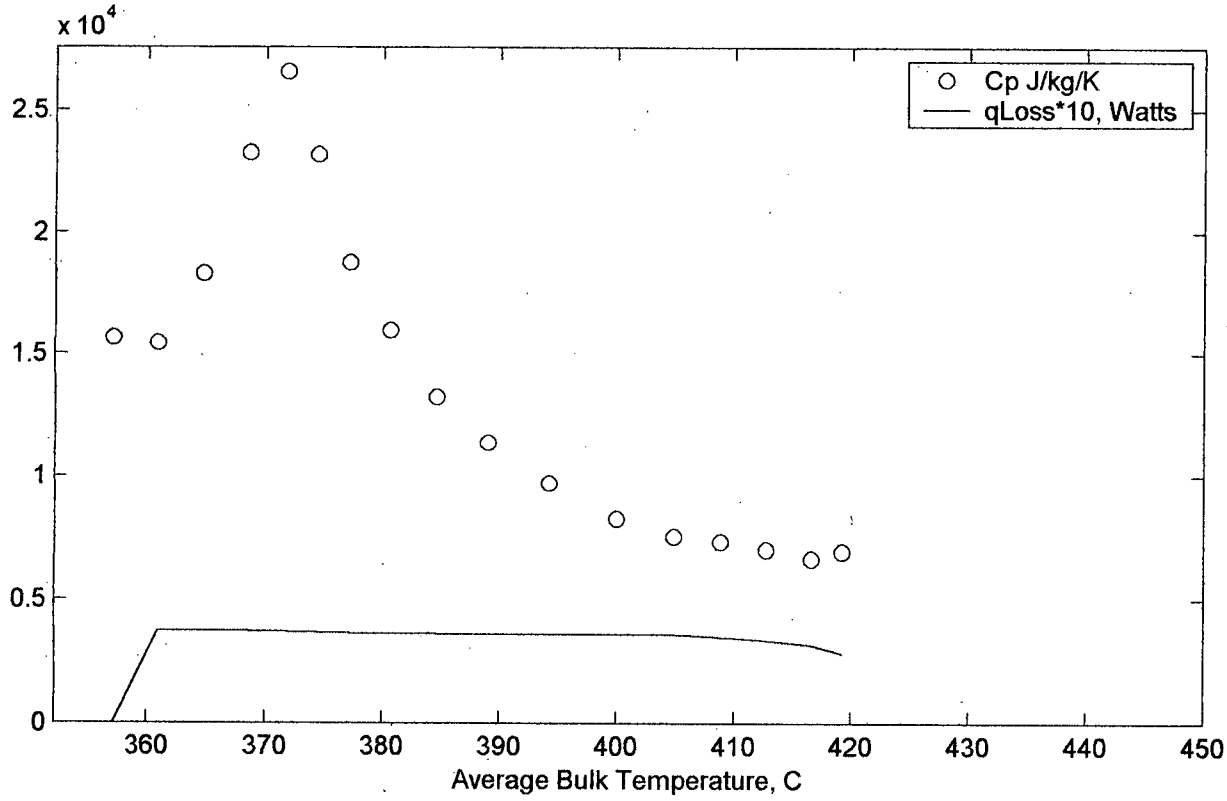

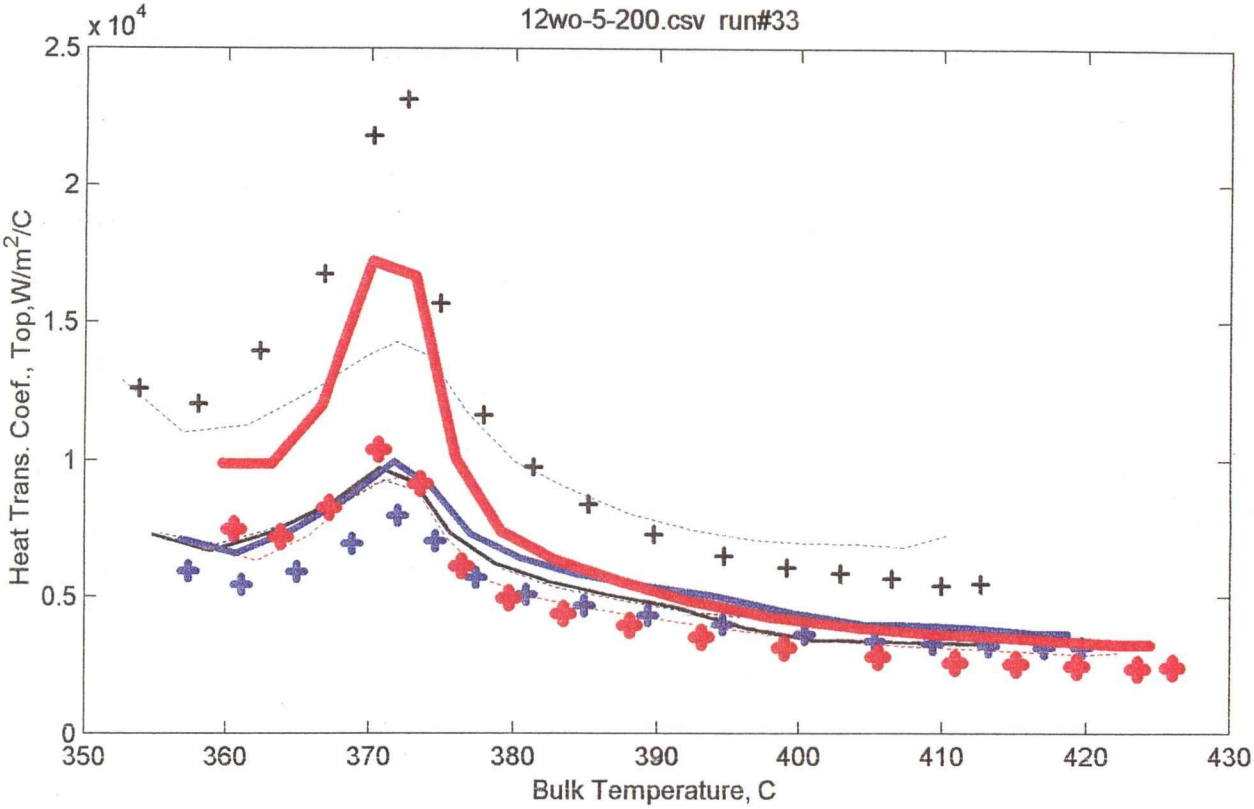

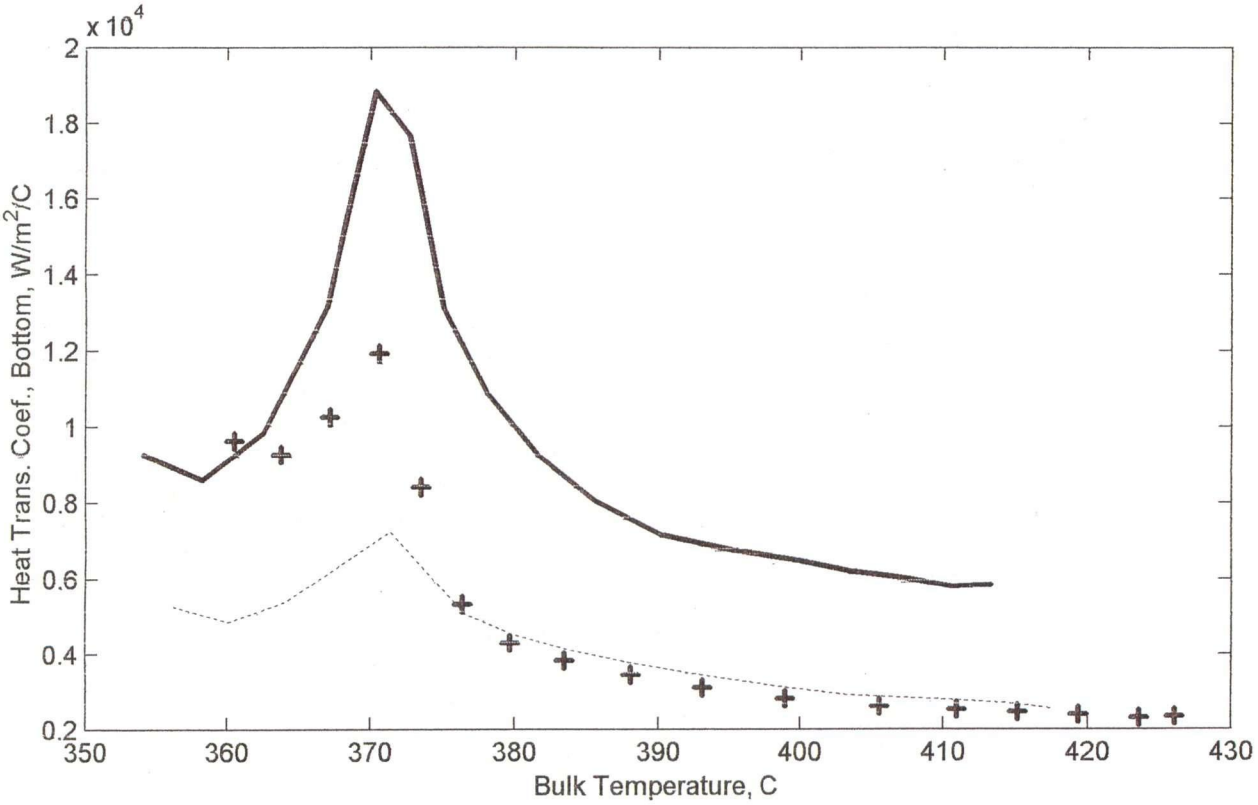

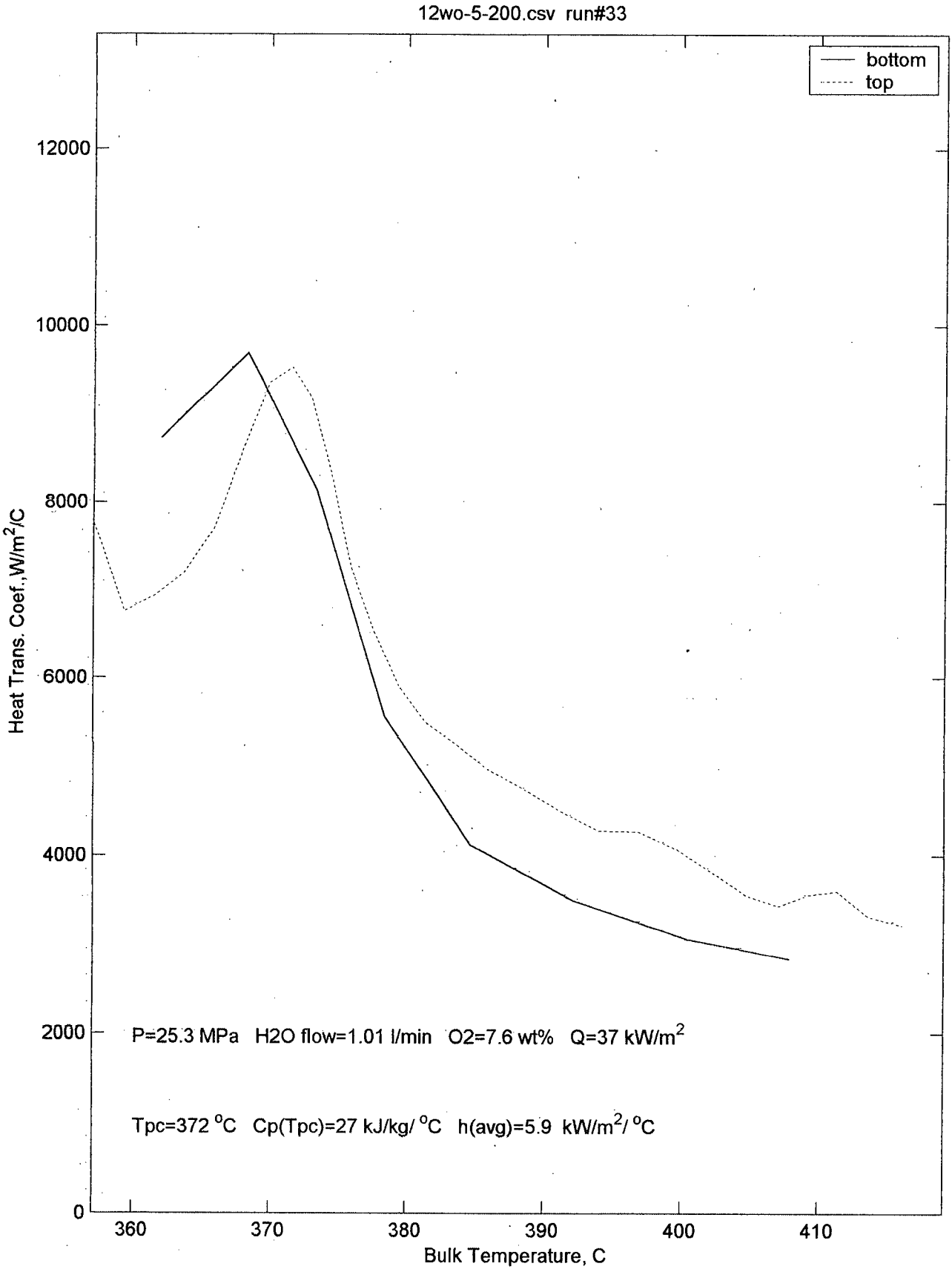

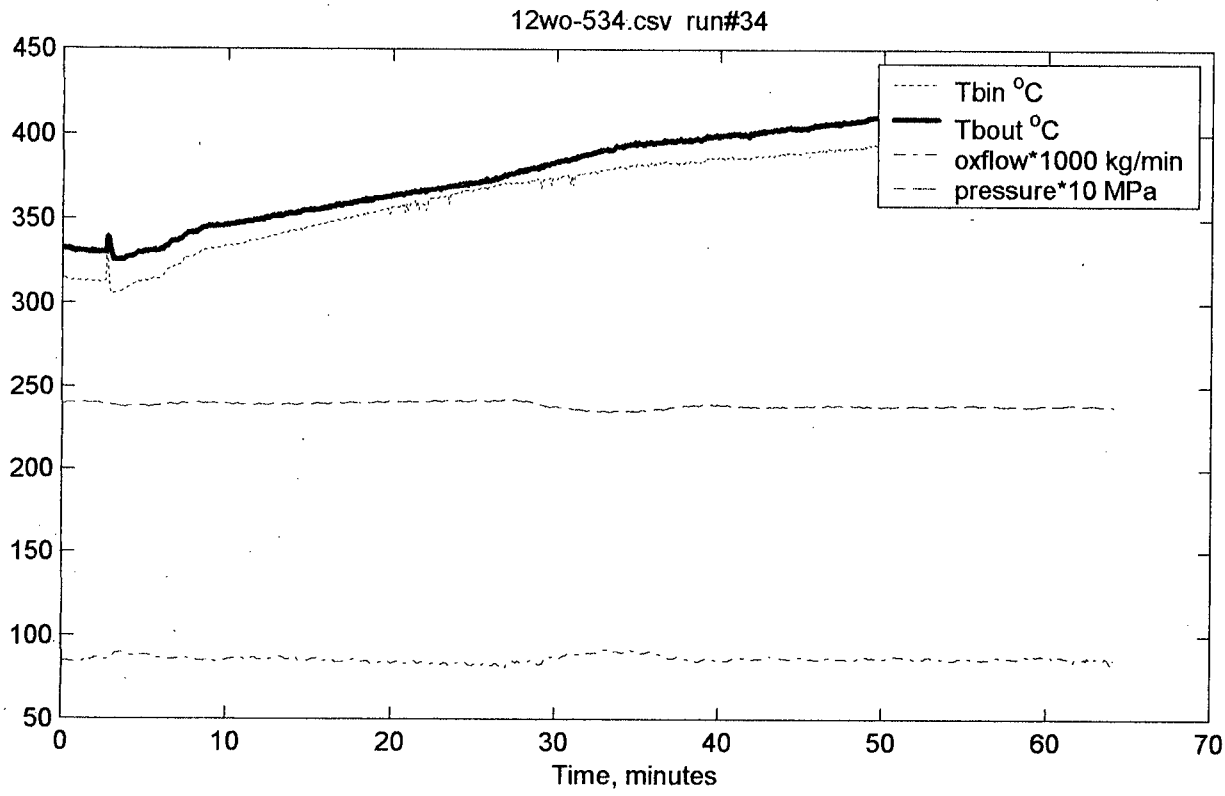

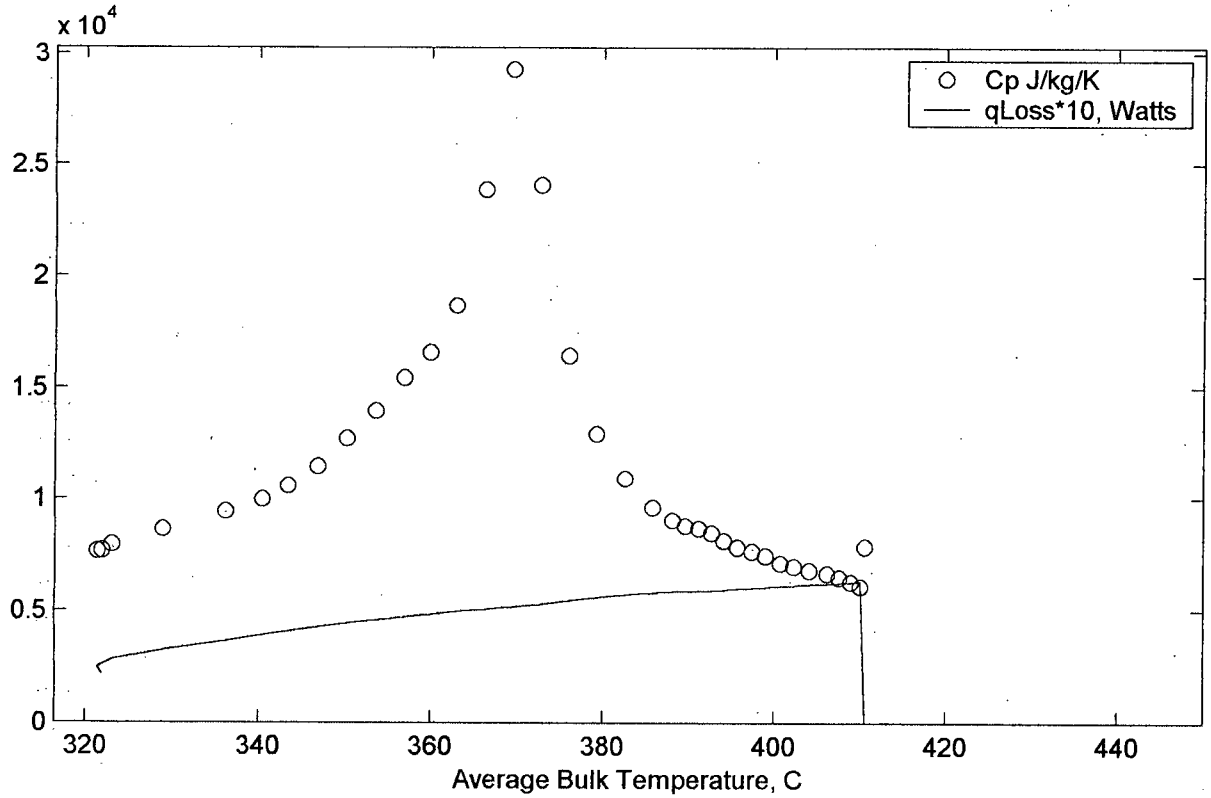

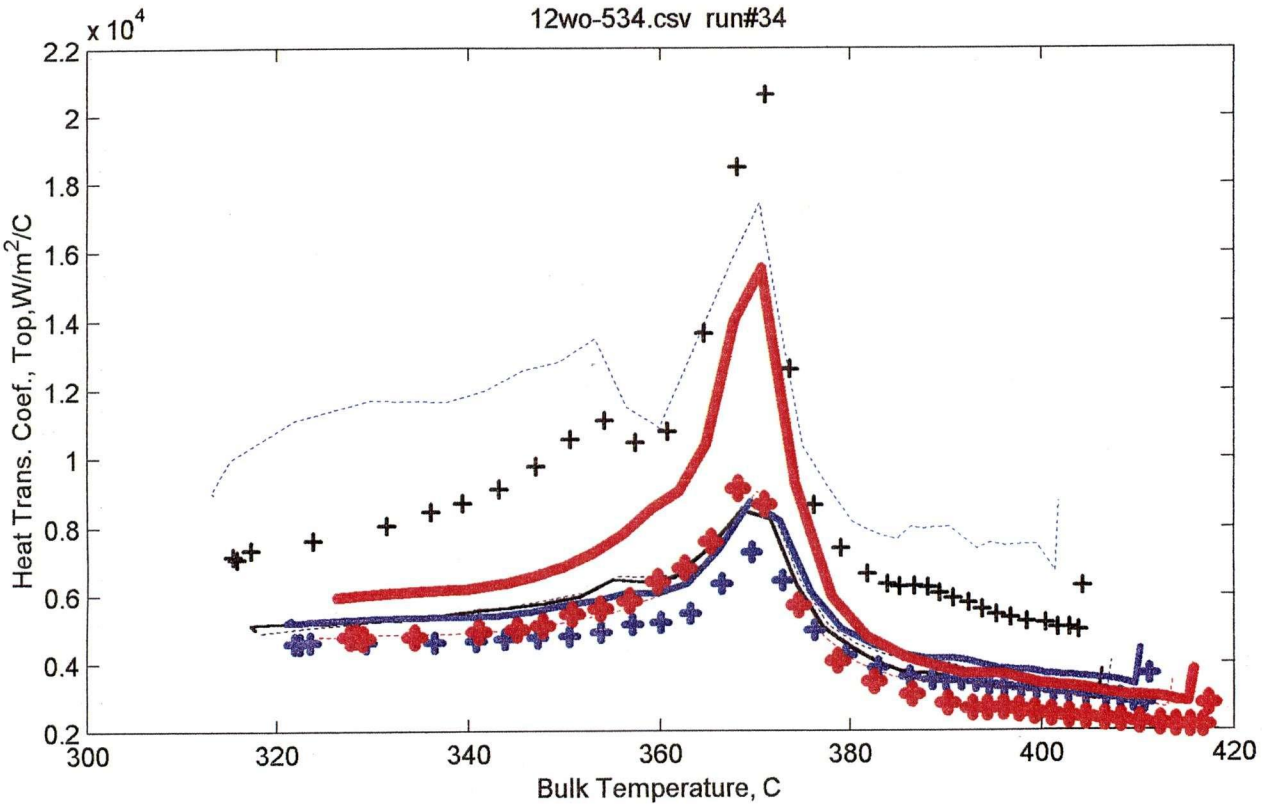

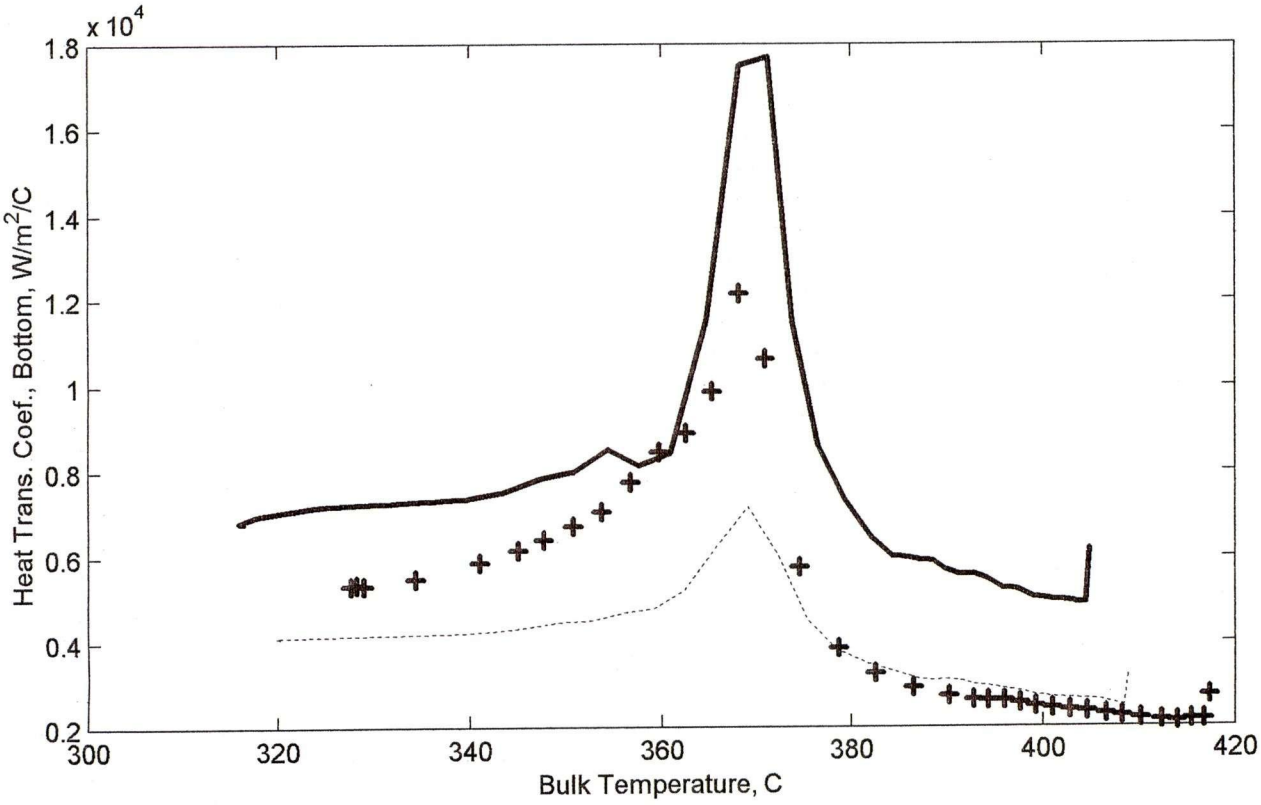

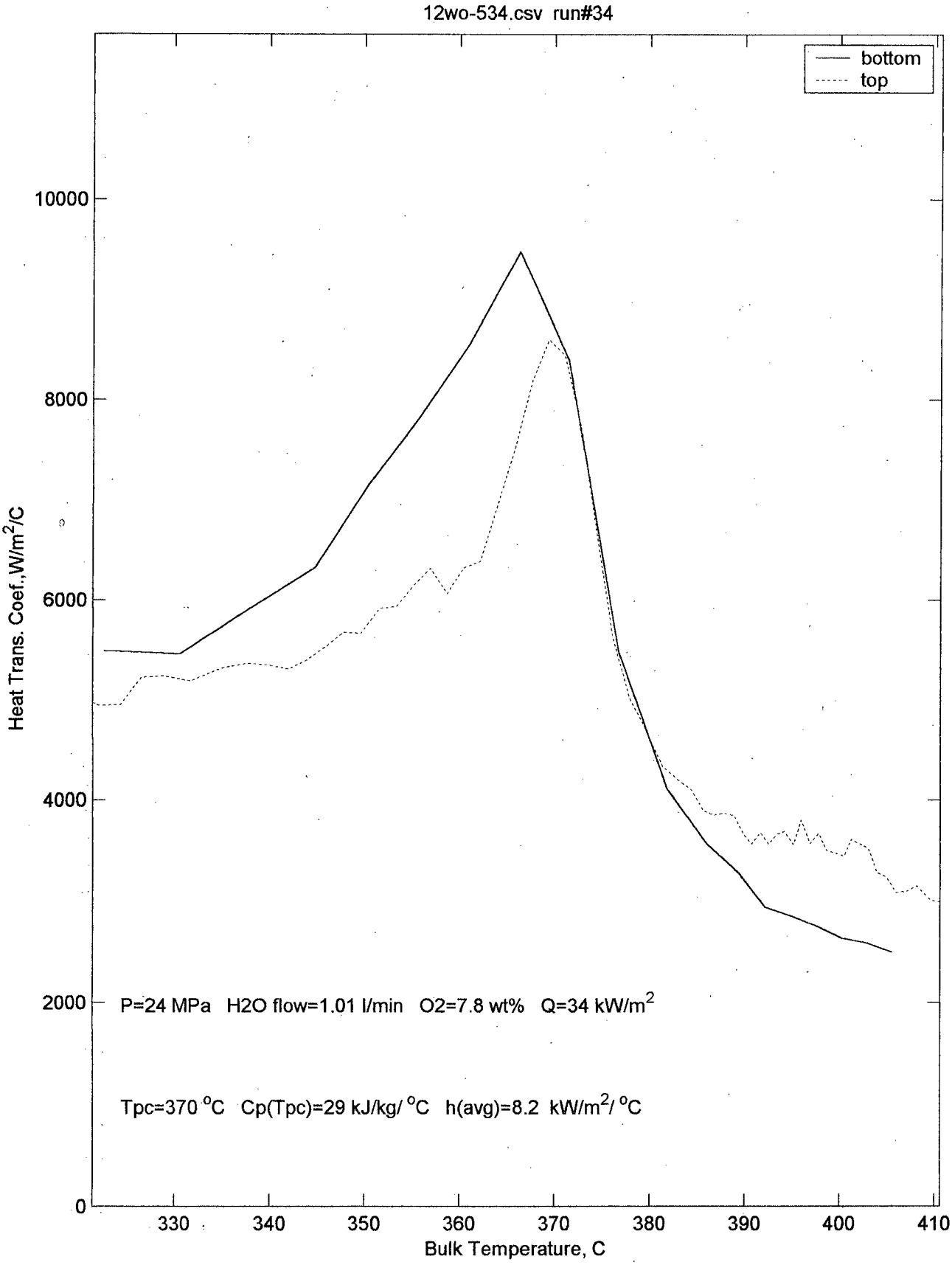

APPENDIX F

MatLab programs outline

Heatdata.m

```
clear
%part 1 Channel Setup,
%each number indicates the channel for:
%bulk in and out thermcouples
Bini=[1,1,3,2,3,3,3,3];
Bouti=[3,3,23,3,5,4,4,5];
%offset for outlet bulk temperature
offsetbout=[-1.5,-1.5,-1.5,-1.5,-1.5,-1.5,-1.5,-1.5]
%length between in, out bulk thermocouples
testL=[2.946,2.946,2.946,2.946,2.946,1.473,1.473,3.259];
%pressure and oxygen channels:
PTi=[18,18,18,22,22,22,22,22];
O2i=[20,20,20,24,24,24,24,24];
%number of top and bottom T/C channels for 8 different configurations
NTOP=[12,10,8,10,8,9,9,9];
NBOT=[0,7,5,5,5,3,3,3];
%make up an array for graphing suface thermocouple data
linetype=char('k:','k-','k +',...
   'b:','b-','b +',...
   'r:','r-','r +',...
   'g-','g +','g:');
%channel numbers for the top and bottom T/C
% each row corresponds to one configuration
top=[4,5,6,7,8,9,10,11,12,13,14,15;...
      4,5,12,13,14,16,21,22,23,24,0,0;...
      10,11,12,13,14,15,21,22,0,0,0,0;...
      5,7,8,10,12,14,16,17,18,20,0,0;...
      6,8,9,14,15,17,18,20,0,0,0,0;...
      7,8,10,11,12,13,14,15,16,0,0,0;...
      7,8,10,11,12,13,14,15,16,0,0,0;...
      7,8,10,11,12,13,14,15,16,0,0,0];
bot=[0,0,0,0,0,0,0,0,0,0,0,0;...
      6,7,8,9,10,11,15,0,0,0,0,0;...
      4,5,7,8,9,0,0,0,0,0,0,0;...
      6,9,11,13,15,0,0,0,0,0,0,0;...
      7,10,11,12,13,0,0,0,0,0,0,0;...
      6,9,17,0,0,0,0,0,0,0,0,0;...
      6,9,17,0,0,0,0,0,0,0,0,0;...
      6,9,17,0,0,0,0,0,0,0,0,0];
%axial location of the thermocouples, for a given config (row)
% and thermocouple number.  All configs use less than 13 T/Cs.
xtop=[0.242,0.447,0.749,0.837,0.969,1.25,1.551,1.721,2.024,2.278,2.414,
2.822;...
      0.749,0.969,2.024,0.837,1.123,1.25,2.822,2.414,0.442,1.41,0,0;...
      0.247,0.612,0.837,1.123,1.25,1.41,1.551,2.822,0,0,0,0;...
      0.612,0.749,0.837,0.969,1.123,1.25,1.41,1.721,2.278,2.822,0,0;...
      .612,.749,.835,1.41,1.721,2.278,2.822,2.874,0,0,0,0;...
      1.031,0.861,.504,.063,1.551,1.721,2.151,2.551,2.822,0,0,0;...
      1.031,0.861,.504,.063,1.551,1.721,2.151,2.551,2.822,0,0,0;...
      1.031,0.861,.504,.063,1.551,1.721,2.151,2.551,2.822,0,0,0];
xbot=[0,0,0,0,0,0,0,0,0,0,0,0;...
      2.822,0.861,1.03,1.179,1.329,0.521,0.776,0,0,0,0,0;...
      0.148,0.521,1.03,1.179,1.329,0,0,0,0,0,0,0;...
      0.691,0.861,1.03,1.179,1.329,0,0,0,0,0,0,0;...
```

```
      .691,.861,1.03,1.179,1.329,0,0,0,0,0,0,0;...
      1.325,.612,2.822,0,0,0,0,0,0,0,0,0;...
      1.325,.612,2.822,0,0,0,0,0,0,0,0,0;...
      1.325,.612,2.822,0,0,0,0,0,0,0,0,0];
%Thermcouple offsets entered here, assumed to be configuration-specific
offsettop=[0,0,0,0,0,0,0,0,0,0,0,0,;...
       0,0,0,0,0,0,0,0,0,0,0,0,;...
       0,0,0,0,0,0,0,0,0,0,0,0,;...
       0,0,0,0,0,0,0,0,0,0,0,0,;...
       0,0,0,0,0,0,0,0,0,0,0,0,;...
       0,0,0,0,0,0,0,0,0,0,0,0,;...
       0,0,0,0,0,0,0,0,0,0,0,0,];
offsetbot=[0,0,0,0,0,0,0,0,0,0,0,0;...
      0,0,0,0,0,0,0,0,0,0,0,0;...
      0,0,0,0,0,0,0,0,0,0,0,0;...
      0,0,0,0,0,0,0,0,0,0,0,0;...
      0,0,0,0,0,0,0,0,0,0,0,0;...
      0,0,0,0,0,0,0,0,0,0,0,0;...
      0,0,0,0,0,0,0,0,0,0,0,0];
%-------------------------- now enter run-specfic information -----
%file names.  The data file should have the first 2 columns of the raw
.txt
% file removed, as well as the header row.  That, is the file is a
comma-separated
% file with each column corresponding to a particular channel.
fname=char('sept2a.csv','sept2b.csv','sept2c.csv','sept2d.csv','sept2e.
csv',...

'sept2e.csv','qhfmtall.csv','qhfmtal2.csv','qhftall.csv','mar10cp.csv',
...

't1june17.csv','t2jun17.csv','t3jun17.csv','t4jun17.csv','t5jun17.csv',
...
   't6jun17.csv','O1Tall.csv',...
   'O2Tall.csv','jun19a.csv','jun19b.csv','jun19c.csv','jun19d.csv',...
   'may24.csv','800w.csv','800w.csv','1600w.csv','1600awo.csv',...
   '14water.csv','14wo.csv','12wo.csv','12wo-5-300.csv','12wo-5-
370.csv',...
   '12wo-5-200.csv'  ,'12wo-
534.csv','12water.csv','O0T120.csv','O0T200.csv','O0T300.csv');
cn=[1,1,1,1,1,1,2,2,2,2,3,3,3,3,3,3,...
   4,4,5,5,5,5,6,7,7,...
   7,7,8,8,8,8,8,8,8,8,4,4,4];
v=[-1,-1,299,299,299,299,-1,-1,-1,-1,...
   300,300,300,300,300,300,...
   300,300,0,0,0,0,...
   -1,300,300,-1,300,300,300,300,...
   300,370,200,200,0,300,300,300];
lpm=[1.2,1.2,1.2,1.2,1.2,1.2,-1,-1,0.94,1.2,...
      1.01,1.01,1.01,1.01,1.01,1.01,1.05...
      1.05,0.636,0.636,1.296,1.296,1.365,1.026,1.026,2.117,2.1168,...

1.269,1.269,1.007,1.007,1.007,1.007,1.007,1.007,1.068,1.068,1.068];
kgps=lpm/60.;
timestep=5;
```

```
%K(1:38)=4.16/60.;
%V0(1:38)=2.;
K(1:38)=(366.76*3950/3980/44.4)^0.5

%---------------------------------------read in data-------------------
-----
run=input('run number?')
nav=input('averaging window size (~20)?')
filename=deblank(fname(run,:))
data=csvread(filename);
titlestr=strcat(filename,'  run# ',num2str(run))
ic=cn(run);
Tbin=data(:,Bini(ic));
Tbout=data(:,Bouti(ic))-offsetbout(ic);
L=testL(ic);
pres=data(:,PTi(ic));
pres=(992.1*pres-22.353)/145
%oxv=max(data(:,O2i(ic))-V0(run),0);
oxv=data(:,O2i(ic))
%voltages less than V0 indicated zero oxygen flow
%oxraw=K(run).*oxv.^.5;
oxraw=K(run).*(oxv.^.5)/60
Ndata=max(size(data))
minutes=timestep/60:timestep/60:timestep*Ndata/60;

%now work on the filtering then analyzing data
oxflow=cleanup(oxraw,nav,1);
short=length(oxflow);
Tbinf=cleanup(Tbin,nav,1);
Tboutf=cleanup(Tbout,nav,1);
Tbavg=(Tbinf+Tboutf)/2;
%++++++++++++++++++++++++++++++++++++++++++++++++++++++++++++++

%now call the transient heat transfer program
for j=1:NTOP(ic)
   i=top(ic,j);
   T=data(:,i)-offsettop(ic,j);
   Tt(:,j)=cleanup(T,nav,1);
end
Ttavg =0.
for j=1:NTOP(ic)
   Ttavg=Ttavg+Tt(:,j)
end
Ttavg=Ttavg/NTOP(ic)


qloss=losses(Ttavg,5*nav,L);
if v(run)==0.
   Qe=0.
else

      Qe=Qelec(Ttavg,v(run),L);
   end
Q=Qe-qloss;
oxraw = 0.
figure(1)
subplot(2,1,1);
```

```
plot(minutes,Tbin,'k:',minutes,Tbout,'k-',...
   minutes,oxraw*1000,'k-.',minutes,abs(pres*10),'k--','LineWidth',2)
legend('Tbin ^oC','Tbout ^oC','oxflow*1000 kg/min','pressure*10 MPa')
title(titlestr)
xlabel('Time, minutes')
mflow=kgps(run)
%mflow=kgps(run)+oxflow/60.;
dT=Tboutf-Tbinf;
Cp=(Q./(dT))./mflow;
%calculate some parameters needed for a quadratic interpolation of
temperature
%dCpdT=gradient(Cp,Tbavg);
%a=0.5*dCpdT;
%b=Cp-Tbavg.*dCpdT;
%c1=0.5*Tbinf.*Tbinf.*dCpdT+Cp.*Tbinf-Tbinf.*Tbavg.*dCpdT;
subplot(2,1,2);
plot(Tbavg,Cp,'k o',Tbavg,qloss*10,'k-')
xlabel('Average Bulk Temperature, C')
axis([min(Tbavg)-5,450,0,max(Cp)+1000])
%notes=strcat(num2str(mean(mflow)),'kg/s    ,'...
%    ,num2str(mean(Q)),'  Watts')
%notes2=strcat( 'points averaged(x0.5)=',num2str(nav))
%text([min(Tbavg)+60],[max(Cp)-3500],notes)
%text([min(Tbavg)+60],[max(Cp)-9500],notes2)
legend('Cp J/kg/K','qLoss*10, Watts')
filename5=strcat('run16a','.out')% can construct a filename using the
run number
M=[Tbavg,Cp]%3 column vectors or more put into one matrix
dlmwrite(filename5,M)%default formate is comma delimited
%now recover file to see that it works
A=dlmread(filename5,',')

%------------------ parse and filter TOP surface temperatures  ----
q=(Q./Cp)./mflow
Ri=0.0031
Ro=0.00475
kin=17
Ariro=2*Ri/(Ro^2-Ri^2)
%a=Ri/Ro
for j=1:NTOP(ic)
   i=top(ic,j);
   T=data(:,i)-offsettop(ic,j);
   Tt(:,j)=cleanup(T,nav,1);
   Tti(:,j)=Tt(:,j)+Qe.*Ariro*(Ro^2-Ri^2)/(4*kin)+(Qe.*Ro*Ariro/2-
qloss)*(log(Ri)-log(Ro))*Ro/kin
   %Tti(:,j)=Tt(:,j)-Q.*Ri*(a^2-2*log(a)-1)/(2*kin*(1-a^2))
   xj=xtop(ic,j);
   Ttb(:,j)=q*xj/L+Tbinf;
end
%------------------ parse and filter BOTTOM surface temperatures  ----
for j=1:NBOT(ic)
   i=bot(ic,j);
   T=data(:,i)-offsetbot(ic,j);
   Tb(:,j)=cleanup(T,nav,1);
   Tbi(:,j)=Tb(:,j)+Qe.*Ariro*(Ro^2-Ri^2)/(4*kin)+(Qe.*Ro*Ariro/2-
qloss)*(log(Ri)-log(Ro))*Ro/kin
   xj=xbot(ic,j);
```

```
   Tbb(:,j)=q*xj/L+Tbinf;
end
%=====================================================================


%------------------  TOP surface heat transfer coefficients  ----
Ttall=[];
htall=[];
A=0.0062*pi*L
figure(2)
subplot(2,1,1);
for j=1:NTOP(ic)
   Qa=Q./A
   ht(:,j)=Qa./(Tti(:,j)-Ttb(:,j));
   Ttall=[Ttall;Ttb(:,j)]
   htall=[htall;ht(:,j)]
   plot(Ttb(:,j),ht(:,j),linetype(j,:),'LineWidth',j/2)
   hold on
end
title(titlestr)
xlabel('Bulk Temperature, C')
ylabel('Heat Trans. Coef., Top,W/m^2/C  ')
hold off
%------------------ Bottom heat transfer coefficients  ----
Tball=[];
hball=[];
subplot(2,1,2);
for j=1:NBOT(ic)
   Qa=Q./A
   hb(:,j)=Qa./(Tbi(:,j)-Tbb(:,j));
   Tball=[Tball;Tbb(:,j)]
   hball=[hball;hb(:,j)]
   plot(Tbb(:,j),hb(:,j),linetype(j,:),'LineWidth',2)
   hold on
end
xlabel('Bulk Temperature, C')
%ylabel('Axial Position, m')
ylabel('Heat Trans. Coef., Bottom, W/m^2/C ')
hold off
%----average top and bottom coefficients----
figure(3)
[Ttallsort,sortindex]=sort(Ttall);
htallsort=htall(sortindex);
[Tballsort,sortindex]=sort(Tball);
hballsort=hball(sortindex);
hballclean=cleanup(hballsort,5,2000)
htallclean=cleanup(htallsort,5,2000)
Tballclean=cleanup(Tballsort,5,2000)
Ttallclean=cleanup(Ttallsort,5,2000)
filename6=strcat('run16b','.out')% can construct a filename using the
run number
N=[Tballclean,hballclean]%3 column vectors or more put into one matrix
dlmwrite(filename6,N)%default formate is comma delimited
filename7=strcat('run16c','.out')% can construct a filename using the
run number
N1=[Ttallclean,htallclean]%3 column vectors or more put into one matrix
dlmwrite(filename7,N1)%default formate is comma delimited
```

```
%diary ('cp and h')
%Tti
%Tt
%Tbi
%Tb
%Tbavg
%Tbinf
%Tboutf
%Cp
%diary of
%Tballclean
%hballclean
%Ttallclean
%htallclean
plot(cleanup(Tballsort,5,2000),cleanup(hballsort,5,2000),'k-')
hold on
plot(cleanup(Ttallsort,5,2000),cleanup(htallsort,5,2000),'k:')
legend('bottom','top')
xlabel('Bulk Temperature, C')
ylabel('Heat Trans. Coef.,W/m^2/C')
title(titlestr)
hold off
%post processing/averageing routines
%The purpose of these calculations is to generate the run summary
information that
% is tabulated in the thesis
% Find the peak Cp and call this the pseudocritical point
[Cpmax,imax]=max(Cp);
Tpc=Tbavg(imax);
% The most important range for the averages is about +/- 15 C of Tpc
low=Tpc-15;
high=Tpc+15;
% create an index that will allow us to calculate averages in this
range of temperatures.
% good is used in "logical subscripting"
good=(Tbavg>low)&(Tbavg<high);
meanP=mean(pres(good))
meanP=abs(meanP)
meanQ=mean(Q(good))/(.0062*pi*L)/1000;
%meanOx=mean(oxflow(good))*60.
meanOx=0.
oxpct=100*meanOx/(meanOx+kgps(run)*3600)
%getting average heat transfer coefficient is more complicated because
% we want an average weighted by the heat capacity.  In a heat
exchanger,
% most of the heat transfer is required where the heat capacity is
highest,
% so the heat transfer coefficient is more important near the peak.
allT=[Ttall;Tball];
allh=[htall;hball];
[allTsort,isort]=sort(allT);
allhsort=allh(isort);
%we will need a Cp value for every temperature; use a lookup table here
[Tsort,isort]=sort(Tbavg);
Cpsort=Cp(isort);
Cpall=interp1(Tsort,Cpsort,allTsort);
good=(allTsort>low)&(allTsort<high);
```

```
dT=gradient(allTsort);
CpdT=Cpall.*dT;
hCpdT=allhsort.*CpdT;
%now the mean value is the integral of hCpdT divided by the integral of
CpdT
% but in Matlab, we use a sumation instead of an integral
meanh=sum(hCpdT(good))/sum(CpdT(good))/1000;
notes3=strcat( 'P=',num2str(meanP,3),' MPa   H2O
flow=',num2str(lpm(run),3),' l/min   O2=',...
 num2str(oxpct,2),' wt%   Q=',num2str(meanQ,2),' kW/m^2 ' );
notes4=strcat( 'Tpc=',num2str(Tpc,3),' ^oC
Cp(Tpc)=',num2str(Cpmax/1000,2),...
   ' kJ/kg/ ^oC   h(avg)= ',num2str(meanh,2),'  kW/m^2/ ^oC' );
%reset the axis limits on the last plot of heat transfer coefficients
so that we
% can be sure that there is room for the text.
xmin=min(Tbavg);
xmax=max(Tbavg);
ymin=0;
%get the y-axis limit
ymax=1.3*max(cleanup(allhsort,5,2000));
axis([xmin,xmax,ymin,ymax]);
text([xmin+3],[ymin+2000],notes3);
text([xmin+3],[ymin+1000],notes4);
%here is how to put vectors together into a fil
Q
dT
```

```
function ql=losses(Tw,deltime,L)
%calculates test section transient heat losses given tube temperature
Tw
% as a function of time.

n=40;
W=.15
k=.35;
thermalmass=0;
rho=480;
cp=710;
Tambient=20;
delr=W/n/2;
h=7;
Fo=k/rho/cp*deltime/delr/delr;
Bi=h*delr/k;
desired=.5/(1+Bi);
extrasteps=round(0.5+Fo/desired)
Fo=Fo/extrasteps;
r0=.0095;
area=L*2*r0*pi;

%make up the "grid"
Adiag=1-2*Fo;
for i=1:n
   r(i)=r0+delr*i;
   Aback(i)=Fo*(1-delr/2/r(i));
   Afor(i)=Fo*(1+delr/2/r(i));
end
%make up a matrix for making the timestep
A=zeros(n,n);
A(1,1)=Adiag;
A(1,1+1)=Afor(1);
for i=2:n-1
   A(i,i-1)=Aback(i);
   A(i,i)=Adiag;
   A(i,i+1)=Afor(i);
end
A(n,n)=1-Fo-Fo*Bi;
A(n,n-1)=Fo;
%-----------Now set initial conditions----------------------------
% for simplicity, use linear variation from inside to outside
i=1:n;
T=Tw(1)-(Tw(1)-Tambient)*i/n;
T=T';
%now march along in time for as many points as contained in Tw
Ntimes=length(Tw);
B=zeros(Ntimes,n+1);
ql=Tw*0;
for j=1:Ntimes-1
   for jj=1:extrasteps
     T=A*T;
     T(1)=T(1)+Aback(1)*Tw(j);
     T(n)=T(n)+Fo*Bi*Tambient;
  end
   B(j,1)=Tw(j);
   B(j,2:n+1)=T';
```

```
      ql(j)=k*area*(Tw(j)-T(1))/delr+(Tw(j+1)-
Tw(j))/deltime*thermalmass;

end

j=1:Ntimes;
i=1:n+1;
figure(5)
contour(i,j,B)
[CS,H]=contour(i,j,B);
clabel(CS,H)
```

```
function q=Qelec(Ttavg,SCRvolts,L)
%calculates electric power input using temperature dependent
resisistivty
F=0.789
rho=(((Ttavg.^3)/1000000000)-
((Ttavg.^2)/1000000)+Ttavg.*0.0004+1.288)./1000000.
area=41.486e-6;
V=0.0491*SCRvolts-1.2564;
R=rho.*1.473/area;
q=2*(F*V^2./R);
end
```

```
function y=cleanup(x,nav,cutoff)
%y=cleanup(x,nav,cutoff)
%takes a vector x and removes outliers according to the parameter
cutoff,...
%and smooths with moving window +/-nav
% It returns a shorter vector (roughly nav times shorter)
% There is no real loss of information because we are averaging over a
number of points
% anyway; the original longer vector is more difficult to work with and
slower.

clean=x;
N=length(x);
for i=nav+1:N-nav
   mid=median(x(i-nav:i+nav));
   if abs(x(i)-mid)>cutoff;
      clean(i)=mid;
   end
end
newndata=(N-mod(N,nav))/nav-2;
y=(1:newndata)';
for j=1:newndata
   i=j*nav+1;
   y(j)=mean(clean(i-nav:i+nav));
end
```

```
% heat transfer correlation
clear
massflow=input('kg/min')/60.;
%tube parameters: roughness and conductivity
eps=.3048*10^-4;
D=.001*input('id mm')
area=pi*D^2/4;
pressure=25.;
%interpolate 2D property tables for the specified pressure
% to get a 1-D table for fast intperpolation of properties
[Tp,rhop,Hp,Cpp,visp,Kp,Prp]=tables(pressure);
maxtemp=max(Tp);
mintemp=min(Tp);
%bulk properties
Hb=1500000:100000:2500000;
Tb=interp1(Hp,Tp,Hb');
visb=interp1(Tp,visp,Tb');
Re=(massflow/area*D)./visb;
Db=interp1(Tp,rhop,Tb');
Q=input('heat flux kW/m^2')
%guess wall temperature to start iteration of heat transfer coefficent
Tw=Tb+10.;
% guess initial friction factor
friction=(-2*log10(eps/D/3.7+2.51./(Re*.02))).^-2;
figure(1)
for i=1:15
%properties at walls and bulks:
  Dw=interp1(Tp,rhop,Tw');
  Hw=interp1(Tp,Hp,Tw');
  visw=interp1(Tp,visp,Tw');
  kw=interp1(Tp,Kp,Tw');
  Pr=(Hb-Hw)./(Tb-Tw)'.*visw./kw;
  Nu = 0.00459*(Re.^0.923).*(Pr.^0.613).*(Dw./Db).^0.231;
  friction=(-2*log10(eps/D/3.7+2.51./(Re.*friction))).^-2;
  heat=kw.*Nu/D;
  % generate new estimate of wall temperature
  Tw=Tb+Q*1000./heat';
end
plot(Tb-273.1,heat/1000,Tb-273.1,friction*1000,Tb-273.1,Tw-Tb)
legend('h kW/m^2/C','f*1000','Tw-Tb')
xlabel('Tb C')
ylabel('h,f')
%here is how to put vectors together into a file
filename=strcat('25.2b','.out')% can construct a filename using the run
number
M=[Tb,heat',friction']%3 column vectors or more put into one matrix
dlmwrite(filename,M)%default formate is comma delimited
%now recover file to see that it works
A=dlmread(filename,',')
```

```
%property loader and plotter
function [T,rhop,Hp,Cpp,visp,Kp,Prp]=tables(Pressure)
%load all the property tables
%all must have the same size and the same T,P spacing
load dens.txt;
load K.txt;
load cp.txt;
load enth.txt;
load prand.txt;
load vis.txt;
% get file sizes from dens, but other files must have same size
[nT,nP]=size(dens);
% the first row contains the pressures in MPa
P=dens(1,2:nP);
% the first column contains the Temperatures in K
T=dens(2:nT,1);
% other than the first rows and columns, we have actual property values
A=dens(2:nT,2:nP);
rhop=interp2(P,T,A,Pressure,T);
A=K(2:nT,2:nP);
Kp=interp2(P,T,A,Pressure,T);
A=enth(2:nT,2:nP);
Hp=interp2(P,T,A,Pressure,T);
A=cp(2:nT,2:nP);
Cpp=interp2(P,T,A,Pressure,T);
A=vis(2:nT,2:nP);
visp=interp2(P,T,A,Pressure,T);
A=prand(2:nT,2:nP);
Prp=interp2(P,T,A,Pressure,T);
figure(2)
plot(T,rhop/1000.,'k:',T,Hp/1e6,'k+',T,Cpp/100000,'ko',T,visp*10.0,'k-
'...
,T,Kp,'g:',T,Prp/10,'bx')
legend('s.g. ','enthalpy MJ','Cp
10^5J/kg/K','vis*10','conductivity','Prandtl/10')
yLABEL('Property')
XLABEL('T K')
title(strcat('properties at pressure=',num2str(Pressure),'MPa'))
```